SEISMIC HAZARD EVALUATION FOR THE PALO VERDE NUCLEAR GENERATING STATION WINTERSBURG, ARIZONA

FINAL REPORT

Prepared for

ARIZONA PUBLIC SERVICE CO.
PHOENIX, ARIZONA

by

Risk Engineering, Inc.
5255 Pine Ridge Road
Golden, Colorado

December 3, 1991

EXECUTIVE SUMMARY

This study presents the results of an investigation of seismic hazard at the site of the Palo Verde Nuclear Generating Station (PVNGS).

This investigation followed a methodology analogous to the EPRI/SOG methodology that was developed for sites in the Central and Eastern United States, with appropriate modifications for the conditions at the PVNGS site. Two Earth-Science Teams identified seismic sources and assessed their activity probabilities and maximum magnitudes. Activity rates and b values for these seismic sources were calculated using a common methodology and data set. The teams then modified these parameters to reflect other information such as slip rates on faults. Interaction and communication between the two teams took place to exchange information, concepts, and results. This interaction helped to ensure that all relevant data, theories, and interpretations were considered by each team in making its evaluations.

Four sets of ground-motion attenuation functions were selected for this study. These attenuation functions are based mostly on California data; they were modified to account for postulated differences in anelastic attenuation in California and Arizona. Site amplification is characterized by the EPRI/SOG amplification factors for soil depths in the 180–400 foot range.

Seismic hazard calculations were performed for peak ground acceleration and spectral velocities at 1, 2.5, 5, 10, and 25 Hz. Results are presented as hazard curves and as uniform-hazard spectra (in both graphical and tabular forms). Results with no site amplification (i.e., corresponding to rock outcrop) are also presented.

The results presented here form a basis for comparing the seismic hazard at the PVNGS to hazard at other nuclear plant sites. For this purpose it would be most relevant to use the EPRI/SOG hazard results for the central and eastern US, rather than the LLNL results, as the methodology applied here follows most closely the EPRI/SOG study.

CONTENTS

LIST OF FIGURES

LIST OF TABLES

Section 1

INTRODUCTION

This study investigates the probabilistic hazard of earthquake-induced ground shaking at the Palo Verde Nuclear Generating Station (PVNGS), Arizona. These results will be used to guide decisions regarding seismic safety and levels of seismic evaluation and seismic retrofit, if any, to be undertaken at the facility. An express purpose of this study is to follow the methodology developed by several recent studies of seismic hazard at nuclear facilities in the central and eastern US (CEUS), so that comparisons can be made between the hazard at the PVNGS and at other nuclear power plants in the country. These other studies make explicit representation of the uncertainty in seismic hazard caused by multiple, alternative hypotheses on the causes and characteristics of earthquakes.

These recent studies of seismic hazard in the central and eastern United States (CEUS) were completed by the Electric Power Research Institute, funded by the Seismicity Owners Group (EPRI/SOG) (1), and by the Lawrence Livermore National Laboratory (LLNL), funded by the U.S. Nuclear Regulatory Commission (2). These studies represent major efforts to characterize the seismic hazard for nuclear power plants in the CEUS, and use the most recent, up-to-date understandings of seismicity and ground motion relations for the region.

These two studies could not be applied to the PVNGS site because the studies consider only sources of earthquakes east of the Rocky Mountains. Further, the two studies treat earthquakes of all magnitudes as point sources. That is, the studies do not consider the rupture size associated with large earthquakes that break a significant section of an active fault. In this study earthquake sources are developed for the region around the PVNGS, and explicit treatment of made of the length of rupture associated with large earthquakes that might occur in the region (including on the southern San Andreas fault). Following the methodology of the EPRI/SOG and LLNL studies, multiple seismic source interpretations are considered here, in order to characterize uncertainty in the seismic hazard, including uncertainty in the finite–rupture analysis.

The PVNGS is located at latitude 33.39 north and longitude 112.86 west. Structures at the site overly sandy silts and clay interspersed with layers of tuffs and breccias, varying from 300

to 400 feet thick, overlying andesite. Consistent with the EPRI/SOG and LLNL analyses, we report the distribution of peak horizontal ground acceleration (PGA) and spectral velocities (PSV) at multiple frequencies; we also show constant hazard spectra to demonstrate typical spectral amplitudes and shapes that might apply for earthquake ground motions of interest.

Section 2 of this report summarizes the calculational methodology for seismic hazard analysis used here, which is a standard methodology used in virtually all studies of this type. Section 2 also discusses the main points of the EPRI/SOG and LLNL methodologies, for background information. Section 3 describes the seismic sources (including faults) that were examined in this study, and Section 4 documents the analysis of historical seismicity that was conducted to estimate seismicity parameters for these sources. Section 5 reports the attenuation equations used to estimate PGA and PSV for the study, and the treatment of soils used to estimate surface ground motions. Section 6 reports the results of the study, including the dominant sources of uncertainty in seismic hazard. Finally, Section 7 presents conclusions of the study and some important qualifications to these results.

1.1 REFERENCES

1. *Seismic Hazard Methodology for the Central and Eastern United States.* Technical Report NP-4726-A, Electric Power Research Institute, July 1986. Revised, 1988. Vol. 1, Part 1: Methodology, Vol. 1, Part 2: Theory, Vol. 2: EQHAZARD Programmer's Manual, Vol. 3: EQHAZARD User's Manual, Vol. 4: Applications, Vols. 5 through 10: Tectonic Interpretations, Vol. 11: Nuclear Regulatory Commission Safety Review.

2. D. L. Bernreuter, J. B. Savy, R. W. Mensing, and J. C. Chen. *Seismic Hazard Characterization of 69 Plant Sites East of the Rocky Mountains.* Technical Report NUREG/CR5250, UCID-21517, U. S. Nuclear Regulatory Commission, 1988.

Section 2

SEISMIC HAZARD METHODOLOGY

2.1 INTRODUCTION

This Section describes the methodology used to calculate seismic hazard in this study. It also describes the EPRI/SOG and LLNL methodologies, as background for the present study.

State–of–the–art seismic hazard studies calculate ground–motion exceedance probabilities using earth–science hypotheses about the causes and characteristics of earthquakes in the region being studies. Scientific uncertainty about the causes of earthquakes and about the physical characteristics of potentially active tectonic features lead to uncertainties in the inputs to the seismic hazard calculations. These uncertainties are quantified by using the tectonic interpretations developed by earth scientists familiar with the region. These experts evaluate the likelihood associated with alternative tectonic features and with alternative characteristics of these potential sources.

These and other uncertainties, for example on the ground motion equations, are carried through the entire analysis. The result of the analysis is a suite of hazard curves and their associated weights; these curves quantify the seismic hazard at the site and its uncertainty.

We describe first the basic probabilistic seismic hazard model used to calculate seismic hazard in this study. The specific applications of the EPRI/SOG and LLNL efforts are then described in the context of this basic model.

2.2 BASIC SEISMIC HAZARD MODEL

2.2.1 Overview

The methodology to calculate seismic hazard at a site is well established in the literature (1,2,3,4,5). Calculation of the hazard requires specification of three inputs:

1. Source geometry: the geographic description of the seismic source. A seismic source is a portion of the earth's crust, associated with a tectonic feature (a fault) or with a concentration of historic seismicity, which may be capable of producing earthquakes. Source geometry determines the probability distribution of distance from the earthquake to the site: $f_R(r)$.

2. Seismicity: the rate of occurrence ν_i and magnitude distribution $f_{M(i)}(m)$ of earthquakes within each cell. Magnitude is usually characterized by the moment magnitude scale M_w in California and the Rocky Mountain region, and by the body-wave magnitude m_b in the central and eastern US (CEUS).

3. Attenuation functions: a relationship that allows the estimation of ground motion at the site as a function of earthquake magnitude and distance.

These inputs are illustrated in Figure 2–1, parts a through c. Figure 2–1a shows the geometry of a seismic source. From the source's geometry, $f_{R(i)}(r)$, can be derived. The density function on magnitude $f_{M(i)}(m)$ is either the doubly truncated exponential distribution as shown in Figure 2-1b, or the characteristic magnitude distribution (6). Seismicity for a source or a fault with the exponential magnitude distribution is completely specified by the minimum magnitude m_0 and parameters a and b. Parameter a is a measure of seismic activity, b is a measure of relative frequency of large versus small events, and $\log[\nu_i f_{M(i)}(m)]$ is proportional to $a + b\,m$ for $m_0 < m \leq m_{max}$. For the characteristic magnitude distribution, it is necessary in addition to specify the "characteristic" part of the distribution, i.e. the magnitude range of earthquakes that act in a characteristic way, and the annual rate of occurrence of magnitudes in that range.

The ground motion is modeled by an attenuation function, as illustrated in figure 2-1c. Attenuation functions are usually of the form $\ln[Y] = f(M, R) + \epsilon$, where Y is ground-motion amplitude, M is magnitude, R is distance, and ϵ is a random variable that represents scatter. The attenuation function is used to calculate $G_{Y|m,r}(y) = P[Y > y|m, r]$: the probability that the ground-motion amplitude be larger than y, for given M and R. The seismic hazard contributed by a source is calculated as :

$$\frac{P[Y > y \text{ in time } t]}{t} \simeq \sum_i \nu_i \int\int P[Y > y|m, r]\, f_{M(i)}(m)\, f_{R(i)}(r)\, dm\, dr \qquad (2-1)$$

in which the summation is performed overall all possible earthquake locations i within the source.

2.2.2 Tectonic and Seismicity Interpretations

The specification of potential sources of future earthquakes is the first step in the evaluation of earthquake hazards. Seismic sources indicate where earthquakes may occur; analysis of historical seismicity within those defined sources indicates the probabilities of occurrence

A. Seismic Source i
(Earthquake locations in space lead to a distribution of epicentral distances $f_R(r|m)$

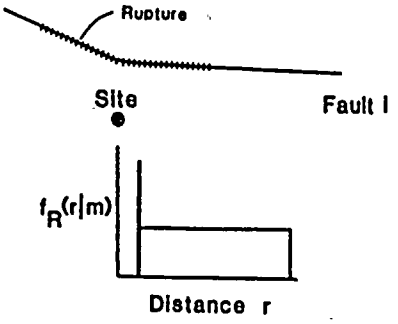

B. Magnitude distribution and rate of occurrence for Source i:

$f_M(m)$, ν_i

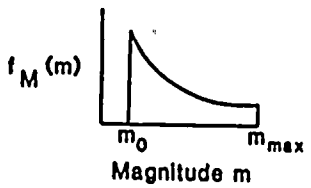

C. Ground motion estimation:

$G_{A|m,r}(a^*)$

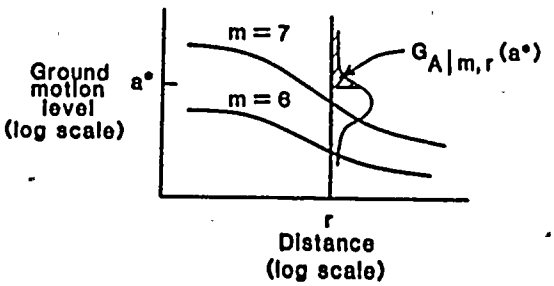

D. Probability analysis:

$$P[A > a^* \text{ in time } t]/t = \sum_i \nu_i \iint G_{A|m,r}(a^*)\, f_M(m)\, f_R(r|m)\, dm\, dr$$

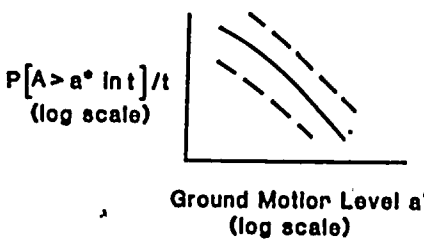

Figure 2-1. Seismic hazard computational model. Source: (7).

and characteristics of future earthquakes (i.e. a magnitude distribution is fit to historical data within the source, once the source is defined).

A seismic source is defined as a region with a single probability of being active, a single magnitude distribution, and a single distribution on maximum magnitude. Within a seismic source the seismicity (quantified by parameters a and b) may vary in space; this generality was used in the EPRI/SOG study, but was not used in the LLNL study and is not used here.

In general, seismic sources are derived based on tectonic features and other evidence (including, in some cases, merely a spatial cluster of historical seismicity). Because of this derivation there is, conceptually, some causal association of earthquakes within a source: they are releasing crustal stresses of the same orientation and amplitude, and/or they are caused by slip on faults with the same general depth, orientation, and sense of slip. Because of these similarities the delineation conforms to the seismic source definition with regard to maximum magnitude and probability of activity.

2.2.3 Seismicity Parameters

Seismicity parameters for earthquake sources are estimated using historical seismicity and other evidence, particularly for identified active faults. Where area sources are used to represent seismicity, earthquake catalogs are analyzed to collect all seismic events that have occurred within each source. For each magnitude level, periods of completeness are picked and the rate of occurrence for that magnitude level is calculated as the number of events divided by the time of complete observation. These data are then fit using the maximum-likelihood procedure (8) to obtain estimates of a and b.

Where slip rates are available on faults (e.g. from paleoseismic studies), they can be converted to rates of seismic activity (e.g. (9)). Also, when the characteristic magnitude distribution is used, the rate of occurrence of events with the characteristic size must generally be estimated using data other than historical seismicity. This is the case because there are few places in the US where a sufficient number of cycles of seismicity have been observed to calculate a rate of characteristic events from observations.

Maximum magnitude distributions are estimated using a combination of techniques. Among these are fault length–magnitude relations, comparison with other regions of similar characteristics, consideration of geophysical characteristics that relate to m_{max}, and consideration of the amount of information known about the region under consideration. Ultimately the choice of m_{max} distribution should be made by analysts familiar with the region.

The choice of minimum magnitude m_0 is based on the characteristics of small earthquakes (i.e. on how damaging are the ground motions associated with these earthquakes), analysis of structural response for the facilities being studied, and field observations of structural performance during low-intensity ground motions. On the basis of these considerations it is concluded that moment magnitude 5.0 is an appropriate minimum magnitude for seismic-hazard calculations for this study (13,14).

2.2.4 Ground Motion Attenuation Equations

Equations estimating seismic ground motion are required for the seismic hazard calculations. These are selected using ground motion studies conducted in the region, available strong motion and seismological data, and inferences from characteristics of earthquakes. Equations are selected for all measures of interest for the study, which typically are peak ground acceleration (PGA) and pseudo-velocity (PSV) for frequencies in the range of 1 to 25 Hz. Ground motion estimates exhibit randomness, and this is characterized in the current study by a standard deviation of ln[ground motion] of 0.5, a common value.

2.2.5 Calculations

Equation 2-1 is formulated using the assumption that earthquakes (most particularly, successive earthquakes) are independent in size and location. In all seismic hazard applications, primary interest is focused on computing probabilities for high (rare) ground motions (as a result, the probability of two exceedances in time t is negligible). Thus, the quantity on the right side of Equation 2-1 — which is the rate of earthquakes with $Y > y$ — is a good approximation to the probability of exceeding amplitude y in time t. The same argument holds when considering hazard at a site from multiple sources. Terms similar to the right hand side of Equation 2-1 are summed to compute, to very good approximation, the total hazard at the site (see Figure 2-1d).

The calculation of hazard from all sources is performed for multiple values of y in order to generate the hazard curve, which gives the annual probability of exceedance as a function of y. This calculation is performed in the current study for 6 different measures of ground motion: PGA and PSV at 5 frequencies (1, 2.5, 5, 10, and 25 Hz, all at 5% damping).

2.2.6 Treatment of Uncertainty

State-of-the-art seismic hazard studies distinguish between two types of variability: randomness and uncertainty. "Randomness" is probabilistic variability that results from natural physical processes. The size, location and time of the next earthquake on a fault and the

details of the ground motion are examples of random events. In concept, these elements cannot be predicted even with collection of additional data, so the randomness component of variability is irreducible. The second category of variability is "uncertainty" which is the statistical or modeling variability that result from lack of knowledge about the true state of nature. In principle, this variability can be reduced with the collection of additional data.

These two types of variability are treated differently in advanced seismic hazard studies, as follows. Integration is carried out over probabilistic variabilities to get a single hazard curve (as indicated by equation 2–1). Modeling uncertainties are expressed by multiple assumptions, hypotheses, or parameter values.

There are uncertainties associated with each of the three inputs to the seismic-hazard evaluation, as follows:

- Uncertainty about seismic sources and faults (i.e., which tectonic features in a region are actually earthquake sources) arises because there are multiple hypotheses about the causes of earthquakes and because there is incomplete knowledge about the physical characteristics of tectonic features. Uncertainty may also arise about the geometry of a seismic source.
- Uncertainty in seismicity is generally divided into uncertainty in maximum magnitude and uncertainty in seismicity parameters a and b. Uncertainty about m_{max}, the maximum magnitude that a given source can generate, arises for the same reasons described above. Estimates of m_{max} are obtained from physical characteristics of the source and from historic seismicity. Uncertainty in seismicity parameters a and b arises from statistical uncertainty and from uncertainty about the accuracy of various catalogs of historical seismicity available with which to estimate parameters. For the characteristic magnitude distribution, additional uncertainties are the magnitude range of the characteristic event, and its annual rate or occurrence.
- Uncertainty in the attenuation functions arises from alternative hypotheses about the dynamic characteristics of earthquakes. This uncertainty often is large, particularly in areas where few direct recordings of strong motion are available.

These multiple interpretations are used to calculate alternative seismic hazard values according to equation 2–1, resulting in a suite of hazard curves. The weight assigned to each seismic hazard curve is calculated from the probabilities given to each of the uncertain inputs used to calculate it; the final weight is calculated as the product of the probabilities of the input variables. From the suite of hazard curves with associated weights, fractile curves or a mean seismic hazard curve are derived.

2.3 EPRI/SOG STUDY OF SEISMIC HAZARD

2.3.1 Development of Seismological Interpretations

This section briefly describes the development of the EPRI/SOG seismic sources and the estimation of their parameters; a complete description is found in Volume 1, Sections 3 and 4, of (10).

Seismic Sources. In the EPRI/SOG methodology, seismic sources have the following characteristics:

- A seismic source is associated with potentially active tectonic features or with a cluster of seismicity.
- The entire source is either active or inactive.
- Every point within the source has the same maximum magnitude.
- The seismic source is composed of individual cells (1 degree latitude by 1 degree longitude). Seismicity parameters a and b may be specified separately for each cell within the source.

The EPRI/SOG seismic sources were developed using a tectonic framework, which was a structured approach to identifying and characterizing tectonic features that may be capable of generating earthquakes. This included interpreting scientific knowledge concerning the causative mechanisms of earthquakes in EUS, delineating seismic sources, and assessing probabilities of activity (P^a) for these sources.

Six Earth Science Teams were used to develop a tectonic framework for the CEUS. In addition to assessing P_a for each seismic source, the teams assessed joint activity probabilities for multiple sources in the same region. In most cases, the Teams specified joint activity probabilities through simple forms of dependence, such as perfect dependence or mutual exclusivity. Activity dependencies have no effect on the mean hazard (because the total hazard is a linear combination of source hazards), but they have an effect on uncertainty. Perfect dependence produces the highest uncertainty, mutual exclusivity produces the lowest uncertainty.

Seismicity Parameters. Seismicity parameters a and b were estimated using the maximum likelihood method. Parameters a and b (especially a) could vary spatially within a seismic

source. For computational convenience, these parameters were assumed to be constant within each 1-degree cell within the source. The degree of spatial variability (or smoothing) of a and b between adjacent cells in each source was controlled by the seismicity option. Each team captured uncertainty on the appropriate degree of smoothing for each source (i.e., whether the source has homogeneous seismicity or has activity rates that follow the within-source pattern of historic activity) by specifying alternative seismicity options, with associated probabilities. In addition, the teams could specify a prior distribution (in the Bayesian sense) on b, and other parameters of the estimation algorithm, with each seismicity option.

Maximum Magnitudes. To calculate seismic hazard at a site, the largest possible earthquake magnitude that can occur in each seismic source must be estimated. This maximum magnitude m_{max} is generally uncertain. This uncertainty is represented by a probability distribution on the maximum magnitude that the source can generate.

Each team in the EPRI/SOG study estimated a probability distribution of m_{max} for each active source that the team had identified. The following considerations were used to constrain the maximum-magnitude estimates:

- Physical Constraints. These approaches related m_{max} to the size of the source or the thickness of the earth's crust.
- Historic Seismicity. These approaches involved the addition of an increment to the maximum historical magnitude, extrapolation of the magnitude-recurrence relation to some justified frequency of occurrence, and the statistical treatment of the earthquake catalog.
- Analogies With Other Sources or Regions. If one is able to identify a number of analogous sources, so that one can assume that they all have the same value of m_{max}, one can improve the precision of m_{max} estimates obtained from statistical analyses. The analyses of earthquakes in other intraplate regions of the world is another way to increase sample size. A study of this type was performed by EPRI (11,12); m_{max} values were obtained for various types of tectonic features.

The EPRI/SOG methodology used discrete distributions to represent uncertainty in m_{max}. When a team specified continuous distributions or discrete distributions with excessive numbers of values, equivalent discrete distributions were developed.

Minimum Magnitude. The minimum magnitude m_0 introduced in Section 2.2 represents the smallest magnitude of interest in the hazard calculations. It is assumed that earthquakes with magnitudes lower than m_0 are incapable of causing damage. Therefore, the choice of m_0 is related to the type of facility being analyzed.

As mentioned above, the EPRI/SOG study used body–wave magnitude m_b as the magnitude measure of interest, because seismological studies in the CEUS use m_b and this value is listed in most earthquake catalogs of the region. The EPRI/SOG methodology used m_b 5.0 as the minimum magnitude. This value was considered sufficiently conservative because of the small probability that an earthquake with $m_b < 5.0$ could cause damage to an engineered structure.

2.3.2 Ground–Motion Attenuation

The EPRI/SOG study used attenuation functions to predict six measures of rock-site ground motions: peak acceleration and spectral velocities at five frequencies. Three sets of attenuation functions, with associated weights, characterized uncertainty in ground-motion predictions. The NRC has indicated acceptance of these attenuation functions for computations of seismic hazard in the CEUS (15).

The attenuation functions used in the EPRI/SOG seismic-hazard calculations are based on simplified physical models of energy release at the seismic source and of wave propagation. The model of energy release describes the Fourier spectrum and duration of shaking at a hypothetical site close to the earthquake, and how these vary with seismic moment (seismic moment is a measure of earthquake size). The model of wave propagation describes how the spectrum and duration of shaking vary as the waves travel through the crust. This model contains the effects of geometric spreading (including *Lg* waves at longer distances), anelastic attenuation, and dispersion. The combined predictions of these models are consistent with seismograph and accelerograph data from the region.

Uncertainty on attenuation functions arises from uncertainty on the parameters of these models and on the derivation of peak time-domain amplitudes from Fourier spectra. The most important of these are uncertainty on source scaling, on the magnitude-moment relation, and on the spectra to time-domain derivation. These uncertainties are captured by considering three alternative formulations of these models, as follows:

1. The attenuation functions obtained by McGuire et al. (16) using an ω-square model with stress drop of 100 bars. This set of attenuation functions is assigned a weight of 0.5.

2. The attenuation functions obtained by Boore and Atkinson (17) using an ω-square model. This set of attenuation functions is assigned a weight of 0.25.

3. The attenuation function obtained from the velocity and acceleration attenuation equations obtained by Nuttli (18) using the "increasing stress-drop" assumption coupled with the dynamic amplification factors by Newmark and Hall (19). The attenuation functions in (18) were derived using a procedure analogous to that of Herrmann and Nuttli (20). This set of attenuation functions is given a weight of 0.25.

Estimation of dynamic soil effects on ground motion was made in the EPRI/SOG study through the use of generic soil categories. These SOG soil amplification factors were developed using an approach analogous to that implemented in the program SHAKE. The rock-motion input to the analysis was specified as a random process with frequency content typical of ground motions in the CEUS [see (16)].

The standard soil profile was chosen to be consistent with the generally stiff soils typical of the CEUS (see Figure 2–2). The profile was based on the sand-like and till-like profiles established by Bernreuter et al. (5). Amplification factors were calculated for five depth categories, as defined in Table 2–1. The modulus reduction and damping curves are shown in Figure 2–3.

Table 2-1

Soil Categories and Depth Ranges

Category	Depth (ft)	Range (ft)
I	20	10–30
II	50	30–80
III	120	80–180
IV	250	180–400
V	500	>400

Soil amplification factors were computed as the ratio of 5% damping response spectral acceleration (Sa) computed at the surface of each site to 5% damping response spectral acceleration (Sa) computed for the surface bedrock motion. In addition, both peak acceleration and peak ground velocity were computed for the site and surface bedrock. Levels of input motion

(rock outcrop) of 0.1, 0.3, 0.5, 0.75, and 1.0 g were used to accommodate effects of material nonlinearity upon soil response. Figures 2-4 through 2-9 show the calculated amplification factors for peak acceleration and spectral velocities. Additional details on the development of these amplification factors are available in Section 6 of (16).

2.3.3 Treatment of Uncertainty

The EPRI/SOG methodology quantified seismic hazard and its uncertainty by using as inputs the tectonic interpretations developed by six multidisciplinary Earth-Science Teams. In addition, each team quantified its uncertainty about seismic sources, maximum magnitudes, and seismicity parameters, as follows:

- Uncertainty about seismic sources was characterized by specifying an activity probability P^a to each seismic source and specifying activity dependencies among sources in the same region.
- Uncertainty about maximum magnitude was characterized by a discrete distribution of m_{max} for each source. That is, multiple values of m_{max} were specified and given weights.
- Uncertainty about seismicity parameters was characterized by considering multiple sets of parameter values of each source, and assigning weights to them. Each set of parameters represented, for instance, different assumptions about spatial continuity of a and b, or different portions of the earthquake catalog.

Ground-motion attenuation in the CEUS, and its uncertainty, was quantified by considering three alternative attenuation functions for each ground-motion measure, and giving them weights (see above). The development and selection of these attenuation equations was documented in (16) and in Appendix A of (7).

In order to organize and display the multiple hypotheses, assumptions, parameter values and their possible combinations, a logic tree approach was used in the EPRI/SOG study. Logic trees are a convenient means to express alternative interpretations and their probabilities. Each level of the logic tree represents one source of uncertainty. The branches emanating from one node represent possible values of a parameter. The probability assigned to a branch represents the likelihood of the parameter value associated with that branch, given certain values of the preceding parameters.

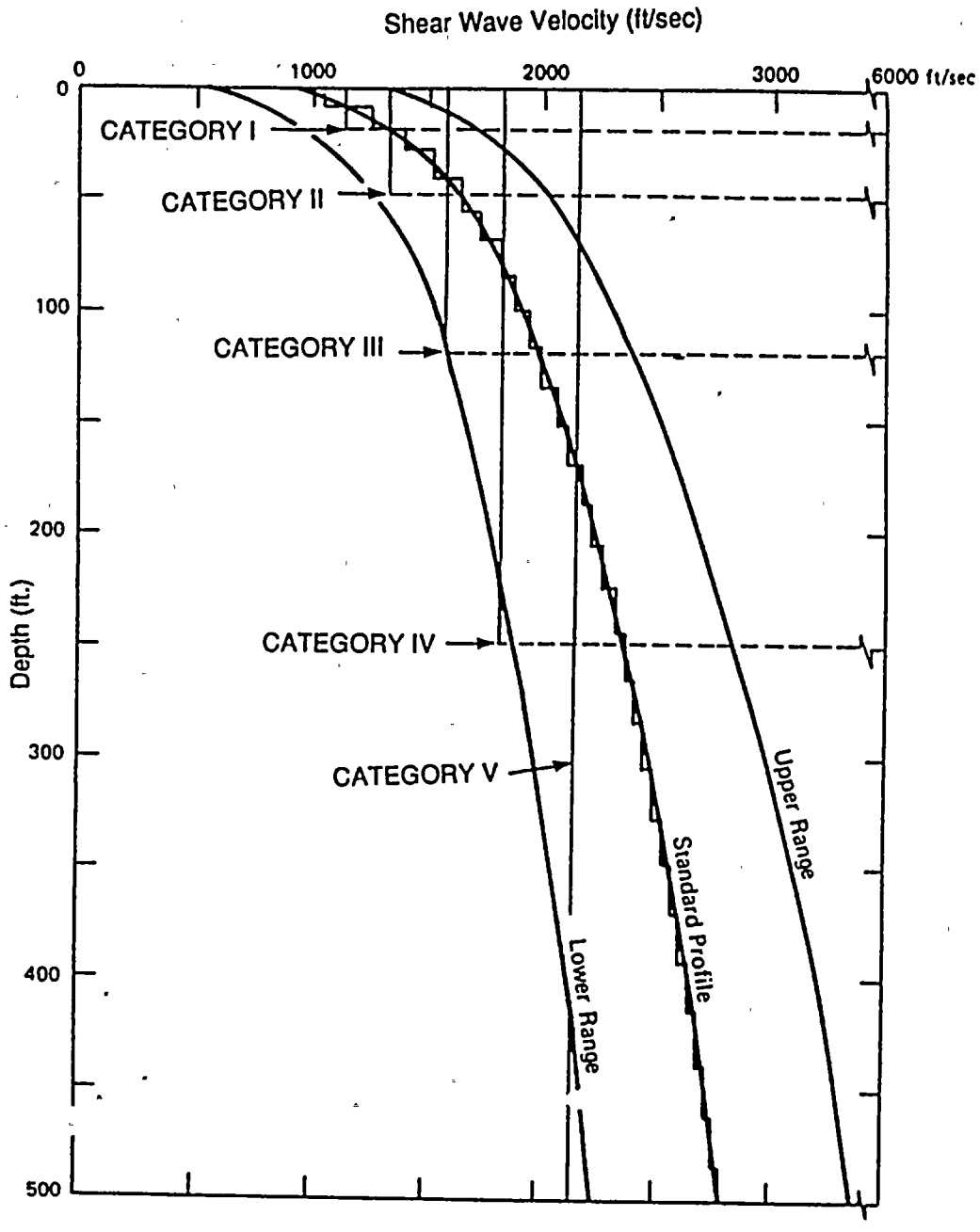

Figure 2-2. Standard soil profile for sand-like Central and Eastern United States sites (gradient). Soil categories I–V are indicated by their respective soil column depths. See Table 2–1 for definition of the soil categories.

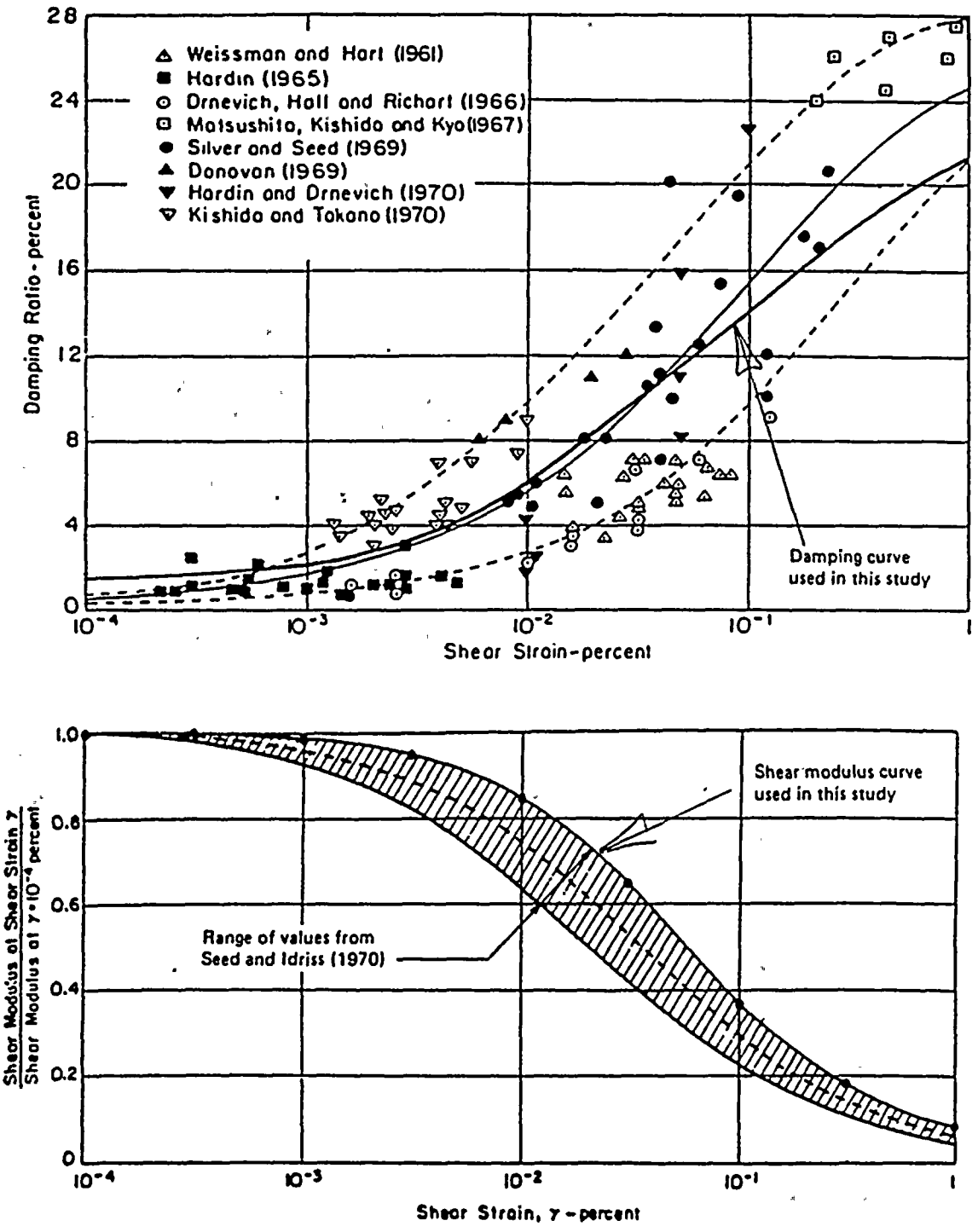

Figure 2-3. Shear-strain dependency of shear-wave damping and shear modulus (from Seed and Idriss).

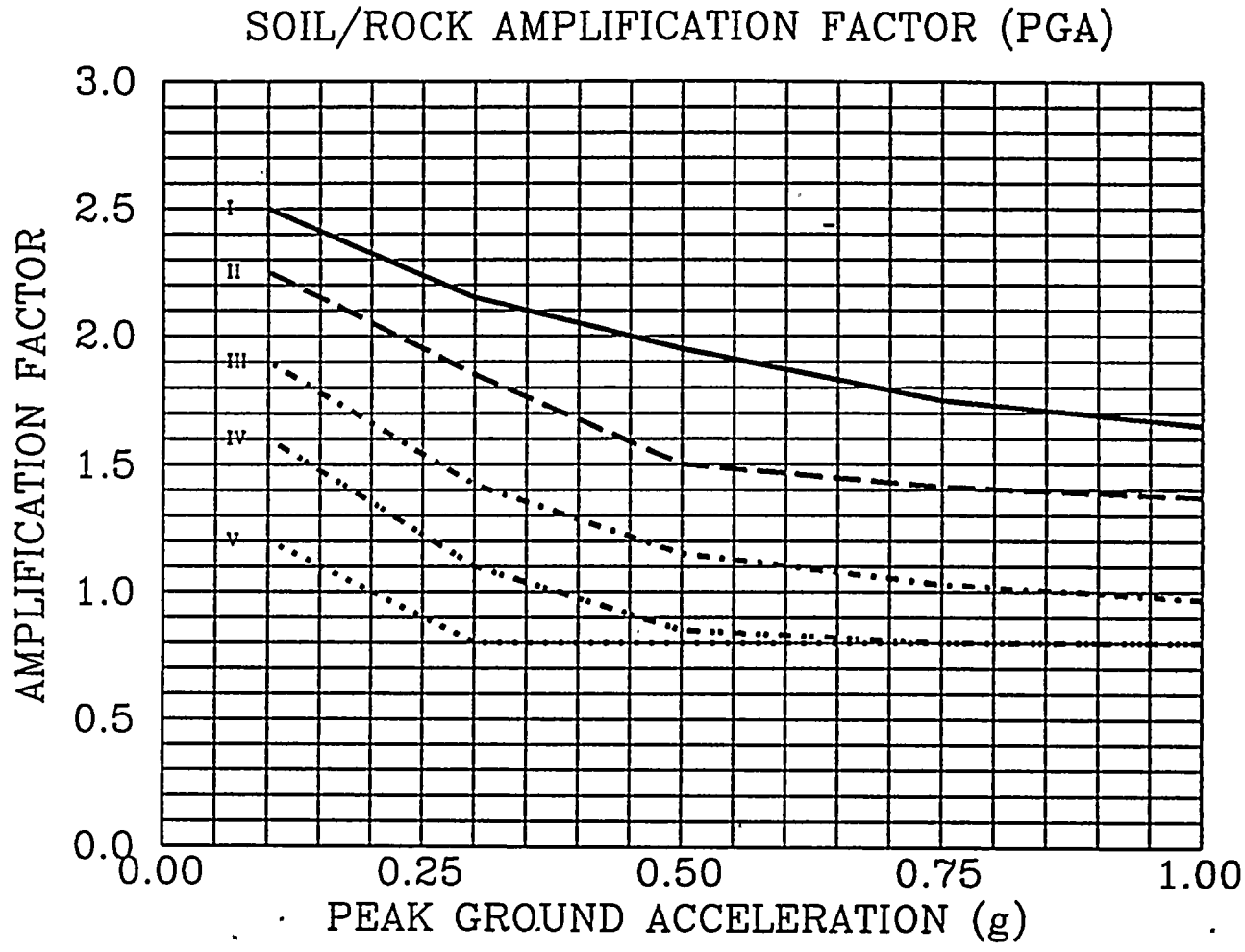

Figure 2-4. Soil amplification factors for peak ground acceleration, for the 5 soil categories. See Table 2–1 for the definition of soil categories.

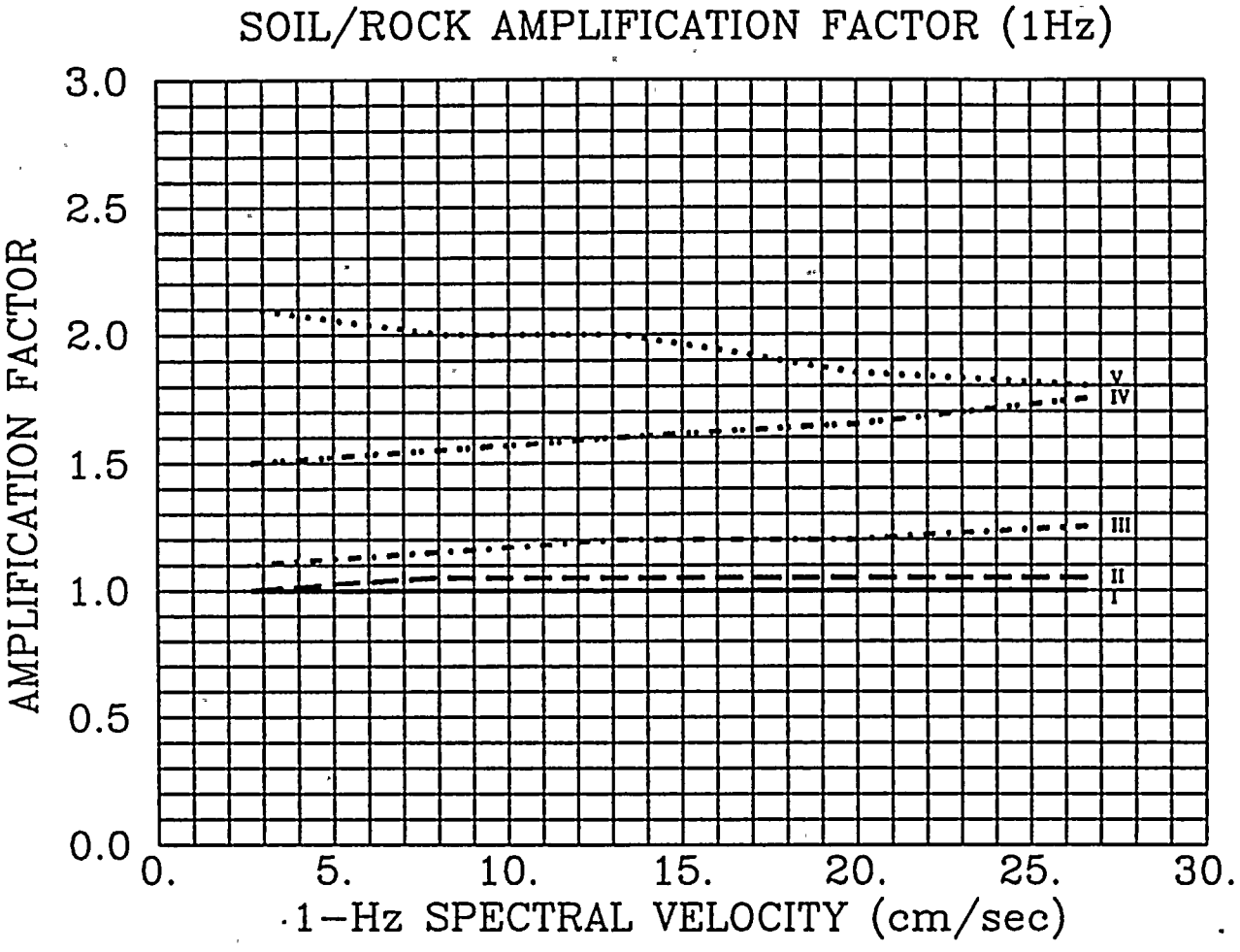

Figure 2-5. Soil amplification factors for 1-Hz spectral velocity (5% damping), for the 5 soil categories. See Table 2–1 for the definition of soil categories.

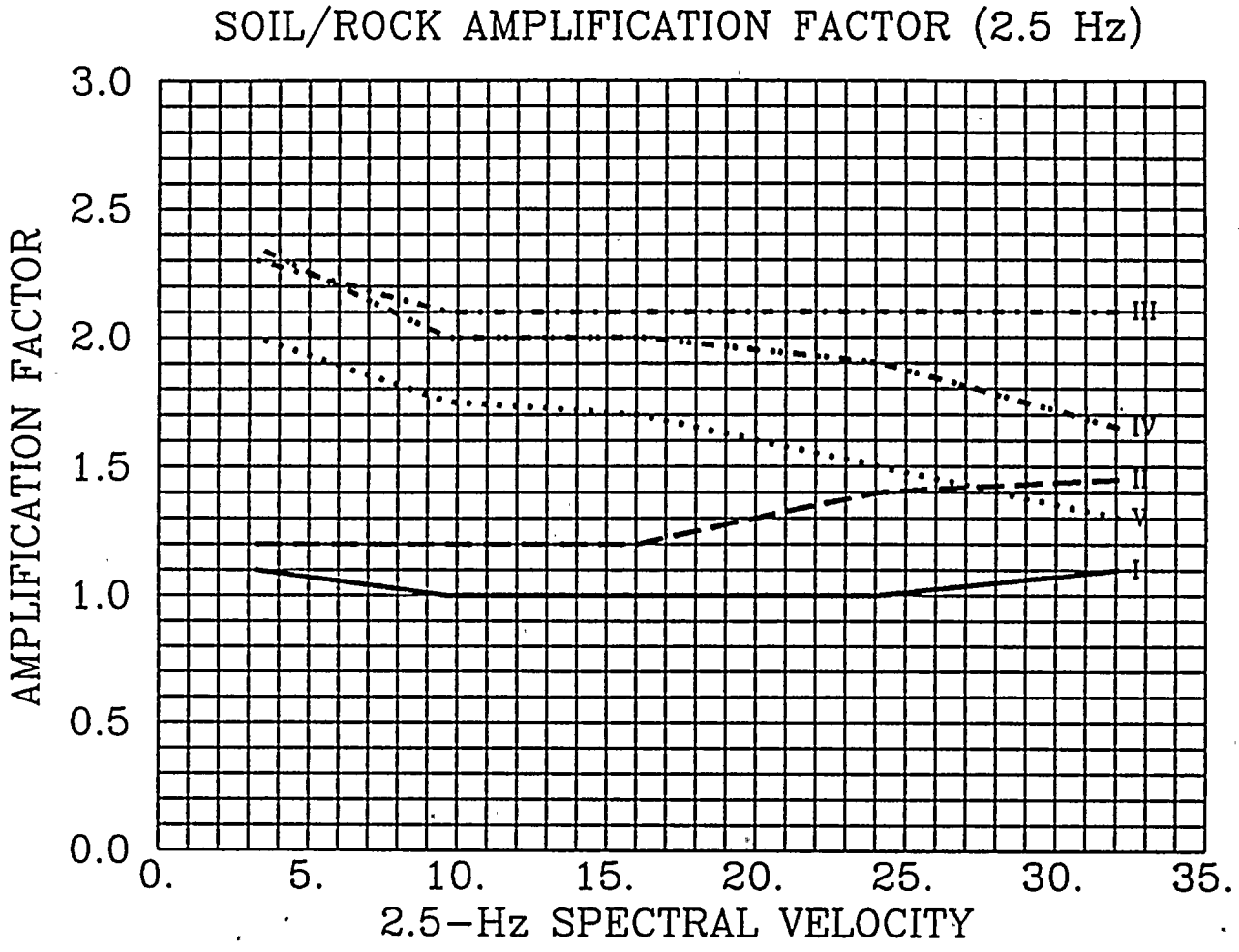

Figure 2-6. Soil amplification factors for 2.5-Hz spectral velocity (5% damping), for the 5 soil categories. See Table 2–1 for the definition of soil categories.

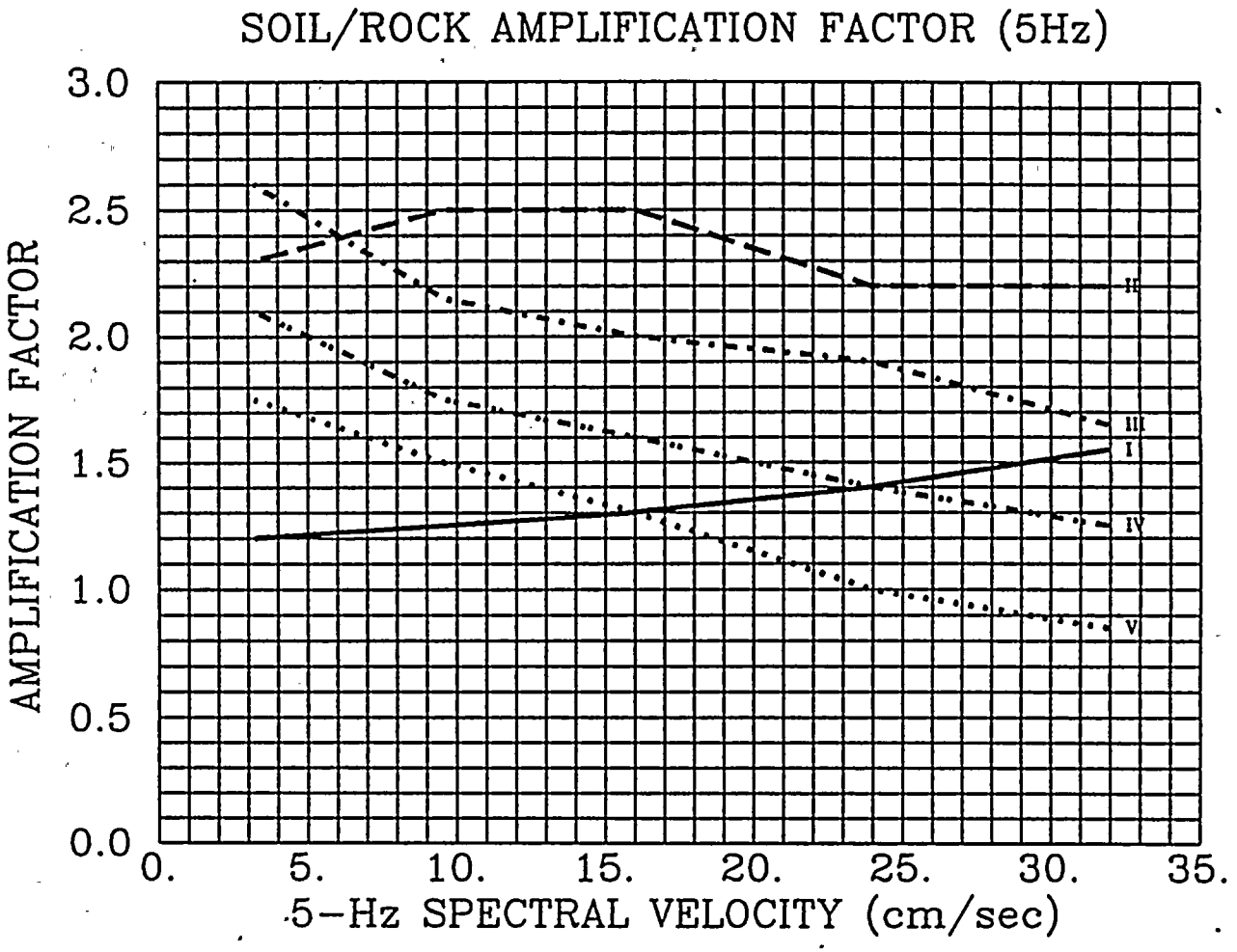

Figure 2-7. Soil amplification factors for 5-Hz spectral velocity (5% damping), for the 5 soil categories. See Table 2-1 for the definition of soil categories.

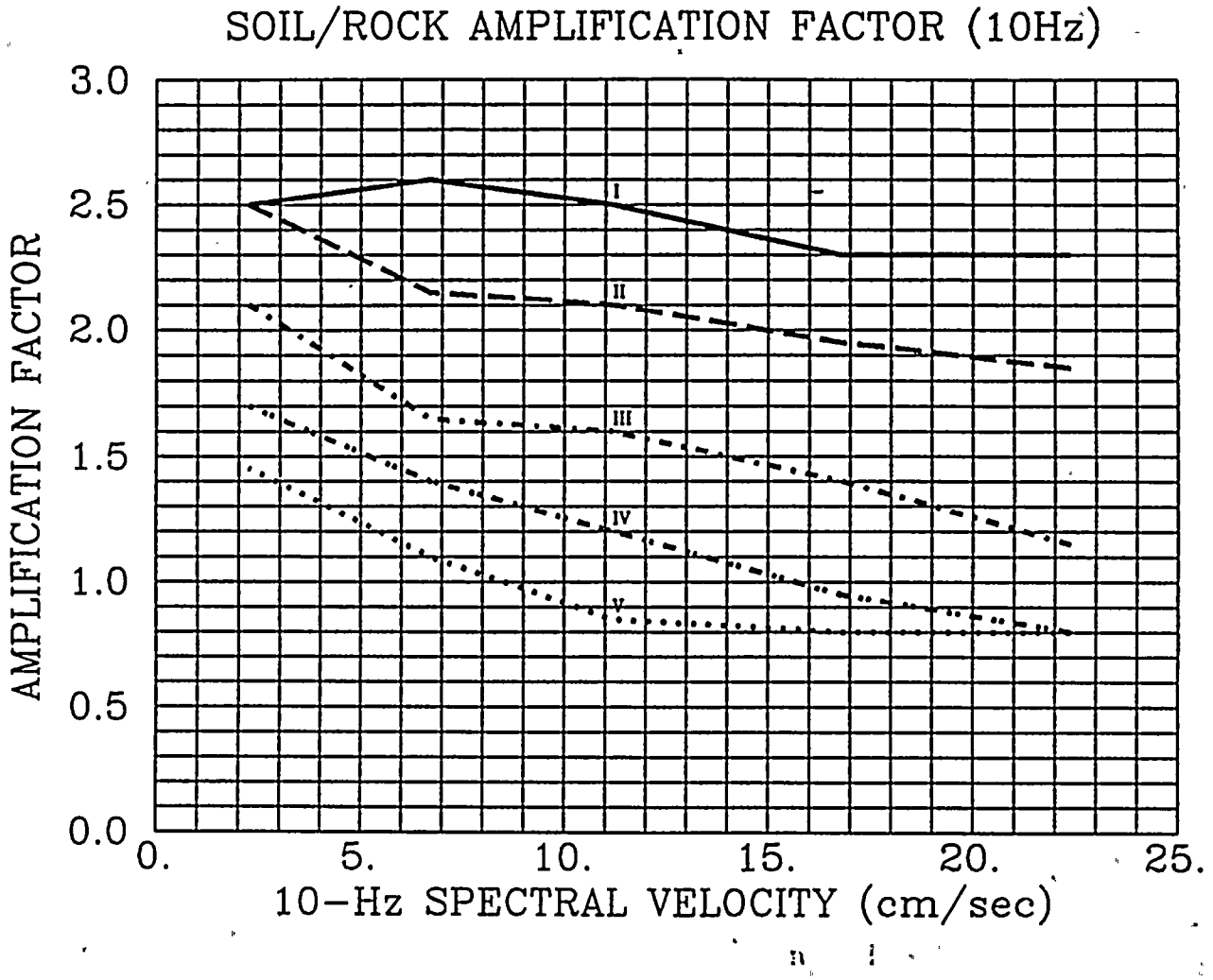

Figure 2-8. Soil amplification factors for 10-Hz spectral velocity (5% damping), for the 5 soil categories. See Table 2–1 for the definition of soil categories.

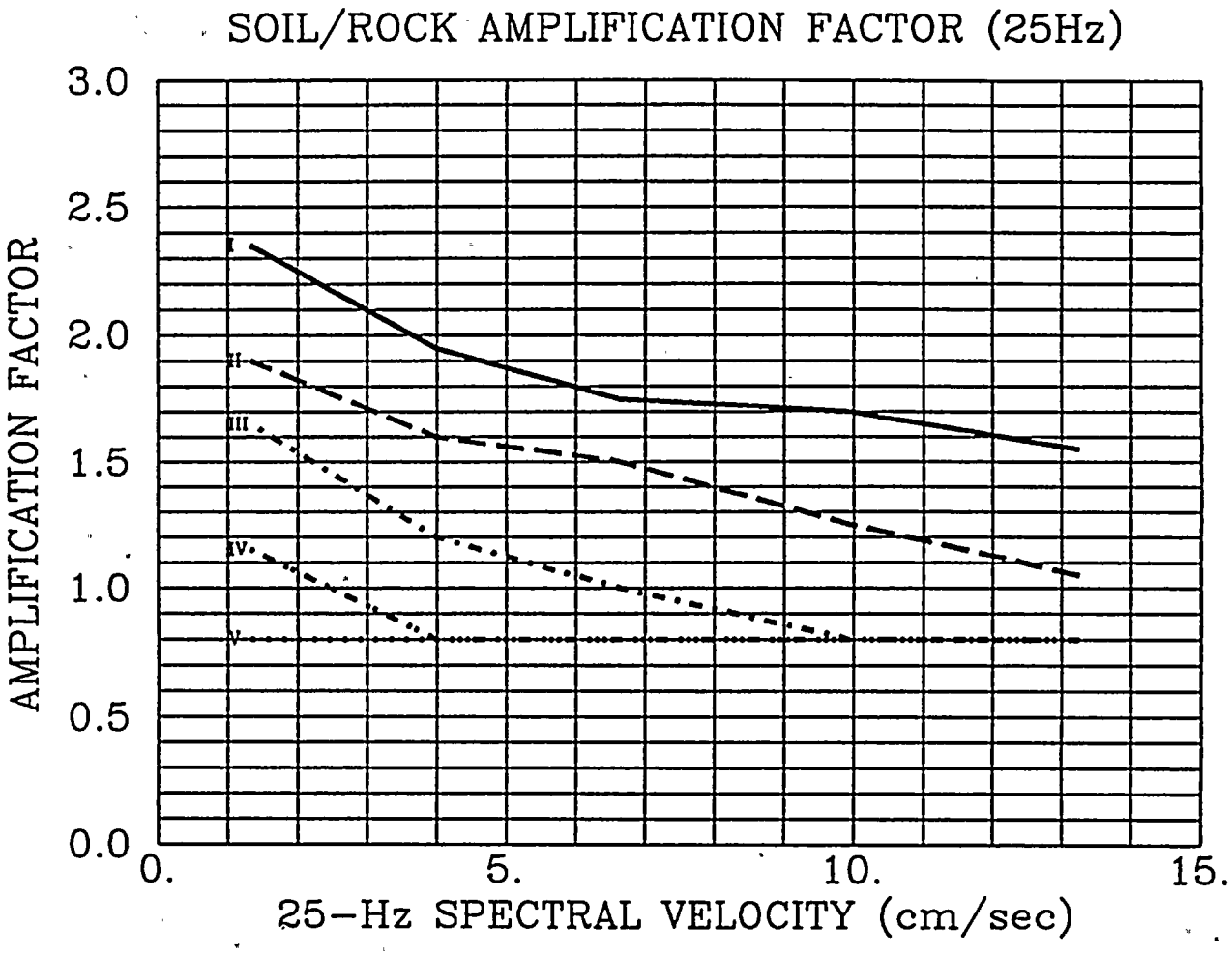

Figure 2-9. Soil amplification factors for 25-Hz spectral velocity (5% damping), for the 5 soil categories. See Table 2–1 for the definition of soil categories.

The logic tree in Figure 2–10 illustrates the treatment of parameter uncertainty in the EPRI/SOG methodology, for one team. Associated with each terminal node, there is one hazard curve, which corresponds to certain sources being active, each active source having a certain m_{max} and certain seismicity parameters, and a certain attenuation function being the true attenuation model. The probability associated with that end branch is the product of the probabilities of all branches traversed to reach that terminal node.

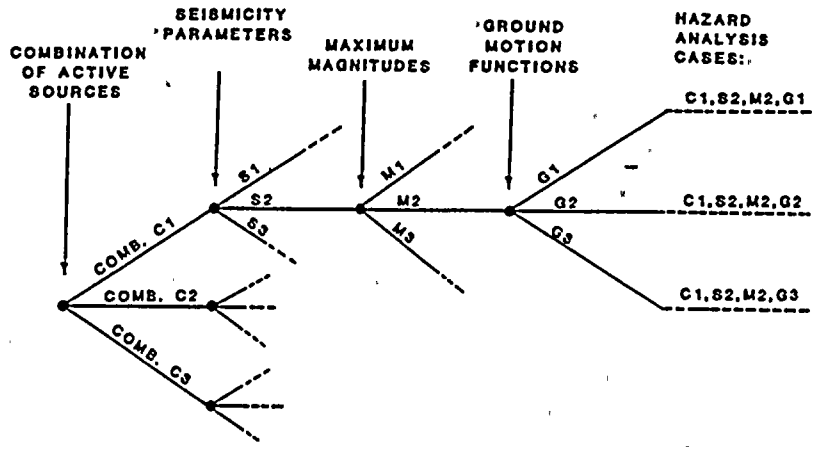

Figure 2-10. Logic tree representation of uncertain parameters in the EPRI/SOG methodology

The hazard curves obtained by the 6 teams were given equal weights in the EPRI/SOG study and then were combined. The resulting family of hazard curves and their associated probabilities, corresponding to all end branches of the six teams' logic trees, contained all the information about seismic hazard at the site, its uncertainty, and the different contributors to that uncertainty.

2.4 LLNL STUDY OF SEISMIC HAZARD

The LLNL study of seismic hazards in the CEUS culminated a decade of effort funded by the U.S. Nuclear Regulatory Commission to characterize earthquake sources, seismicity parameters, and ground motion estimates for the region. Two panels of experts were formed. Eleven seismicity experts familiar with the region were polled for interpretations of seismic sources and ground motion parameter values, and five ground motion experts were polled for opinions on appropriate attenuation equations to estimate PGA and response spectrum amplitudes.

Uncertainties in the interpretations were represented by discrete and continuous distributions, and uncertainty in the seismic hazard was derived by Monte Carlo sampling of the

input distributions, producing a seismic hazard curve for each set of simulated variables and thus representing the uncertainty in the seismic hazard as a function of uncertainty in expert interpretation.

2.4.1 Seismicity Interpretations

The eleven seismicity experts provided sets of seismic sources for the CEUS. These were generally in the form of a single set of seismic sources for the entire CEUS. Some LLNL experts also specified alternative geometries of sources. By contrast to the EPRI study, which specified uncertainty on the seismic activity of each source separately, the LLNL experts specified global alternatives for sets of sources that might be active simultaneously.

Seismicity parameters (rates of activity and Richter *b*-values) for the sources were provided by the seismicity experts, although the LLNL team made available the results of calculations of these parameters using a standard method and an earthquake catalog specified by the expert. Distributions and correlations were also specified to represent the uncertainty of these parameters. In addition, the distribution of maximum possible earthquake size was specified for each source by each expert. (Most of them used magnitude to characterize earthquake size; one used MM intensity, and a second used a combination of the two.)

2.4.2 Ground-Motion Attenuation

Five earth scientists and engineers were asked to derive ground motion estimation equations for the EUS for the LLNL study. These equations were to estimate PGA and response spectrum amplitude as a function of earthquake magnitude and distance. Estimating such equations for the CEUS is problematic because of the lack of recorded strong earthquake motions in the area with which to calibrate empirical techniques or validate theoretical models. Any method thought to be adequate by the five experts was acceptable. The five participants were asked to specify uncertainty in their choice of ground motion equations by designating multiple models with subjective weights.

One set of models—the models selected by ground-motion Expert 5—gives substantially higher ground motion estimates than the others for PGA and response spectrum amplitudes. This set of models was derived by a combination of two equations, the first a correlation between PGA and MM intensity published by Trifunac from California data, and the second an MM intensity attenuation equation published by Gupta and Nuttli. This selection, and the corresponding models for spectral velocity, received 100% weight from LLNL Expert 5, and zero weight from the other panelists. Comparing the predictions from this equation to data available from EUS seismographs and accelerographs indicates that the method severely

over-estimates ground motions in the CEUS, particularly at distances greater than 20 km from the earthquake source. (See Figures 5–123 through 5–125 of (21) for these comparisons.) As a result of this over–estimation, results of this method have received less emphasis than results from the other four LLNL experts.

2.4.3 Site Amplification Factors

LLNL developed generic site amplification factors using a modeling approach similar to that used by EPRI/SOG. The two main differences between the LLNL and EPRI/SOG computations are as follows: (1) LLNL did not consider soil nonlinearity, and (2) LLNL used input ground motions typical of the western United States. Additional details on the LLNL site-amplification factors are contained in (22); comparisons of the LLNL and EPRI/SOG amplification factors are contained in (21). In the LLNL methodology, a site is assigned to one of the ten soil categories based on its depth to bedrock and shear-wave velocity.

Four of the five LLNL ground-motion experts adopted the above site-amplification factors. Ground-motion Expert 5 selected a different set of amplification factors, which are used in connection with this expert's attenuation functions.

2.4.4 Calculations

A Monte Carlo simulation procedure was used by LLNL to express uncertainty in seismic hazard as a function of uncertain input. There were 55 possible combinations of the eleven seismicity experts and the five ground motion experts, and each combination was considered separately. For each combination, 50 simulations of uncertain parameters were made, drawing from the distributions on seismicity parameters, ground motion equations, and attenuation randomness terms specified by each expert. This resulted in 2750 combinations of parameters from which a family of 2750 seismic hazard curves could be calculated. Each of these seismic hazard curves was then assigned a weight based on a self-weighting provided by the experts. This led to an uncertainty distribution on the frequency of exceedance for any PGA or PSV level, from which fractiles of seismic hazard could be computed and plotted as fractile seismic hazard curves.

2.5 REFERENCES

1. C. A. Cornell. "Engineering Seismic Risk Analysis". *Bulletin of the Seismological Society of America*, 58(5):1583–1606, October 1968.

2. C. A. Cornell. *Dynamic Waves in Civil Engineering*, chapter 27: "Probabilistic Analysis of Damage to Structures under Seismic Loads". Wiley Interscience, 1971.

3. A. Der Kiureghian and A. H. S. Ang. *A Line Source Model for Seismic Risk Analysis.* Technical Report UILU-ENG-75-2023, Univ. of Illinois, October 1975. pp. 134.

4. R. K. McGuire. *FORTRAN Computer Program for Seismic Risk Analysis.* Open File Report 76-67, U. S. Geological Survey, 1976. pp. 1-90.

5. D. L. Bernreuter, J. B. Savy, R. W. Mensing, J. C. Chen, and B. C. Davis. *Seismic Hazard Characterization of the Eastern United States.* Technical Report LLNL UCID-20421, Volumes 1 and 2, Lawrence Livermore National Laboratory, Livermore, Ca., 1985.

6. D. Schwartz and K. J. Coppersmith. "Fault Behavior and Characteristic Earthquakes: Examples from the Wasatch and San Andreas Fault Zones". *Journal of Geophysical Research*, 89:5681–5698, 1984.

7. R. K. McGuire, G. R. Toro, J. P. Jacobson, T. F. O'Hara, and W. J. Silva. *Probabilistic Seismic Hazard Evaluations in the Central and Eastern United States: Resolution of the Charleston Earthquake Issue.* Special Report NP-6395-D, Electric Power Research Institute, April 1989.

8. D. H. Weichert. "Estimation of the Earthquake Recurrence Parameters for Unequal Observations Periods for Different Magnitudes". *Bulletin of the Seismological Society of America*, 70:1337–1346, 1980.

9. K. M. Shedlock, R. K. McGuire, and D. G. Herd. *Earthquake Recurrence in the San Francisco Bay Region, California, from Fault Slip and Seismic Moment.* Open-File Report, US Geological Survey, 1980. pp. 80-999.

10. *Seismic Hazard Methodology for the Central and Eastern United States.* Technical Report NP-4726-A, Electric Power Research Institute, July 1986. Revised, 1988. Vol. 1, Part 1: Methodology, Vol. 1, Part 2: Theory, Vol. 2: EQHAZARD Programmer's Manual, Vol. 3: EQHAZARD User's Manual, Vol. 4: Applications, Vols. 5 through 10: Tectonic Interpretations, Vol. 11: Nuclear Regulatory Commission Safety Review.

11. K. J. Coppersmith, A. C. Johnston, and W. J. Arabasz. "Assessment of Maximum Earthquake Magnitudes in the Eastern United States". *Earthquake Notes*, 57–1:12, 1986.

12. A. C. Johnston, A. G. Metzger, K. J. Coppersmith, and W. J. Arabasz. "A Systematic Global Overview of Large Intraplate Earthquakes". *Earthquake Notes*, 57–1:12, 1986.

13. M. W. McCann and J. W. Reed. *Selection of a Lower Bound Magnitude for Seismic Hazard Assessment.* Technical Report, Electric Power Research Institute, Palo Alto, California, 1988.

14. M. W. McCann and J. W. Reed, editors. *Engineering Characterization of Small-Magnitude Earthquakes*, Electric Power Research Institute, Palo Alto, California, 1988.

15. L. Reiter. EPRI Ground Motion Models for Eastern North America. NRC Letter to R.A. Thomas, August 3, 1988.

16. R. K. McGuire, G. R. Toro, and W. J. Silva. *Engineering Model of Earthquake Ground Motion for Eastern North America.* Technical Report NP-6074, Electric Power Research Institute, 1988.

17. D. M. Boore and G. M. Atkinson. "Stochastic Prediction of Ground Motion and Spectral Response Parameters at Hard-Rock Sites in Eastern North America". *Bulletin of the Seismological Society of America*, 77(2):440–467, 1987.

18. O. W. Nuttli. Letter dated September 19, 1986 to J. B. Savy. Reproduced in: D. Bernreuter, J. Savy, R. Mensing, J. Chen, and B. Davis. *Seismic Hazard Characterization of 69 Nuclear Plant Sites East of the Rocky Muntains: Questionnaires.* U. S. Nuclear Regulatory Commission, Technical Report NUREG/CR-5250, UCID-21517, Volume 7, 1989. Prepared by the Lawrence Livermore National Laboratory.

19. N. M. Newmark and W. J. Hall. *Earthquake Spectra and Design.* Earthquake Engineering Research Institute, Berkeley, CA, 1982.

20. R. B. Herrmann and O. W. Nuttli. "Strong Motion Investigations in the Central United States". In *Proceedings: 7th World Conference on Earthquake Engineering, Istanbul*, pp. 533–536, 1980.

21. R. K. McGuire, G. R. Toro, and W. J. Silva. *Probabilistic Seismic Hazard Evaluations in the Central and Eastern United States — Appendix A: Model of Earthquake Ground Motion for the Central and Eastern United States.* Technical Report, Electric Power Research Institute, 1989. EPRI Project RP101-53, prepared by Risk Engineering, Inc.

22. D. L. Bernreuter, J. B. Savy, R. W. Mensing, and J. C. Chen. *Seismic Hazard Characterization of 69 Plant Sites East of the Rocky Mountains.* Technical Report NUREG/CR5250, UCID-21517, U. S. Nuclear Regulatory Commission, 1988.

Section 3
SEISMIC SOURCES

3.1 OVERVIEW

This Section describes the seismic sources derived in this study for calculation of seismic hazard at the PVNGS. Two teams of earth science experts were used in the study for this phase. The Geomatrix Consultants, Inc. ("Geomatrix") team was lead by R. Youngs and included K. Coppersmith and R. Perman. The J.M. Montgomery Consulting Engineers, Inc. ("JMM") team was lead by J. Scott and included D. West and B. Schell. Each team provided interpretations of seismic sources and seismicity parameters for possible sources of earthquakes within 300 km of the PVNGS. This distance includes the southern section of the San Andreas Fault, which is a possible contributor to hazard for low frequencies and low probabilities, because of the large magnitude earthquakes that might be generated. A summary of each team's results are presented here; details are given in Appendices A and B.

3.2 GEOMATRIX SOURCES

The Geomatrix team identified twenty-seven potential sources of seismicity within 300 km of the PVNGS, including seventeen seismogenic zones and ten faults. These sources are shown in Figure 3-1. For each of these sources a probability of activity is specified, as shown in Table 3-1. These probabilities were based on historical and instrumental activity, tectonics of the southern Basin and Range province, knowledge of active faults mapped in the region, and other factors. Details of these considerations are given in Appendix A. For each of these sources, seismicity parameters have been calculated as specified in Section 4.

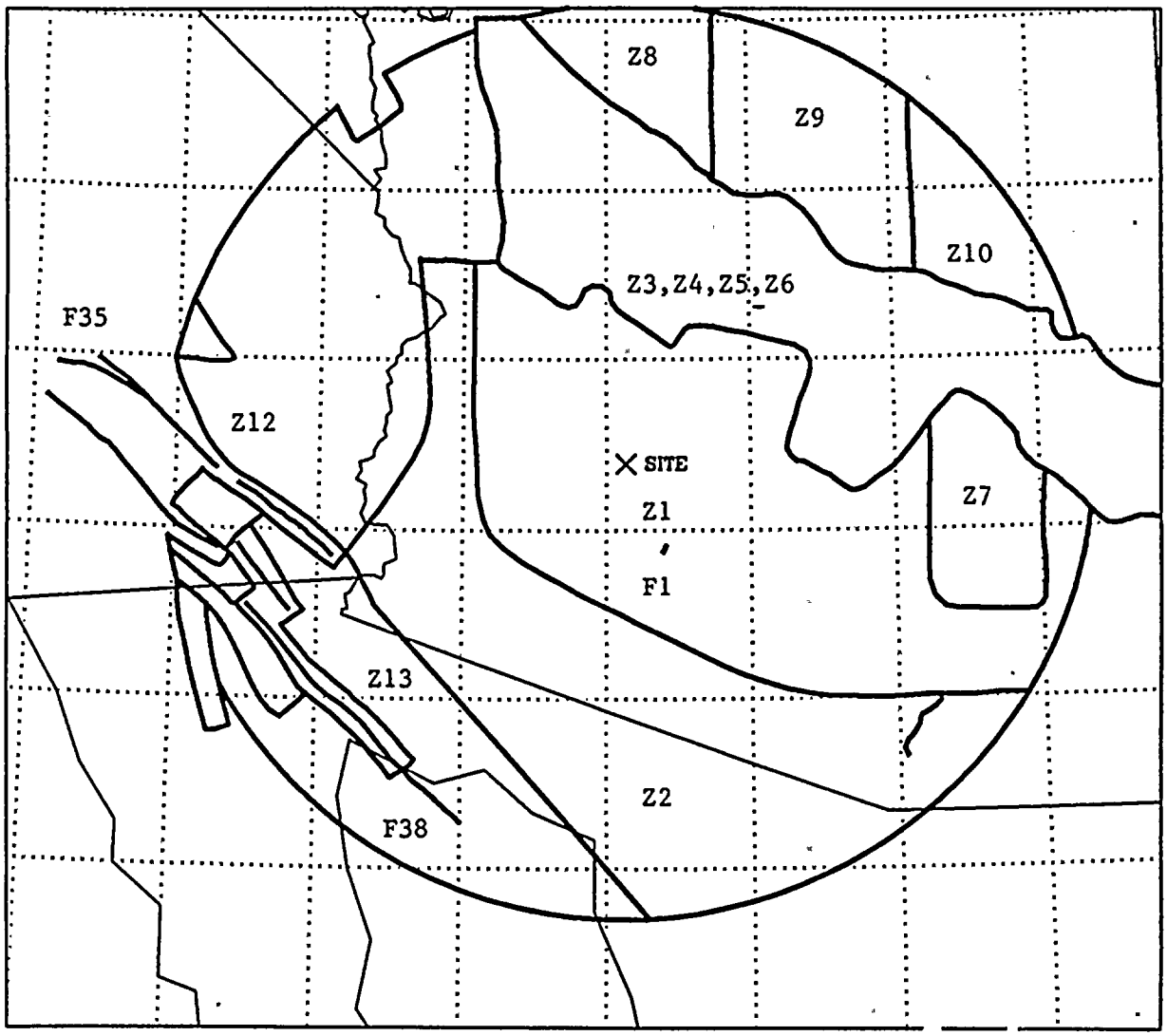

Figure 3-1. Seismic Sources for Geomatrix Team.

Table 3-1

Probabilities of Activity for Geomatrix Team Sources

Type	No.	Source	Prob. of Activity
Zone	Z1	Zone 1	1.0
Zone	Z2	Zone 2	1.0
Zone	Z3	Zone 3	1.0
Zone	Z4	Zone 4	0.3
Zone	Z5	Zone 5	0.3
Zone	Z6	Zone 6	0.3
Zone	Z7	Zone 7	1.0
Zone	Z8	Colorado Plateau	1.0
Zone	Z9	Colorado Plateau	1.0
Zone	Z10	Colorado Plateau	1.0
Zone	Z11+Z12	Southern Basin & Range	1.0
Zone	Z13	Salton Trough/Gulf of Calif.	1.0
Zone	Z14	Pinto Mtn. Faults	1.0
Zone	Z17	Imperial/San Andreas Stepover	1.0
Zone	Z22	Laguna Salada	1.0
Zone	Z23	Sierra Juarez	1.0
Zone	Z24	No. Exten. of Cerro Prieto	0.5
Fault	F1	Sand Tank	1.0
Fault	F4	Santa Rita	1.0
Fault	F35	San Andreas	1.0
Fault	F36	Sand Hills	0.30
Fault	F37	Imperial	1.0
Fault	F38	Cerro Prieto	1.0
Fault	F41	San Jacinto	1.0

3.3 JMM SOURCES

The JMM Team sources are illustrated in Figure 3–2 for the 300 km region around the PVNGS site. They consist of eleven seismogenic zones and twenty–three faults. These also were derived considering historical and instrumental seismicity, the tectonics of the Basin and Range province, and other factors, as described in Appendix B. The probabilities of activity of these sources are listed in Table 3–2; details of how these probabilities were derived are described in Appendix B.

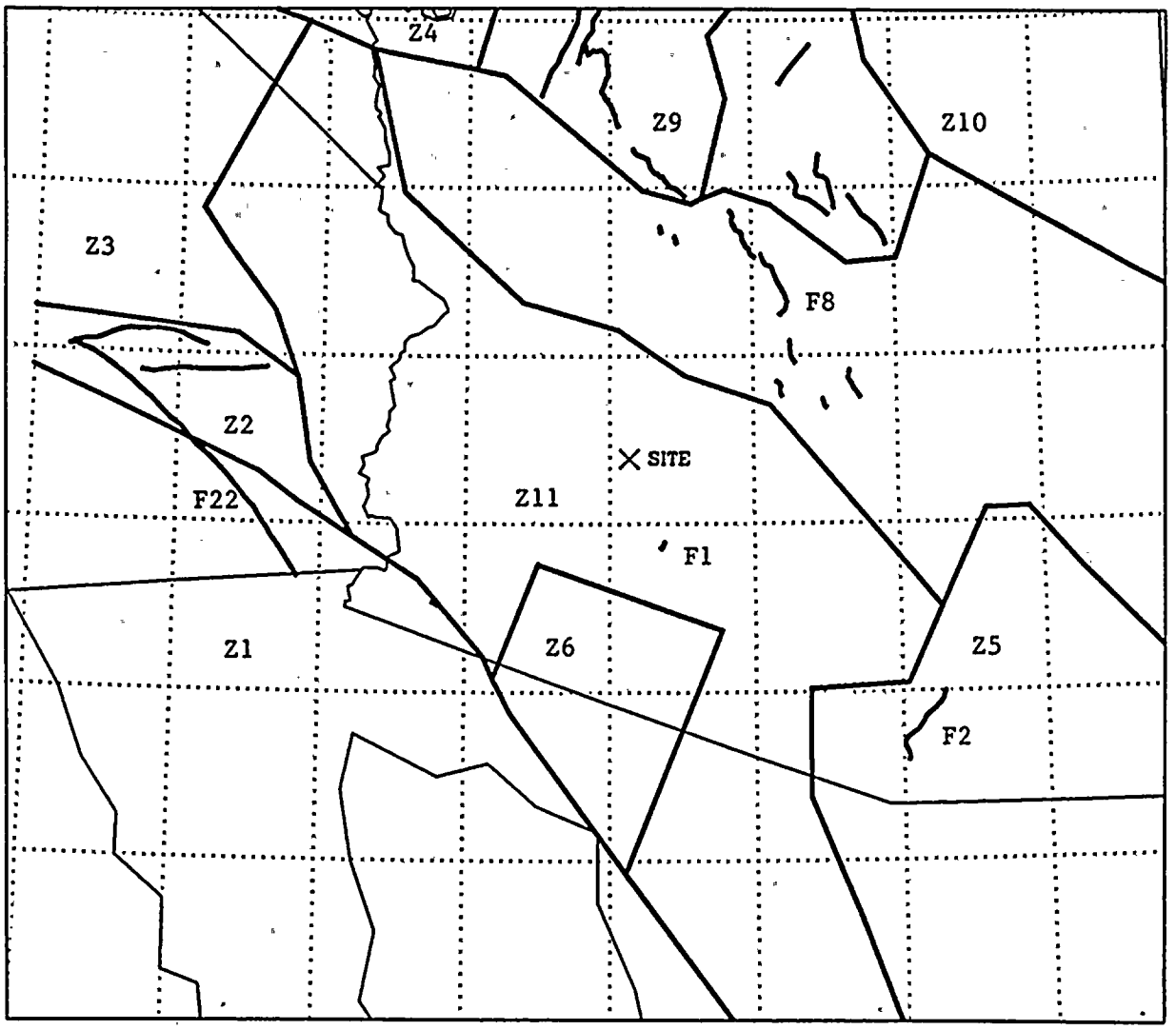

Figure 3-2. Seismic Sources for JMM Team.

Table 3-2

Probabilities of Activity for JMM Team Sources

Type	No.	Source	Prob. of Activity
Zone	1	Salton Trough	1.0
Zone	2	Transverse Ranges	1.0
Zone	3	Mojave Desert Basin & Range	1.0
Zone	4	Lake Mead Basin & Range	1.0
Zone	5	Mexican Basin & Range	1.0
Zone	6	Pinacate Volcanic Field	1.0
Zone	7	Arizona Mountains	1.0
Zone	8	Hurricane/Wasatch	1.0
Zone	9	San Francisco Volcanic Field	1.0
Zone	10	Colorado Plateau	1.0
Zone	11	Sonoran Desert Basin & Range	1.0
Fault	1	Sand Tank	0.78
Fault	2	Ranta Rita	0.78
Fault	3	Sugarloaf Peak	0.80
Fault	4	Carefree	0.81
Fault	5	Tonto Basin	0.94
Fault	6	Horseshoe Dam	0.88
Fault	7	Turret Peak	0.68
Fault	8	Verde	0.93
Fault	9	Prescott Valley	0.71
Fault	10	Williamson Valley	0.71
Fault	11	Chavez Mountain	0.73
Fault	12	Lake Mary/Mormon Lake	0.73
Fault	13	Munds Park	0.73
Fault	14	Big Chino	0.98
Fault	15	Mesa Butte	0.85
Fault	16	Bright Angel	0.70
Fault	17	Aubrey	0.88
Fault	18	Toroweap	1.0
Fault	19	Hurricane	1.0
Fault	20	Pinto Mountain	1.0
Fault	21	Blue Cut	1.0
Fault	22	San Andreas	1.0
Fault	23	Gila Mountain	0.60

Section 4

SEISMICITY PARAMETERS

To derive seismicity parameters for the seismic sources shown in Figures 3–1 and 3–2, two earthquake catalogs were found to be appropriate. The first is the Decade of North American Geology (DNAG) catalog (1), published in 1989, which consists of events through 1985. This catalog provides good coverage of southern California, but less extensive coverage of Arizona. Figures 4–1 and 4–2 show the Geomatrix Team and JMM Team seismic sources plotted with the DNAG seismicity data. The second catalog is the Stover et al. catalog of seismicity for Arizona (2), which includes events through 1982. Figures 4–3 and 4–4 shown plot the Geomatrix Team and JMM Team seismic sources with the Stover et al. seismicity; comparison of these plots with those of the DNAG catalog indicate the more complete coverage of the Stover et al. data in Arizona and the lack of coverage in Southern California. For the Stover et al. catalog, earthquakes described with only a Modified Mercalli intensity MMI were converted to magnitude using the Richter relation $M = 1 + 2MMI/3$. As a result of the differences in coverage between the two catalogs, the Stover et al. catalog was used for analysis of earthquake data for sources in Arizona, and the DNAG catalog was used for analysis of earthquake data for sources in southern California. The only change to both catalogs was to modify the location of the 1852 Fort Yuma earthquake, based on the work of Balderman et al. (3) and Agnew (4). Through analysis of contemporary reports, these authors concluded that this earthquake occurred in the Salton Trough, and we have used this location in the data analysis conducted for each team. The DNAG and Stover et al. catalogs are listed in Appendix C for the larger events within 300 km of PVNGS.

In addition to these two catalogs, the earthquakes reported in the FSAR for the PVNGS were also analyzed. These are based on the NOAA catalog of seismicity through 1980, and on work by DuBois et al. (5,6). These earthquakes gave results very similar to the Stover et al. catalog, which is not surprising as both the NOAA data and the DuBois work are cited by Stover et al.

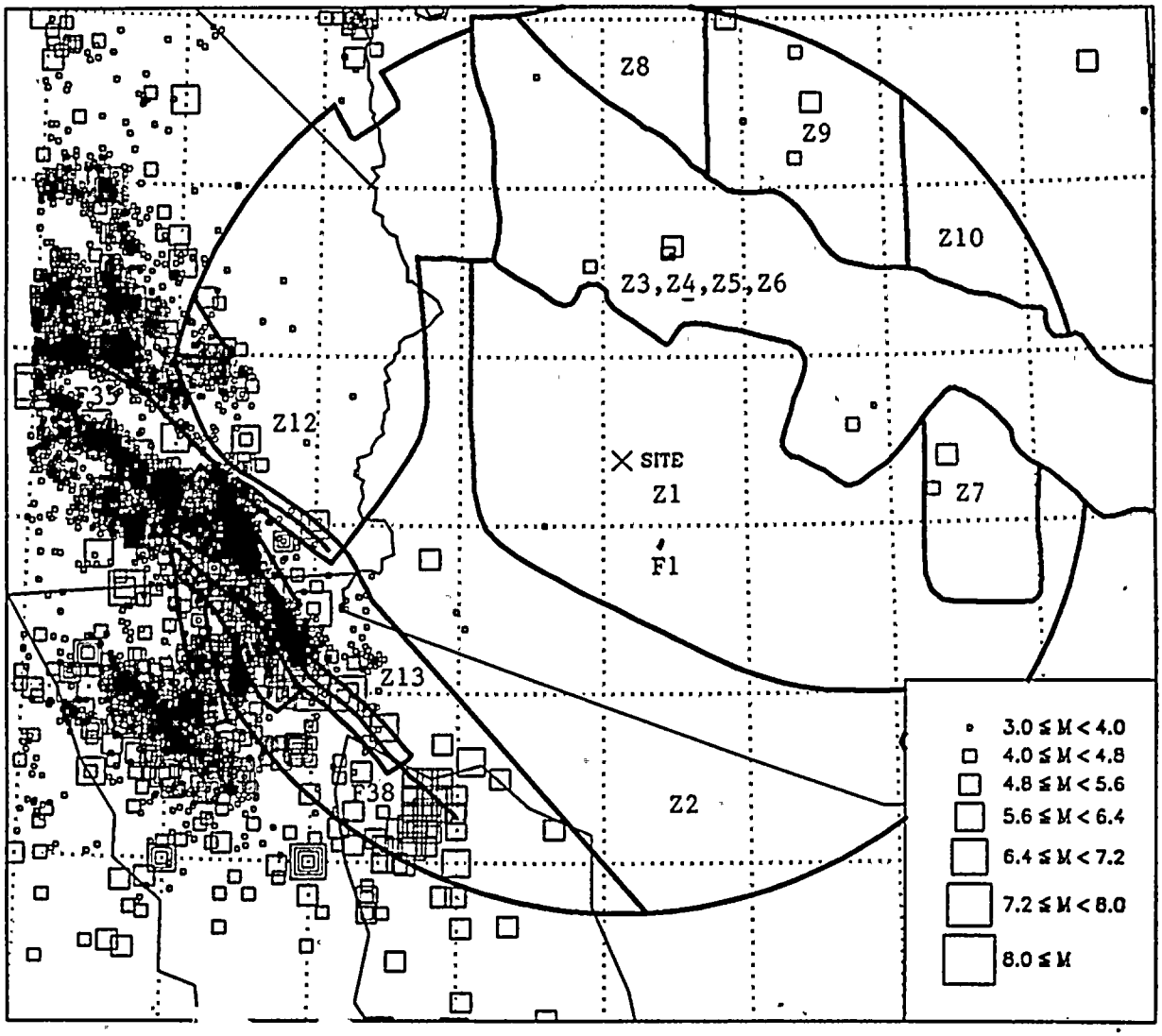

Figure 4-1. DNAG Catalog of Seismicity with Geomatrix Team Sources

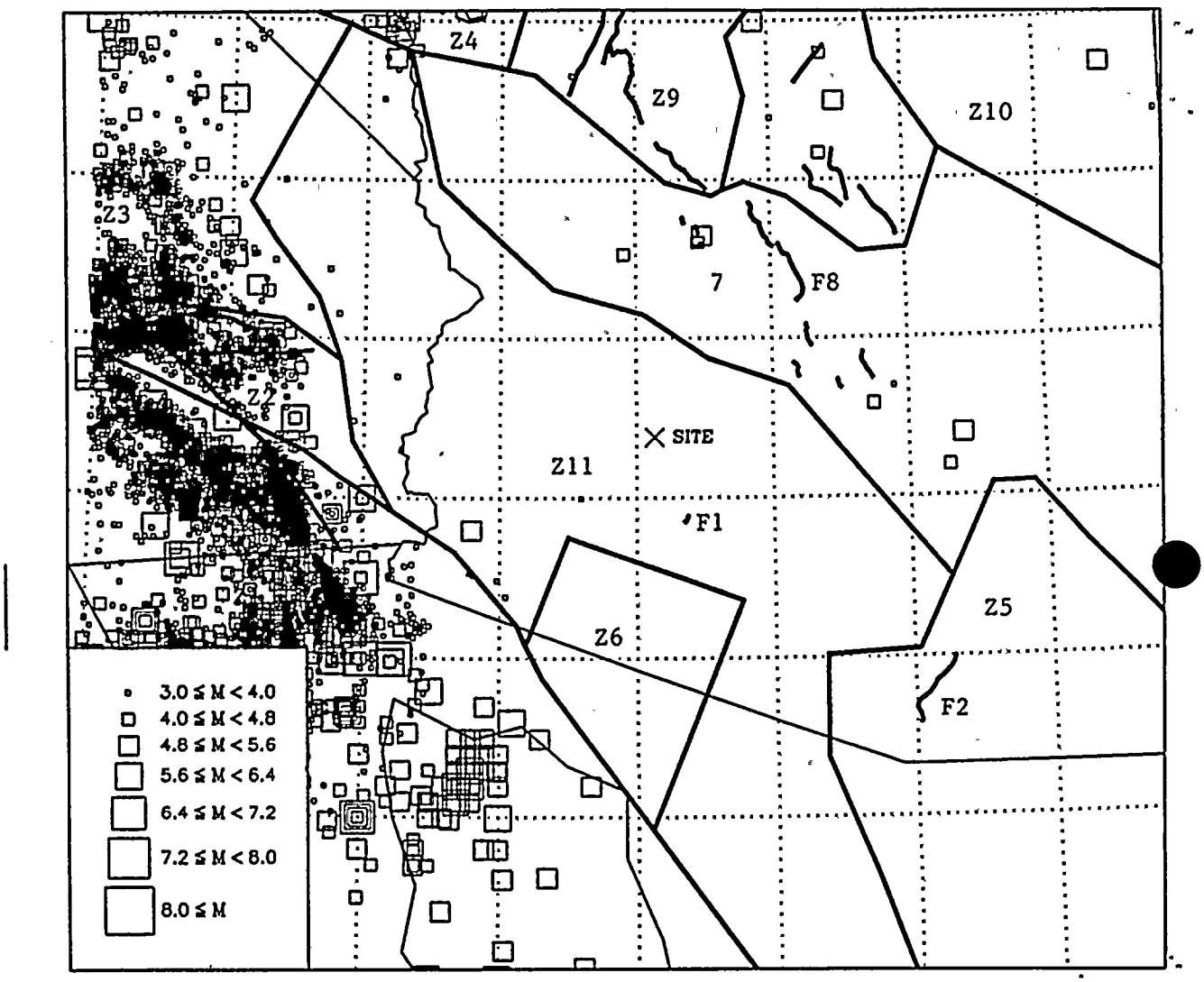

Figure 4-2. DNAG Catalog of Seismicity with JMM Team Sources

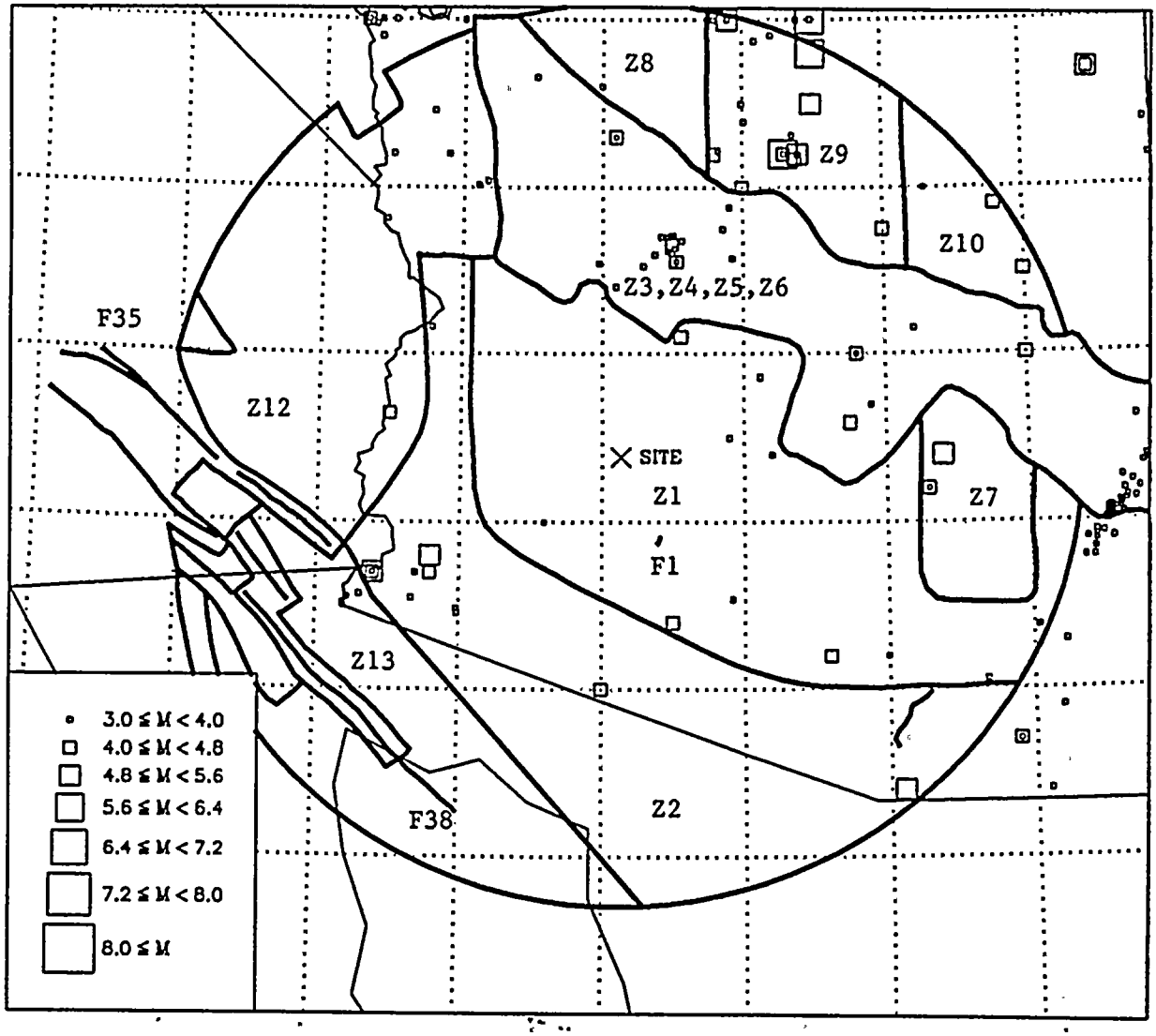

Figure 4-3. Stover Catalog of Seismicity with Geomatrix Team Sources

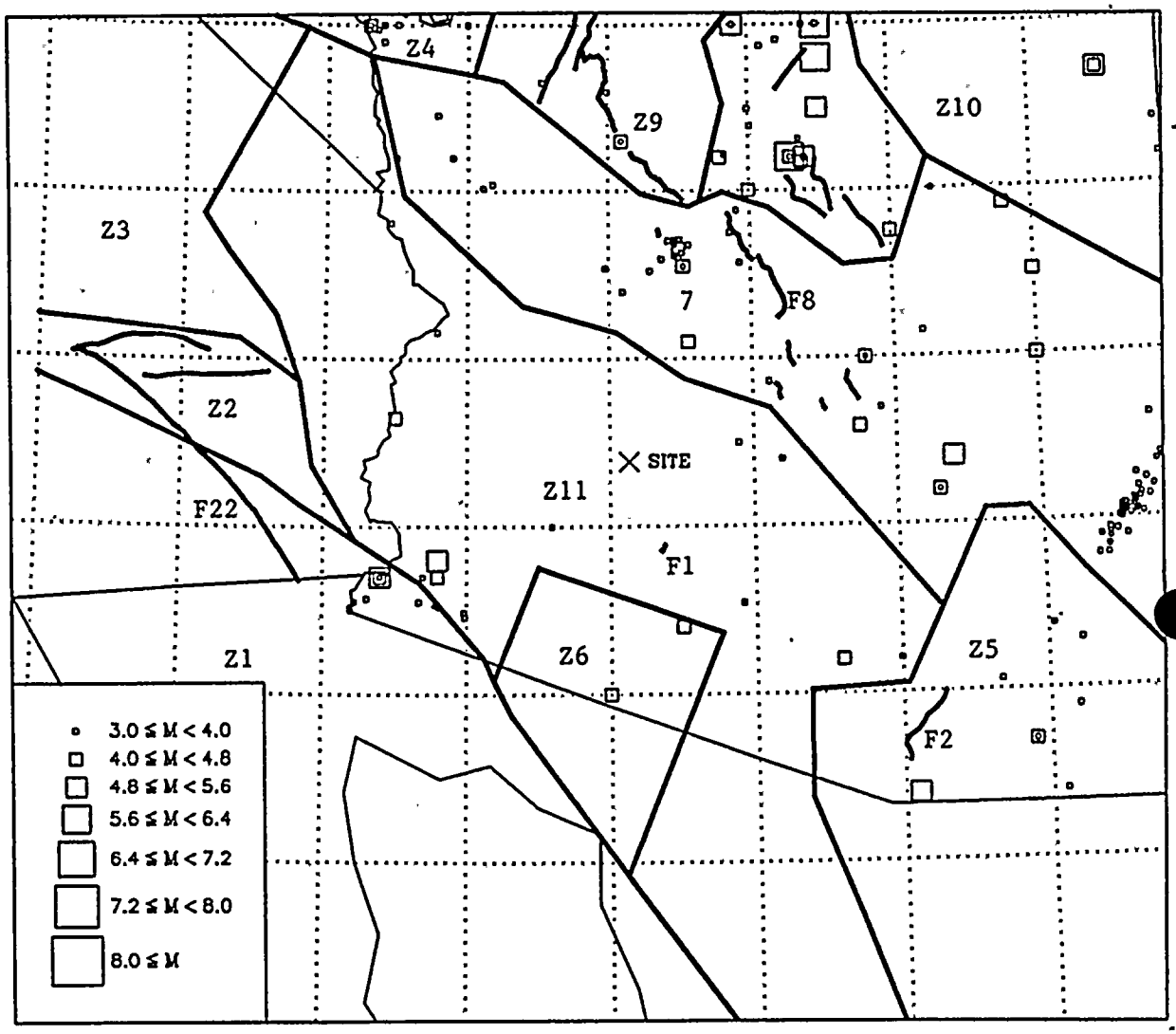

Figure 4-4. Stover Catalog of Seismicity with JMM Team Sources

For both earth science teams and both catalogs, an analysis was conducted to determine rates of activity and b-values for each seismogenic zone. This analysis proceeded with the following steps:

1. For each seismogenic zone, determine earthquakes that fall within the boundaries of that zone.

2. For each event in the source, determine the magnitude most equivalent to the moment magnitude. For specific magnitude ranges, estimate the time of completeness based on the observed occurrences, and calculate a mean rate of activity by dividing the observed numbers of events by the time of completeness.

3. Use the maximum-likelihood procedure of Weichert (7) to calculate an activity rate and b value for seismicity in the zone.

For these calculations, preliminary estimates of the upper-bound magnitude were used; this is sufficient because the calculated activity rates and b values are insensitive to the choice of m_{max} value.

The calculations were reviewed by the earth science teams, who determined appropriate choices of rates $\nu_{5.0}$ and b values for specification of the distribution of these parameters. That is, for each source, values of $\nu_{5.0}$ and b were specified along with weights, in order to quantify the uncertainty in these parameters for the seismic hazard calculations. The selected values are listed in Tables 4-1 and 4-2 for the Geomatrix and JMM Teams, respectively.

For reference purposes, the areas of seismic sources that contribute most to the seismic hazard are shown in Table 4-3, along with activity rates normalized by area. In the case of the Sonoran Desert source of the JMM Team, the activity rate used in the hazard calculations was a factor of 2.0 times that derived from the historical seismicity, because the Stover et al. catalog only covered one-half of the source. (Failure to account for this lack of coverage would result in underestimating the seismicity in the vicinity of the site.)

Figures 4-4 and 4-6 show plots of the historical seismicity and predictive curves for magnitudes above 5.0 for zones Z1 and Z2 of the Geomatrix Team (these sources contributed most to the seismic hazard at the PVNGS, as discussed below in Section 6). Figures 4-7 and 4-8 present similar plots for the JMM Team, for sources that contributed most to seismic hazard

Table 4-1

Seismicity Parameters for Geomatrix Team Sources

Type	No.	Source	Range of Act. Rates*	Range of b-values	Range of Max. Mags.
Zone	Z1	Zone 1	0.003–0.027	0.68–0.98	5.5–6.5
Zone	Z2	Zone 2	0.001–0.017	0.66–0.95	5.5–6.5
Zone	Z3	Zone 3	0.009–0.053	0.76–1.04	6.0–6.7
Zone	Z4	Zone 4	0.007–0.045	0.71–0.99	6.0–6.7
Zone	Z5	Zone 5	0.007–0.045	0.71–0.99	6.0–6.7
Zone	Z6	Zone 6	0.002–0.022	0.71–1.01	6.0–6.7
Zone	Z7	Zone 7	0.004–0.034	0.67–0.98	6.0–6.7
Zone	Z8	Colorado Plateau	0.002–0.010	0.67–0.96	6.2–7.0
Zone	Z9	Colorado Plateau	0.009–0.052	0.67–0.96	6.2–7.0
Zone	Z10	Colorado Plateau	0.002–0.010	0.67–0.96	6.2–7.0
Zone	Z11+Z12	Southern Basin & Range	0.007–0.069	0.54–1.00	6.0–6.7
Zone	Z13	Salton Trough/Gulf of Calif.	0.77–1.11	0.97–1.19	6.0–7.0
Zone	Z14	Pinto Mtn. Faults	0.014–0.085	0.48–0.95	6.5–7.2
Zone	Z17	Imperial/San Andreas Stepover	0.19–0.36	0.72–0.89	6.2–6.7
Zone	Z22	Laguna Salada	0.16–0.32	0.68–0.87	7.2–7.5
Zone	Z23	Sierra Juarez	0.13–0.24	0.69–0.77	7.0–7.2
Zone	Z24	No. Exten. of Cerro Prieto	0.008–0.037	0.72–0.92	6.5–7.2
Fault	F1	Sand Tank	5E-5–3E-3	0.70–1.00	6.3–6.8
Fault	F4	Santa Rita	5E-5–5E-3	0.70–1.00	6.3–7.0
Fault	F35	San Andreas	0.052–0.138	0.7–0.9	7.5–8.1
Fault	F36	Sand Hills	6E-4–3E-2	0.7–0.9	7.0–7.5
Fault	F37	Imperial	0.16–0.77	0.7–0.9	7.0–7.2
Fault	F38	Cerro Prieto	0.04–0.22	0.7–0.9	7.4–8.0
Fault	F41	San Jacinto	0.18–1.1	0.7–0.9	7.0–7.2

* Activity rates shown are annual rates of $M_w \geq 5$ for each source for the exponential model; refer to Appendix A for distributions of characteristic model

Table 4-2

Seismicity Parameters for JMM Team Sources

Type	No.	Source	Range of Act. Rates*	Range of b-values	Range of Max. Mags.
Zone	1	Salton Trough	0.77	0.77	6.9–8.5
Zone	2	Transverse Ranges	0.23	1.0	6.0–6.5
Zone	3	Mojave Desert Basin & Range	0.30	0.81	6.8–7.3
Zone	4	Lake Mead Basin & Range	0.17	0.63	6.8–7.3
Zone	5	Mexican Basin & Range	4.5E-3	0.99	5.0–5.5
Zone	6	Pinacate Volcanic Field	3E-4	1.4	5.0–5.5
Zone	7	Arizona Mountains	4.5E-3	0.99	5.0–5.5
Zone	8	Hurricane/Wasatch	1.5E-2	0.61	6.0–7.3
Zone	9	San Francisco Volcanic Field	1.7E-2	0.66	5.5–6.0
Zone	10	Colorado Plateau	7.2E-3	0.67	5.8–6.0
Zone	11	Sonoran Desert Basin & Range	3E-4–2.5E-02	0.80–1.36	5.0–6.0
Fault	1	Sand Tank	3E-4	1.36	5.4–7.0
Fault	2	Santa Rita	4.5E-3	0.99	5.7–7.2
Fault	3	Sugarloaf Peak	4.5E-3	0.99	5.7–6.7
Fault	4	Carefree	4.5E-3	0.99	5.5–6.8
Fault	5	Tonto Basin	4.5E-3	0.99	6.0–6.8
Fault	6	Horseshoe Dam	4.5E-3	0.99	5.8–6.8
Fault	7	Turret Peak	4.5E-3	0.99	5.8–6.8
Fault	8	Verde	4.5E-3	0.99	6.2–7.2
Fault	9	Prescott Valley	4.5E-3	0.99	5.6–6.8
Fault	10	Williamson Valley	4.5E-3	0.99	5.5–6.8
Fault	11	Chavez Mountain	1.7E-2	0.79	6.1–7.1
Fault	12	Lake Mary/Mormon Lake	1.7E-2	0.79	6.1–7.0
Fault	13	Munds Park	1.7E-2	0.79	6.0–7.0
Fault	14	Big Chino	1.7E-3	1.08	6.2–7.3
Fault	15	Mesa Butte	1.7E-2	0.79	6.6–7.4
Fault	16	Bright Angel	1.7E-2	0.79	6.4–7.6
Fault	17	Aubrey	1.7E-3	1.08	6.3–7.4
Fault	18	Toroweap	1.7E-3	1.08	6.9–7.4
Fault	19	Hurricane	1.7E-3	1.08	6.5–7.7
Fault	20	Pinto Mountain	9.8E-2	0.83	6.1–8.1
Fault	21	Blue Cut	9.8E-2	0.83	5.6–7.2
Fault	22	San Andreas	0.77	0.77	6.6–9.2
Fault	23	Gila Mountain	3E-4	1.4	5.4–6.8

* Activity rates shown are annual rates of $M_w \geq 5$ for each source for the exponential model; refer to Appendix A for more a detailed distribution.

Table 4-3

Rates per Unit Area for Critical Sources

Team	Source	Area (km^2	Annual Activity Rate per km^2
Geomatrix	Z1	6.09E+4	4.9E-8–4.4E-7
Geomatrix	Z2	5.69E+4	1.7E-8–3.0E-7
JMM	Sonoran Desert	1.2E+5	5.0E-9–1.4E-7
JMM	Salton Trough	2.9E+4	2.6E-5

at the PVNGS under this team's interpretations. These plots show annual rates with which various magnitudes will be exceeded. The uncertainty bands on the observed data show plus and minus one standard deviation values; these bands were calculated based on the number of earthquakes used to estimate the rate (7). These uncertainties are smaller for the lower magnitudes because more events were used in the estimates.

Exponential magnitude distributions were used to represent earthquake occurrences on most of the seismic sources designated by the two earth science teams. The maximum magnitude distribution was specified using methods similar to those derived in the EPRI/SOG study, i.e. the potential fault length, rupture area, surface displacement, slip rate, and other factors were evaluated and used to derive a distribution on maximum possible magnitude that could occur in each seismic source. The resulting evaluations of maximum magnitude are given in Tables 4–1 and 4–2 for the Geomatrix and JMM Teams, respectively.

For some sources, the Geomatrix Team determined that a characteristic magnitude distribution was most appropriate to represent the occurrences of the largest events. These in all cases were faults where the largest earthquakes were thought to occur at a different average rate from that indicated by extrapolation of lower seismicity. Appendix A contains details of these faults and of the parameters used for the characteristic magnitude distribution; none of these faults contributed significantly to the seismic hazard at PVNGS, as is shown in Section 6.

4.1 REFERENCES

1. E. R. Engdahl and W. A. Rinehart. "Seismicity Map of North America". In *Observatory Seismology*, ed. by J. J. Litehiser, Univ. of Calif. Press, Berkeley, Calif., 1989.

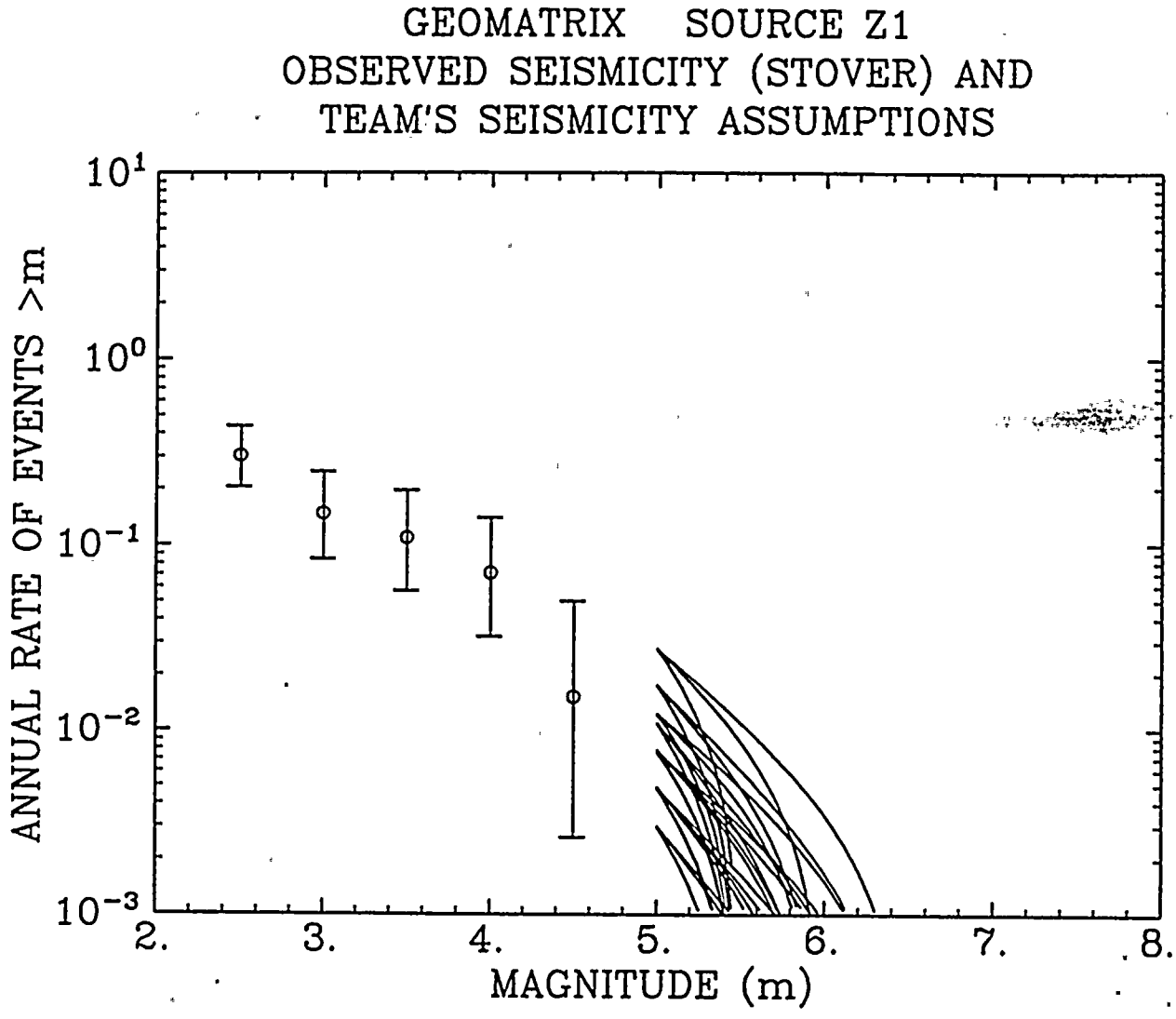

Figure 4-5. Historical Seismicity for Geomatrix Team Source Z1

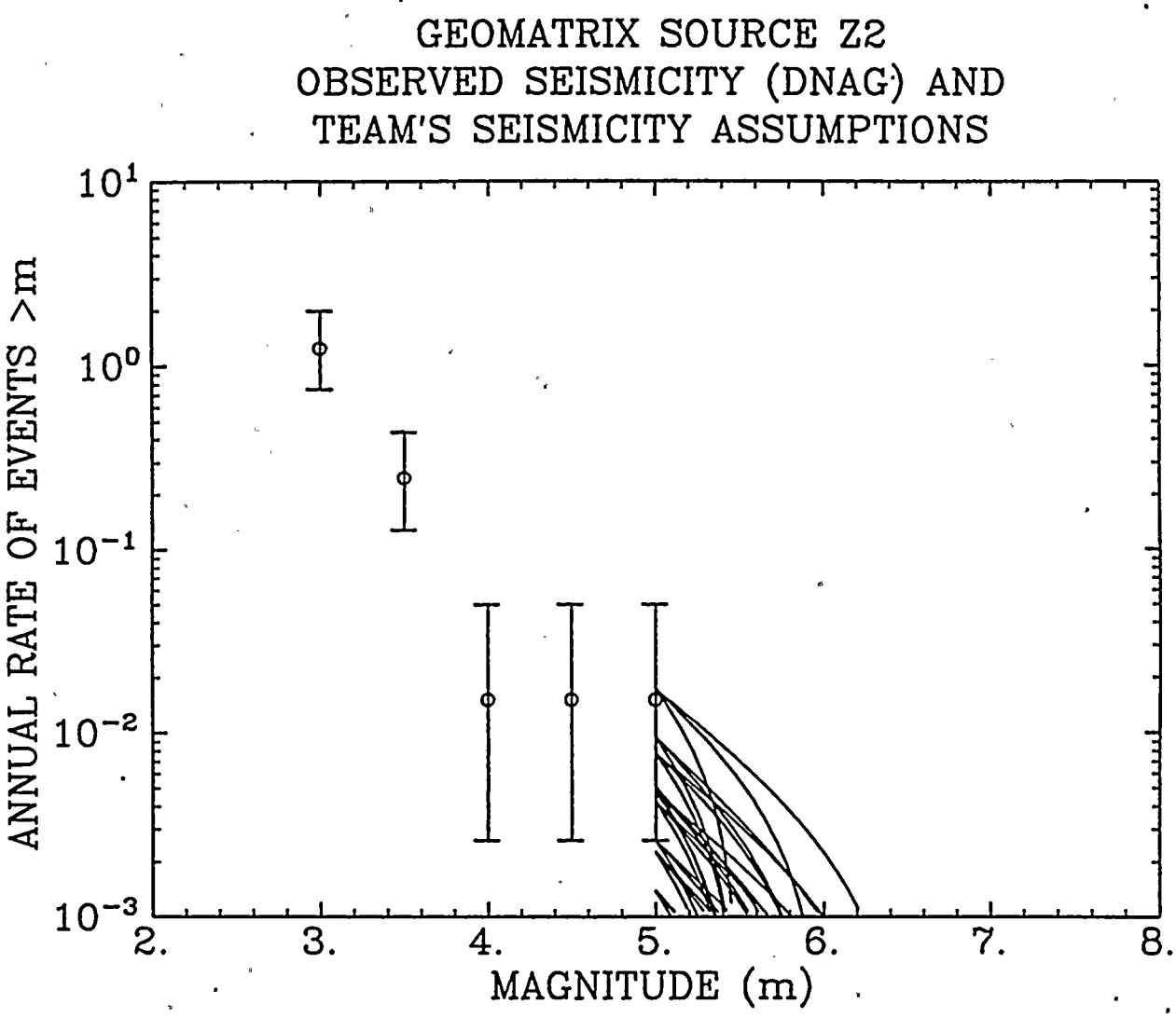

Figure 4-6. Historical Seismicity for Geomatrix Team Source Z2

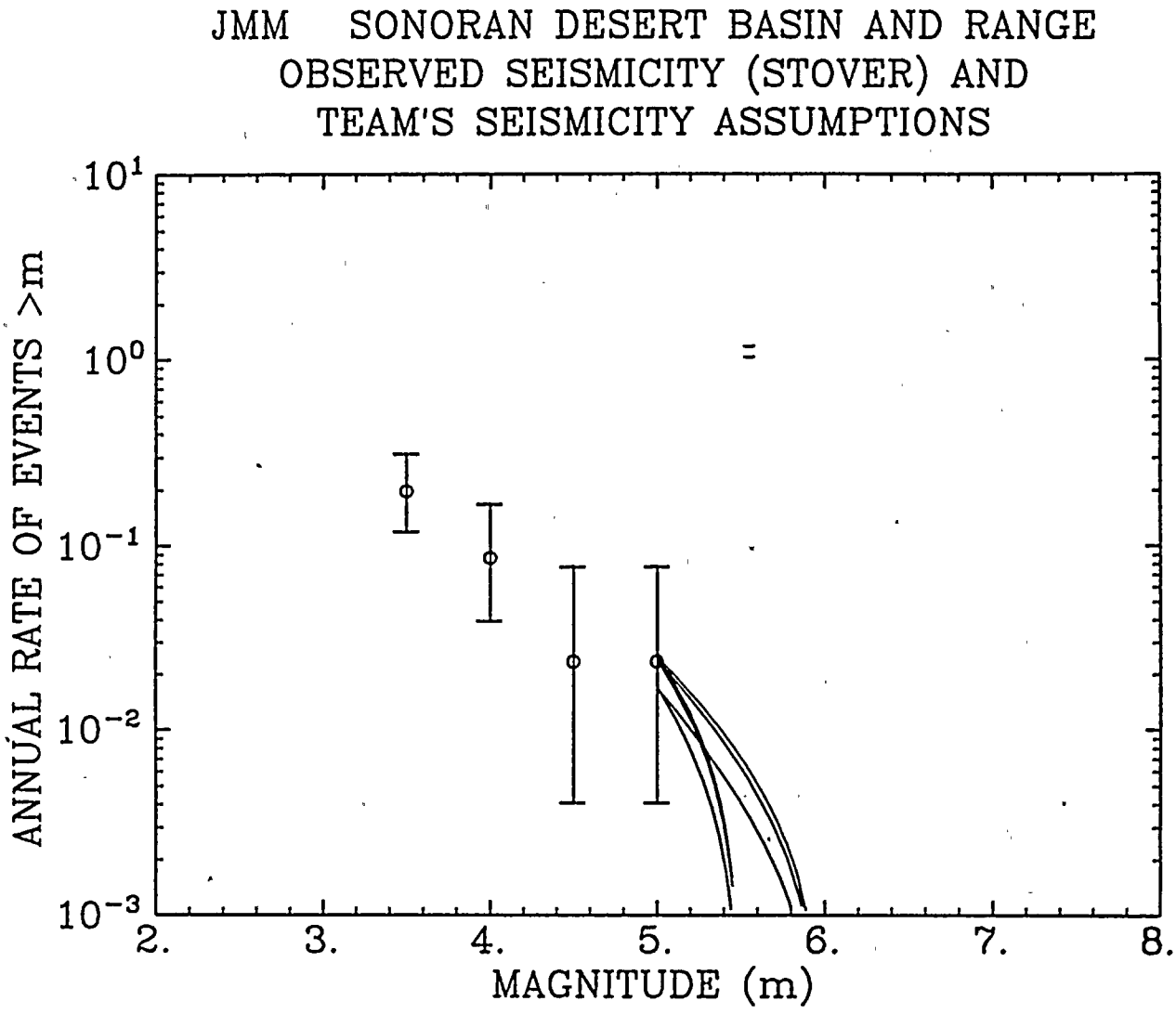

Figure 4-7. Historical Seismicity for JMM Team Sonoran Desert Source. Observed rates have been multiplied by a factor of 2 because the Stover catalog covers only half the area of this source.

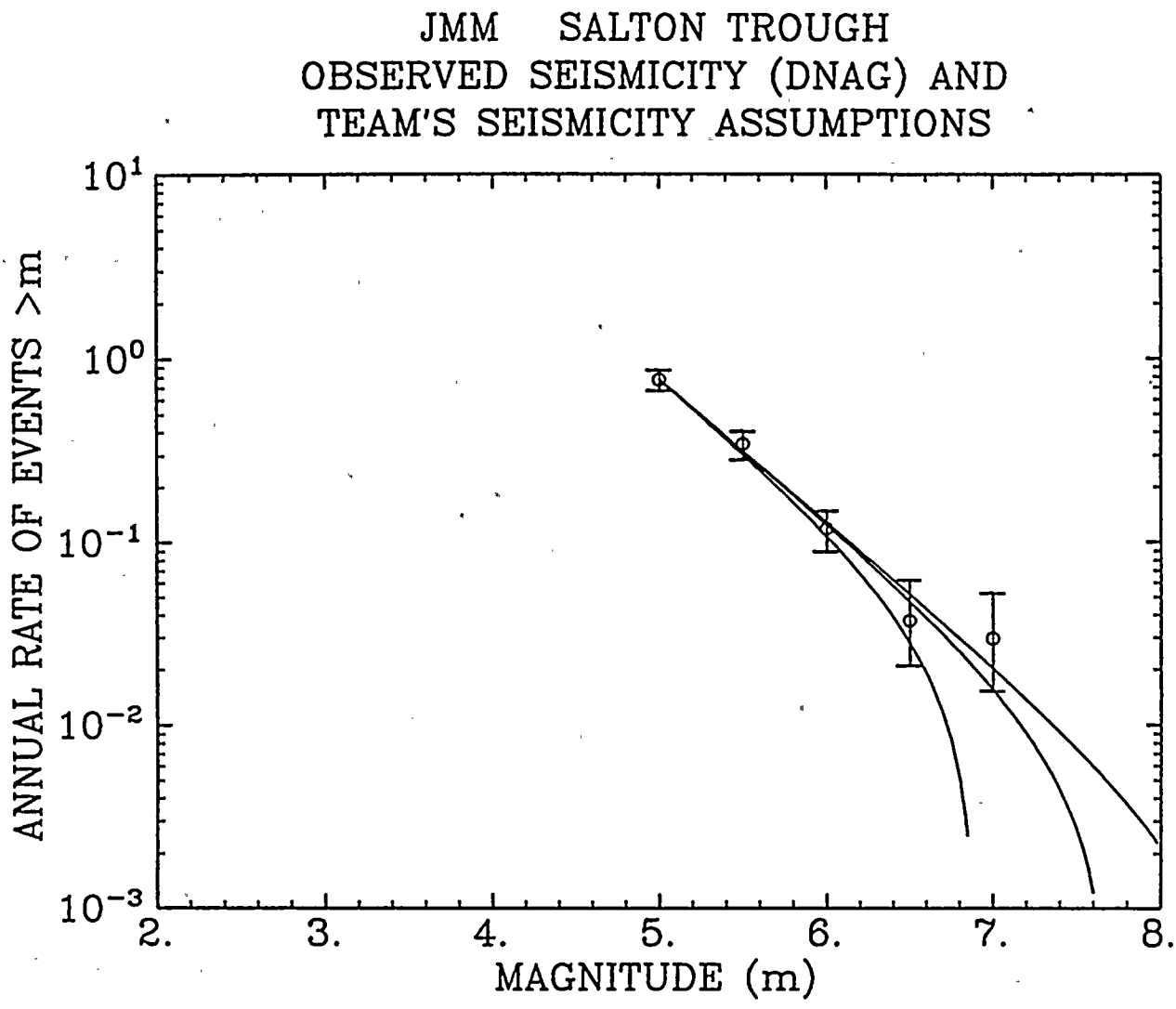

Figure 4-8. Historical Seismicity for JMM Team Salton Trough Source

2. C. W. Stover, B. G. Reagor, and S. T. Algermissen. *Seismicity Map of the State of Arizona.* Miscellaneous Field Studies Map MF-1852, US Geological Survey, 1986.

3. M. A. Balderman, C. A. Johnson, D. G. Miller, and D. L. Schmidt. "The 1852 Fort Yuma Earthquake". *Bull. Seism. Soc. of America*, 68(3):699–710, June 1978.

4. D. C. Agnew. "The 1852 Fort Yuma Earthquake–Two Additional Accounts". *Bull. Seism. Soc. of America*, 68(6):1761–1762, December 1978.

5. S. M. DuBois, A. W. Smith, N. K. Nye, and T. A. Novak. *Arizona Earthquakes, 1776–1980.* Bulletin 193, Arizona Bureau of Geology and Mineral Technology, 1982.

6. S. M. DuBois, M. L. Sbar, and T. A. Novak. *Historical Seismicity in Arizona.* Open-File Rept. 82-2, Arizona Bureau of Geology and Mineral Technology, 1982.

7. D. H. Weichert. "Estimation of the Earthquake Recurrence Parameters for Unequal Observations Periods for Different Magnitudes". *Bulletin of the Seismological Society of America*, 70:1337–1346, 1980.

Section 5

GROUND MOTION ATTENUATION FUNCTIONS

5.1 OVERVIEW

This Section describes and compares the ground motion attenuation functions and site-amplification factors used in the evaluation of seismic hazard at the PVNGS site. This study uses separate attenuation functions for each of the five ground-motion measures (i.e., peak ground acceleration and spectral velocities at of 1, 2.5, 5, 10, and 25 Hz). Multiple attenuation functions are used for each ground-motion measure, in order to characterize uncertainty in ground-motion attenuation.

We use ground-motion attenuation functions for rock conditions and then modify the predicted rock ground motions using amplitude and frequency-dependent amplification factors.

5.2 METHODOLOGY

The PVNGS site is located on the Basin and Range physiographic province, a region of extensional tectonic stress bounded by the Sierra Nevada and the Rocky Mountains.

The number of available strong-motion earthquake records from the Basin and Range province are not sufficient for the development of empirically based attenuation functions based solely on these records. As a result, one must use data or attenuation relationships from other regions (mostly California), an understanding of the region's tectonics and wave propagation, and comparisons with earthquake recordings from the region, in order to select or construct attenuation functions for the Basin and Range (1,2,3, for example).

In this study, we utilize attenuation functions in the literature (based on mostly California data), which we modify as appropriate to reflect conditions in the Basin and Range province. Section 5.3 discusses the tectonics and wave-propagation in the region. Section 5.4 presents and compares the resulting attenuation equations. Finally, Section 5.5 describes the site-amplification factors used in this study.

5.3 FACTORS AFFECTING GROUND MOTIONS IN THE BASIN AND RANGE PROVINCE

5.3.1 Tectonic Stresses

McGarr (4) has postulated that earthquakes from regions with extensional tectonic stresses, such as the Basin and Range, generate lower ground motions than earthquakes of similar magnitudes in regions with compressional tectonic stresses, such as California. A study by Campbell (5), which compared ground motions earthquakes in the Mammoth region to earthquakes from elsewhere in California, do not support McGarr's hypothesis. Similarly, Westaway and Smith (6) compared peak accelerations from normal-faulting earthquakes throughout the world with predictions by California attenuation functions, and found similar amplitudes.

Based on the latter two studies, we will assume that there are no differences in near-source ground motions between the Basin and Range and California. As a corollary, California attenuation functions are applicable to the Basin and Range, at least as short and moderate distances (< 50 km; i.e., distances for which anelastic attenuation is not important).

5.3.2 Anelastic Attenuation

Anelastic attenuation (i.e, damping in the earth's crust) has little effect on ground motions at short and moderate distances (< 50km), but becomes important at distances of 100 km or more.

Studies of anelastic attenuation in the Basin and Range have obtained a wide range of results (see Campbell (3) for a discussion). Some recent studies (see Mitchell (7)) have obtained consistent estimates, which suggest lower anelastic attenuation in the Basin and Range than in California.

This study will use two assumptions for anelastic attenuation. The first assumption is that anelastic attenuation is the same for the Basin and Range and California (this assumption is equivalent to using California attenuation equations, without modification). The second assumption will adopt the anelastic attenuation model obtained by Xie and Mitchell (8) for the Basin and Range, which is consistent with results from other studies. The model by Xie and Mitchell is characterized by the frequency-dependent quality factor[1] $Q(f) = 267f^{0.37}$.

[1]Anelastic attenuation is characterized by the dimensionless quality factor Q, defined such that the energy loss of a wave of frequency f, as it travels a distance of one wavelength, is equal to a factor of $\exp[-2\pi/Q(f)]$.

5.3.3 Crustal Reflections

Seismic waves reflected from strong velocity discontinuities in the earth's crust have been shown to affect ground motions at distances of 80 km or more (9). These effects are not included in most attenuation equations, which implicitly assume a homogeneous crust. The effect of these crustal reflections on seismic hazard is believed to be minimal, but has never been quantified.

Consideration of crustal-reflection effects on ground motions in the Basin and Range is beyond the scope of this study.

5.4 ATTENUATION EQUATIONS FOR ROCK SITE CONDITIONS

We select the attenuation equations by Joyner and Boore (10) and Campbell (11) as the starting points for the development of attenuation functions for this study. These attenuation equations were obtained through regression, using mostly California data. Both the Joyner-Boore and Campbell studies contain attenuation equations for peak acceleration and spectral velocities at multiple frequencies.

The Joyner and Boore set of attenuation equations does not contain an attenuation equation for 25-Hz spectral velocity. We used Joyner and Boore's attenuation function for peak acceleration and the Newmark-Hall amplification factors to construct the corresponding 25-Hz attenuation equation.

We extended the Campbell attenuation functions to longer distances by adding a term of the form $\gamma(R-50)$ to Campbell's expression for ln[Ground-Motion Amplitude], where γ is the anelastic attenuation term in the corresponding Joyner-Boore attenuation equation.

To construct attenuation equations consistent Xie and Mitchell's (8) Basin and Range anelastic attenuation model, we introduce new values of γ, which are calculated as

$$\gamma = \frac{\pi f}{Q\beta} \qquad (5-1)$$

where f is frequency (Hz) and β is the average shear-wave velocity. Following Campbell (5), we use a central frequency of 5 Hz to compute the value of γ for peak acceleration.

These two sets of attenuation functions, combined with two anelastic-attenuation assumptions, yield four attenuation functions for each ground-motion measure. These four sets of attenuation functions are given equal weights in the seismic hazard calculations.

Tables 5–1 through 5–4 contain the functional forms and coefficients of the four sets of attenuation equations. Figure 5–1 compares predictions by these attenuation equations, for magnitudes 5 and 7. Differences among the attenuation equations provide a reasonable representation of uncertainty in ground-motion predictions in the Basin and Range province.

5.5 SITE AMPLIFICATION FACTORS

According to the PVNGS FSAR, structures in PVNGS are founded on soil with 300 to 400 foot thickness. Therefore, we will characterize site response at PVNGS using the EPRI/SOG amplification factors for category IV (180–400'). These amplification factors are given in Figures 2–4 through 2–9.

Because the EPRI/SOG amplification factors were developed for ground motions with frequency content typical of the eastern U.S., they are not consistent with the western-U.S. attenuation equations developed in Section 5-4. In particular, the category-IV amplification factors for 25-Hz spectral velocity (Figure 2-9) is significantly lower than the corresponding amplification factor for PGA (Figure 2-4). This may lead to calculated 25-Hz spectral accelerations that are lower than the corresponding peak ground accelerations.

The effect of this difference in frequency content is largest for 25-Hz PSV, is expected to be moderate for 10-Hz PSV and PGA, and is small for PSV at 5 Hz or less.

5.6 REFERENCES

1. K. W. Campbell. "A Preliminary Methodology for the Regional Zonation of Peak Ground Acceleration". In *Proceedings: 3rd International Earthquake Microzonation Conference, Seattle, WA*, pp. 365–376, June 1982.

2. R. K. McGuire. *Estimation of Seismic Ground Motion in Northern Utah.* Contract Report 14-08-001-19825, U. S. Geological Survey, September 1983.

3. K. W. Campbell. "Predicting Strong Ground Motion in Utah". In W. Hays and P. Gori, editors, *Evaluation of Urban and Regional Earthquake Hazard and Risk and Utah*, 1988. in preparation.

4. A. McGarr. "Scaling of Ground Motion Parameters, State of Stress and Focal Depth". *Journal of Geophysical Research*, 6969–6979, 1984.

5. K. W. Campbell. "Strong Motion Attenuation Relations: A Ten Year Perspective". *Earthquake Spectra*, 1:759–804, 1985.

6. R. Westaway and R. B. Smith. "Strong Ground Motion in Normal Faulting Earthquakes". *Geophysics Journal*, 96:529–560, 1989.

7. B. J. Mitchell. "Frequency Dependence of Q_{Lg} and its Relationship to Crustal Anelasticity in the Basin and Range Province". *Geophysical Research Letters*, 18(4):621–624, 1991.

8. J. Xie and B. J. Mitchell. "Attenuation of Multiphase Surface Waves in the Basin and Range Province; Part 1: *Lg* and *Lg* Coda". *Geophys. J. Int.*, 102:121–137, 1990.

9. R. W. Burger, P. G. Somerville, J. S. Barker, R. B. Herrmann, and D. V. Helmberger. "The Effect of Crustal Structure on Strong Ground Motion Attenuation Relations in Eastern North America". *Bulletin of the Seismological Society of America*, 77(2):420–439, 1987.

10. W. B. Joyner and D. M. Boore. *Prediction of Earthquake Response Spectra.* Open-File Report 82-977, U. S. Geological Survey, 1982.

11. K. C. Campbell. *Empirical Prediction of Near-Source Ground Motion For the Diablo Canyon Power Plant Site, San Luis Obispo County California.* Open File Report 89-484, U. S. Geological Survey, 1989.

Table 5-1

Joyner and Boore Attenuation Equations (original)

$$\ln Y = a + b(M-6) + c(M-6)^2 + d \ln R_h + \gamma R_h \ ^{1}$$

Y [2]	a	b	c	d	γ	h (km)
1-Hz PSV	5.244	1.541	-0.391	-1.000	-0.00897	4.7
2.5-Hz PSV	5.612	1.081	-0.299	-1.000	-0.01242	5.7
5-Hz PSV	5.658	0.805	-0.207	-1.000	-0.01449	9.6
10-Hz PSV	4.968	0.575	-0.138	-1.000	-0.01679	11.3
25-Hz PSV	6.967	0.529	0.000	-1.000	-0.00621	8.0
PGA	7.878	0.529	0.000	-1.000	-0.00621	8.0

[1] These equation apply to rock site conditions. Distance R_h is defined as $R_h = \sqrt{R^2 + h^2}$, where R is epicentral distance.

[2] Pseudo spectral velocity (PSV) is given in cm/sec; peak ground acceleration (PGA) is given in cm/sec^2.

Table 5-2

Joyner and Boore Attenuation Equations (alternative Q)

$$\ln Y = a + b(M-6) + c(M-6)^2 + d \ln R_h + \gamma R_h \ ^{1}$$

Y [2]	a	b	c	d	γ	h (km)
1-Hz PSV	5.244	1.541	-0.391	-1.000	-0.00336	4.7
2.5-Hz PSV	5.612	1.081	-0.299	-1.000	-0.00599	5.7
5-Hz PSV	5.658	0.805	-0.207	-1.000	-0.00927	9.6
10-Hz PSV	4.968	0.575	-0.138	-1.000	-0.01434	11.3
25-Hz PSV	6.967	0.529	0.000	-1.000	-0.00927	8.0
PGA	7.878	0.529	0.000	-1.000	-0.00927	8.0

[1] These equation apply to rock site conditions. Distance R_h is defined as $R_h = \sqrt{R^2 + h^2}$, where R is epicentral distance.

[2] Pseudo spectral velocity (PSV) is given in cm/sec; peak ground acceleration (PGA) is given in cm/sec^2.

Table 5-3

Campbell Attenuation Equations (original)

$$\ln Y = a + bM + f_1 \tanh[f_2(M + f_3)] + d\ln[R_h + 0.311\exp(0.597M)] + \gamma(R_h - 50)$$ [1]

Y [2]	a	b	f_1	f_2	f_3	d	γ
1-Hz PSV	1.260	1.108	1.740	0.570	-4.7	-1.81	-0.00897
2.5-Hz PSV	2.009	1.108	0.425	0.570	-4.7	-1.81	-0.01242
5-Hz PSV	1.788	1.108	0.000	0.570	-4.7	-1.81	-0.01449
10-Hz PSV	0.754	1.108	0.000	0.570	-4.7	-1.81	-0.01679
25-Hz PSV	-0.648	1.108	0.000	0.570	-4.7	-1.81	-0.00621
PGA	4.420	1.108	0.000	0.570	-4.7	-1.81	-0.00621

[1] These equation apply to rock site conditions, strike-slip faults, and no building effects. Distance R_h is defined as $R_h = \sqrt{R^2 + h^2}$, where R is epicentral distance and h is given in Tables 5–1 and 5–2.

[2] Pseudo spectral velocity (PSV) is given in cm/sec; peak ground acceleration (PGA) is given in cm/sec^2.

Table 5-4

Campbell Attenuation Equations (alternative Q)

$$\ln Y = a + bM + f_1 \tanh[f_2(M + f_3)] + d\ln[R_h + 0.311\exp(0.597M)] + \gamma(R_h - 50)$$ [1]

Y [2]	a	b	f_1	f_2	f_3	d	γ
1-Hz PSV	1.260	1.108	1.740	0.570	-4.7	-1.81	-0.00336
2.5-Hz PSV	2.009	1.108	0.425	0.570	-4.7	-1.81	-0.00599
5-Hz PSV	1.788	1.108	0.000	0.570	-4.7	-1.81	-0.00927
10-Hz PSV	0.754	1.108	0.000	0.570	-4.7	-1.81	-0.01434
25-Hz PSV	-0.648	1.108	0.000	0.570	-4.7	-1.81	-0.00927
PGA	4.420	1.108	0.000	0.570	-4.7	-1.81	-0.00927

[1] These equation apply to rock site conditions, strike-slip faults, and no building effects. Distance R_h is defined as $R_h = \sqrt{R^2 + h^2}$, where R is epicentral distance and h is given in Tables 5–1 and 5–2.

[2] Pseudo spectral velocity (PSV) is given in cm/sec; peak ground acceleration (PGA) is given in cm/sec^2.

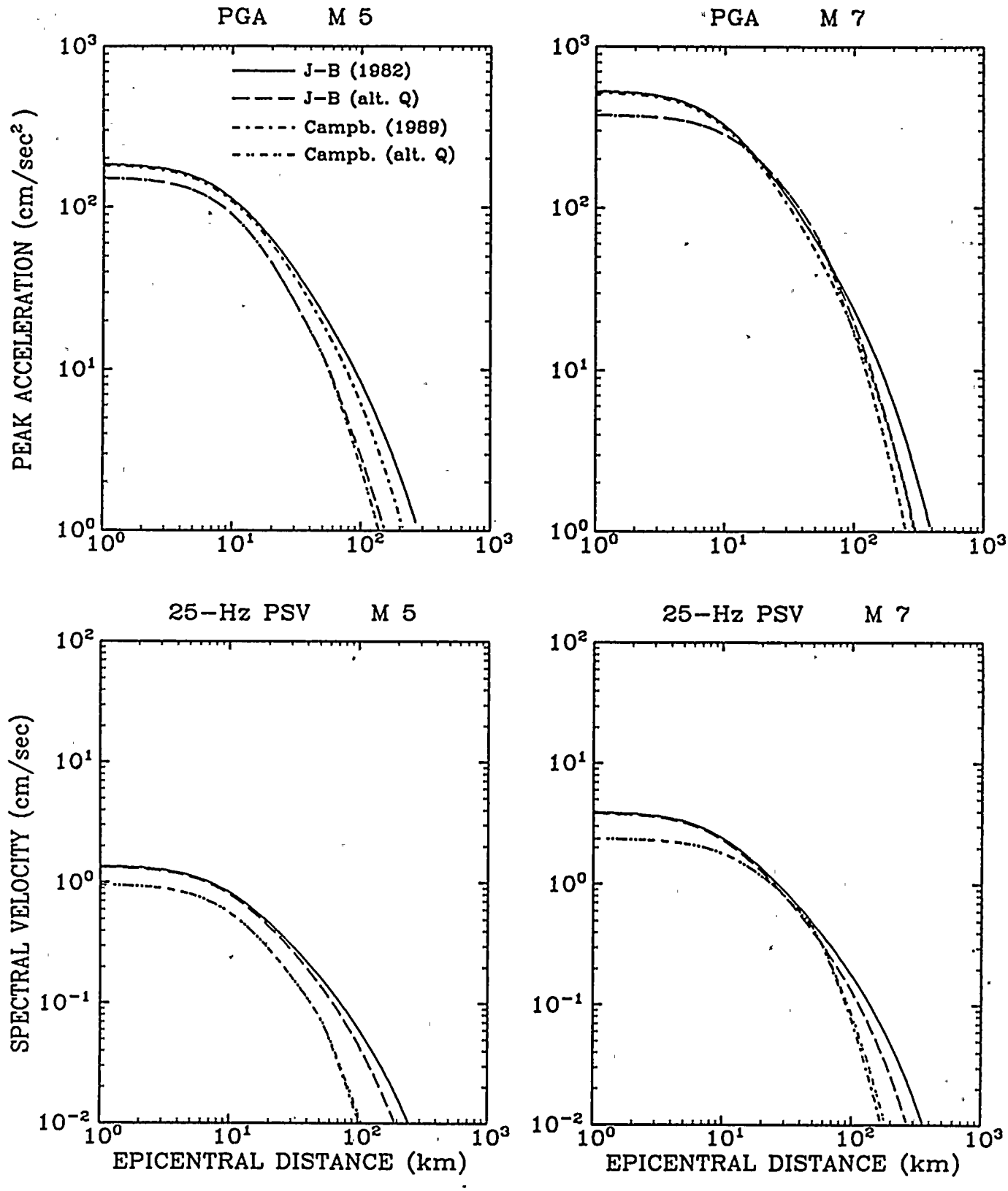

Figure 5-1. Attenuation equations used in this study: predicted ground motions for magnitudes 5 and 7; peak acceleration and 25-Hz spectral velocity

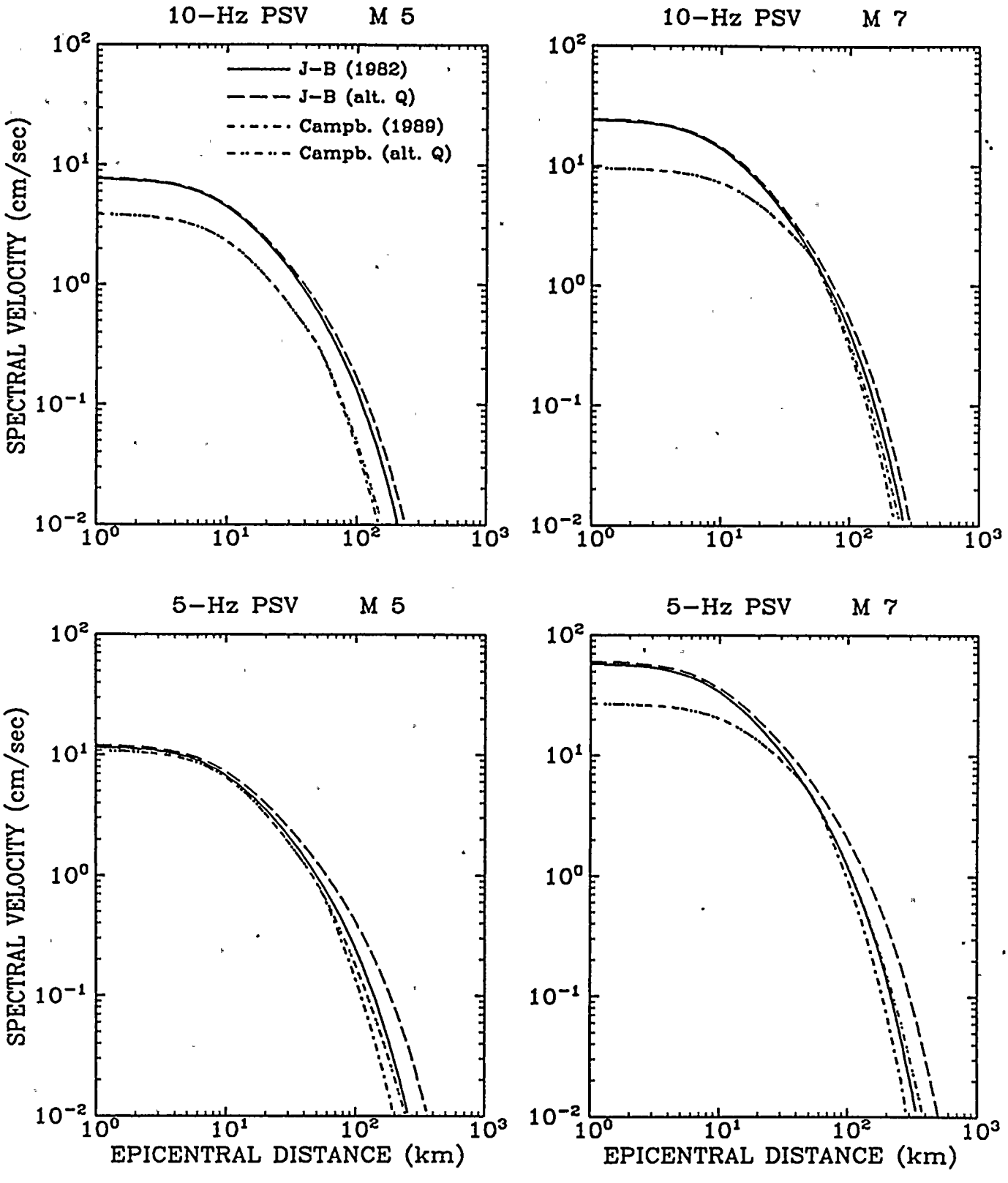

Figure 5-1 (continued). Attenuation equations used in this study: predicted ground motions for magnitudes 5 and 7; spectral velocities at 10 and 5 Hz.

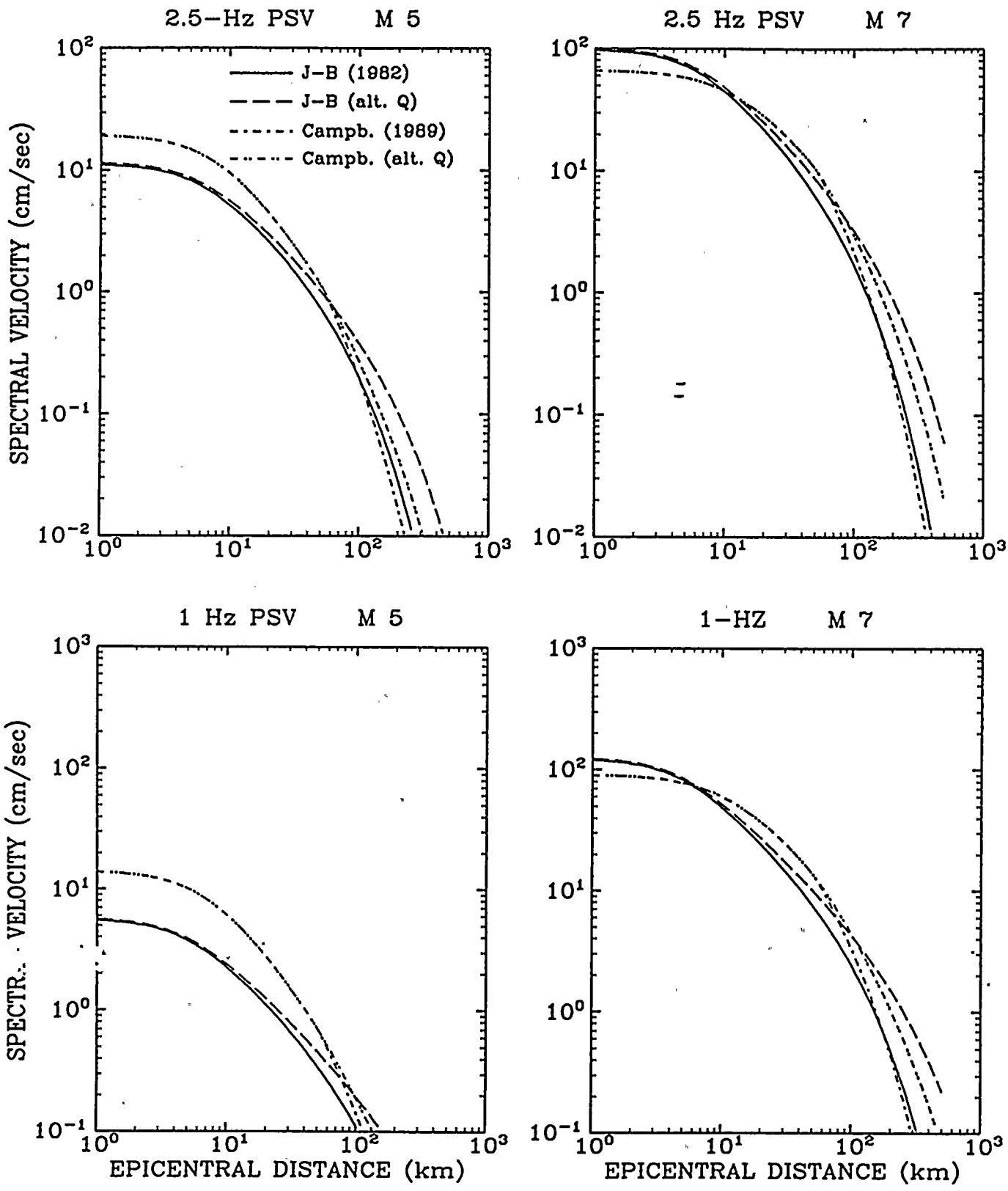

Figure 5-1 (continued). Attenuation equations used in this study: predicted ground motions for magnitudes 5 and 7; spectral velocities at 2.5 and 1 Hz.

Section 6
SEISMIC HAZARD RESULTS

This Section reports the seismic hazard results calculated with the inputs described in Sections 3 through 5. These results were obtained with the computer program FRISK88, which incorporates uncertainties in inputs to seismic hazard analyses and produces explicit hazard curves for each combination of uncertain parameters. The calculations are, in all ways, equivalent to the calculations performed under the EPRI/SOG study. Most of the results presented in this section include the effects of deep soil on the ground motions, as described in Section 5. Additional results are presented at the end of this section that correspond to rock outcrop motions, i.e. hazard results without the effects of deep soil amplification/deamplification of the ground motion. The latter results are presented in the event that future results are desired with soil effects different from those described in Section 5.

Figures 6–1 through 6–3 display the seismic hazard (annual probability of exceedance versus ground motion level) for the Geomatrix Team, for PGA and 1- and 2.5-Hz spectral velocity, respectively. The curves shown are mean curves for each source indicated on Figure 3–1, the mean being over all uncertainties in activity rates, b–values, and m_{max} values for that source, and over all attenuation equations. For the Geomatrix team it is evident that sources Z1 (the host source), F38 (Cerro Prieto Fault) and F1 (Sand Tank Fault) dominate the seismic hazard at the PVNGS.

A similar presentation is made in Figures 6–4 through 6–6 for the JMM Team, for PGA and 1- and 2.5-Hz spectral velocity, respectively, for the JMM sources (Figure 3–2). Here it is evident that the Sonoran Desert (host source), the Salton Trough, the San Andreas Fault, and the Sand Tank Fault contribute most to the seismic hazard.

Note that the distant, more active sources contribute to the seismic hazard for low-frequency ground motions such as 1-Hz PSV, but only for low amplitudes. For peak acceleration, the seismic hazard is controlled by the host sources, for all amplitudes of interest.

Figures 6–7 through 6–12 display the mean and fractiles of total seismic hazard at the PVNGS for the six ground motion measures, the fractiles being over all uncertainties considered.

For these plots the two earth science teams were weighted equally. Table 6-1 lists annual probabilities of exceedance for three fractiles and the mean, from Figure 6-7. Table 6-2 lists fractiles of spectral velocity for four annual probabilities of exceedance, from Figures 6-8 through 6-12.

The hazard results are presented in a different format in Figures 6-13 through 6-16. These are fractiles of spectra for frequencies of 25 to 1 Hz (periods of 0.04 to 1 sec). Figure 6-17 shows median spectra (that is, the 50% fractile) for annual probabilities of exceedance of 10^{-3}, 10^{-4}, and 10^{-5}.

In addition to the total hazard results presented in Figures 6-7 to 6-17, it is useful to show the sensitivity of hazard to the various assumptions specified as inputs. In all of the following sensitivity plots, results are given for both PGA and spectral velocity at 1 and 2.5 Hz, because different elements of the input will have different effects at different frequencies. Figures 6-1 through 6-6, which show hazard results by source, have already indicated that the host source contributes most to the total hazard for both earth science teams, especially for high-frequency ground motions at moderate amplitudes.

Figures 6-18 through 6-20 indicate the mean hazard curves for the two earth science teams, for PGA and spectral velocity at 1 and 2.5 Hz, respectively. The seismological assumptions by the Geomatrix and JMM Teams lead to similar hazards, except for high amplitudes for which the Geomatrix Team predicts higher hazards.

Sensitivity to the choice of attenuation equation is presented in Figures 6-21 for PGA and Figures 6-22 and 6-23 for 1-Hz and 2.5-Hz spectral velocity. These figures show the mean hazards calculated with each of the four ground motion models described in Section 5. The uncertainty in attenuation equations is a major contributor to uncertainty in 1-Hz and 2.5-Hz hazard, but is a moderate contributor to uncertainty in PGA hazard.

The uncertainty in hazard caused by seismicity parameters (i.e., activity rates, b values, and maximum magnitudes) is illustrated in Figures 6-24 through 6-26. This is shown by plotting the uncertainty in hazard, using a single attenuation function and team. These figures show that seismicity parameters are a major contributor to uncertainty at high amplitudes, but is a moderate contributor at lower amplitudes

The uncertainties presented here for the PVNGS site are similar to results obtained in the EPRI/SOG study, in the sense that it contains the same sources of uncertainty.

For reference purposes the basic results presented in Figures 6–7 through 6–17 are repeated in Figures 6–27 through 6–38, without the soil amplification/deamplification factors. Tables 6–3 and 6–4 present the corresponding results in numerical form. These results allow an alternative soil dynamic model to be incorporated, in the event that the deep soil factors described in Section 5 (and used in other Figures and Tables in this Section) wish to be changed.

6.1 COMPARISON WITH SELECTED SITES IN THE EASTERN UNITED STATES

It is useful to compare the seismic hazard results obtained here for PVNGS to results obtained in (1) for sites in the Central and Eastern United States (CEUS). One pertinent site is Pilgrim, which is founded on category-III soil (see Table 2–10) and is located in New England, an area of relatively high seismicity.

Focusing on the spectral velocities at 2.5 Hz, we observe that the hazard at PVNGS is slightly higher than the hazard at Pilgrim for the amplitudes of interest. Comparing the teams' seismological interpretations for both sites, we note that the activity rate per unit area of the host source is slightly higher for PVNGS than for Pilgrim.

The generic site-amplification factors applied at both sites (categories III and IV) are comparable at 2.5 Hz, and are significantly higher than those for the other site categories. The same is true, to a lesser extent, for the amplification factors at 5 Hz. For peak acceleration and for frequencies other than 2.5 and 5 Hz, the site amplification factors for category IV are significantly less severe and the results for PVNGS are more comparable to those of CEUS plants.

Comparisons with other CEUS sites in soil categories III and IV indicate that differences in hazard at 2.5 Hz are consistent with differences in the host source's rate per unit area.

6.2 REFERENCES

1. R. K. McGuire, G. R. Toro, J. P. Jacobson, T. F. O'Hara, and W. J. Silva. *Probabilistic Seismic Hazard Evaluations in the Central and Eastern United States: Resolution of the Charleston Earthquake Issue.* Special Report NP-6395-D, Electric Power Research Institute, April 1989.

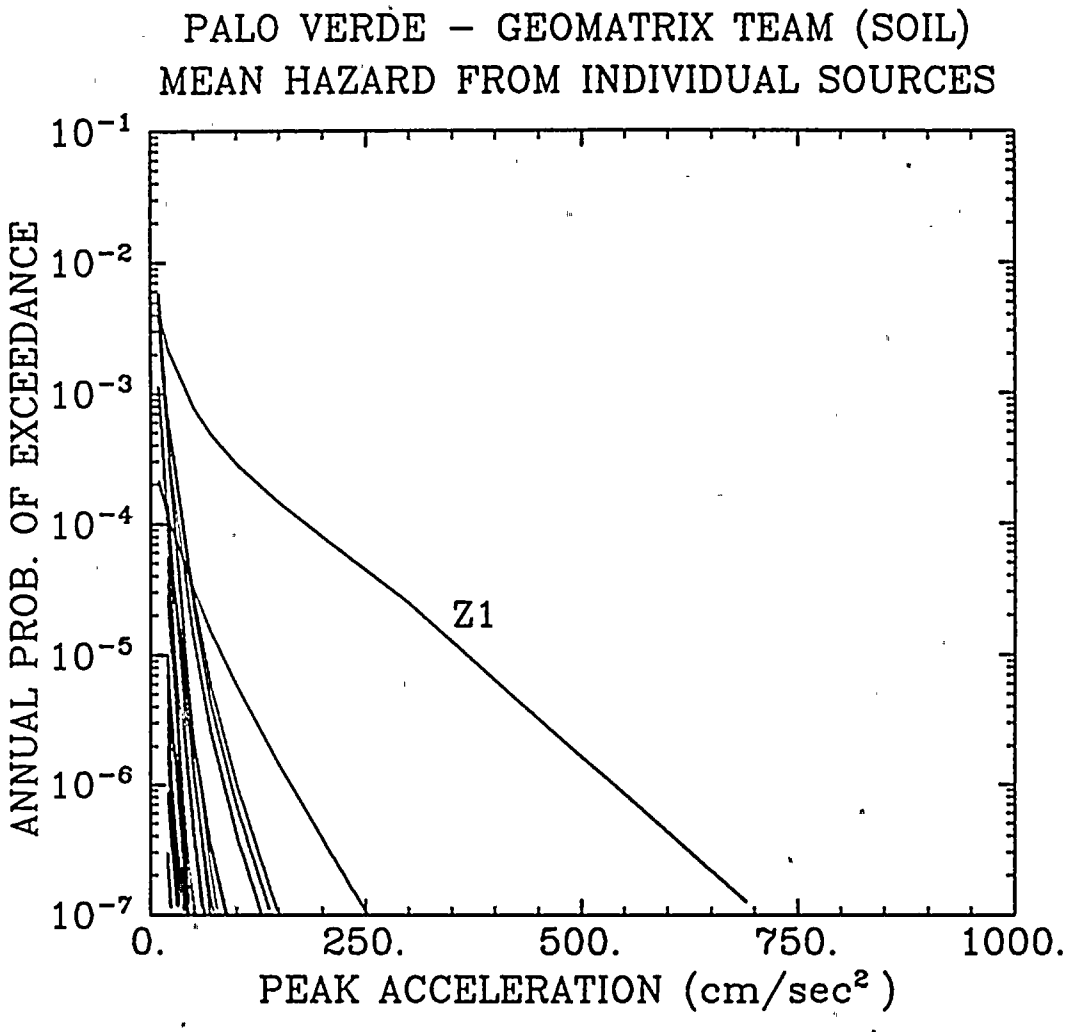

Figure 6-1. Annual probability of exceedance of peak ground acceleration. Mean hazard contributed by each Geomatrix seismic source.

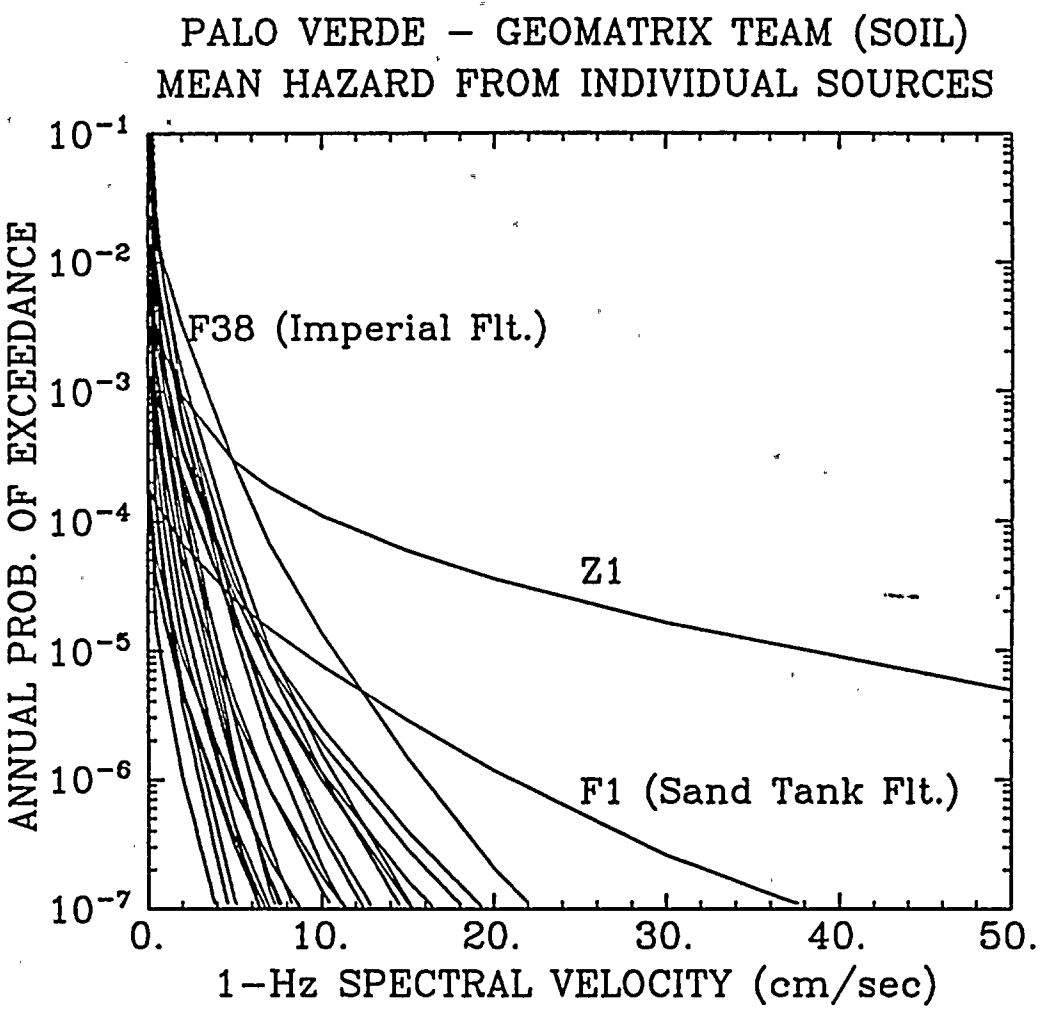

Figure 6-2. Annual probability of exceedance of 1-Hz spectral velocity. Mean hazard contributed by each Geomatrix seismic source.

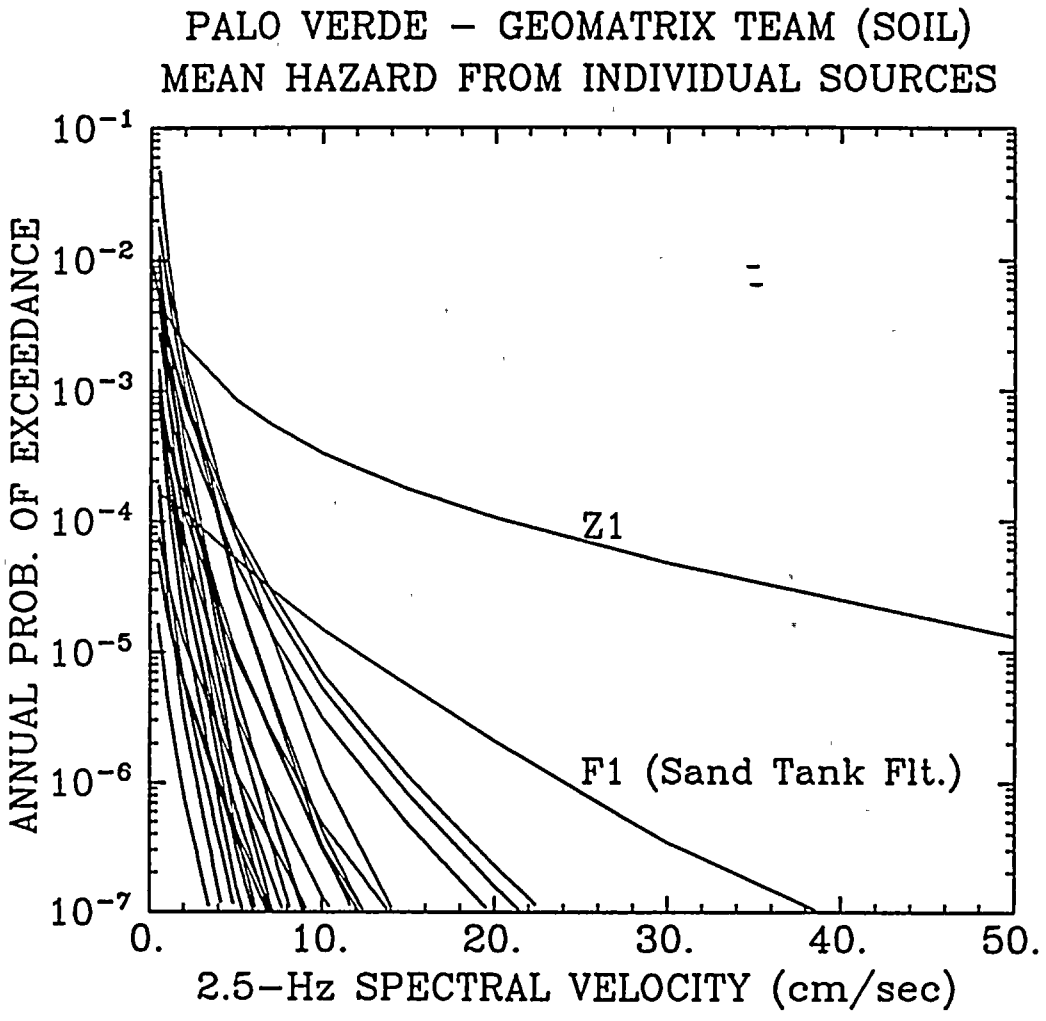

Figure 6-3. Annual probability of exceedance of 2.5-Hz spectral velocity. Mean hazard contributed by each Geomatrix seismic source.

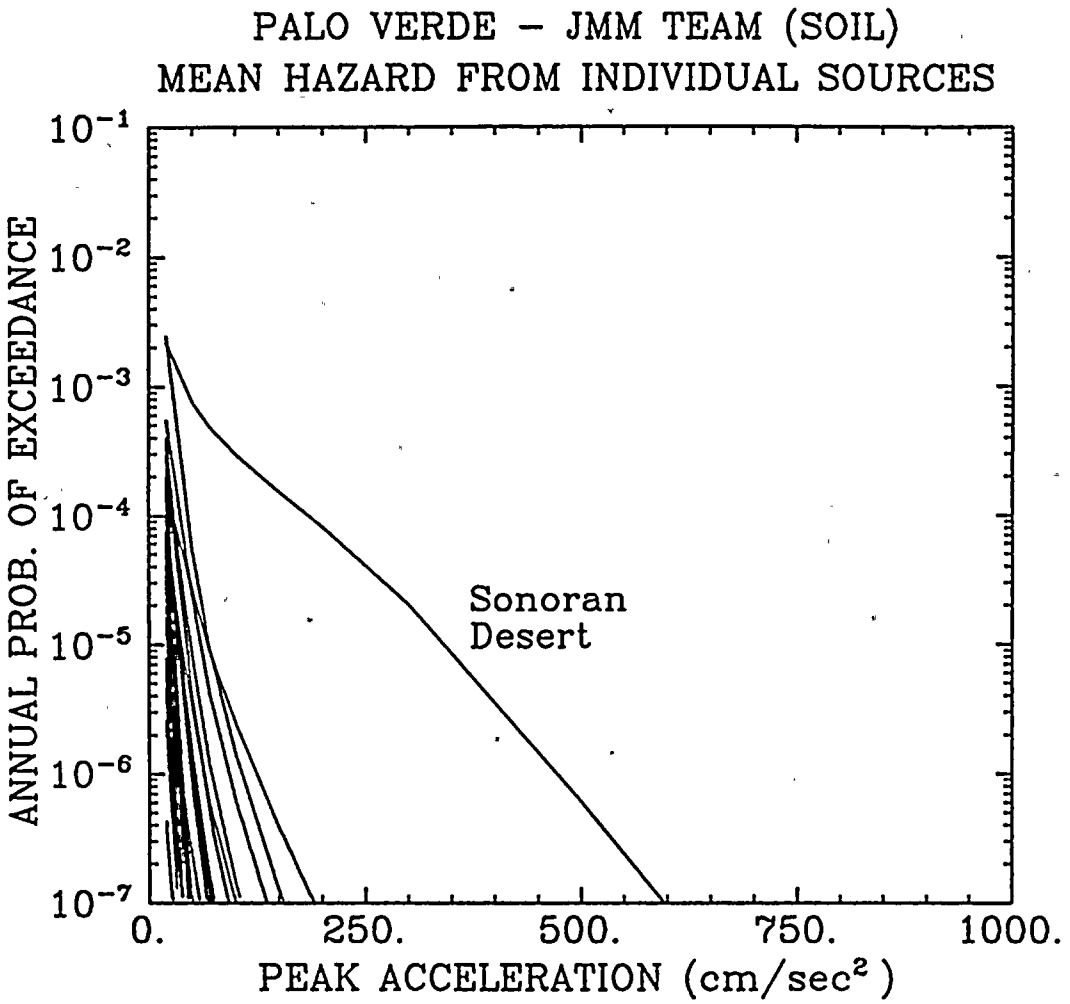

Figure 6-4. Annual probability of exceedance of peak ground acceleration. Mean hazard contributed by each JMM seismic source.

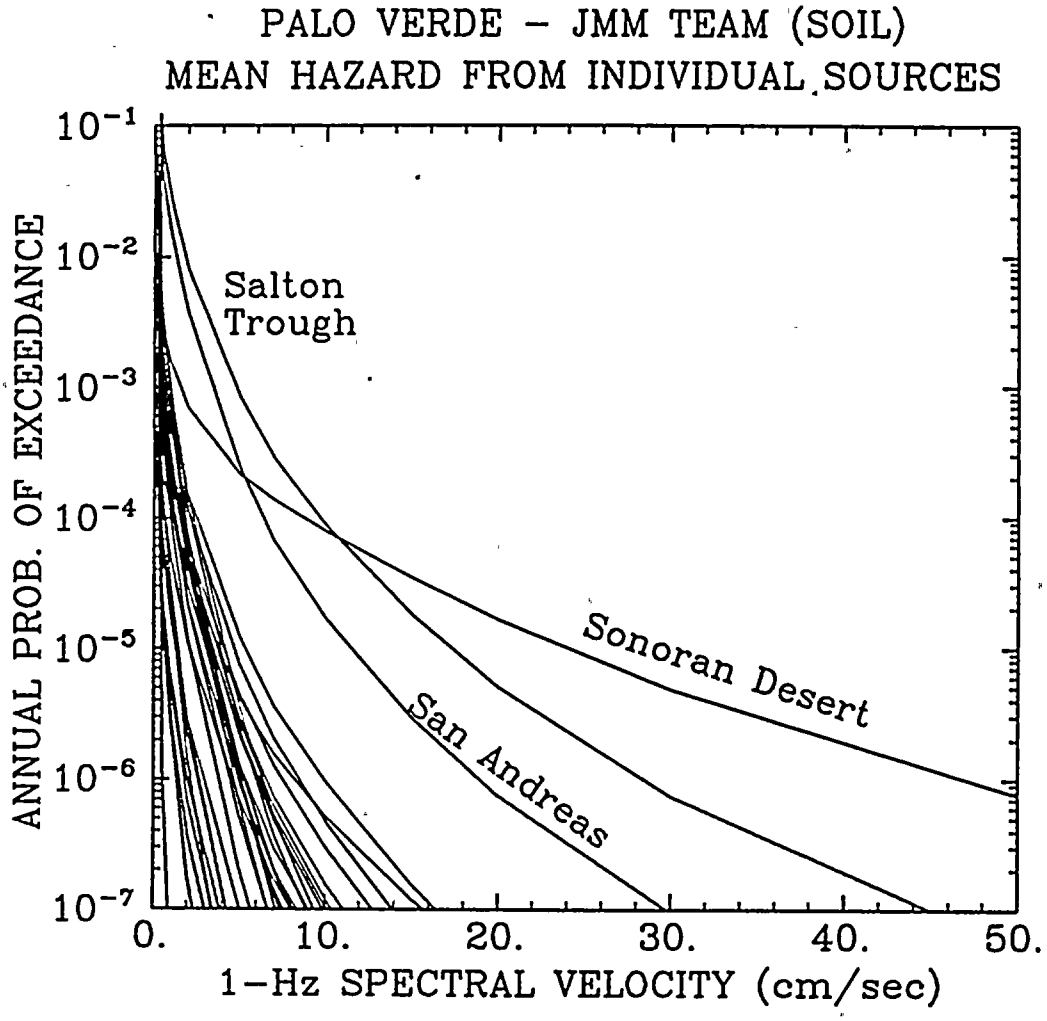

Figure 6-5. Annual probability of exceedance of 1-Hz spectral velocity. Mean hazard contributed by each JMM seismic source.

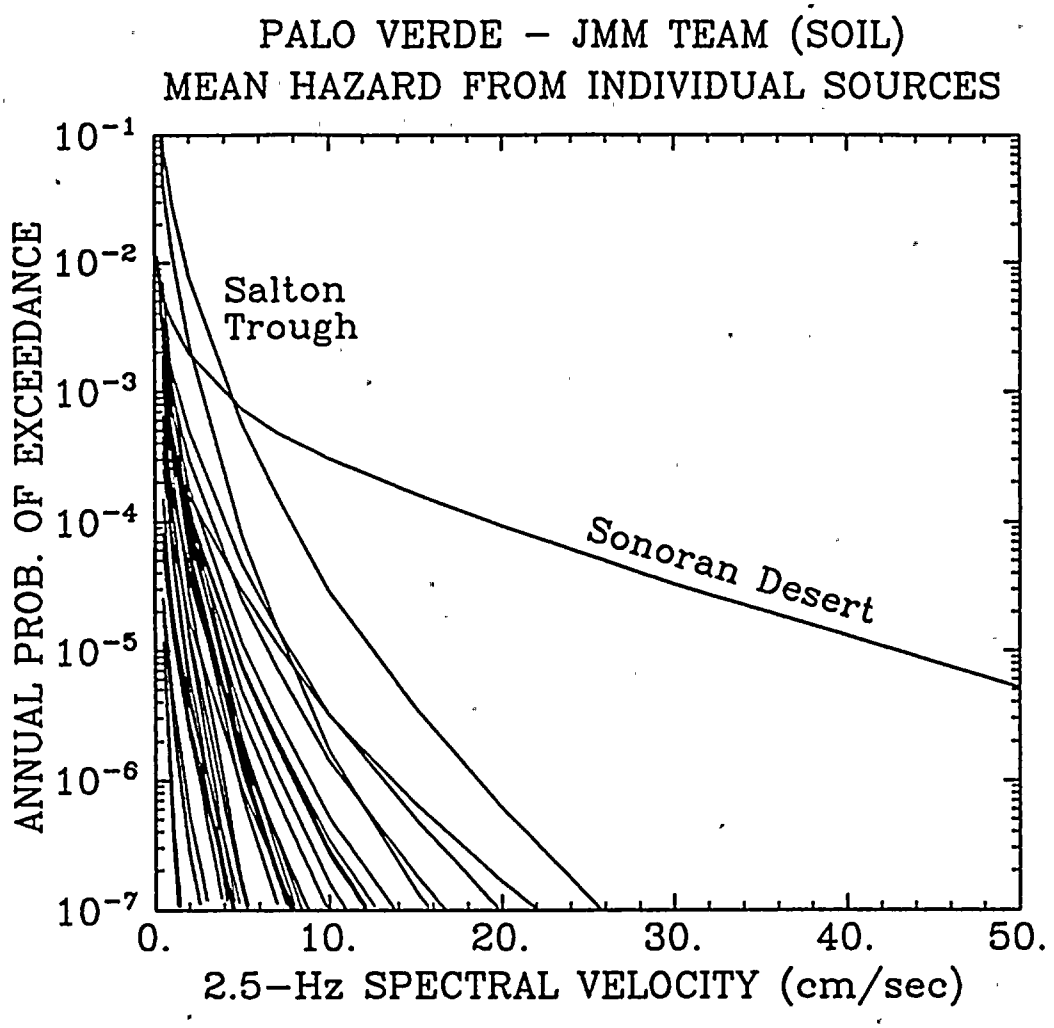

Figure 6-6. Annual probability of exceedance of 2.5-Hz spectral velocity. Mean hazard contributed by each JMM seismic source.

Table 6-1

ANNUAL PROBABILITY OF EXCEEDANCE FOR
PEAK GROUND ACCELERATION:
PALO VERDE SITE (SOIL)

Acceleration (cm/sec^2)	Mean	Percentiles		
		15	50	85
10	3.0E−02	3.7E−03	1.0E−02	4.8E−02
20	5.7E−03	1.3E−03	3.0E−03	9.8E−03
50	9.1E−04	3.1E−04	7.1E−04	1.5E−03
70	5.3E−04	1.8E−04	4.1E−04	8.7E−04
100	3.0E−04	1.0E−04	2.5E−04	5.0E−04
150	1.5E−04	3.6E−05	1.2E−04	2.7E−04
200	7.9E−05	6.9E−06	5.5E−05	1.5E−04
300	2.2E−05	5.6E−07	7.4E−06	5.0E−05
500	1.1E−06	6.0E−09	6.8E−08	1.4E−06
1000	9.3E−10	3.6E−12	1.7E−10	1.6E−09

Table 6-2

SPECTRAL VELOCITIES (cm/sec) FOR
VARIOUS EXCEEDANCE PROBABILITIES:
PALO VERDE SITE (SOIL)

		Frequency (Hz)				
		25	10	5	2.5	1
Exceedance		Period (sec)				
Probability	Percentile	0.04	0.1	0.2	0.4	1
1.E−03	15	0.11	0.55	1.90	2.84	2.00
	50	0.19	1.06	3.24	4.80	3.79
	85	0.34	2.00	5.44	7.58	6.54
2.E−04	15	0.29	1.93	5.99	7.60	4.07
	50	0.54	3.34	10.10	12.20	7.46
	85	0.86	5.99	15.10	19.40	12.20
1.E−04	15	0.45	2.61	8.45	10.60	5.45
	50	0.75	5.04	13.20	17.00	9.82
	85	1.17	8.45	20.10	26.80	16.00
1.E−05	15	1.08	6.07	17.20	22.40	11.20
	50	1.63	10.10	25.20	36.30	21.30
	85	2.23	15.50	36.40	56.40	39.40

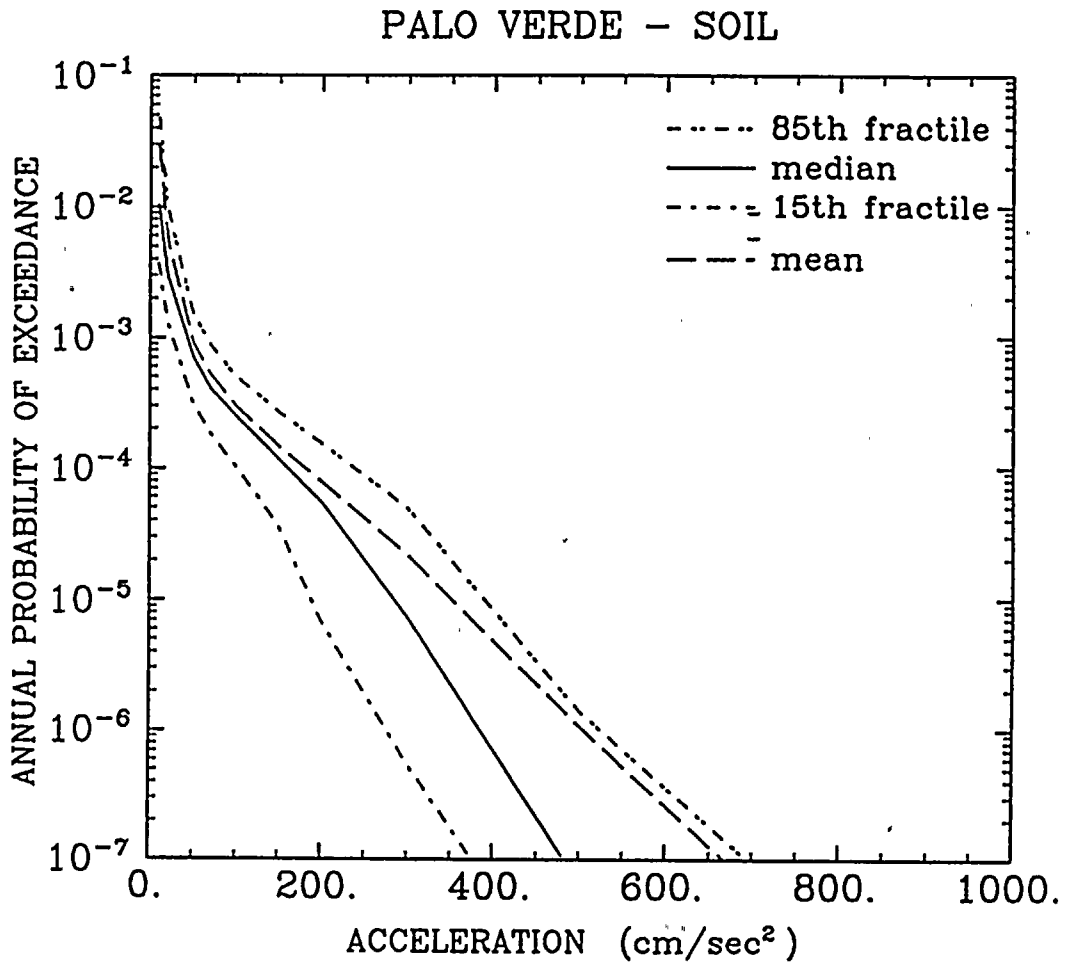

Figure 6-7. Annual probability of exceedance of peak acceleration: Palo Verde site (soil site conditions).

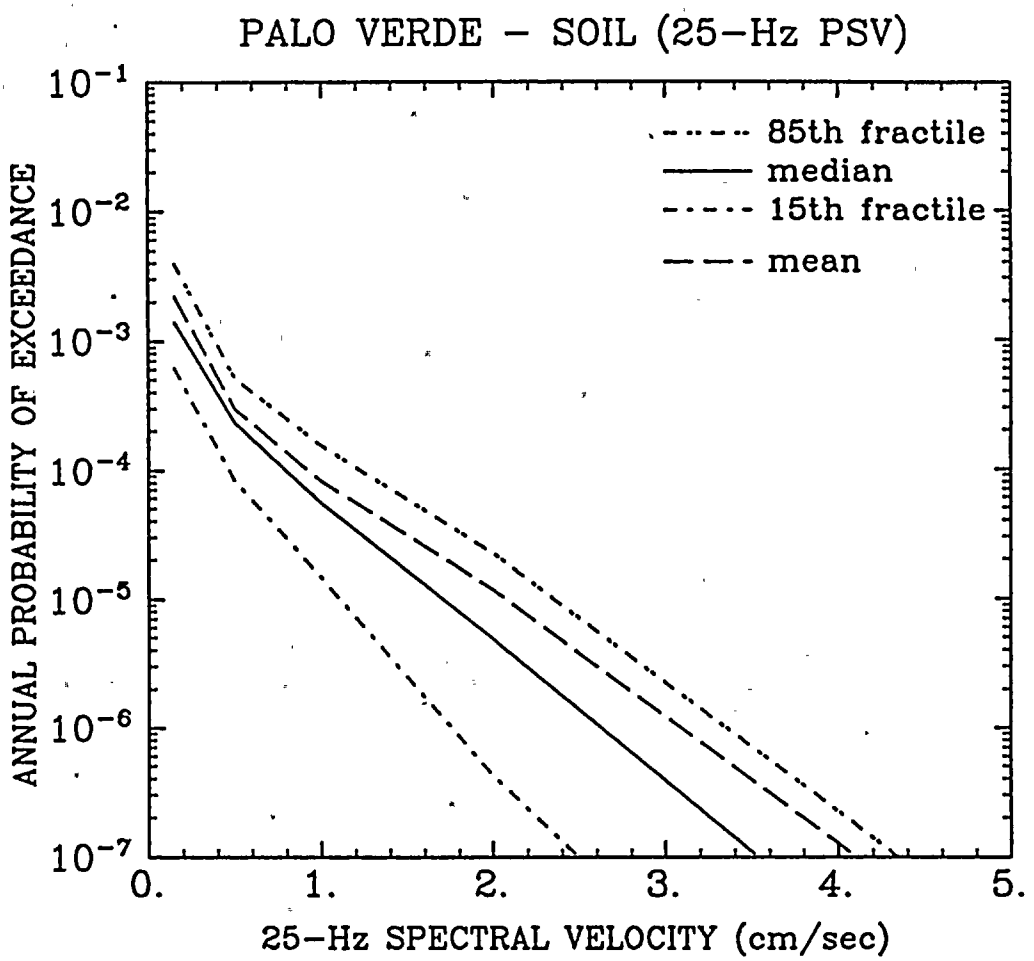

Figure 6-8. Annual probability of exceedance of 25-Hz spectral velocity: Palo Verde site (soil site conditions).

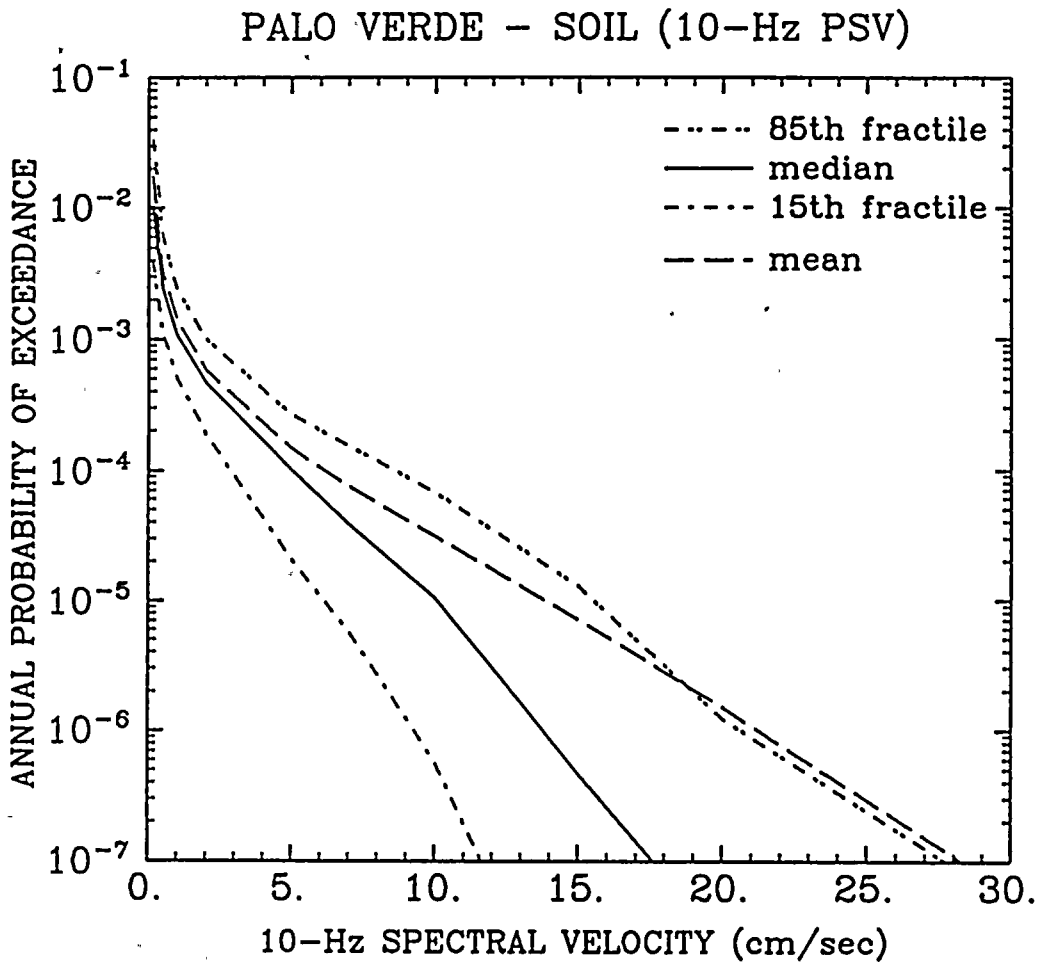

Figure 6-9. Annual probability of exceedance of 10-Hz spectral velocity: Palo Verde site (soil site conditions).

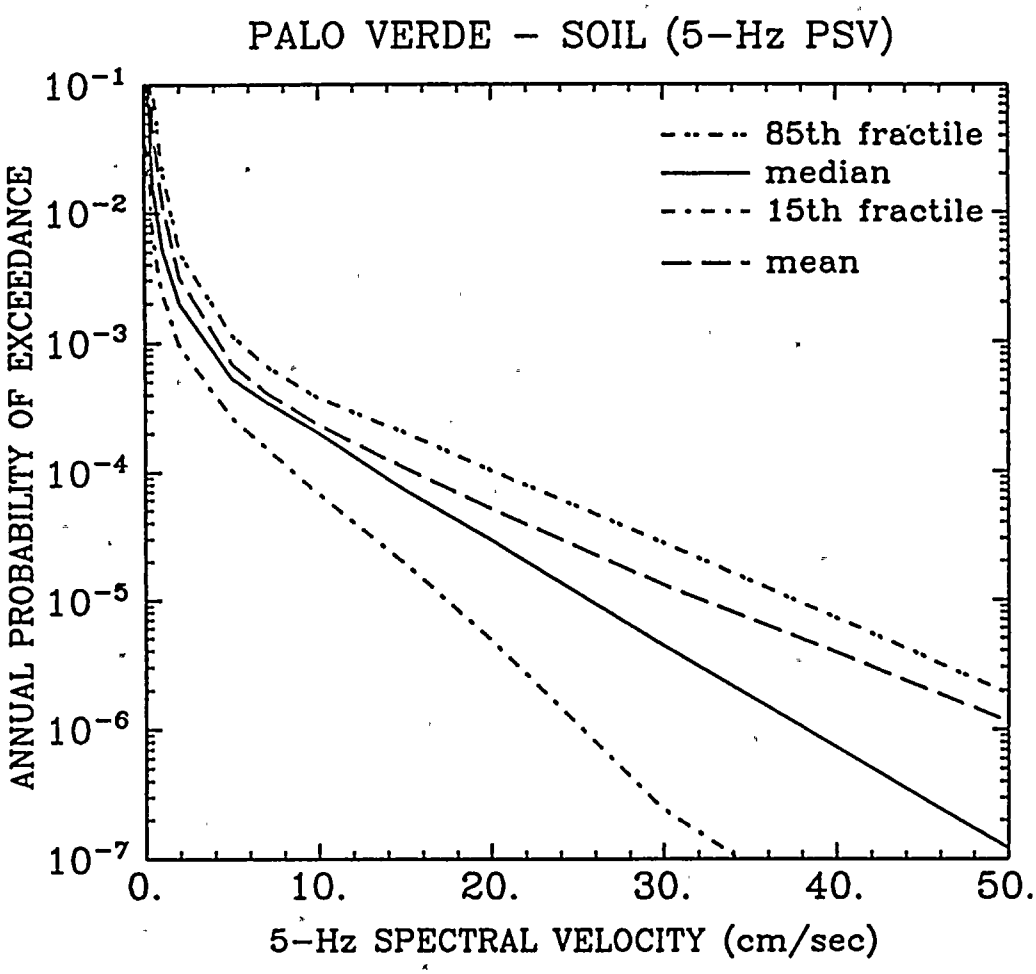

Figure 6-10. Annual probability of exceedance of 5-Hz spectral velocity: Palo Verde site (soil site conditions).

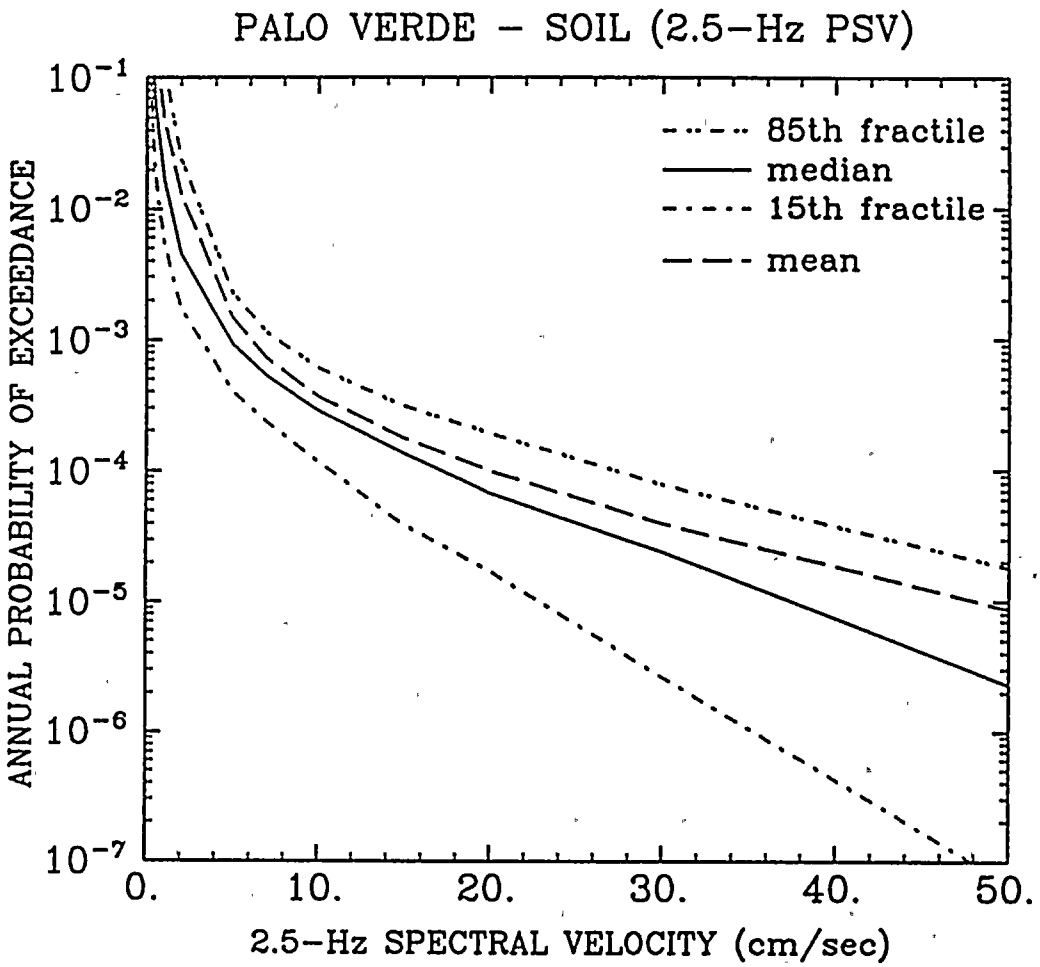

Figure 6-11. Annual probability of exceedance of 2.5-Hz spectral velocity: Palo Verde site (soil site conditions).

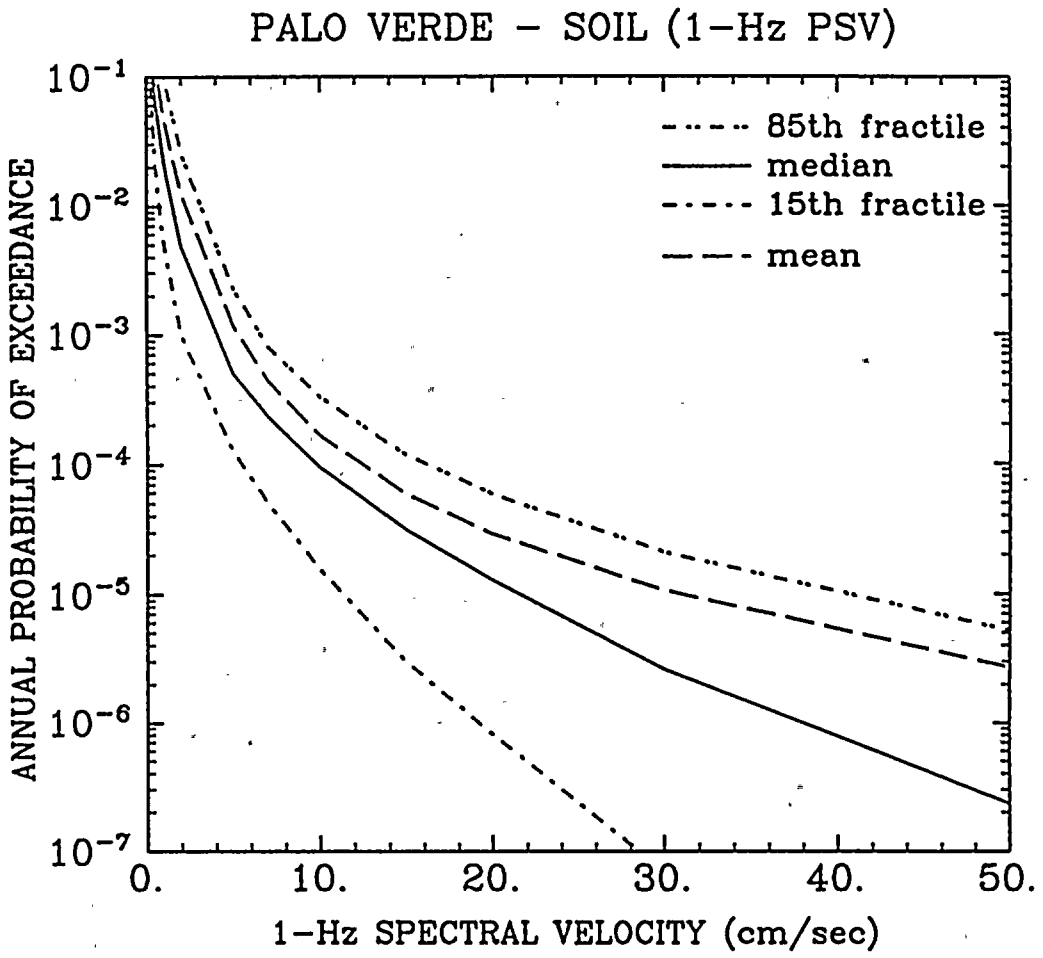

Figure 6-12. Annual probability of exceedance of 1-Hz spectral velocity: Palo Verde site (soil site conditions).

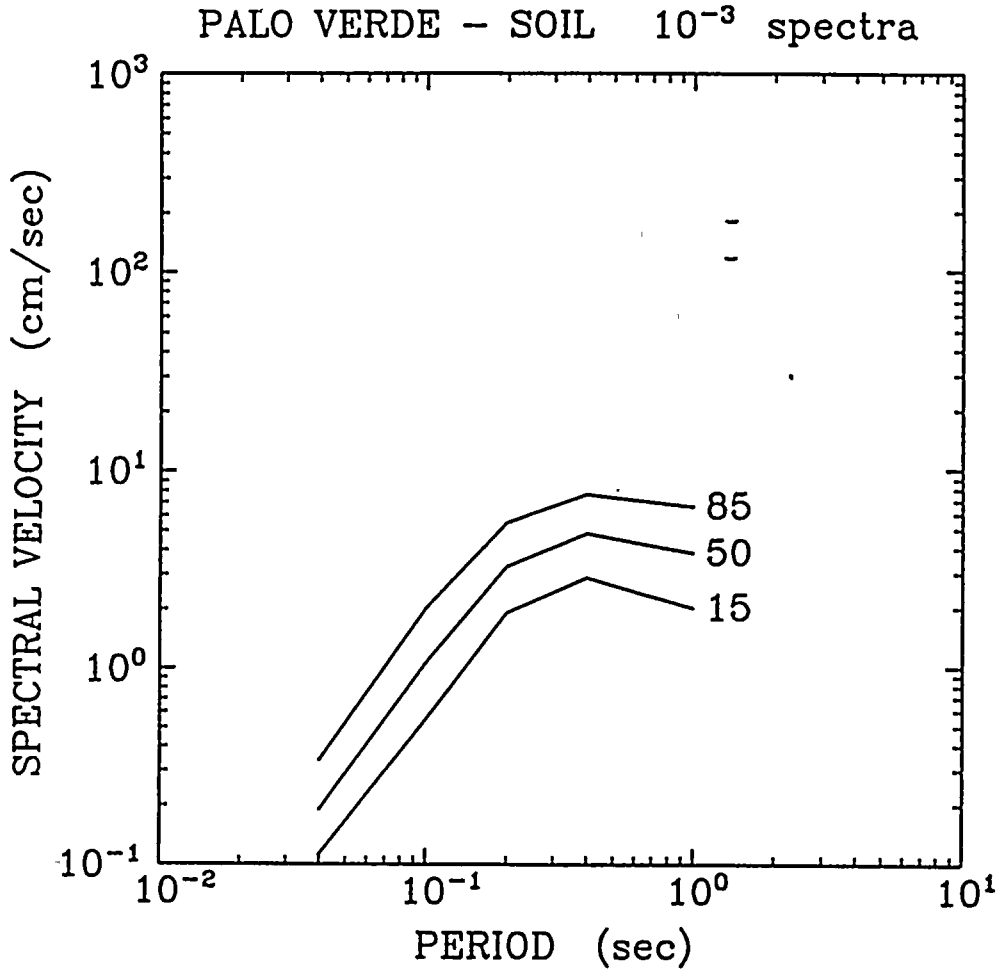

Figure 6-13. Uniform hazard spectra for the 10^{-3} annual probability of exceedance: Palo Verde site (soil site conditions). Spectra shown for three percentiles: 15^{th}, 50^{th}, and 85^{th}.

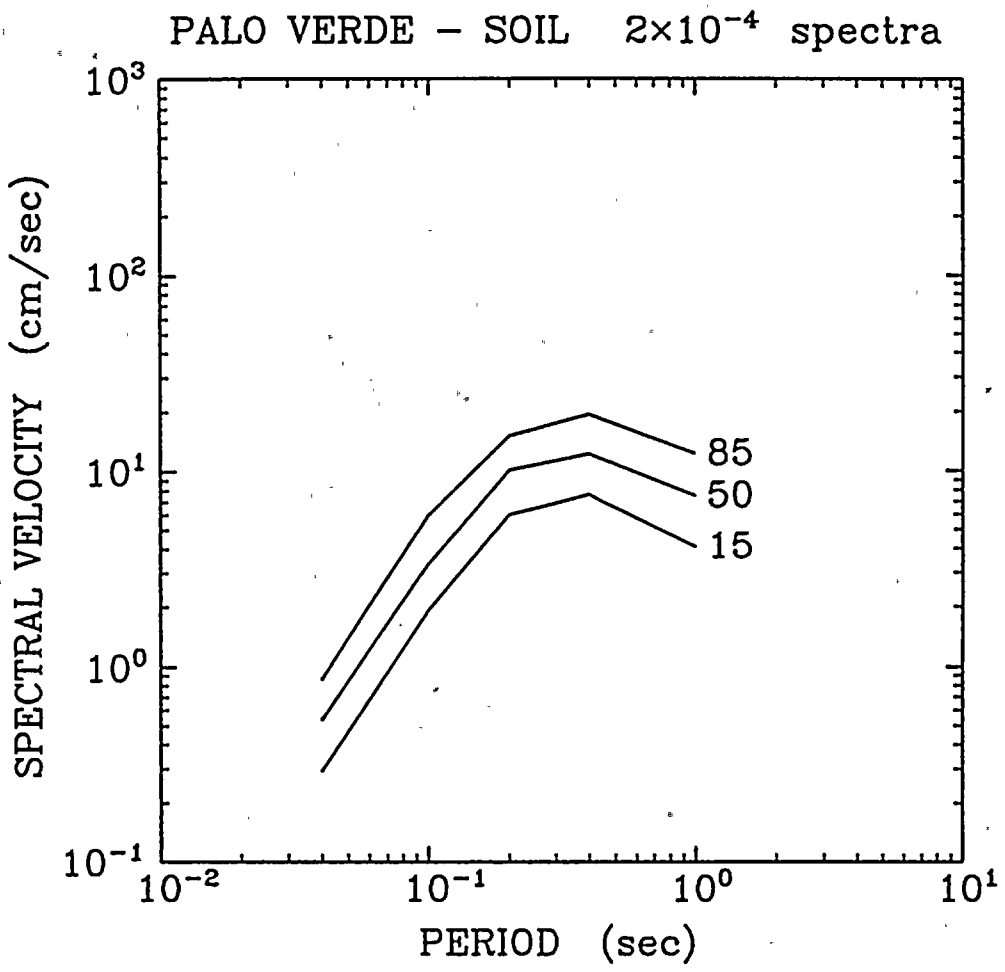

Figure 6-14. Uniform hazard spectra for the 2×10^{-4} annual probability of exceedance: Palo Verde site (soil site conditions). Spectra shown for three percentiles: 15^{th}, 50^{th}, and 85^{th}.

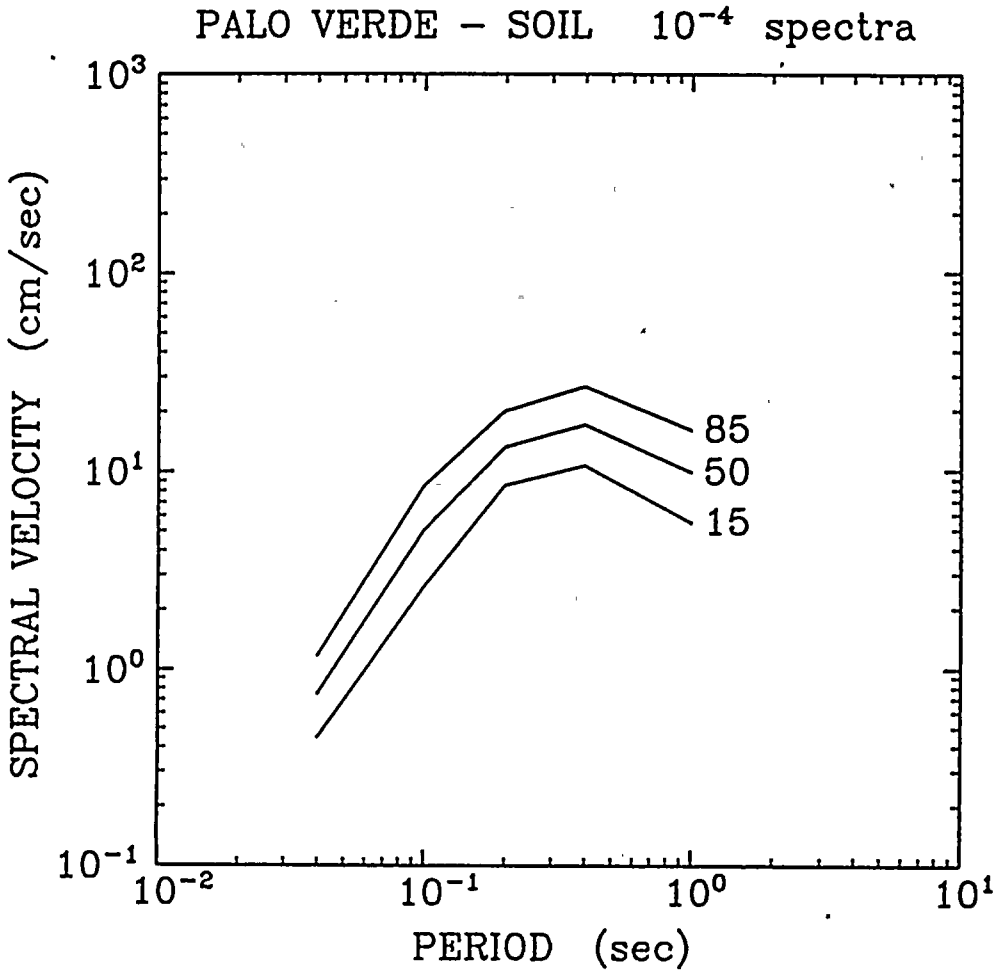

Figure 6-15. Uniform hazard spectra for the 10^{-4} annual probability of exceedance: Palo Verde site (soil site conditions). Spectra shown for three percentiles: 15^{th}, 50^{th}, and 85^{th}.

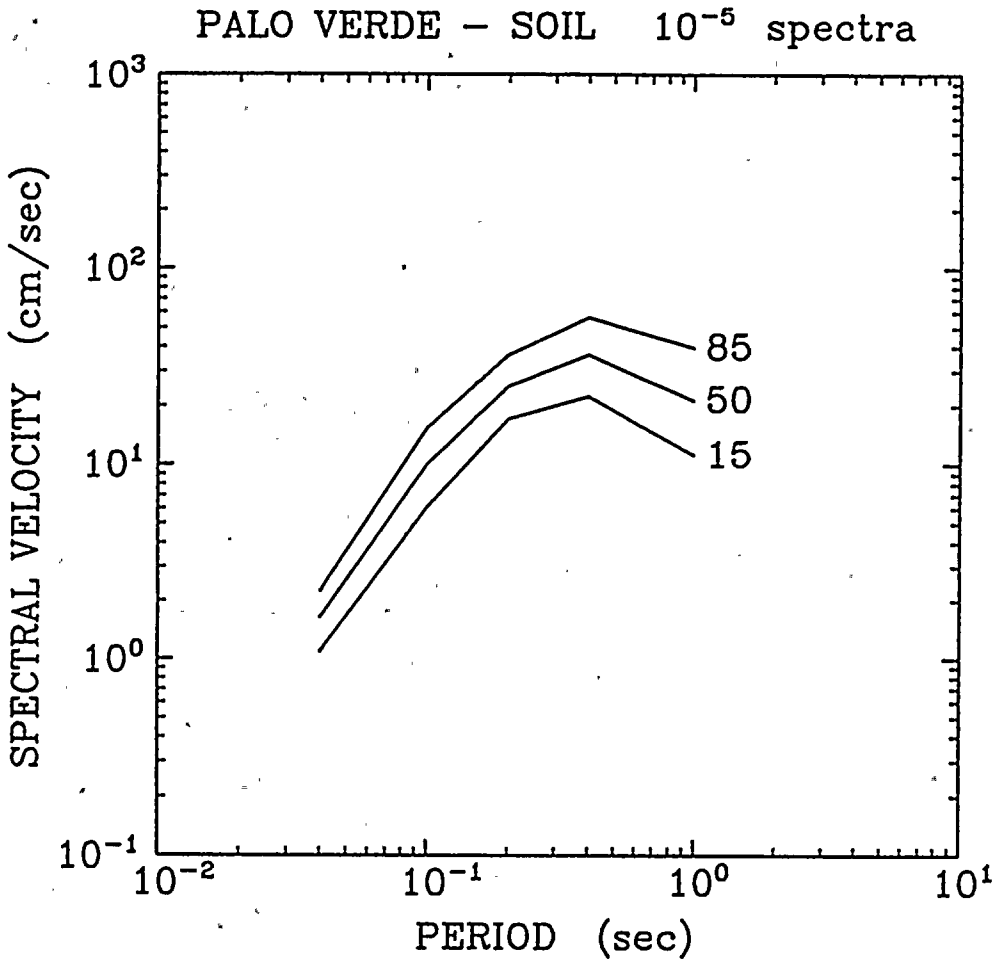

Figure 6-16. Uniform hazard spectra for the 10^{-5} annual probability of exceedance: Palo Verde site (soil site conditions). Spectra shown for three percentiles: 15^{th}, 50^{th}, and 85^{th}.

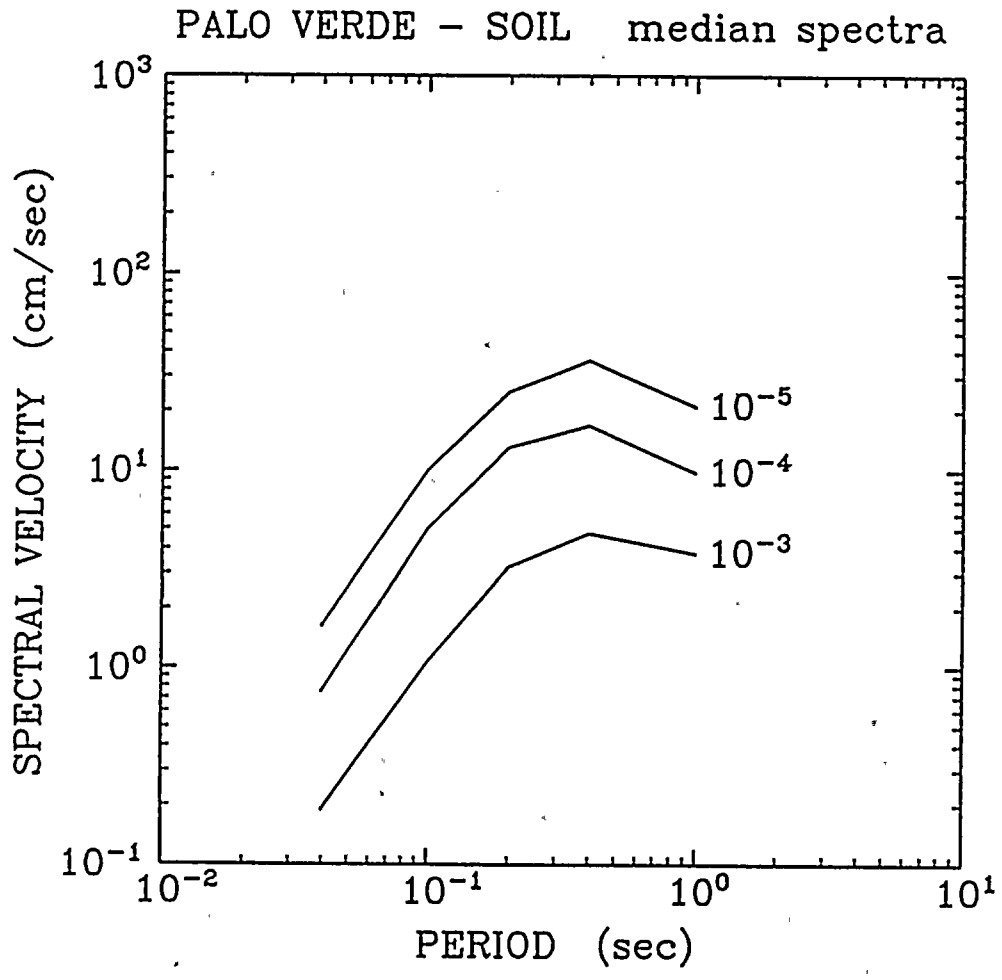

Figure 6-17. Median uniform hazard spectra for the 10^{-3},10^{-4}, and 10^{-5}probability of exceedance: Palo Verde site.

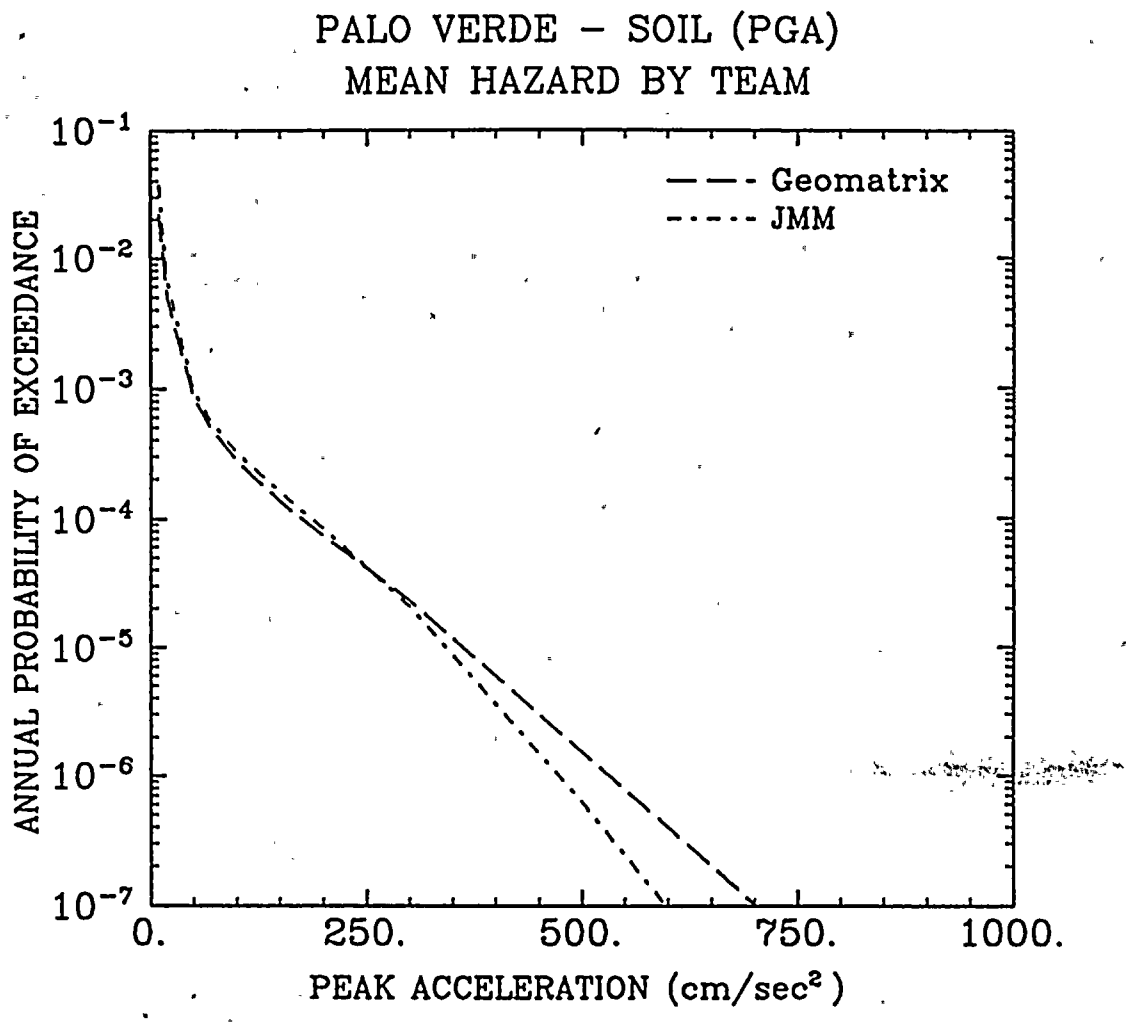

Figure 6-18. Annual probability of exceedance of peak acceleration. Mean hazard calculated by each team.

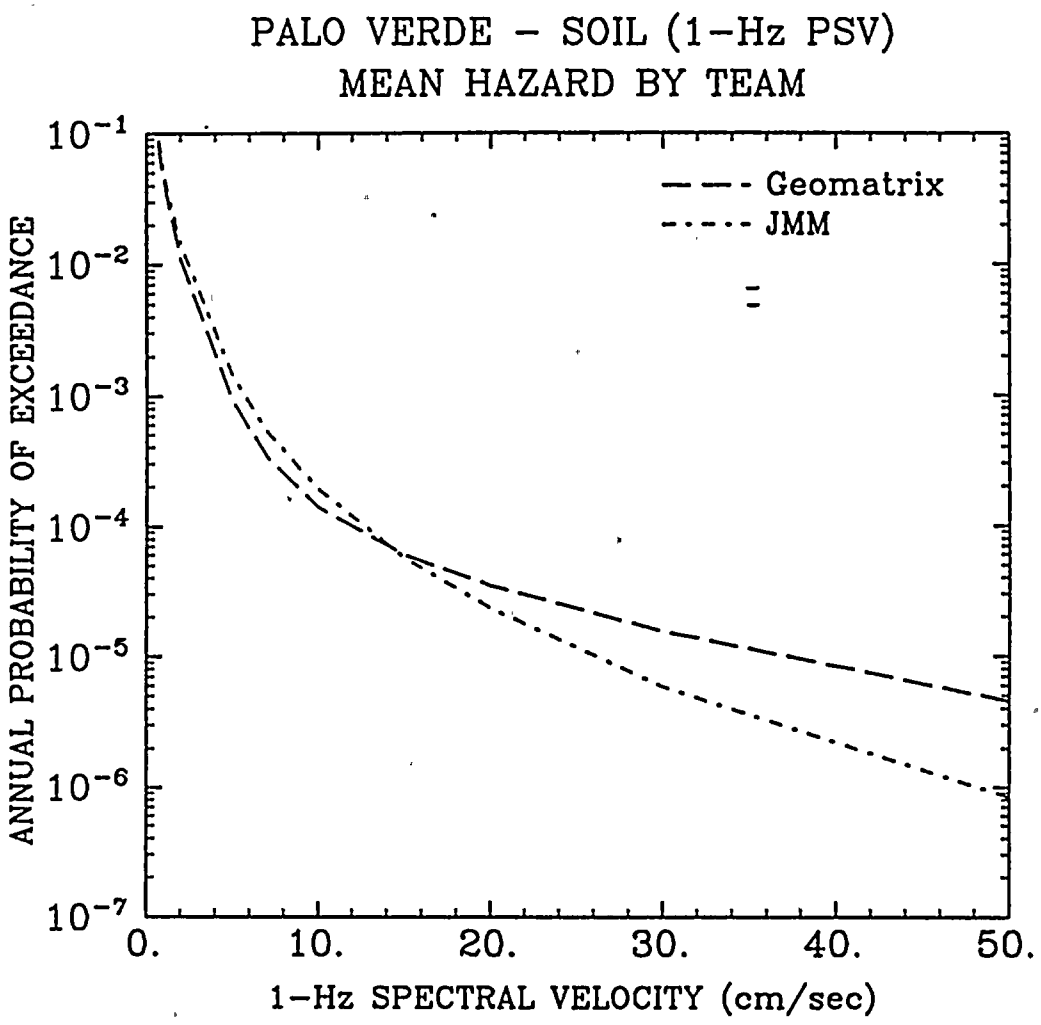

Figure 6-19. Annual probability of exceedance of 1-Hz spectral velocity. Mean hazard calculated by each team.

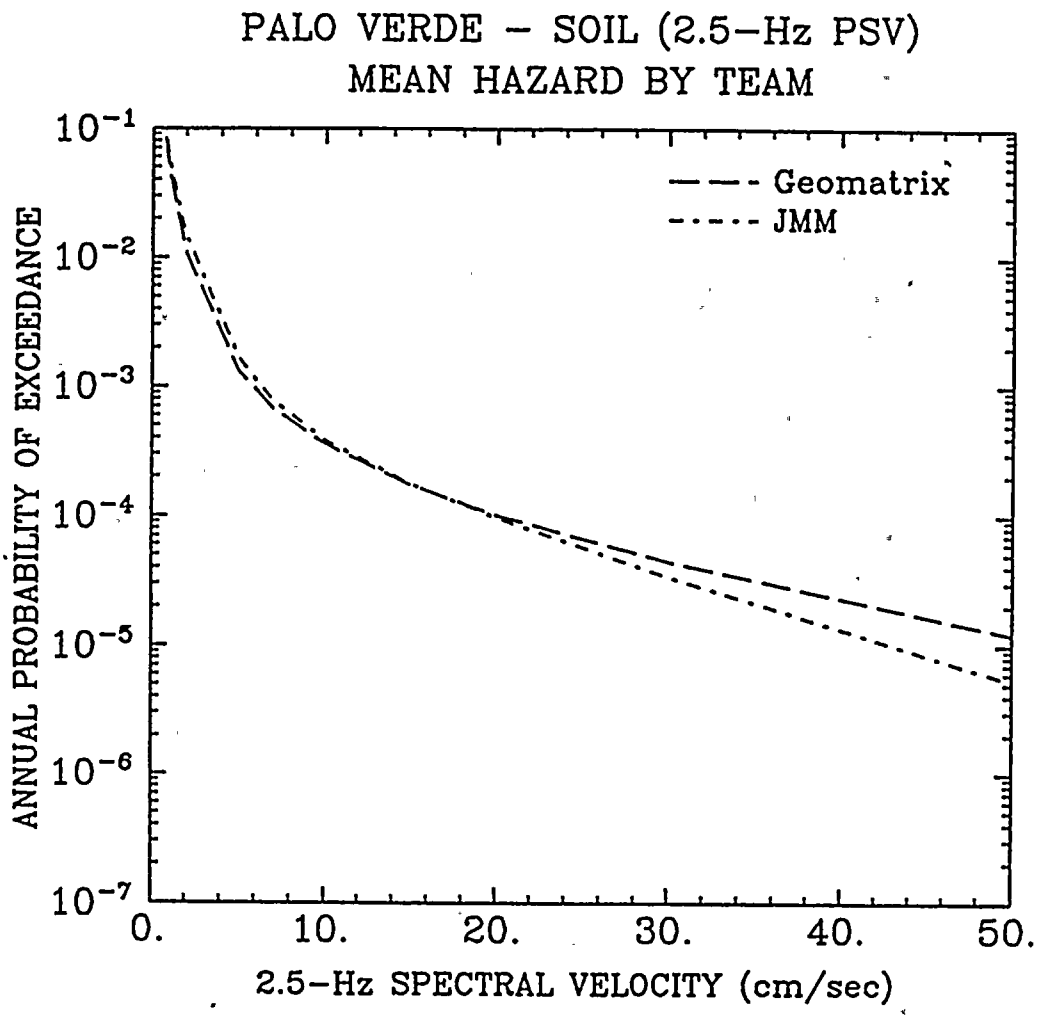

Figure 6-20. Annual probability of exceedance of 2.5-Hz spectral velocity. Mean hazard calculated by each team.

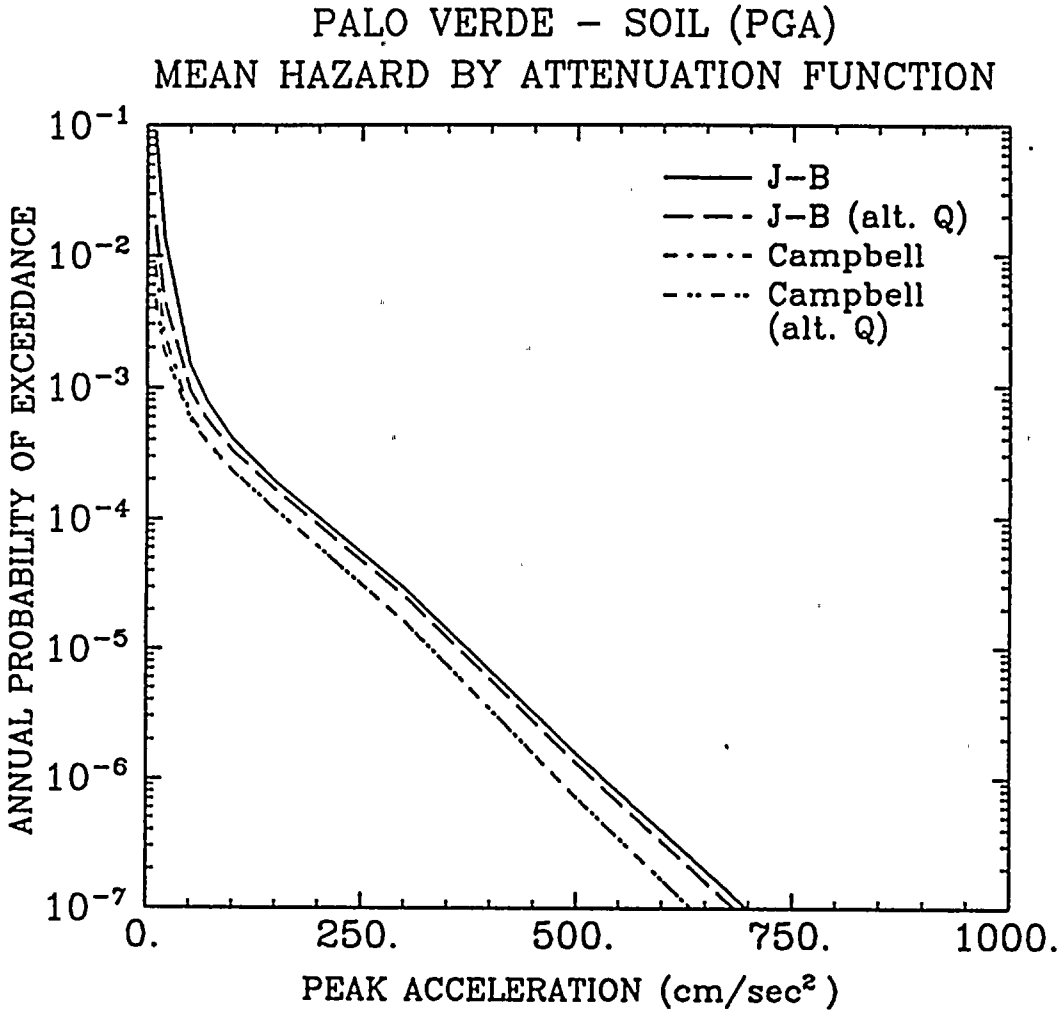

Figure 6-21. Annual probability of exceedance of peak acceleration. Sensitivity to attenuation functions.

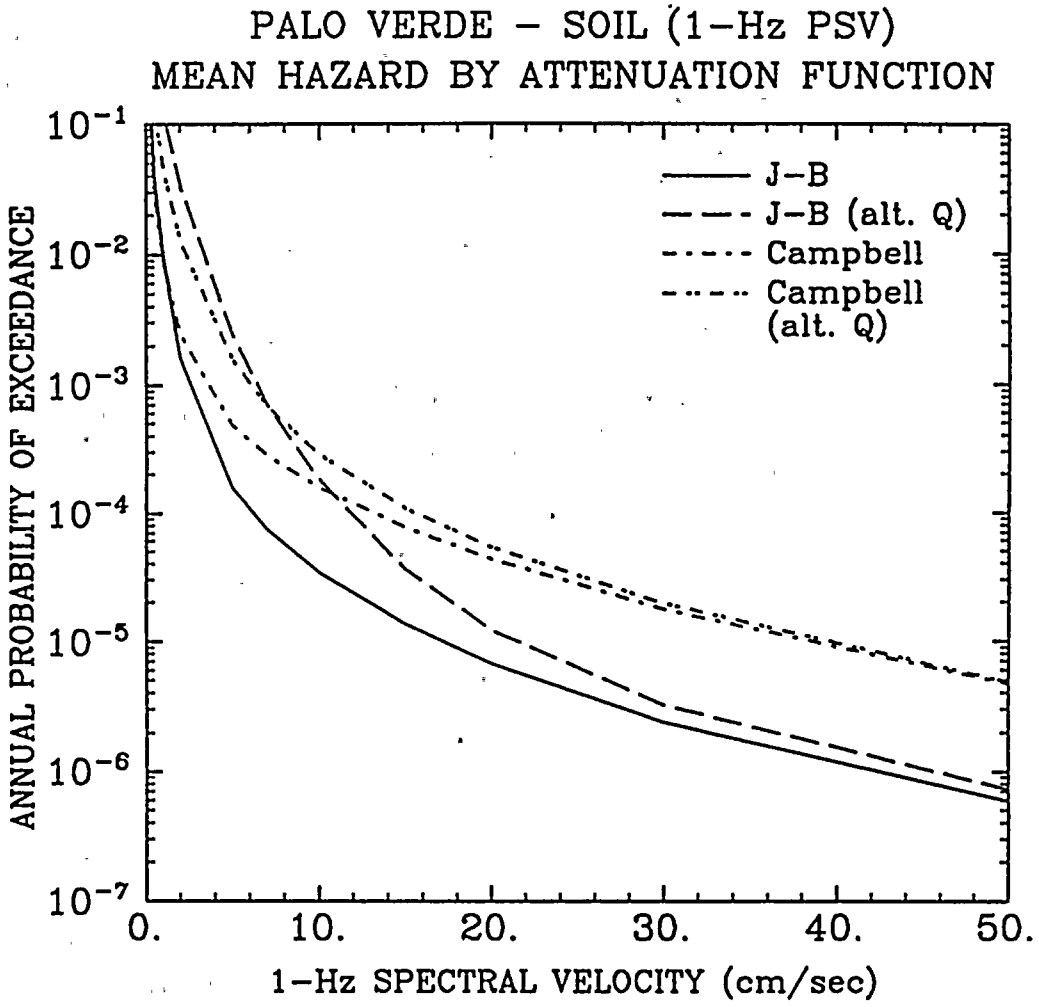

Figure 6-22. Annual probability of exceedance of 1-Hz spectral velocity. Sensitivity to attenuation functions.

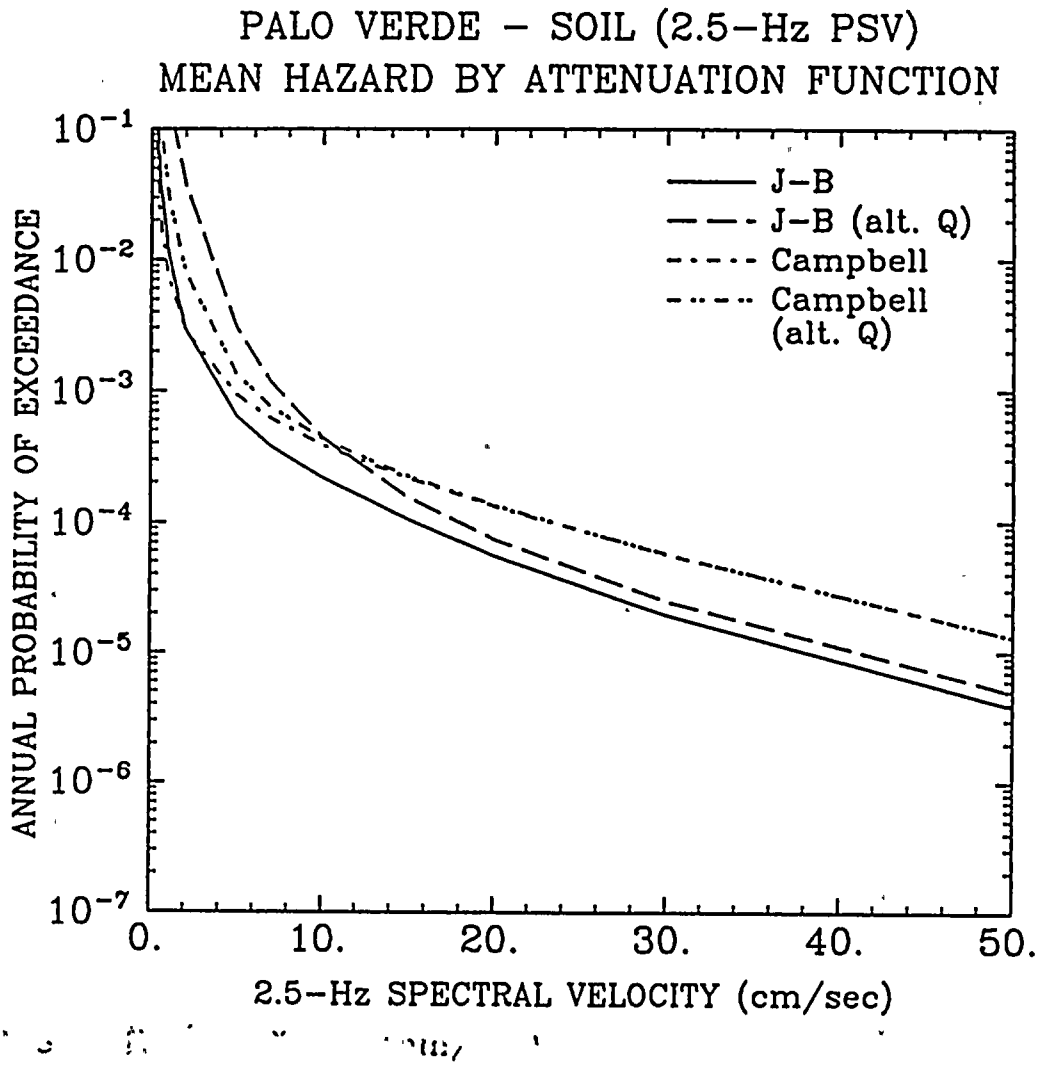

Figure 6-23. Annual probability of exceedance of 2.5-Hz spectral velocity. Sensitivity to attenuation functions.

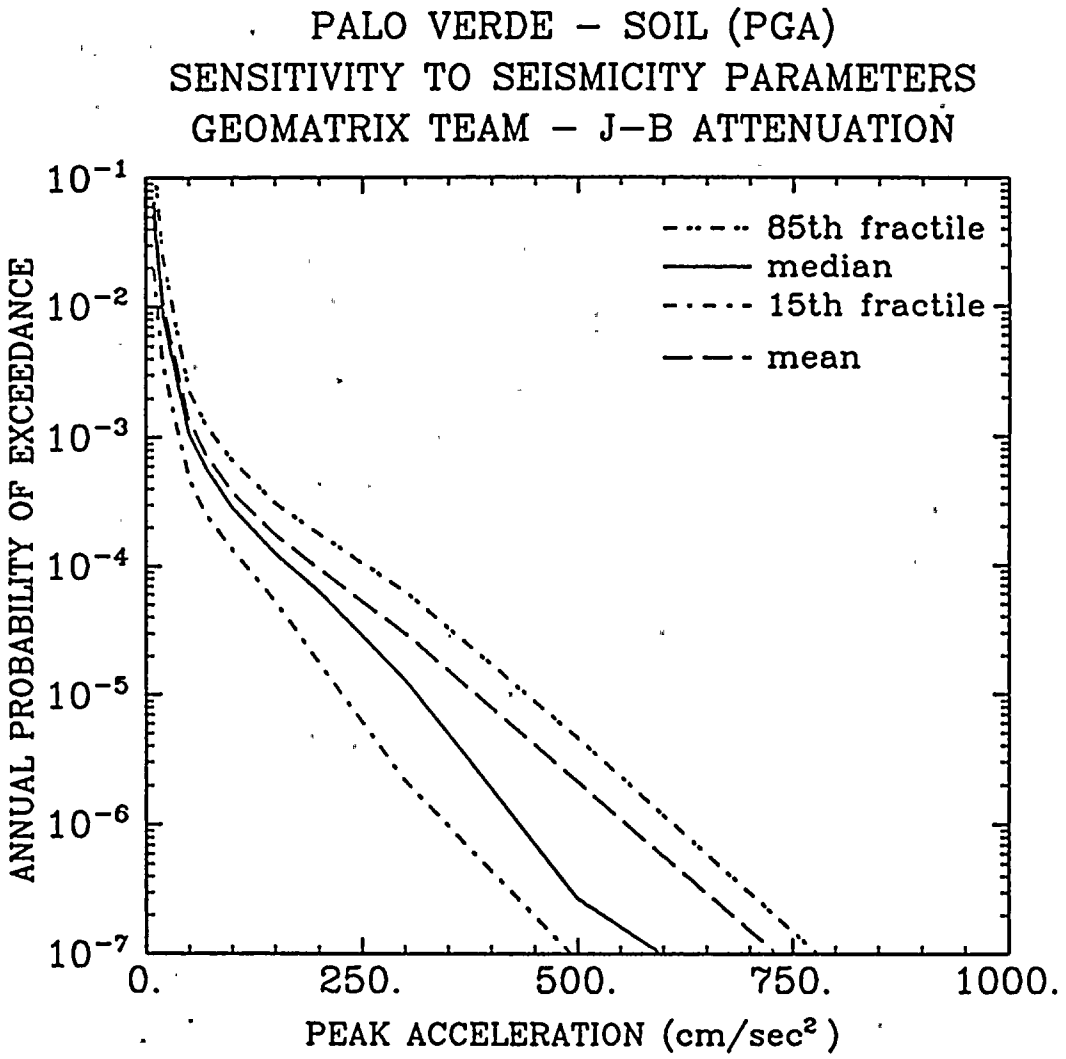

Figure 6-24. Annual probability of exceedance of peak acceleration. Sensitivity to seismicity parameters: Geomatrix team.

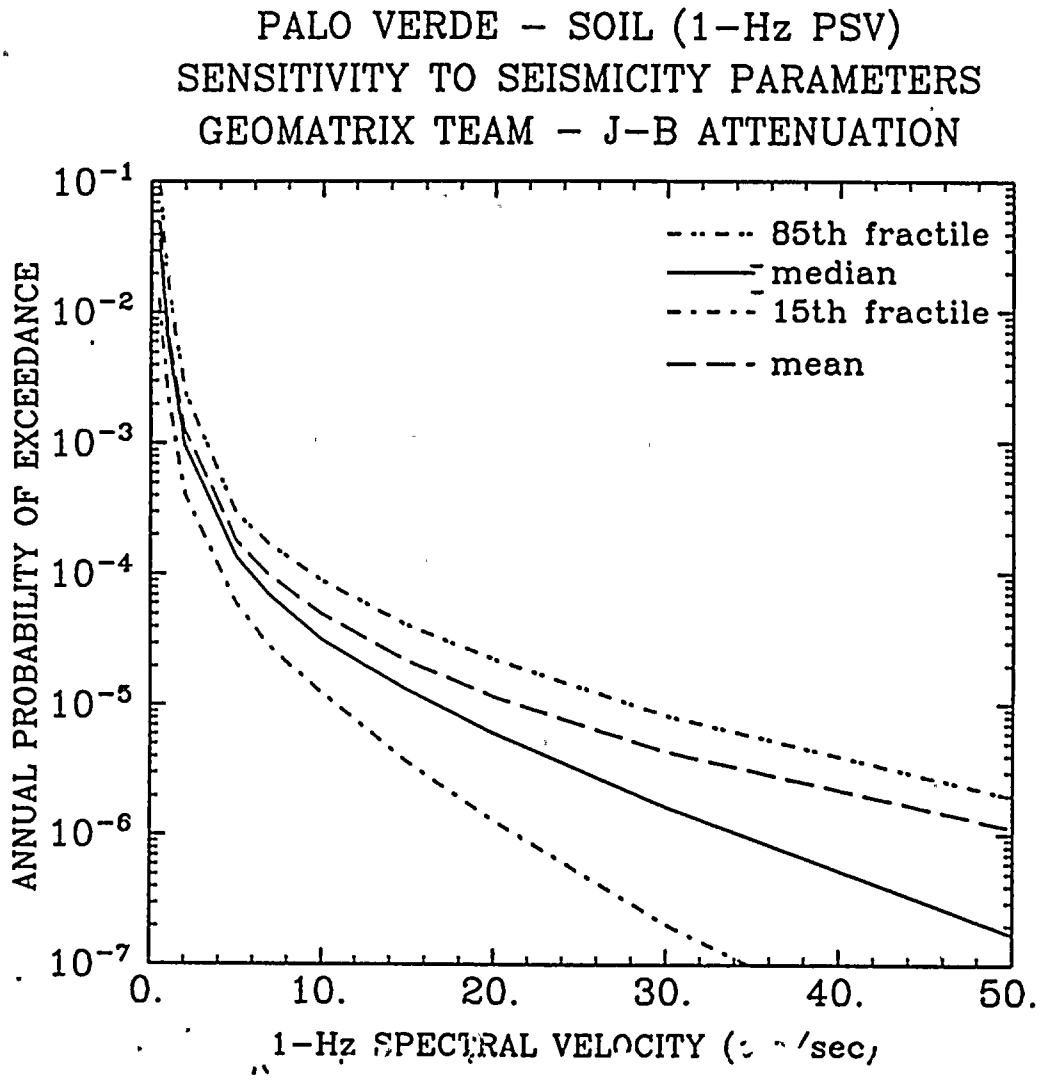

Figure 6-25. Annual probability of exceedance of 1-Hz spectral velocity. Sensitivity to seismicity parameters: Geomatrix team.

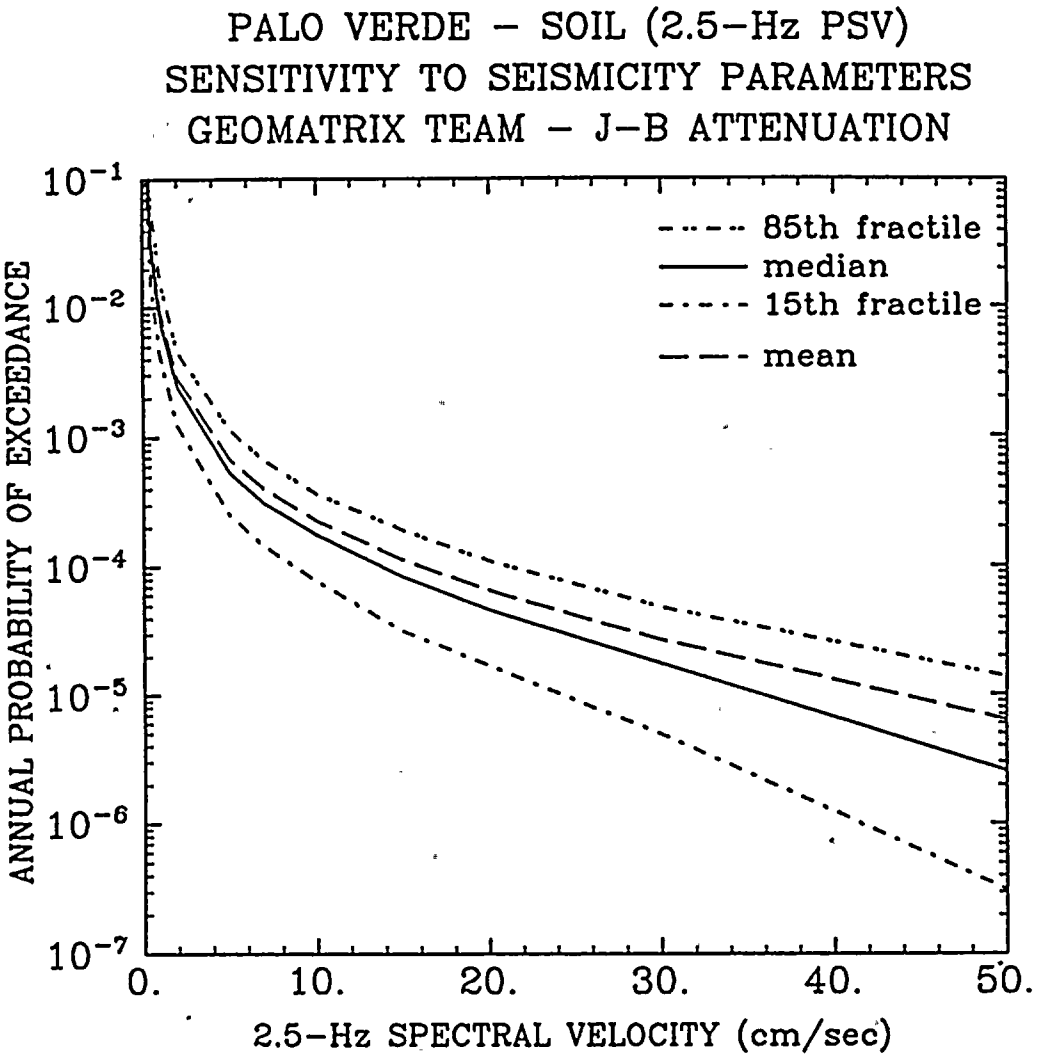

Figure 6-26. Annual probability of exceedance of 2.5-Hz spectral velocity. Sensitivity to seismicity parameters: Geomatrix team.

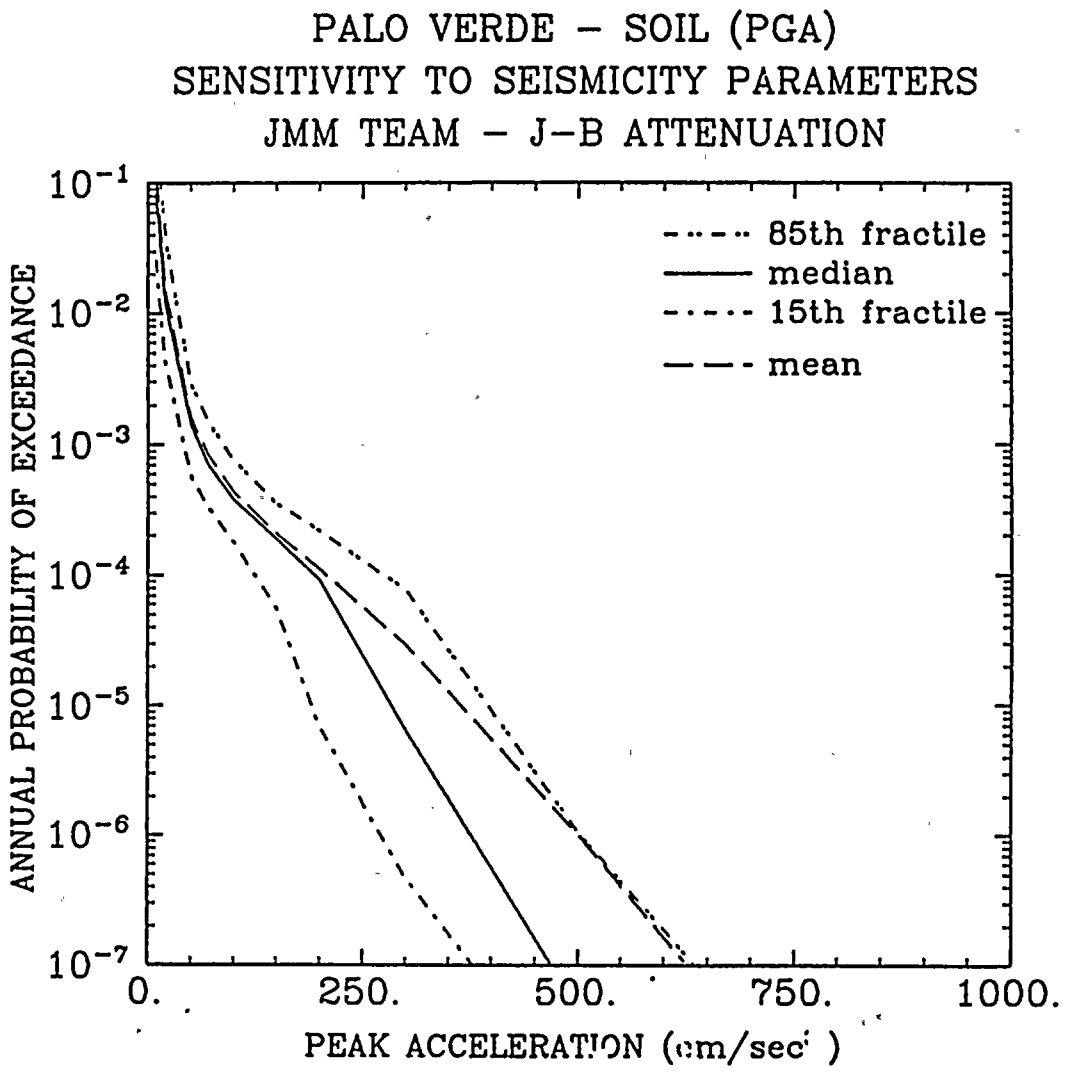

Figure 6-27. Annual probability of exceedance of peak acceleration. Sensitivity to seismicity parameters: JMM team.

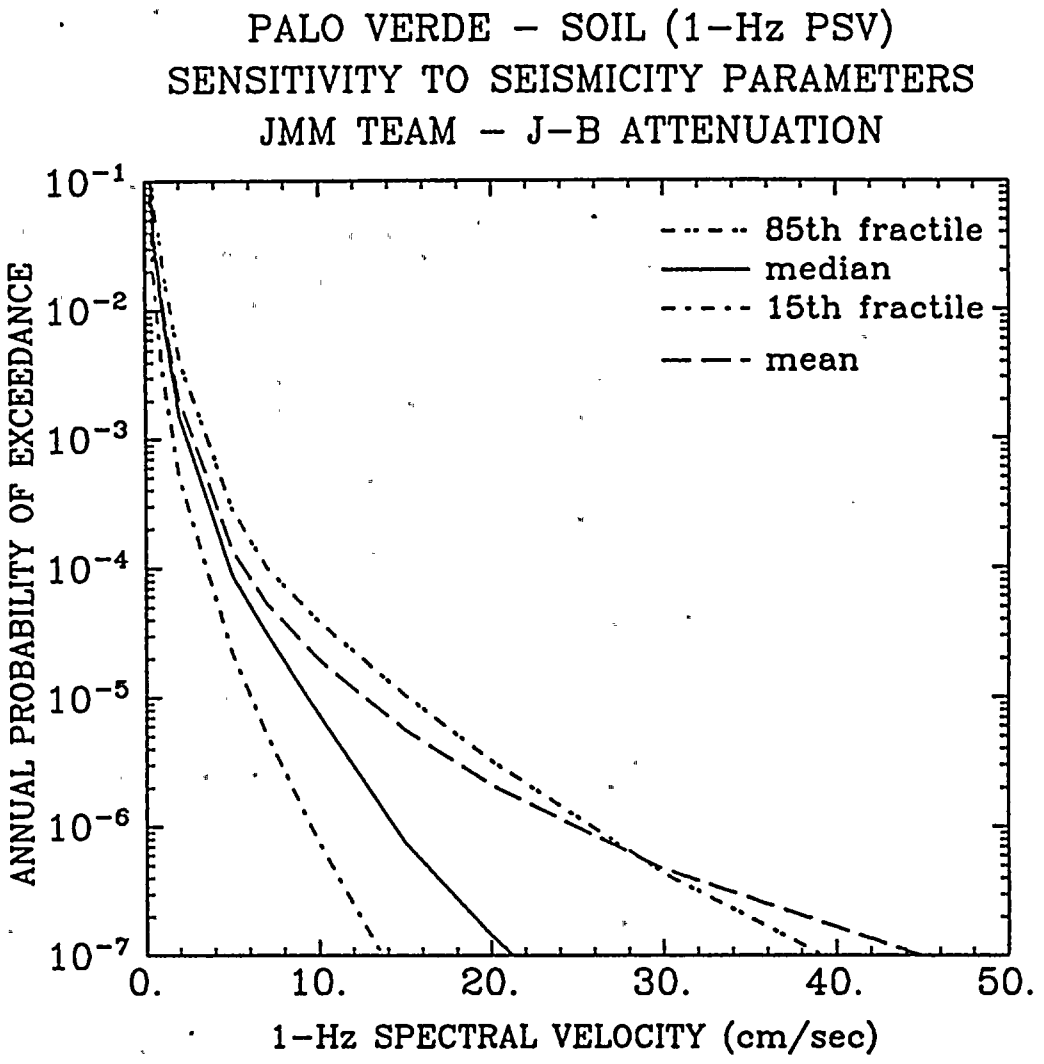

Figure 6-28. Annual probability of exceedance of 1-Hz spectral velocity. Sensitivity to seismicity parameters: JMM team.

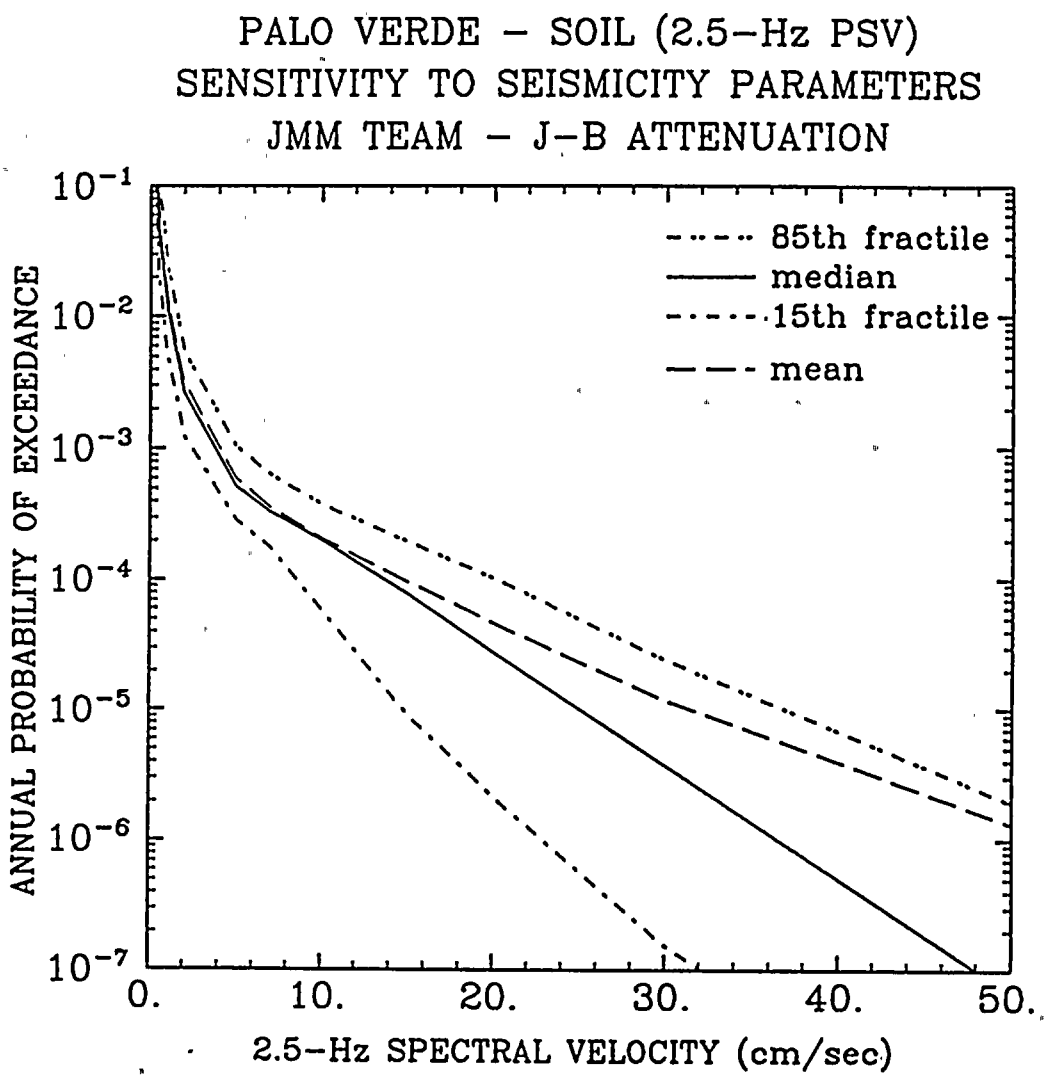

Figure 6-29. Annual probability of exceedance of 2.5-Hz spectral velocity. Sensitivity to seismicity parameters: JMM team.

Table 6-3

ANNUAL PROBABILITY OF EXCEEDANCE FOR
PEAK GROUND ACCELERATION:
PALO VERDE SITE (ROCK)

Acceleration (cm/sec^2)	Mean	Percentiles		
		15	50	85
10	7.6E−03	2.1E−03	4.3E−03	1.7E−02
20	1.7E−03	7.6E−04	1.4E−03	3.0E−03
50	3.8E−04	1.9E−04	3.8E−04	5.8E−04
70	2.3E−04	1.1E−04	2.3E−04	3.5E−04
100	1.2E−04	5.1E−05	1.2E−04	1.9E−04
150	4.9E−05	2.2E−05	4.5E−05	7.8E−05
200	2.1E−05	8.5E−06	1.8E−05	3.4E−05
300	4.6E−06	1.0E−06	3.7E−06	7.4E−06
500	3.9E−07	2.6E−08	2.2E−07	7.1E−07
1000	4.2E−09	3.4E−11	1.1E−09	7.4E−09

Table 6-4

SPECTRAL VELOCITIES (cm/sec) FOR
VARIOUS EXCEEDANCE PROBABHLITIES:
PALO VERDE SITE (ROCK)

		Frequency (Hz)				
		25	10	5	2.5	1
Exceedance		Period (sec)				
Probability	Percentile	0.04	0.1	0.2	0.4	1
1.E−03	15	0.11	0.36	1.00	1.35	1.37
	50	0.17	0.63	1.56	2.09	2.71
	85	0.27	1.11	2.31	3.13	3.93
2.E−04	15	0.31	1.26	3.17	3.73	2.71
	50	0.48	2.02	5.06	5.66	5.16
	85	0.68	3.51	6.57	8.16	6.79
1.E−04	15	0.49	1.94	4.86	5.63	3.65
	50	0.68	2.84	7.48	8.17	6.57
	85	0.98	5.34	9.74	11.70	9.75
1.E−05	15	1.15	4.95	13.70	12.20	8.31
	50	1.58	7.32	16.50	20.50	13.10
	85	2.02	11.90	21.30	27.30	21.20

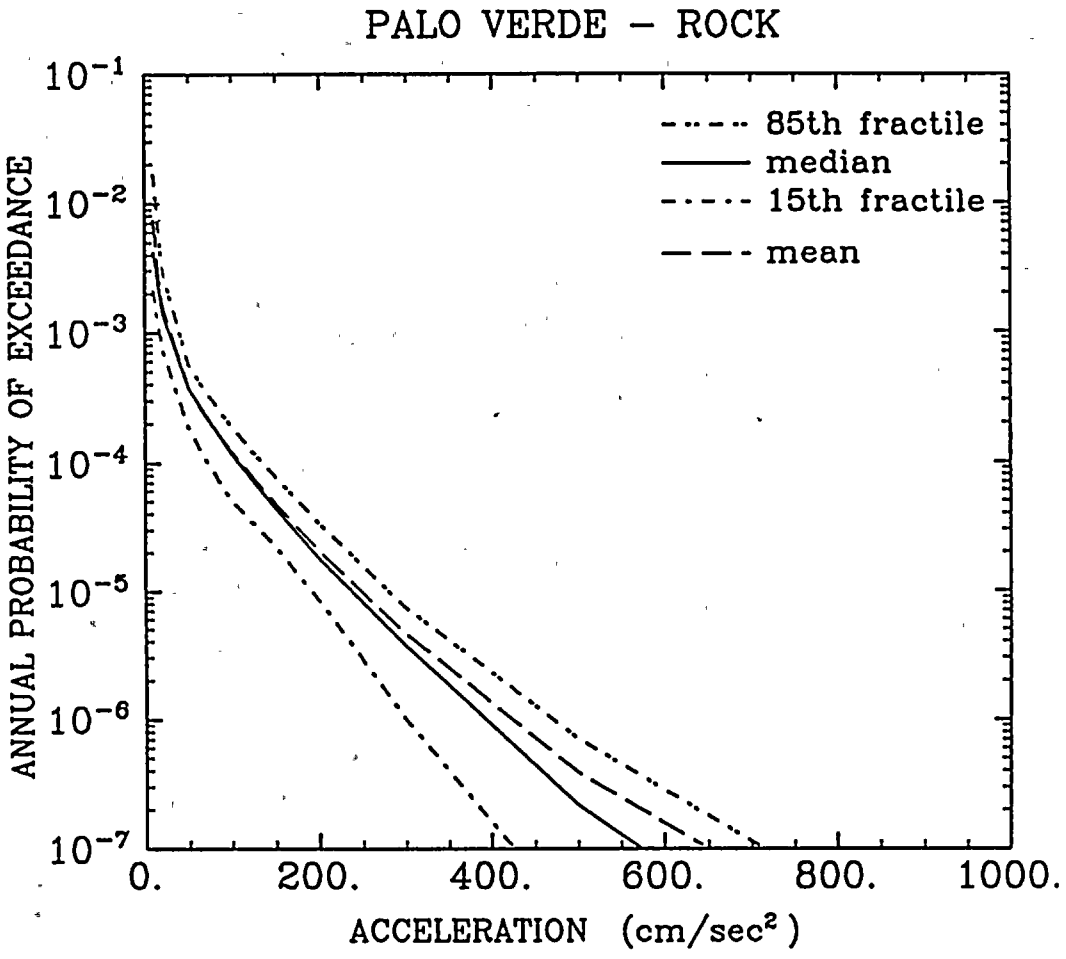

Figure 6-30. Annual probability of exceedance of peak acceleration: Palo Verde site (rock site conditions).

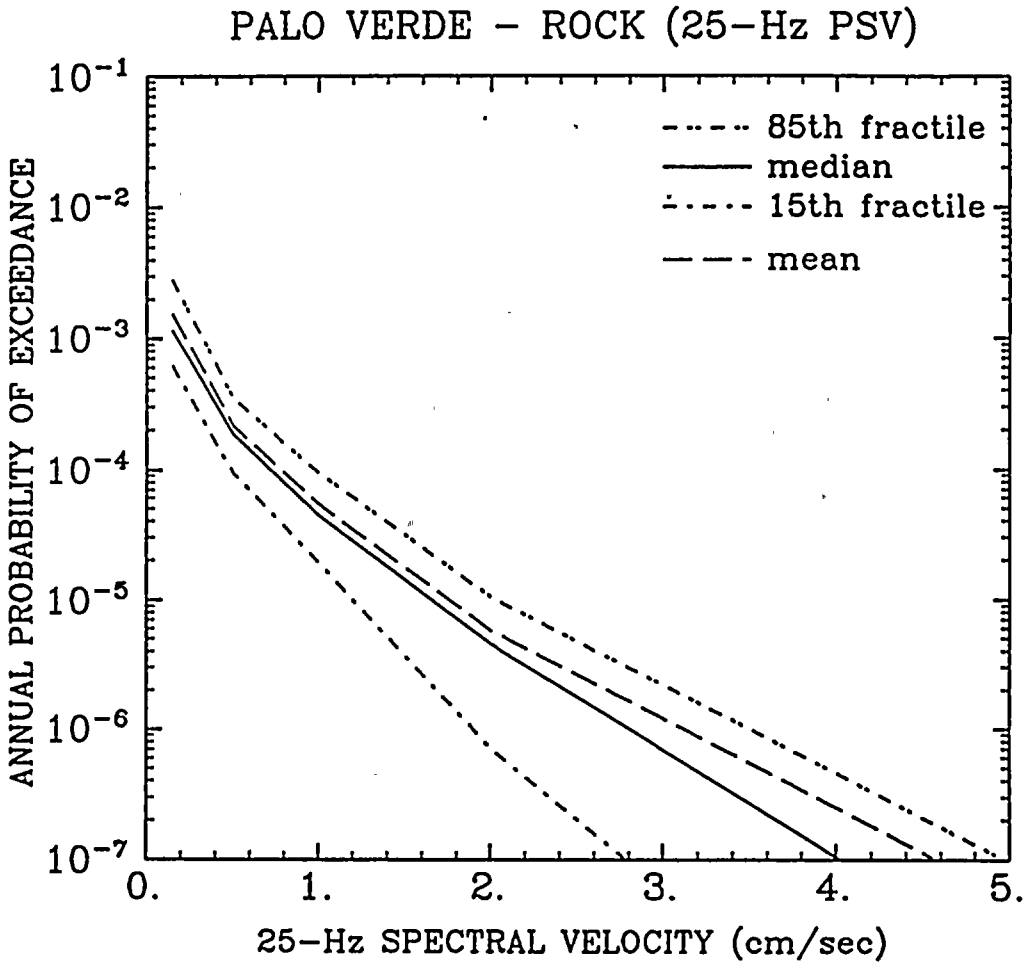

Figure 6-31. Annual probability of exceedance of 25-Hz spectral velocity: Palo Verde site (rock site conditions).

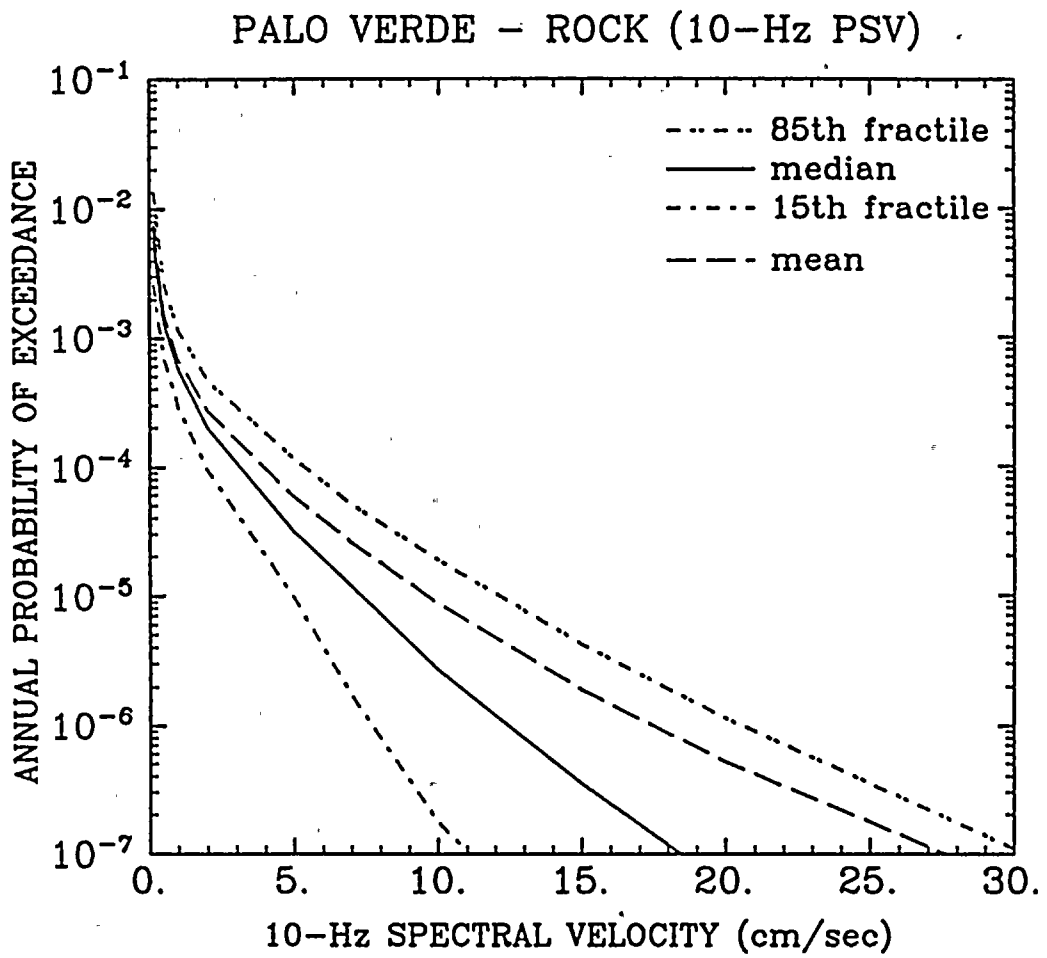

Figure 6-32. Annual probability of exceedance of 10-Hz spectral velocity: Palo Verde site (rock site conditions).

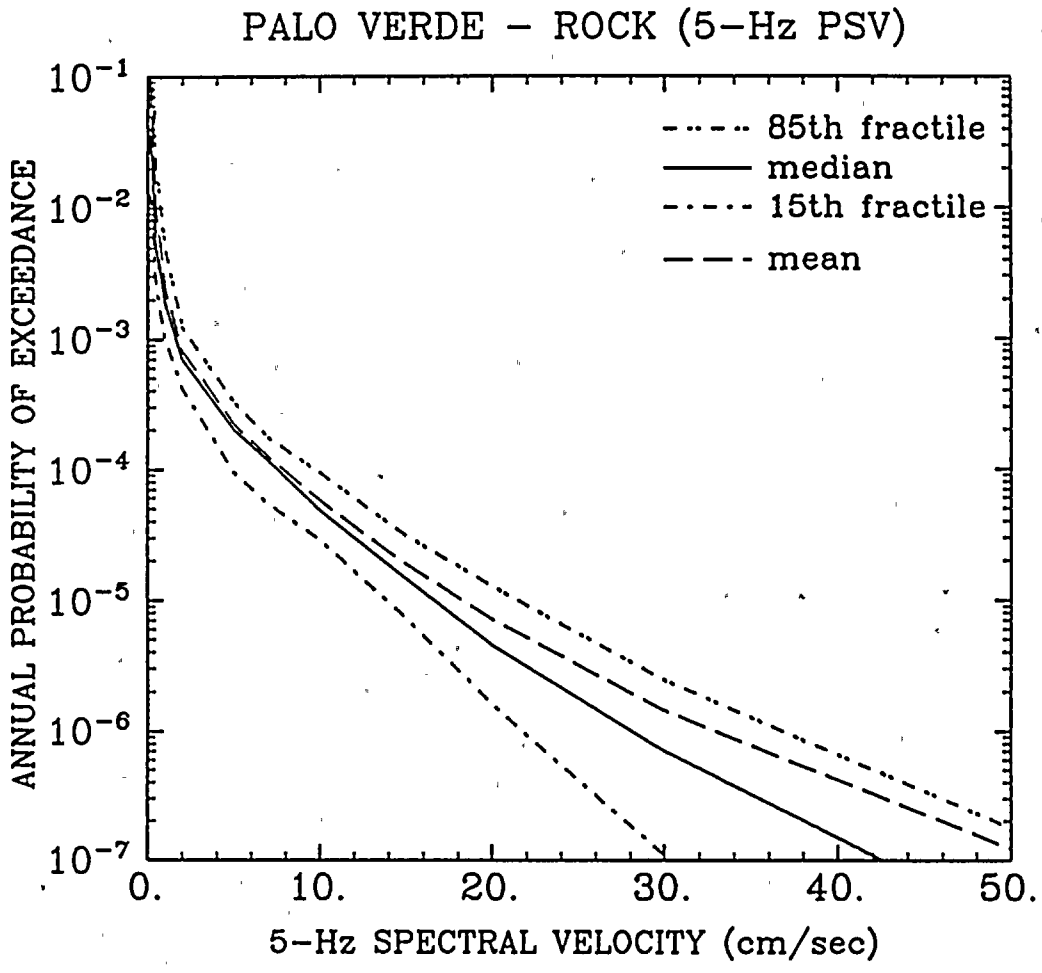

Figure 6-33. Annual probability of exceedance of 5-Hz spectral velocity: Palo Verde site (rock site conditions).

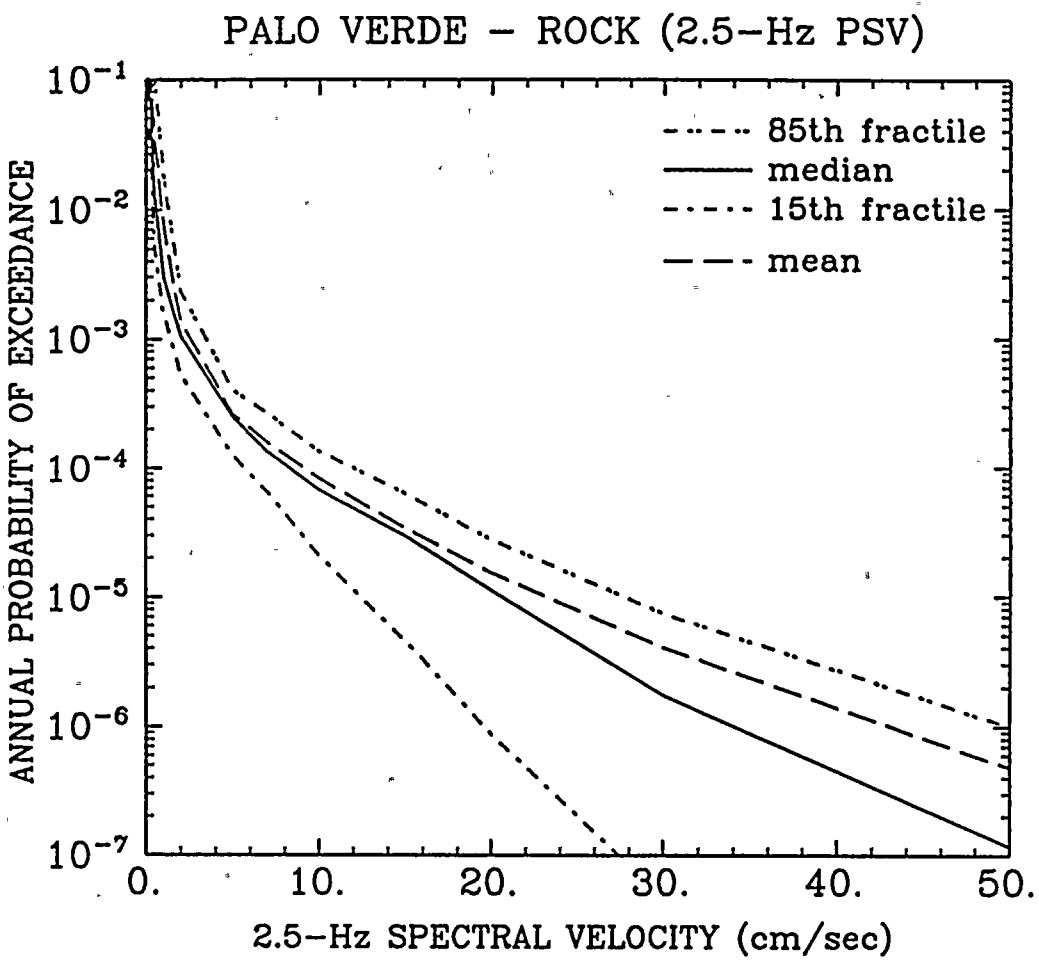

Figure 6-34. Annual probability of exceedance of 2.5-Hz spectral velocity: Palo Verde site (rock site conditions).

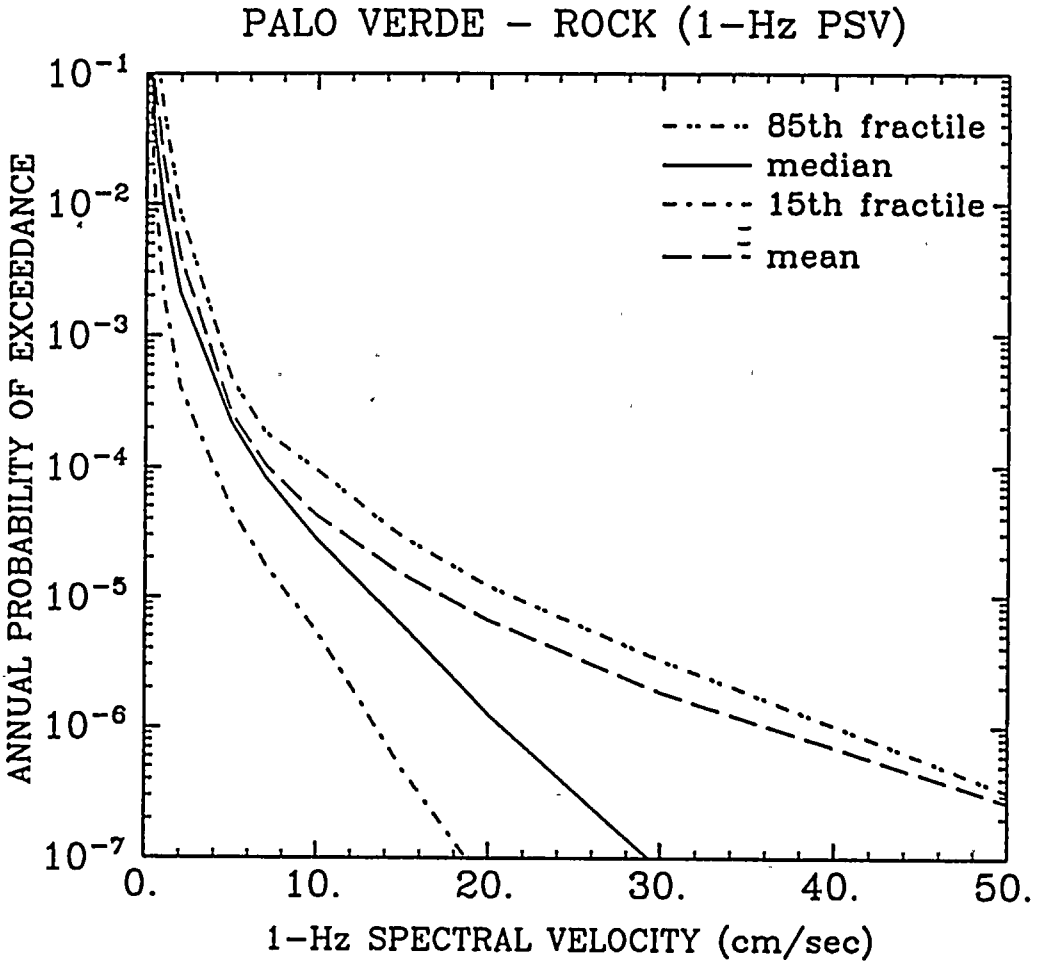

Figure 6-35. Annual probability of exceedance of 1-Hz spectral velocity: Palo Verde site (rock site conditions).

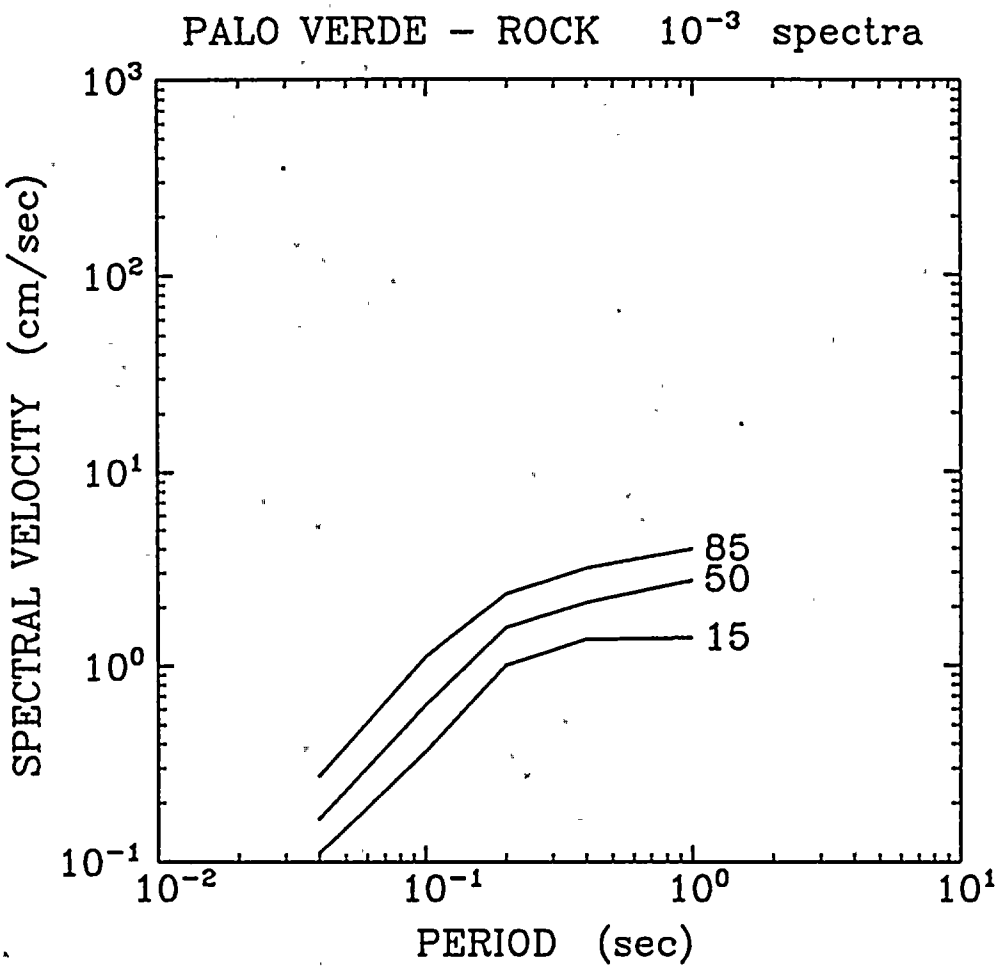

Figure 6-36. Uniform hazard spectra for the 10^{-3} annual probability of exceedance: Palo Verde site (rock site conditions). Spectra shown for three percentiles: 15^{th}, 50^{th}, and 85^{th}.

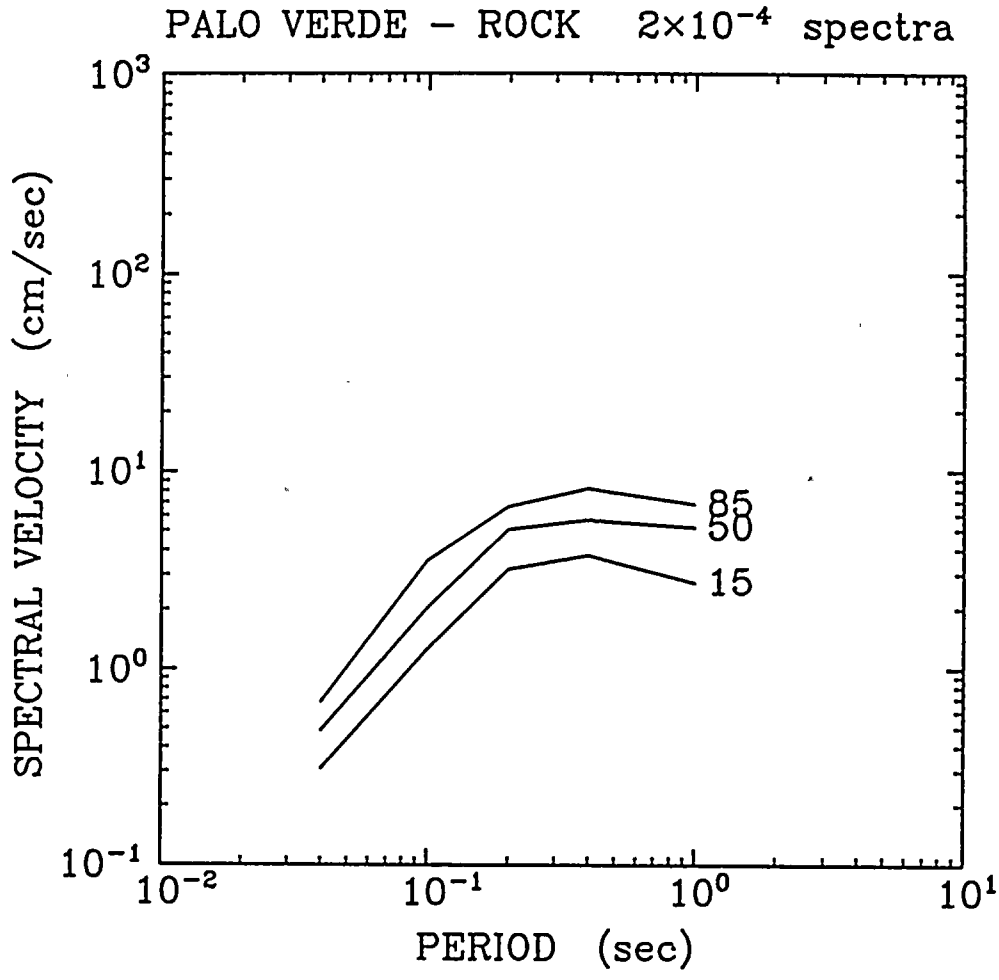

Figure 6-37. Uniform hazard spectra for the 2×10^{-4} annual probability of exceedance: Palo Verde site (rock site conditions). Spectra shown for three percentiles: 15^{th}, 50^{th}, and 85^{th}.

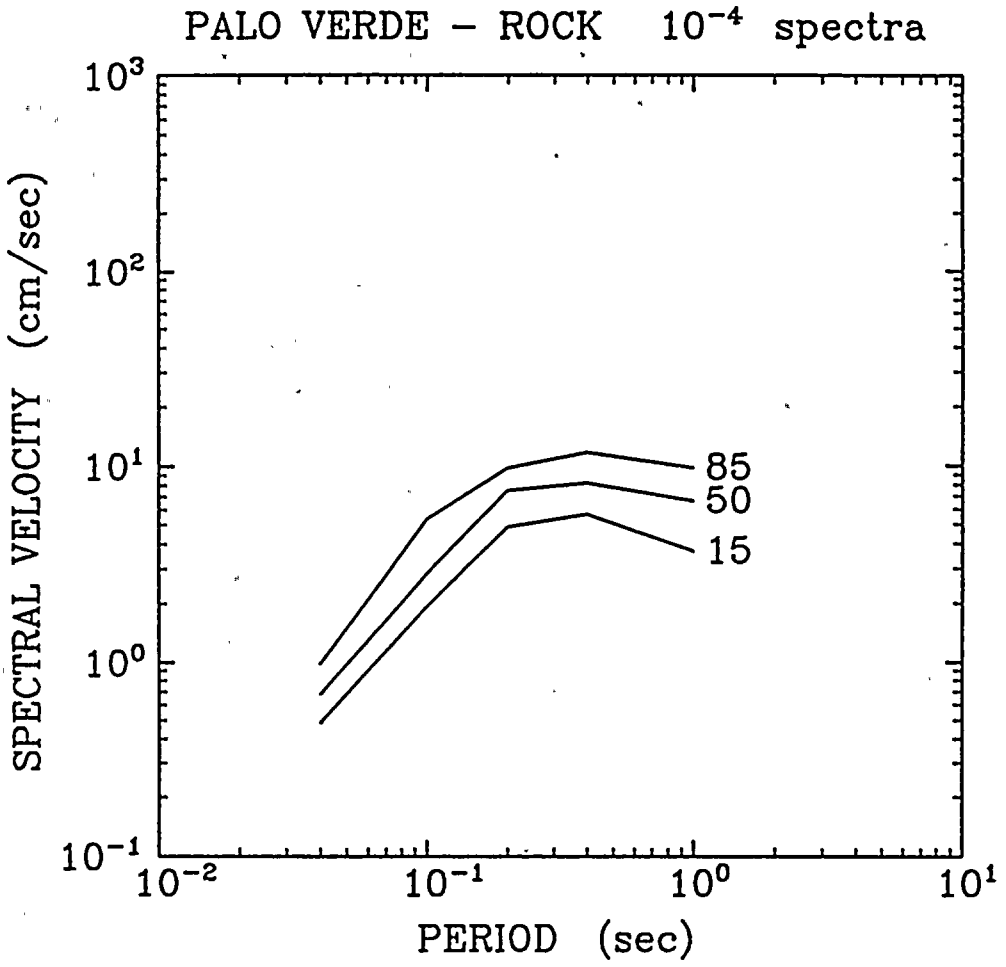

Figure 6-38. Uniform hazard spectra for the 10^{-4} annual probability of exceedance: Palo Verde site (rock site conditions). Spectra shown for three percentiles: 15^{th}, 50^{th}, and 85^{th}.

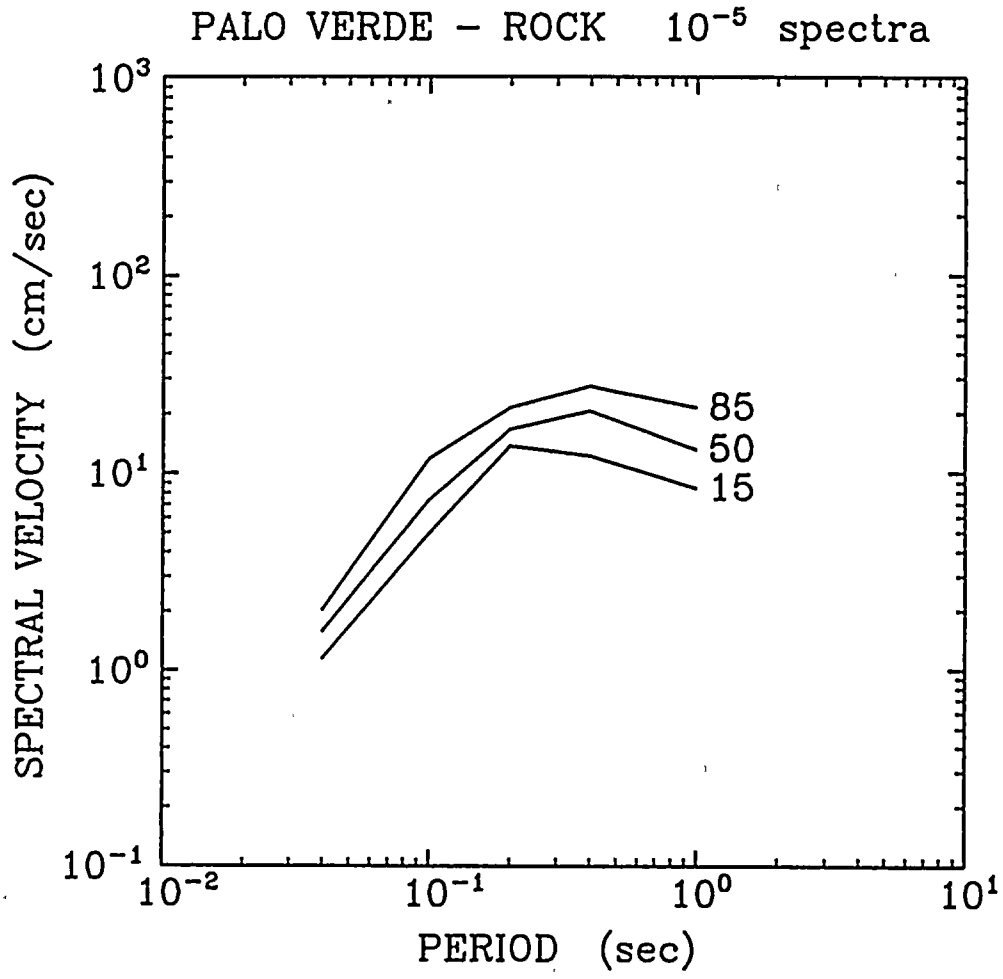

Figure 6-39. Uniform hazard spectra for the 10^{-5} annual probability of exceedance: Palo Verde site (rock site conditions). Spectra shown for three percentiles: 15^{th}, 50^{th}, and 85^{th}.

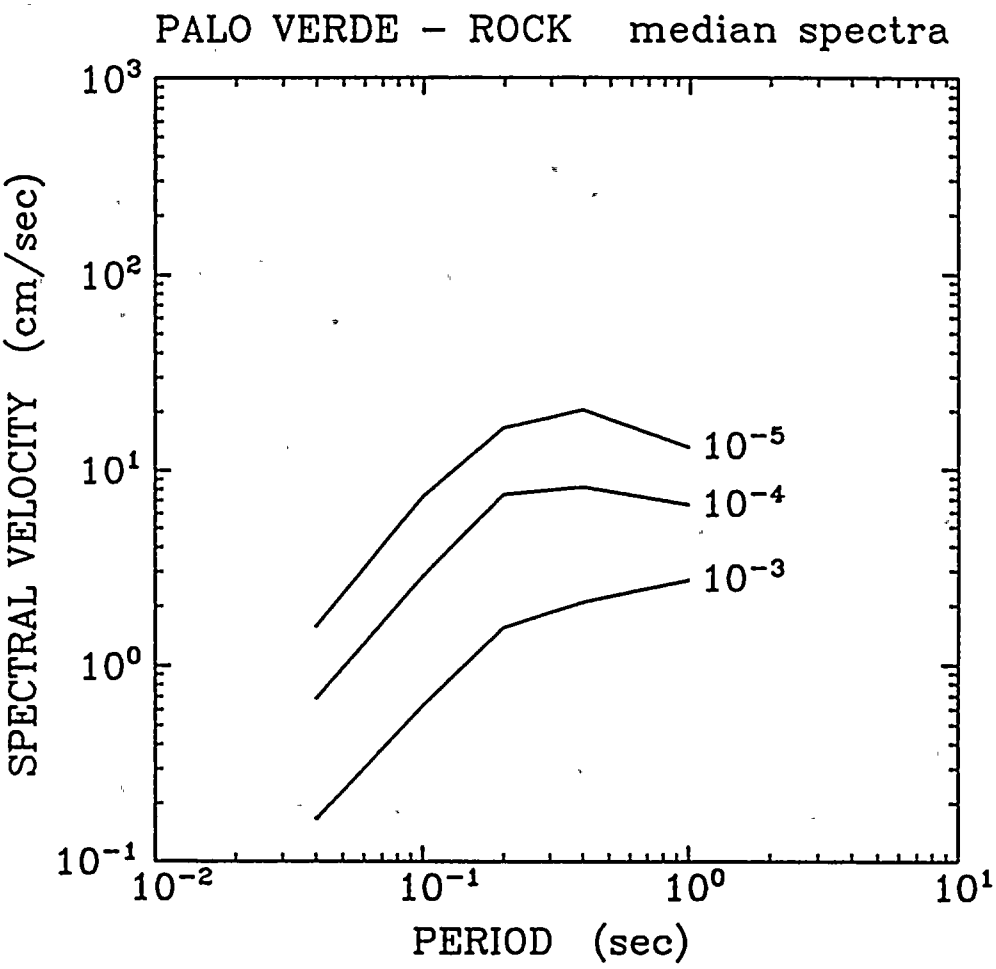

Figure 6-40. Median uniform hazard spectra for the 10^{-3}, 10^{-4}, and 10^{-5} probability of exceedance: Palo Verde site.

Section 7
CONCLUSIONS

This study presents seismic hazard results that represent the annual frequency of exceedance of various ground motion levels at the PVNGS site, and the uncertainty in the annual frequency of exceedance. These results are represented as a family of fractile seismic hazard curves, and as uniform-hazard spectra corresponding to annual probabilities of 2×10^{-3}, 1×10^{-3}, and 2×10^{-4}. The uncertainties in hazard derive from uncertainties on input assumptions regarding seismic sources, seismicity parameters, and ground motion attenuation equations. In this sense the analysis presented here is state-of-the-art, because it incorporates and presents uncertainties in the major factors affecting seismic hazard in the region around the site.

Two earth science teams were used, Geomatrix Consultants Inc. and James M. Montgomery Consulting Engineers, Inc. These teams specified inputs to the analysis as seismic sources (tectonic regions and faults) and seismicity parameters for those sources. Differences in interpretations between the two teams in terms of seismic sources in the area, and of parameters describing those sources, contribute to uncertainties in the seismic hazard. In addition, there are uncertainties in the ground motion equation appropriate for Arizona. We have used here attenuation equations proposed by Joyner and Boore and by Campbell, modified to reflect uncertainty in the anelastic term appropriate for Arizona. These uncertainties also contribute to uncertainty in hazard.

The methodology used in this study follows closely that used in the EPRI/SOG study of seismic hazards at nuclear plant sites in the central and eastern US. The derivation of seismic sources is specified by the earth science teams; a common analysis of historical seismicity is performed to aid in estimation of seismicity parameters; and interaction and communication between the two teams took place to exchange information, concepts, and results. This theme of interaction helps to ensure that all relevant data, theories, and interpretations are considered by each team in making its evaluations. Even after this effort at interaction and communication, however, important differences remain between the two teams. This is to be expected; differences among experts providing seismological input to hazard analyses was a result observed in both the EPRI/SOG and LLNL studies of seismic hazard in the central and eastern US.

Several qualifications to these results are appropriate. Only two earth science teams were used here, although we spent a significant effort attempting to identify additional teams who would be familiar with the region and who might participate. If such teams are used in a similar study in the future, their interpretations may lead to results that are higher or lower than those obtained here. i.e., there is no guarantee that we have spanned the entire range of seismological interpretations available for Arizona. (It should be noted that no study of this type could make that guarantee.) A similar comment applies to the selection of ground motion attenuation equations. Regarding the analysis of earthquake data, we have not conducted an extensive evaluation of the earthquake catalogs used in this study and described in Section 4. Issues such as the accuracy of specific event locations and magnitudes, the conversion of intensity to magnitude, and the completion of earthquake coverage represented by the catalogs have not been addressed in detail. Similarly, the specific soil conditions at PVNGS have not been considered; we have used generic (though depth- and amplitude-dependent) factors to estimate the dynamic response of average soils that are 300 to 400 feet deep. Site-specific studies of soil response under earthquake loads might yield results different from those used here, with a corresponding effect on the hazard results. We have no reason to believe that more detailed studies in any of these areas would either increase or decrease the hazard results calculated here.

The site-amplification factors used in this study were developed during the EPRI/SOG program for eastern-U.S. ground motions (which contain more high-frequency energy than western-U.S. ground motions). These factors were applied here on a preliminary basis to obtain results consistent in methodology with the EPRI/SOG results. As a results of differences in frequency content, the calculated spectral acceleration at 25 Hz is lower than the calculated peak ground acceleration. In view of this inconsistency, the 25-Hz soil results should be disregarded and other soil results should be viewed as approximate. These approximations should be removed by performing a site-specific soil amplification study, using rock-motion inputs typical of the western U.S.

The results presented here form a basis for comparing the seismic hazard at the PVNGS to hazard at other nuclear plant sites. For this purpose it would be most relevant to use the EPRI/SOG hazard results for the central and eastern US, rather than the LLNL results, as the methodology applied here follows most closely the EPRI/SOG study.

APPENDIX A

Seismic Source and Seismicity Parameter Interpretation, Geomatrix Consultants Team

TABLE OF CONTENTS

SEISMIC SOURCE CHARACTERIZATION FOR PALO VERDE NUCLEAR GENERATING STATION

INTRODUCTION

This draft report presents the seismic sources and associated parameters to be used for a probabilistic seismic hazard analysis of the Palo Verde Nuclear Generating Station, Arizona. The seismic sources (including both zones and linear faults) within a 300-km-radius of the site, their maximum magnitudes, activity rates and b-values are described in this report. Plate 1 is a map that shows the locations of the identified seismic zones and faults.

REGIONAL TECTONIC SETTING

The Palo Verde site lies within the broad deforming region between the interiors of the Pacific and North America plate. According to the NUVEL-1 plate motion model (DeMets and others, 1990), which incorporates spreading rates in the Gulf of California (DeMets and others, 1987) and along the East Pacific Rise and Pacific-Antarctica Rise (DeMets and others, 1990), the rate of relative Pacific-North America motion in southern California at the approximate latitude of the Palo Verde site is approximately 46 $\pm$ 1 mm/yr, and oriented about N41W. Relative motion between the plates is characterized by transpressive dextral shear and is accommodated largely by dextral strike-slip centered along the San Andreas fault system and, to a lesser degree, by a component of Basin and Range extension parallel to the plate boundary, extension in the Gulf of California, faults in the borderlands of southern and Baja California, and contractional structures in the Transverse Ranges (Zoback and others, 1981; Weldon and Humphreys, 1986; Argus and Gordon, 1988).

GENERAL APPROACH IN SEISMIC SOURCE CHARACTERIZATION

SOURCE DEFINITION

Two types of earthquake sources are included in this seismic hazard analysis: fault-specific sources representing the mapped active faults that may be the source of moderate-to-large magnitude earthquakes; and areal sources, or zones, that model the background seismicity of smaller-magnitude earthquakes that may be occurring on faults that are not mapped as active in the Quaternary. Alternative interpretations of seismic zonation were made where appropriate.

MAXIMUM MAGNITUDE ASSESSMENT

Maximum magnitudes were assessed for each of the source zones on the basis of the physical dimensions of faulting that could be expected. Maximum magnitudes for fault-specific sources were estimated using the physical dimensions of the maximum size of earthquake rupture assessed directly from the dimensions of the faults. The expected magnitudes associated with these rupture dimensions were then obtained using empirical correlations between earthquake rupture dimension and earthquake magnitude (Wells and Coppersmith, in review). Maximum magnitudes for areal sources were assessed on the basis of the size of earthquakes that have occurred where specific faults have not been readily identified and by analogy with other regions with similar tectonics. Uncertainty in maximum magnitude appropriate for each zone was assessed subjectively considering the relative credibilities of various alternative values.

EARTHQUAKE RECURRENCE RATES

The earthquake recurrence parameters for areal source zones were determined from the analysis of the historical and instrumental seismicity provided by Risk Engineering (1991).

These data were fit to a truncated exponential distribution (Cornell and Van Marke, 1969) of the form

$$N(m) = \alpha(m^o)\frac{10^{-b(m-m^o)} - 10^{-b(m^u-m^o)}}{1 - 10^{-b(m^u-m^o)}} \qquad (1)$$

where $\alpha(m^o)$ is the annual frequency of occurrence of earthquakes of magnitude greater than a minimum magnitude, m^o, b is the Gutenberg-Richter b-value parameter, m^u is the maximum magnitude event than can occur on the source, and $N(m)$ is the annual frequency of occurrence of earthquakes of magnitude greater than m. The exponential frequency-magnitude distribution is considered to be the appropriate distribution for source zones representing the cumulative effect of many individual features and was originally developed by Gutenberg and Richter (1954) from examination of seismicity in large regions.

The parameters $\alpha(m^o)$ and b of equation 1 were obtained using the maximum likelihood algorithm of Weichert (1980) which allows for variable periods of complete reporting in the catalog for different magnitude intervals. The catalog completeness for the study region was evaluated on the basis of the completeness estimates for the individual source zones provided by Risk Engineering (1991) and the general completeness estimates given by Engdahl and Rinehart (in press). The nominal values selected for Arizona are:

Magnitude Interval	Completeness Period
2.0-4.0	1975-1985
4.0-5.0	1960-1985
5.0-6.0	1932-1985
6.0+	1900-1985

The periods of completeness for the Imperial Valley region of California are much longer and the nominal values selected are.

Magnitude Interval	Completeness Period
2.0-4.0	1975-1985
4.0-6.0	1932-1985
6.0+	1900-1985

No attempt was made to remove dependent events (foreshocks and aftershocks) prior to estimating recurrence parameters. Although dependent events should be removed in order to develop recurrence parameters consistent with the Poisson model of independent events, the influence of aftershocks on the seismic hazard at the Palo Verde site was judged to be insignificant. There do not appear to be any foreshocks and aftershocks reported in the earthquake catalog for the source zones near the site where smaller magnitude events could influence the hazard and those zones in the Imperial Valley where there may be significant numbers of dependent events present are at a great enough distance from the site that small magnitude events are not likely to have significant impact on the hazard.

Uncertainty in the recurrence parameters $\alpha(m^o=5)$ and b were assessed in a quantitative fashion by assigning a range of plus-or-minus one standard deviation to each parameter and then computing the relative likelihoods of observing the reported catalog given the specified recurrence parameters. These relative likelihoods were used as weighting functions for the various combinations of $\alpha(m^o=5)$ and b values, and account for the dependence between the two parameters.

Earthquake recurrence parameters for fault-specific sources were estimated based on an assessment of either fault slip rate and a translation of the slip rate to seismic moment rate or recurrence intervals for the largest events. Development of earthquake recurrence relationships from slip rate requires partitioning the seismic moment rate into earthquakes of various magnitudes according to an earthquake recurrence model (e.g. Anderson, 1979; youngs and Coppersmith, 1985b). Two recurrence models were considered in this analysis: The characteristic earthquake model (Schwartz and Coppersmith, 1984) and the truncated

exponential model. These models describe the distribution of earthquake magnitudes. Youngs and Coppersmith (1985a,b) have shown that the characteristic earthquake model is more appropriate for fault sources and areal source zones are typically modeled using the exponential recurrence model. For recurrence relationships developed on the basis of recurrence intervals for the largest events, the two models are used to define the recurrence for smaller earthquakes.

In applying Youngs and Coppersmith's (1985a,b) characteristic magnitude distribution to individual sources, the maximum magnitude assessed for the fault, m_{max}, was taken to be the expected magnitude for the characteristic size event, with individual events uniformly distributed in the range of $m_{max} \pm ¼$ magnitude units. The cumulative frequency for earthquakes of magnitude m_{max}-¼ is then set equal to the annual frequency of maximum, or characteristic events assessed for the fault and the upper bound magnitude, m^u, is equal to m_{max}+¼. The truncated exponential distribution was applied to fault-specific sources in a consistent manner with the upperbound magnitude set equal to m_{max}+¼ and the rate for the maximum or characteristic events specified by the cumulative frequency for earthquakes of magnitude m_{max}-¼.

Figure 1 compares the shape of the truncated exponential and characteristic magnitude distributions. Shown on the left are the distributions developed for an assessed fault m_{max} of 7.25 with the frequency of events larger than magnitude 7 held constant. Shown on the right in Figure 1 are the magnitude distributions developed on the basis of equal rate of seismic moment release. The characteristic magnitude distribution results in about a factor of 3 reduction in the frequency of small magnitude events compared to the exponential model when the absolute level of the distribution is fixed by either the frequency of the largest events or by the rate of moment release.

Uncertainty in recurrence rates for fault-specific sources was specified by weighting alternative values for fault slip rate or return period of maximum events. In addition, relative

credibilities were assigned to the two recurrence models. The uncertainty in the b-value for the truncated exponential portion of the recurrence relationships was estimated from the observed seismicity.

All earthquake magnitudes were assumed to be equivalent to moment magnitude M. The magnitudes reported in the DNAG catalog for the western United States are typically either local magnitudes, M_L, or surface wave magnitude, M_S, which are equivalent to M in the magnitude range of interest in this study (Hanks and Kanamori, 1979). The maximum magnitudes assessed for each of the sources are in terms of moment magnitude.

SEISMIC SOURCE CHARACTERIZATION

The region within 300 km of the Palo Verde site may be divided into several tectonic/physiographic provinces, including: 1) Southern Basin and Range, 2) Arizona Transition Zone, 3) Colorado Plateau, and 4) Salton Trough/Gulf of California (Jahns, 1954; Hendricks and Plescia, 1991). Because the tectonic style, seismicity, geophysical signature, and surface geology are distinctly different between each of these provinces, we have used these provinces as a basis for the identification of regional seismic zones. The source zones defined within each of these provinces are shown on Plate 1 and are described below, together with the basis for the seismicity parameter estimates. Table 1 lists the distributions for seismicity parameters developed for each seismic source.

SOUTHERN BASIN AND RANGE

The Palo Verde site lies within the Basin and Range province, a region of broad continental rifting, characterized by extensional fault-block mountains and deep, sediment-filled basins. Features characteristic of this extension include widespread seismicity, young Cenozoic fault scarps, and abundant Cenozoic intrusive and extrusive igneous activity. Crustal thickness,

which is thin throughout the Basin and Range province, is about 25-30 km thick in west-central Arizona (Hendricks and Plescia, 1991).

The southern Basin and Range province (Arizona and southwestern New Mexico) has been tectonically quiescent for about the past 10 m.y. (Eberly and Stanley, 1978), although moderate, low-level seismicity still persists in this region (Brumbaugh, 1987). Stratigraphic-geomorphic studies in the Basin and Range province of southeastern Arizona and adjacent Sonora, Mexico, indicate that Quaternary faults are rare and have histories of infrequent ruptures (Menges and others, 1982). These studies suggest that large scale Basin and Range tectonism had ceased in southeastern Arizona by the latest Miocene to Pliocene. In addition, these data imply localized and widely-dispersed late Pliocene-Quaternary reactivation of basin-margin normal faulting in the region, at lower rates than the earlier Basin and Range event.

Zones 1, 2, and 11-12

Three subdivisions of the southern Great Basin tectonic/physiographic province were defined primarily on the basis of their variable seismicity. The seismicity is lowest in Zone 1 and highest in Zone 11-12. The higher rate of seismicity in Zone 2 relative to Zone 1 may be at least partially related to volcanic activity in the Pinacate volcanic field, centered on the international border. Earthquakes related to volcanic processes are typically small. No active faults have been recognized in the Pinacate field (Pearthree, pers. comm.). Because the rate of seismicity in Zones 1 and 2 are not greatly different and the two zones have generally similar levels of tectonic deformation, we have included an alternative scenario in which Zones 1 and 2 are combined into a single seismic source. Because of the presence of volcanic activity in Zone 2 we favor the two zones being separate sources (weight 0.67) over the alternative of a single combined source (weight 0.33).

A small number of Quaternary faults have been mapped in Zones 1 and 2 by Menges and Pearthree (1983) as part of a study presenting data and interpretations concerning the

distribution, amounts and timing of neotectonic (latest Pliocene to Quaternary) faulting in Arizona. The primary data source for the study is photointerpretation of black-and-white high-altitude (U2) aerial photography supplemented by ground and aerial reconnaissance concentrated on the major fault scarps in the state. These faults are treated separately from Zones 1 and 2.

The maximum magnitude associated with Zones 1 and 2 is an important assessment. Because the studies by Menges and Pearthree (1983) appear to be regional in nature, it is reasonable to assume that additional minor faults not identified by Menges and Pearthree (1983) may exist within Zones 1 and 2. The threshold of surface faulting is about M 5½ to 6, as demonstrated by recent moderate magnitude earthquakes in the San Francisco area (Greenville, Hall's Valley, Coyote Lake) that were accompanied by very minor surface slip. The crust, and presumably the seismogenic crust, is of "normal" thickness in Zones 1 and 2, which would allow for subsurface ruptures having significant downdip widths (e.g., 10 km) without necessarily rupturing the surface. Empirical regressions between fault rupture area and magnitude (Wyss, 1979; Wells and Coppersmith, in review) indicate that the magnitude associated with a 10 km x 10 km rupture is about 6 - 6¼ Concealed ("blind") thrust faults have produced earthquakes in the M 6 to 7 range (e.g., the 1983 Coalinga, California earthquake (M_L 6.5), the 1985 Nahanni, Canada earthquakes (M_S 6.6 and 6.9), and the 1989 Loma Prieta, California earthquake (M 7.0). Although blind thrust faults are characteristic of compressional rather than extensional tectonic regimes, the possibility of blind faulting should be considered.

On the basis of the above considerations, we conclude that the likely values of maximum magnitude for Zones 1 and 2 are 5.5 (0.65) or 6.0 (0.3). Because of the possibility of blind faulting and the lack of detailed mapping throughout the entire zone we have included the possibility that the maximum is as high as 6.5 with a low likelihood (0.05).

The maximum magnitudes for Zone 11-12 are higher than in Zones 1 and 2, ranging from 6.0 to 6.75. Zone 11-12 borders and may include portions of the Mojave Desert tectonic/physiographic province, which includes a higher density of Quaternary active faults than the southern Basin and Range. The higher magnitudes reflect the higher seismicity and rates of tectonic deformation within the zone.

Earthquake recurrence rates for Zones 1, 2, and 12 were estimated on the basis of the observed historical and instrumental seismicity. Because of the very limited recorded seismicity in the region, *b*-value estimates for individual source zones are very uncertain. Accordingly, the seismicity from all source zones lying to the east of the Salton Trough/Gulf of California was combined to estimate a regional b-value (see Figure 2). The resulting *b*-value of 0.83 ± 0.15 was used as a prior on b in the maximum likelihood estimation of $\alpha(m^o=5)$ and b. The resulting values and their relative weights are listed in Table 1.

Fault 1 (Sand Tank Fault)

The Sand Tank fault (Fault 1) is located within Zone 1 approximately 60 km from the site. The late Quaternary history and seismic hazard of this fault were studied in detail by Demsey and Pearthree (1987) during studies for the proposed superconducting super collider site in Maricopa County. The fault is characterized by an approximately 3.5 km-long northeast-trending piedmont fault scarp. The Demsey and Pearthree (1987) study concludes that the approximately 2 m displacement on the fault was formed in a single earthquake about 8,000 to 20,000 years BP (before present). Using empirical relationships between surface rupture length and displacement, Demsey and Pearthree (1987) estimate that maximum earthquake magnitudes range from M 6.2 (assuming a minimum rupture length of 3.5 km) to M 6.6 (assuming a maximum rupture length of 30 km). They estimate a minimum potential rupture recurrence interval of about 50,000 to 200,000 years, and state that the likelihood for surface rupture on the Sand Tank fault within the next several thousand years is extremely low.

The maximum magnitudes selected as source parameters for the Sand Tank fault are based on the work of Demsey and Pearthree (1987). The recurrence intervals selected are based on analogy with other faults in the Basin and Range province. In a study of late Quaternary faulting and seismic hazard in southeastern Arizona and adjacent portions of New Mexico and Sonora, Mexico, Pearthree (1986) concluded that faults active during the late Quaternary are characterized by extremely long recurrence intervals between surface ruptures ($> 10^5$ years). This information, combined with the limited data on slip rates for faults in Arizona (e.g., 0.005-0.1 mm/yr on the Big Chino fault, Fault 26 in this study), are the basis for the selected return periods for maximum events assigned to Fault 1, as well as other faults in central Arizona (see Table 1). The characteristic magnitude distribution was favored (0.8) over the truncated exponential model (0.2) because of the lack of observed small magnitude seismicity in association with any of the mapped active faults in Arizona.

Fault 4 (Santa Rita Fault)

The Santa Rita fault (Fault 4) is a discontinuous zone of subdued fault scarps that offset Quaternary alluvium for about 55 km. Trenching across the fault suggests at least two faulting events within the last 200,000 years; the most recent event probably occurred between about 60,000 and 100,000 BP (Johnson and others, 1991). Magnitude estimates for these events range from 6.4 to 7.3 (Pearthree, 1986; Pearthree and Calvo, 1987; Johnson and others, 1990).

The maximum magnitudes selected for the Santa Rita fault are based on the published magnitude estimates, and empirical relationships between earthquake magnitude and specific fault parameters (selected by analogy with other earthquakes in the Basin and Range). Recurrence parameters are the same as described for Fault 1.

ARIZONA TRANSITION ZONE

The Arizona Transition Zone, an area of complex geology and geophysics, represents the region of transition between the high Colorado Plateau province of northern Arizona and the low deserts of the Basin and Range province to the south. The Transition Zone reflects geophysical and geologic changes between the two fundamentally different provinces that surround it (Hendricks and Plescia, 1991). The Transition Zone exhibits geologic features common to both the Colorado Plateau and the Basin and Range. Regional stratigraphic units are nearly continuous between the Transition Zone and the Colorado Plateau, implying that there is no large vertical offset associated with the physiographic boundary. Structurally, the Transition Zone is characterized by 1) northeast-trending structures that extend into the Colorado Plateau and represent reactivation of Precambrian structures within the last 75 million years, and 2) Tertiary to late Quaternary north-to-northwest-trending normal faults more typical of the adjacent Basin and Range. The latter structures suggest that Basin and Range-style extensional tectonism has encroached upon the margins of the Colorado Plateau (Zoback and Zoback, 1980; 1989).

Results of recent seismic and gravity studies suggest that a change from thin crust (25-30 km) in the Basin and Range to thick crust (about 40 km) in the southern Colorado Plateau may occur as a series of steps across the Transition Zone (Hendricks and Plescia, 1991). In addition, these studies suggest that this region is unique and displays anomalous crustal and upper mantle seismic properties, shallow Curie isotherms, high heat flow, and steep down-to-the-plateau Bouguer gravity gradients.

nes 3, 4, 5, 6, and 7

The Arizona Transition Zone was divided in two primary zones, Zone 3 and Zone 7. Zone 3 encompasses the entire zone. Zone 7 is a subregion of the southern Basin and Range province. However, it was delineated as a separate zone on the basis of increased seismicity and a higher density of Quaternary faults than observed in the adjacent Zone 1.. These characteristics suggest the zone is more closely related to the Arizona Transition zone than to Zone 1. Zones 4, 5, and 6 represent sub-areas of the Transition zone that have been

subdivided on the basis of the occurrence of Quaternary-active faults or the spatial distribution of seismicity. Zone 4 has a higher density of Quaternary faults, as mapped by Menges and Pearthree (1983). Zones 5 and 6 enclose areas of higher seismicity than other parts of the Transition Zone.

The maximum magnitudes selected as source parameters for Zones 3 through 6 (and the adjacent Zone 7) range from 6.0 to 6.75. These magnitudes reflect both the higher seismicity and increased density of Quaternary faults relative to areas in Zones 1 and 2 to the south.

Four alternatives were considered in defining the appropriate zonation for determining seismicity rates in the Arizona Transition zone. The assumption that the seismicity rate is uniform throughout the Transition Zone 3 is slightly preferred (0.4). This alterative is further divided into two alternatives. The preferred model (conditional probability 0.7) is that Zone 7 is a separate source, because it is a portion of the Basin and Range province. Alternatively, zones 3 and 7 were considered to be a single source zone (conditional probability 0.3). The two additional interpretations considered were that either zone 4 or zones 5 and 6 represent sub-areas of zone 3. These two cases were considered equally likely (0.3). Recurrence parameters for the various zones and zone combinations were estimated from the earthquake catalog using the regional *b*-value shown in Figure 2 for a prior on *b*.

<u>Faults 16-22 (Verde-Cottonwood Fault Zone), 26 (Big Chino Fault), and 29 (Hualapai Mountain Scarp)</u>

The Verde-Cottonwood fault zone (Fault 16-22), Big Chino fault (Fault 26), and Hualapai Mountains scarp (fault 29) have greater lengths than the Quaternary faults that typically occur in the Arizona Transition zone. Based on empirical relationships between magnitude and surface rupture length and between magnitude and displacement, it is judged that these faults could be the source of larger earthquakes than would be expected within Zone 3. The maximum magnitudes selected as source parameters for these faults are therefore higher than

for the surrounding zones. Recurrence estimates for these faults were assumed to be the same as those developed for Fault 4.

COLORADO PLATEAU

The Colorado Plateau province comprises flat-lying, relatively undeformed, Paleozoic through early Tertiary strata overlying deformed Precambrian basement. This region is topographically high and does not display much internal Quaternary geologic deformation. Extensive late Tertiary and Quaternary volcanism that is localized on the fringes of the Colorado Plateau Province adjacent to the Transition Zone (Ratté and others, 1984; Tanaka and others, 1986) provides evidence of recent release of heat and fluids from the deep crust or mantle from beneath this region. Most of the present tectonic activity also occurs along the margins in zones such as the Wasatch-Hurricane frontal fault system on the west, the southern Rocky Mountains and Rio Grande rift on the east, and the Transition Zone on the south and southwest. Crustal thickness in the southern Colorado Plateau is approximately 40 km. Heat flow in the Colorado Plateau is lower than that in the southwest Arizona Basin and Range and Transition Zone provinces, but higher on the average than heat flow characteristics of the stable interior (Klein, 1991).

Zones 8, 9, and 10

The Colorado Plateau was separated into three zones on the basis of the observed seismicity distribution. Zones 8 and 10 have similar low levels of seismicity and Zone 9 has a relatively high level of seismicity. Menges and Pearthree (1983) map a relatively high density of Quaternary faults in the three zones and adjoining areas of the Colorado Plateau.

The maximum magnitudes selected as source parameters for Zones 8, 9, and 10 range from 6.25 to 7.0. These magnitudes are based on the historic seismicity and numerous Quaternary faults recognized in the southern portion of the Colorado Plateau.

Recurrence parameters for the zones 8 and 9 were estimated from the recorded seismicity using the *b*-value prior shown in Figure 2. Zone 10 was assumed to have a similar seismicity rate as Zone 9.

SALTON TROUGH/GULF OF CALIFORNIA

The Salton Trough province is a structural trough between the Basin and Range and Peninsular Ranges provinces. The Salton Trough deepens gradually to the south and appears to be structurally continuous with the Gulf of California. Most of the dextral displacement of the Pacific/North American plate motion is accommodated by faults within the San Andreas fault system and the transtensional regime in the Gulf of California. The transtensional regime of the Gulf of California and the southern Salton Sea area is characterized by small spreading centers interconnected by right transform faults. This region contains the most seismically active faults in the site region: the San Andreas fault, the Imperial and Cerro Prieto faults of Imperial Valley, the San Jacinto fault zone and the Elsinore-Laguna Salada fault system.

Zone 13

The largest earthquakes in this region are expected to occur on the longer transform faults, which are identified as separate seismic zones. The largest magnitude earthquakes expected in the remaining region, designated Zone 13, are likely to be along normal rift faults or associated with volcanic activity along the short ridge segments. Based on analogy to historical seismicity in rift zones worldwide, which rarely exceed M_S 6.0, we expect the maximum magnitude earthquake to be in the range of M 6.0 to 6.5. We give a small probability to the likelihood that a larger event (M 7.0) will occur. Recurrence parameters for the zone were estimated from the recorded seismicity.

Zone 14 (Pinto Mountain Fault)

The Pinto Mountain fault is an east-west trending, Quaternary active fault that lies along the north flank of the Pinto Mountains in the eastern Transverse Ranges. The eastern ~15 km of the approximately 65 km-long fault extends into the 300 km-radius of the Palo Verde site. This is the longest fault within the region designated Zone 14. Offset streams and lithologic contacts indicate up to 16 km of left-lateral movement on this fault, with the maximum displacement near the central portion of the fault (Ref #53, PVNGS updated FSAR). There have been no known surface ruptures on this fault, but a magnitude 5.9 earthquake in 1949 occurred near its eastern end. This earthquake may have been associated with the Pinto Mountain fault or with nearby northwest-trending strike-slip faults within the Mojave Desert to the north. Based on empirical relationships (Wells and Coppersmith, in review) between magnitude and fault parameters, including fault length and area, we estimate that a maximum magnitude earthquake that would occur along faults within Zone 14 would be M 6.8 to 7.2. Given the uncertainties in the seismic potential of this fault and the surrounding region, however, we allow for a range between 6.5 and 7.25 for the expected maximum magnitude. Given that earthquakes in this zone may occur on the Pinto Mountain fault or other faults, the recurrence parameters were determined from the recorded seismicity.

Zone 15 (San Andreas Fault)

The San Andreas fault (Fault 35) is an active right-lateral strike-slip fault that accommodates about 36 mm/yr of slip in the Carrizo Plain (Sieh and Jahns, 1984), about 24 mm/yr at Cajon Pass (Weldon and Sieh, 1985) and about 30 mm/yr in the Salton Trough (Sieh, 1986).

Recent geologic and geophysical measurements suggest that the historically dormant southern segment of the San Andreas fault , which lies within 300 km of the Palo Verde site, is currently locked and slips primarily during great earthquakes (Rayleigh and others, 1982; Lindh, 1983; Sykes and Nishenko, 1984; and Sieh and Williams, 1990). If the rate of strain accumulation along this segment has been steady during the past three centuries, an average of 6-8 m of surficial fault slip could be expected during a future large earthquake (Sieh and Williams, 1990). The largest historical earthquakes along the San Andreas fault have been

the 1857 Fort Tejon, which ruptured approximately 380 km, and 1906 San Francisco earthquakes, both estimated to be M 7.9. Using regression relationships between fault length and magnitude (Wells and Coppersmith, in review), estimated maximum magnitudes for an event that would rupture the southern segments of the San Andreas fault, the Indio (130 km) and Palmdale (175 km) segments as shown by Anderson and others (1989) are in the range of M 7.1 and M 7.7. Given the scenario that multiple segments will rupture for a total length of 400 km, comparable to the maximum historical events, area-magnitude relationships (Wells and Coppersmith, in review) suggest an expected maximum magnitude of M 7.6 to 7.7. Based on these relationships and the historical record, we estimate that the expected maximum magnitude of a future event on the southern San Andreas fault will be no greater than M 7.9, and more likely in the M 7.3 to 7.5 range. In order to accommodate the rupture associated with the various assigned maximum magnitudes, three total lengths for the southern San Andreas are proposed: a length of 130 km for M 7.3, a length of 175 km for M 7.5, and a length of 400 km for M 7.9.

The southern San Andreas has a relatively high probability for a major earthquake in the near future, based on statistical analyses of the fault's paleoseismic record (Sykes and Nishenko, 1984; Wesnousky, 1986). Paleoseismic trenching investigations at sites along the San Andreas fault in the Carrizo Plain to the Salton Trough (Sieh and Jahns, 1984; Weldon and Sieh, 1985; and Sieh, 1986) have demonstrated that large earthquakes recur every 150-300 years, depending on the proximity of the site to segment boundaries. Although the southernmost 200 km of the San Andreas fault has been dormant during the historical period, studies of the prehistoric earthquake history of the fault at the Indio site along this segment of the fault led Sieh (1986) to conclude that this segment of the fault generates a large earthquake at least once every 200 to 300 years. The last earthquake at the Indio site occurred about 300 years ago (Sieh, 1986). Weldon and Sieh (1985) estimated a recurrence time of about 250 years for large earthquakes along the San Andreas fault at Cajon Pass, with the last earthquake possibly being in the early 18th century (250 years ago). The earthquake recurrence rates obtained from fault slip rates (Table 1) are consistent with these estimated

repeat times. Given the low level of recorded seismicity along this portion of the San Andreas, the characteristic recurrence model was assumed to be the only appropriate recurrence model.

Zone 16 (Sand Hills Fault)

Kovach and others (1939) postulated a subsurface fault in the vicinity of Sand Hills referred to as the Sand Hills fault (Fault 36). This inferred fault as shown by Jennings (1973) is approximately 60 km long and lies along the southern projection of the San Andreas fault. Merriam (1951) has suggested that the San Andreas fault continues through the Yuma, Arizona area into Mexico east of the Gulf of California. There is little information available concerning the seismic potential of this postulated fault. The Sand Hills fault is not defined by an alignment of historical seismicity and is not recognized in the relatively young deposits at the surface. Accordingly we judge that there is only a 30 percent likelihood that there is a seismically active structure in Zone 16. Using empirical relationships between magnitude and fault parameters (Wells and Coppersmith, in review), we estimate that the maximum magnitude for this fault most likely would lie in the range of M 6¾ to 7¼. In the absence of slip rate data for this fault we assume a broad range of 0.5 to 10 mm/yr. The high value, to which we assign a low probability, is based on the assumption that a significant amount of the slip carried by the San Andreas fault north of the Salton Sea continues along the Sand Hills fault trend. However, based on the lack of seismicity and geomorphic expression, we infer that the slip rate is more likely to be $\leq$ 1mm/yr. Given the low level of recorded seismicity along this portion of the San Andreas fault zone, the characteristic recurrence model was assumed to be the only appropriate recurrence model.

Zone 17 (Imperial/San Andreas Stepover Region)

The Brawley seismic zone, which lies between the San Andreas and Imperial faults, has been considered the northernmost ridge segment of the ridge/transform system in the Gulf of California (Lomnitz and others, 1970). Within this area a series of faults that trend northeast between bounding northwest-trending faults with right-lateral slip also have been identified.

Basement morphology (Fuis and others, 1984) indicates that dip slip on these faults has occurred in the past. However, these faults, which are termed "cross-faults", experienced left-lateral slip during the 1987 seismic events in the Superstition Hills, Imperial Valley, California (Hudnut and others, 1989). The 1987 surface ruptures were on pre-existing faults displacing consolidated and deformed strata of the Pleistocene Brawley Formation and locally showed geomorphic expression of prior slip (Hudnut and others,1989). Surface rupture associated with the 1987 Elmore Ranch earthquake (M 6.2), the maximum historical event on these faults, occurred in a zone 10 km long and about 10 km wide; seismicity indicates a 20- to 25-km-long rupture during this event. The maximum length of other cross faults in this region is inferred to be approximately 30 km, the maximum distance between the San Andreas and Imperial and San Jacinto fault zones. Given a maximum length of 30 km, empirical relationships between magnitude to subsurface length and area (Wells and Coppersmith, in review) indicate that the maximum magnitude event that would occur on these faults is M 6.6. Therefore, we assign a high probability to an estimated maximum magnitude of M 6.75. Because this zone contains multiple faults, the truncated exponential model was considered the appropriate recurrence model and the recurrence parameters were derived from the recorded seismicity.

Zone 19 (Imperial Fault) and Zone 21 (Cerro Prieto Fault)

The paleoseismic history and slip rate of the Imperial (Fault 37) and Cerro Prieto (Fault 38) faults in southernmost California and northern Baja California is not well known. These faults are thought to carry all of the San Andreas and San Jacinto slip (3-4 cm/yr). However, unpublished trenching investigations along the Imperial fault at sites just north the international border by Robert Sharp (USGS) and just south of the border by Thomas Rockwell (San Diego State University) suggest that the only significant slip to have occurred along the Imperial fault in this region in the past 500 years was in the 1940 earthquake (M 6.9) (Rockwell, pers. comm.). If large earthquakes are spaced relatively evenly in time, a slip rate of about 1 cm or less would be inferred (Rockwell, pers. comm.). No paleoseismological or slip rate studies have been undertaken for the Cerro Prieto fault.

Historical events along the Imperial fault include the M 6.9 1940 and M 6.5 1979 earthquakes. A M 7.2 earthquake probably occurred along the Cerro Prieto fault in 1934 (Anderson and others, 1989). Based on postulated rupture of most or all of the entire fault, we estimate that the maximum magnitudes for the Imperial and Cerro Prieto faults are M 7.0 and M 7.8, respectively. It is more likely that in the case of the Cerro Prieto fault, the entire fault does not rupture during a single event. Therefore, we provide a range in estimated maximum magnitudes of M 7.2 to 7.8 for the Cerro Prieto fault that captures the uncertainties in fault parameters, particularly relating to segmentation and probable rupture lengths.

Figures 3 and 4 compare the observed seismicity rates for the two fault zones with the recurrence relationships computed using slip rate and the truncated and characteristic recurrence models. The exponential model provides a better fit to the data for the Imperial fault (Figure 3), but the catalog likely contains many aftershocks and the two recurrence models were judged equally likely. The characteristic model provides a good fit for the Cerro Prieto fault (Figure 4) and was judged to be the appropriate model.

Zone 20 (San Jacinto Fault Zone)

The San Jacinto fault zone (Fault 41) in southern California consists of a series of primarily right-lateral strike-slip faults. Sharp (1981) determined a minimum mid-Quaternary to present slip rate of 8-12 mm/yr for the central part of the fault near Anza. Also at this location, 4,000 to 29,000 year old ponded sediments and displaced fan deposits suggest a slip rate of 12 mm/yr (Merifield and others, 1987; Rockwell and others, 1990).

Based on geological and seismological data, Sanders (1989) identified twenty principal fault segments ranging in length from 7 to 35 km in the 250-km-long San Jacinto fault zone. Anderson and others (1989), however, identify only nine segments ranging in length from 17 to 55 km. Sanders (1989) notes that the characteristics of large earthquakes in the fault zone, each limited in size to less than M 7, and often limited in rupture extent by discontinuities,

indicate that segmentation of the fault zone is important in influencing the size of earthquakes. He concludes, therefore, that the relatively short lengths of the segments of the San Jacinto fault zone suggest that most future earthquakes will be similarly limited in size. Based on lengths of the southern segments and combined lengths of multiple segments of the fault, maximum magnitudes are estimated to range from M 6¾ to 7.

Only the southern third of the San Jacinto fault zone lies within 300 km of the Palo Verde site. Available data indicate that most of the segments of the fault that lie within 300 km of Palo Verde can be considered to have low potential for a large earthquake in the near future. These include the Arroyo Salada, Borrego Mountain, and Superstition Hills segments which ruptured during the 1954, 1968, and 1987 earthquakes, respectively. In this region of the fault zone, the Superstition Mountain fault has the potential for an earthquake similar to the Superstition Hills earthquake. A large earthquake has not occurred on the Superstition Mountain fault since at least 1892 (Sanders, 1989). Paleoseismic investigations along the Superstition Hills fault indicate that during the past 300 years, the average interval between large surface faulting events has been between about 150 and 300 years. The predicted recurrence rates using slip rate are slightly larger than these estimates. The characteristic and truncated exponential models were judged equally likely for the same reasons as the Imperial fault.

Zone 22 (Elsinore-Laguna Salada Fault Zone)

The northwest-trending Elsinore fault extends over 260 km from the Los Angeles Basin in southern California southeasterly across the International Border into Mexico as the Laguna Salada fault (Lamar and Rockwell, 1986). The fault zone is a dominantly right-lateral strike-slip fault, although there is locally a vertical component of slip along parts of the Laguna Salada fault zone (Lamar, 1961; Millman, 1986; Millman and Rockwell,1986; Pinault, 1984; Pinault and Rockwell, 1984). Recent studies at several sites along the fault suggest a slip rate of about 5-6 mm/yr (Millman and Rockwell, 1986; Vaughan, 1987: Vaughan and Rockwell, 1986; and Pinault and Rockwell, 1984).

Only the southern part of the fault zone, including the Laguna Salada (38 km), the Chupamiertos (22 km), and Sierra Mayor (49km) segments as defined by Anderson and others (1989), lies within 300 km of the Palo Verde site. The Laguna Salada fault has experienced repeated Holocene surface rupture with oblique-slip events measuring up to 5 m each (Mueller and Rockwell, 1984, Mueller, 1984). The last earthquake along this section of the fault produced up to 5 m of vertical slip and probably 1-2 m of right slip over at least 20 km of the fault (Mueller, 1984). Based on the evidence for this very recent and probably historical earthquake, Mueller and Rockwell (1984) concluded that the February 1892 earthquake ($_M$ 7, Anderson and others, 1989) occurred along the Laguna Salada fault. Another earthquake, the 1934 M 6.5-6.7, is thought to have occurred farther to the south along the Chupamierotos segment of the fault (Anderson and others, 1989). Along the Coyote Mountain segment of the Elsinore fault just north of the International Border, paleoseismological investigations suggest repeated late Holocene surface-faulting events with displacements of 80 to 185 cm per event, corresponding to about M 6.5 to 7 events (Rockwell and Pinault, 1986). Based on these observations, the total length (109 km) of the fault zone south of the border and lengths of inferred segments of the fault zone (22 to 49 km) in this region, we estimate that the expected maximum magnitude event would most likely be a M 7.25, with a lesser probability of a M 7.5.

Paleoseismological investigations at sites along the Glen Ivy segment of the Elsinore fault (Rockwell and others, 1986) and the Coyote Mountain segment just north of the International Border (Pinault and Rockwell, 1984) suggest late Holocene recurrence intervals of 200 and 350 years, respectively, for surface-rupture events. Along the Coyote Mountain segment, the most recent event was prehistoric.

Within the study region this fault zone consists of several segments and associated splay faults. Therefore, the recurrence estimates were based on a fit of the truncated exponential model to the recorded seismicity.

Zone 23 (Sierra Juarez Fault Zone)

The Sierra Juarez fault zone is the main fault bounding the west side of the Salton Trough south of the international border. Based on its relatively high sinuosity and lack of expression of recent faulting, it does not appear to have been active in the late Quaternary (Anderson and others, 1989). However, due to uncertainties in the capability of this fault, we have characterized it as a separate source zone. Given a fault length of approximately 110 km, we estimate an expected maximum magnitude of M 7.0 to 7.25. Recurrence estimates were based on the recorded seismicity.

Zone 24 (Inferred Northern Extension of Cerro Prieto Fault)

Rockwell (pers. comm., 1991) suggests that there may be additional faults west of the Imperial fault that are carrying substantial slip. Based on an alignment of recent seismicity along the northwestern projection of the Cerro Prieto fault north of the International Border, Rockwell hypothesizes that some of the Cerro Prieto slip does not transfer to the Imperial fault, but may transfer to the San Jacinto fault. We have given this hypothesis a probability of 0.5. Assuming that an active fault is present in this region , we characterize this fault segment as about 20 to 40 km long, having a slip rate of 10 ± 5 mm/yr comparable to the San Jacinto fault . We assign a maximum magnitude ranging from M 6.5, based on the most likely length of this proposed segment (20 to 40 km), to M 7.2, based on the possibility of a connection to the mapped trace of the Cerro Prieto fault south of the border. Recurrence estimates were based on recorded seismicity.

REFERENCES

Anderson, J.G., 1979, Estimating the seismicity from geological structure for seismic risk studies: Bulletin of the Seismological Society of America, v. 69, p. 135-158.

Anderson, J., Rockwell, T., and Agnew, D., 1989, Past and possible future earthquakes of significance to the San Diego region: Earthquake Spectra, v. 5, no. 2, p. 299-335.

Argus,D. F., and Gordon, R. G., 1988, Sierra Nevada-North America motion from VLBI and paleomagnetic data--implications for the kinematics of the Basin and Range, Colorado Plateau, and California Coast Ranges: Eos Transactions, American Geophysical Union, v. 69, p. 1418.

Cornell, C.A. and E.H. Van Marke, 1969, The major influences on seismic risk: in Proceedings of the Third World Conference on Earthquake Engineering, Santiago Chile, v. A-1, p. 69-93.

DeMets, C. R., Gordon, G., Stein, S., and Argus, D.F., 1987,A revised estimate of Pacific-North America motion and implications for western North America plate boundary zone tectonics: Geophysical Research Letters, v. 14, p. 911-914.

DeMets, C.R., Gordon, G., Argus, D.F., and Stein, S., 1990, Current plate motions: Geophys. J. Int., v. 101, p. 425-478.

Eberly, L.D., and Stanley, T.B., Jr., 1978, Cenozoic stratigraphy and geologic history of southwestern Arizona: Geological Society of America Bulletin, v. 89, p. 921-940.

Engdahl, E.R., and W.A. Rinehart, Seismicity map of North America project: in Slemmons, D.B., E.R. Engdahl, M.D. Zoback, M.L. Zoback, and D. Blackwell, eds., Neotectonics of North America, The Geological Society of America, Boulder, Colorado, in press.

Fuis, G.S., Mooney, W.D., Helaey, J.H., McMechan, G.A., and Lutter, W.J., 1984, Crustal structure of the Imperial Valley region, California, *in* Rugsby, C.A., ed., The Imperial Basin--Tectonics, Sedimentation, and Thermal Aspects: Pacific Section Society of Economic Paleontologists and Mineralogists, p. 1-13.

Gutenberg B. and C.F. Richter, 1954, Seismicity of the Earth and Associated Phenomena, 2nd ed., Princeton University Press, Princeton, New Jersey, 310 p.

Hanks, T.C., and H. Kanamori, 1979, A moment magnitude scale: Journal of Geophysical Research, v. 84, p. 2348-2350.

Hendricks, J.D., and Plescia, J.B., 1991, A review of the regional geophysics of the Arizona transition zone: Journal of Geophysical Research, v. 96, no. B7, p.12,351-12,373.

Hudnut K., Seeber, L., Rockwell, T.K., Goodmacher, J., Klinger, R., Lindvall, S., and McElwain, R., 1989, Surface ruptures on cross-faults in the 24 November, 1987 Superstition Hills, California, earthquake sequence: Bulletin of the Seismological Society of America, v. 79, no. 2, p. 282-296.

Jahns, R.M., 1954, Investigations and problems of southern California: California Division of Mines Bulletin 170, p. 5-29.

Jennings, C.W., 1983, Fault map of California with locations of volcanoes, thermal springs, and thermal wells: California Division of Mines and Geology Geologic Data Map No. 1.

Johnson, R.A., Loy, K., and Wallace, T., 1990, The Santa Rita fault--reactivation of a low-angle detachment fault?: Geological Society of America Abstracts with Programs, v. 22, no. 3, p. 32.

Klein, D. P., 1991, Crustal resistivity structure from magetotelluric soundings in the Colorado Plateau-Basin and Range provinces, central and western Arizona: Journal of Geophysical Research, v. 96, no. B7, p. 12,313-12,332.

Kovach and others (#39 in PVNGS updated FSAR)

Lamar, D.L., and Rockwell, T.K., 1986, An overview of the tectonics of the Elsinore fault zone, in Ehlig, P., ed., Guidebook and Volume on Neotectonics and Faulting in Southern California: Cordilleran section, Geological Society of America, p. 149-158.

Lamar, D.L., 1961, Structural evolution of the northern margin of the Los Angeles basin: Ph.D. thesis, University of California at Los Angeles, 142 p.

Lindh, A. G., 1983, Preliminary assessment of long-term probabilities for large earthquakes along selected segments of the San Andreas fault system in California: U.S. Geological Survey Open File Report 83-63, 15 p.

Lomnitz, C., Mooser, F., Allen, C.R., Brune, J.N., and Thatcher, W., 1970, Seismicity and tectonics of the northern Gulf of California region, Mexico--preliminary results: Geofisica Internacional, v. 10, p. 37-48.

Menges, C.M., and Pearthree, P.A., 1990, Late Quaternary surface-rupture history of the Sand Tank fault: Arizona Geological Survey Open-File Report 90-1, 45 p.

Menges, C.R., Pearthree, P.A., and Calvo, S.,1982, Quaternary faulting in southeast Arizona and adjacent Sonora, Mexico, (abs.): Geological Society of America Abstracts with Programs, v. 14, no. 4, p. 215.

Menges, C.M., and Pearthree, P.A., 1983, Map of neotectonic (latest Pliocene-Quaternary) deformation in Arizona: Arizona Geological Survey Open-File Report 83-22, 48 p.

Merifield, P.M., Rockwell, T.K., and Loughman, C.C., 1987, Slip rate on the San Jacinto fault zone in the Anza seismic gap, southern California (abs): Geological Society of America Abstracts with Programs, v. 19, no. 6, p. 431-432.

Merriam (#51 in PVNGS updated FSAR)

Millman, D.E., and Rockwell, T.K., 1986, Neotectonics of the Elsinore fault in Temescal Valley, California: in Ehlig, P., ed., Guidebook and Volume on Neotectonics and Faulting in Southern California : Cordilleran Section, Geological Society of America, p. 159-166.

Mueller, K.J., 1984, Neotectonics, alluvial history and soil chronology of the southwestern margin of the Sierra de los Cucapas, Baja California Norte, unpublished M.S. Thesis, San Diego State University, California, 363 p.

Mueller, K.J., and Rockwell, T.K., 1984, Sense, recency and rates of faulting along the Laguna Salada and Canon Rojo faults, NE Baja California: Geological Society of America Abstracts with Programs, p. 602.

Pearthree, P.A., 1986, Late Quaternary faulting and seismic hazard in southeastern Arizona and adjacent portions of New Mexico and Sonora, Mexico: Arizona Bureau of Geology and Mineral Technology Open-File Report 86-8, 20 p.

Pearthree, P.A., and Calvo, S.S., 1987, The Santa Rita fault zone--evidence for large magnitude earthquakes with very long recurrence intervals, Basin and Range province of southeastern Arizona: Bulletin of the Seismological Society of America, v. 77, no. 1, p. 97-116.

Pinault, C.T., 1984, Structure, tectonic geomorphology and neotectonics of the Elsinore fault zone between Banner Canyon and the Coyote Mountains, southern California: M.S. thesis, San Diego State University.

Pinault, C.T., and Rockwell, T., 1984, Rates and sense of Holocene faulting on the southern Elsinore fault: further constraints on the distribution of dextral shear between the Pacific and North American plates: GSA Abstracts with Programs, v. 16, no. 6, p. 624.

Raleigh, C.B., Sieh, K.E., Sykes, L.R., and Anderson, D.L.,1982, Forecasting southern California earthquakes: Science, v. 217, 1097-1104.

Ratte, J.C., Marvin, R.F., and Naeser, C.W., 1984, Calderas and ashflow tuffs of the Mogollon Mountains, southwestern New Mexico: Journal of Geophysical Research, v. 89, p. 8713-8732.

Risk Engineering, 1991, Palo Verde, seismicity calculations for Geomatrix source zones: unpublished memorandum by Risk Engineering, Golden Colorado, dated October 10, 1991.

Rockwell, R.K. and Pinault, C.T., 1986, Holocene slip events on the southern Elsinore fault, Coyote Mountains, southern California: in Ehlig, P., ed., Guidebook and Volume on Neotectonics and Faulting in Southern California : Cordilleran Section, Geological Society of America, p. 193-196.

Rockwell, T.K., Loughman, C., and Merifield, P., 1990, Late Quaternary rate of slip along the San Jacinto fault zone near Anza, southern California: Journal of Geophysical Research, v. 95, p. 8593-8605.

Rockwell, T.K, McElwain, R.S., Millman, D.E., and Lamr, D.L., 1986, Recurrent late Holocene faulting on the Glen Ivy North strand of the Elsinore fault at Glen Ivy Marsh, in Ehlig, P., ed., Guidebook and Volume on Neotectonics and Faulting in Southern California : Cordilleran Section, Geological Society of America, p. 167-176.

Sanders, C.O., 1989, Fault segmentation and earthquake occurrence in the strike-slip San Jacinto fault zone, California, in Schwartz, D.P., and Sibson, R.H., eds., Fault Segmentation and Controls of Rupture Initiation and Termination: U. S. Geological Survey Open-File Report 89-315, p. 324-349.

Schwartz, D.P., and K.J. Coppersmith, 1984, Fault behavior and characteristic earthquakes from the Wasatch and San Andreas faults: Journal of Geophysical Research, v. 89, p. 5681-5698.

Sharp, R. V., 1981, Variable rates of late Quaternary strike slip on the San Jacinto fault zone, southern California: Journal of Geophysical Research, v. 86, p. 1754-1762.

Sieh, K.E., and Jahns, R., 1984, Holocene rate of slip and tentative recurrence interval for large earthquakes on the San Andreas fault, Cajon Pass, southern California: Geological Society of America Bulletin, v. 95, p. 883-896.

Sieh, K.E., and Williams, P.L., 1990, Behavior of the southernmost San Andreas fault during the past 300 years: Journal of Geophysical Research, v. 95, no. B5, p. 6629-6645.

Sieh, K.E., 1986, Slip rate across the San Andreas fault and prehistoric earthquakes at Indio, California: Eos American Geophysical Union, v. 67, no. 44, p. 1200.

Sykes, L.R., and Nishenko, S.P., 1984, Probabilities of occurrence of large plate rupturing earthquakes for the San Andreas, San Jacinto, and Imperial faults, California, 1983-2003: Journal of Geophysical Research, v. 89, p. 5905-5927.

Tanaka, K.L., Shoemaker, E.M., Ulrich, G.E., and Wolfe, E.W., 1986, Migration of volcanism in the San Francisco volcanic field, Arizona: Geological Society of America Bulletin, v. 97, p. 129-141.

Vaughan, P., and Rockwell, T.K., 1986, Alluvial stratigraphy and neotectonics of the Elsinore fault zone at Agua Tibia Mountain, southern California, in Ehlig, P., ed., Guidebook and Volume on Neotectonics and Faulting in Southern California: Cordilleran Section, Geological Society of America, p. 177-191.

Vaughn, P.R., 1987, Alluvial stratigraphy and neotectonics along the Elsinore fault at Agua Tibia Mountain, California: unpublished Masters Thesis, University of Colorado, Boulder, 182 p.

Weichert, D.H., 1980, Estimation of the earthquake recurrence parameters for unequal observation periods for different magnitudes: Bulletin of the Seismological Society of America, v. 70, p. 1337-1346.

Weldon, R.J., II, and Sieh, K.E., 1985, Holocene rate of slip and tentative recurrence interval for large earthquakes on the San Andreas fault, Cajon Pass, southern California: Geological Society of America Bulletin, v. 96, no. 6, p. 793-812.

Weldon, R., and Humphreys, E., 1986, A kinematic model of southern California: Tectonics, v. 5, no. 1, p. 33-48.

Wells, D. and K.J. Coppersmith, New earthquake magnitude and fault rupture parameters: Part I surface rupture length and rupture area relationships (abs.): Seismological Research Letters, v. 60, n. 1, p. 27, paper submitted to Journal of Geophysical Research.

Wells, D., and Coppersmith, K., in preparation 1991, Relationships among magnitude, rupture length, rupture area, and surface displacement: Authors affiliated with Geomatrix Consultants, Inc., San Francisco, California.

Wesnousky, S., 1986, Earthquakes, Quaternary faults, and seismic hazard in California: Journal of Geophysical Research, v. 91, p. 12,587-12,631.

Wyss, M., 1979, Estimating maximum expectable magnitude of earthquakes from fault dimensions: Geology, v. 7, p. 336-340.

Youngs, R.R. and K.J. Coppersmith, 1985b, Implications of fault slip rates and earthquake recurrence models to probabilistic seismic hazard estimates: Bulletin of the Seismological Society of America, v. 75, p. 939-964.

Youngs, R.R. and K.J. Coppersmith, 1985a, Development of a fault-specific recurrence model: Earthquake Notes (abs.), v. 56, p. 16.

Zoback, M.L., and Zoback, M., 1980,State of stress in the conterminous United States: Journal of Geophysical Research, v. 85, p. 6113-6156.

Zoback, M.L., and Zoback, M., 1989, Tectonic stress field of the continental United States, *in* Pakiser, L.C., and Mooney, W.D., eds., Geophysical Framework of the Continental United States: Geological Society of America Memoir 172, p. 523-539.

Zoback, M.L., Anderson, R.E., and Thompson, G.A.,1981, Cenozoic evolution of the state of stress and style of tectonism in the western United States: Philosophical Transactions of the Royal Society of London, Ser. A., v. 300, p. 407-434.

GEOMATRIX

Table 1
Seismicity Parameters for Palo Verde Seismic Source Zones

****

Zones 1 and 2 are related as follows
(note faults F1 and F4 are separate line sources within Zones 1 and 2)

Case 1 (0.67) Zones 1 and 2 as separate sources
Case 2 (0.33) Zones 1 and 2 combined into a single source

(note faults F1 and F4 are separate line sources within Zones 1 and 2)

These represent alternative interpretations of the lower southern Basin and Range

Probability active = 1.0

Maximum Magnitudes for zones 1 and 2 are: 5.5 (0.65), 6.0 (0.3), 6.5 (0.05)

Recurrence model Truncated exponental (1.0)

Activity Rates for Zone 1			Activity Rates for Zone 2			Activity Rates for Zones 1&2 Combined		
N(M>5)	b-value	Weight	N(M>5)	b-value	Weight	N(M>5)	b-value	Weight
0.7522E-02	0.685	0.111	0.4737E-02	0.660	0.111	0.1140E-01	0.640	0.109
0.4782E-02	0.834	0.163	0.2595E-02	0.806	0.164	0.7368E-02	0.786	0.156
0.2988E-02	0.983	0.096	0.1392E-02	0.952	0.098	0.4676E-02	0.932	0.089
0.1222E-01	0.685	0.128	0.7698E-02	0.660	0.128	0.1810E-01	0.640	0.130
0.7772E-02	0.834	0.209	0.4218E-02	0.806	0.210	0.1170E-01	0.786	0.213
0.4855E-02	0.983	0.134	0.2263E-02	0.952	0.135	0.7425E-02	0.932	0.137
0.2743E-01	0.685	0.034	0.1727E-01	0.660	0.034	0.3654E-01	0.640	0.034
0.1744E-01	0.834	0.070	0.9464E-02	0.806	0.070	0.2363E-01	0.786	0.073
0.1090E-01	0.983	0.054	0.5078E-02	0.952	0.052	0.1499E-01	0.932	0.058

****

Fault F1 - Sand Tank fault

Probability active = 1.0

Maximum Magnitudes 6.25 (0.4), 6.5 (0.4), 6.85 (0.2)

Return Period for Maximum Events 10,000 yrs (0.3), 50,000 yrs (0.5), 100,000 yrs (0.2)

b-values 0.6 (0.2), 0.85 (0.6), 1.0 (0.2)

Recurrence model - truncated exponential (0.2)

Return	Activity Rates for: Mmax=6.25		Mmax=6.5		Mmax=6.85	
Period	N(m=5)	b-value	N(m=5)	b-value	N(m=5)	b-value
10,000	5.25E-04	0.70	8.25E-04	0.70	1.51E-03	0.70
10,000	6.35E-04	0.85	1.07E-03	0.85	2.19E-03	0.85
10,000	7.76E-04	1.00	1.42E-03	1.00	3.23E-03	1.00
50,000	1.05E-04	0.70	1.65E-04	0.70	3.02E-04	0.70
50,000	1.27E-04	0.85	2.15E-04	0.85	4.38E-04	0.85
50,000	1.55E-04	1.00	2.83E-04	1.00	6.46E-04	1.00
100,000	5.25E-05	0.70	8.25E-05	0.70	1.51E-04	0.70
100,000	6.35E-05	0.85	1.07E-04	0.85	2.19E-04	0.85
100,000	7.76E-05	1.00	1.42E-04	1.00	3.23E-04	1.00

GEOMATRIX

Table 1 (cont'd)
Seismicity Parameters for Palo Verde Seismic Source Zones

Recurrence model - characteristic (0.8)

Activity Rates for:

Return	Mmax=6.25			Mmax=6.5			Mmax=6.85		
	exponential		characteristic	exponential		characteristic	exponential		characteristic
Period	N(m=5.00-5.75)	b-val	N(m=5.75-6.25)	N(m=5.00-6.00)	b-val	N(m=6.00-6.50)	N(m=5.00-6.35)	b-val	N(m=6.35-6.85)
10,000	5.82E-05	0.70	1.00E-04	9.93E-05	0.70	1.00E-04	1.93E-04	0.70	1.00E-04
10,000	4.82E-05	0.85	1.00E-04	8.78E-05	0.85	1.00E-04	1.88E-04	0.85	1.00E-04
10,000	4.02E-05	1.00	1.00E-04	7.82E-05	1.00	1.00E-04	1.86E-04	1.00	1.00E-04
50,000	1.16E-05	0.70	2.00E-05	1.99E-05	0.70	2.00E-05	3.87E-05	0.70	2.00E-05
50,000	9.64E-06	0.85	2.00E-05	1.76E-05	0.85	2.00E-05	3.77E-05	0.85	2.00E-05
50,000	8.03E-06	1.00	2.00E-05	1.56E-05	1.00	2.00E-05	3.72E-05	1.00	2.00E-05
100,000	5.82E-06	0.70	1.00E-05	9.93E-06	0.70	1.00E-05	1.93E-05	0.70	1.00E-05
100,000	4.82E-06	0.85	1.00E-05	8.78E-06	0.85	1.00E-05	1.88E-05	0.85	1.00E-05
100,000	4.02E-06	1.00	1.00E-05	7.82E-06	1.00	1.00E-05	1.86E-05	1.00	1.00E-05

****

Fault F4 - Santa Rita fault

Probability active = 1.0

Maximum Magnitudes 6.25 (0.4), 6.75 (0.4), 7.0 (0.2)

Return Period for Maximum Events 10,000 yrs (0.3), 50,000 yrs (0.5), 100,000 yrs (0.2)

b-values 0.6 (0.2), 0.85 (0.6), 1.0 (0.2)

Recurrence model - truncated exponential (0.2)

Activity Rates for:

Return	Mmax=6.25		Mmax=6.75		Mmax=7.0	
Period	N(m=5)	b-value	N(m=5)	b-value	N(m=5)	b-value
10,000	5.25E-04	0.70	1.27E-03	0.70	1.95E-03	0.70
10,000	6.35E-04	0.85	1.79E-03	0.85	2.96E-03	0.85
10,000	7.76E-04	1.00	2.55E-03	1.00	4.58E-03	1.00
50,000	1.05E-04	0.70	2.55E-04	0.70	3.89E-04	0.70
50,000	1.27E-04	0.85	3.58E-04	0.85	5.92E-04	0.85
50,000	1.55E-04	1.00	5.11E-04	1.00	9.16E-04	1.00
100,000	5.25E-05	0.70	1.27E-04	0.70	1.95E-04	0.70
100,000	6.35E-05	0.85	1.79E-04	0.85	2.96E-04	0.85
100,000	7.76E-05	1.00	2.55E-04	1.00	4.58E-04	1.00

Recurrence model - characteristic (0.8)

Activity Rates for:

Return	Mmax=6.25			Mmax=6.75			Mmax=7.0		
	exponential		characteristic	exponential		characteristic	exponential		characteristic
Period	N(m=5.00-5.75)	b-val	N(m=5.75-6.25)	N(m=5.00-6.25)	b-val	N(m=6.25-6.75)	N(m=5.00-6.50)	b-val	N(m=6.50-7.00)
10,000	5.82E-05	0.70	1.00E-04	1.61E-04	0.70	1.00E-04	2.53E-04	0.70	1.00E-04
10,000	4.82E-05	0.85	1.00E-04	1.52E-04	0.85	1.00E-04	2.57E-04	0.85	1.00E-04
10,000	4.02E-05	1.00	1.00E-04	1.46E-04	1.00	1.00E-04	2.66E-04	1.00	1.00E-04
50,000	1.16E-05	0.70	2.00E-05	3.22E-05	0.70	2.00E-05	5.06E-05	0.70	2.00E-05
50,000	9.64E-06	0.85	2.00E-05	3.05E-05	0.85	2.00E-05	5.15E-05	0.85	2.00E-05
50,000	8.03E-06	1.00	2.00E-05	2.92E-05	1.00	2.00E-05	5.32E-05	1.00	2.00E-05
100,000	5.82E-06	0.70	1.00E-05	1.61E-05	0.70	1.00E-05	2.53E-05	0.70	1.00E-05
100,000	4.82E-06	0.85	1.00E-05	1.52E-05	0.85	1.00E-05	2.57E-05	0.85	1.00E-05
100,000	4.02E-06	1.00	1.00E-05	1.46E-05	1.00	1.00E-05	2.66E-05	1.00	1.00E-05

GEOMATRIX

Table 1 (cont'd)
Seismicity Parameters for Palo Verde Seismic Source Zones

****

Zones 3, 4, 5, 6, and 7 - Arizona Transition Zone

Zones are related as follows
Case 1 (0.28) Zones 3 and 7 as separate sources (zones 4, 5, and 6 not present)
Case 2 (0.12) Zones 3 and 7 combined into a single source (zones 4, 5, and 6 not present)
Case 3 (0.30) Zones 4, 7, and 3 minus 4 as separate sources (zones 5 and 6 not present)
Case 4 (0.30) Zones 5, 6, 7, and 3 minus 5 and 6 as separate sources (zone 4 not present)

Maximum Magnitudes for zones 3, 4, 5, 6, and 7 are: 6.0 (0.1), 6.5 (0.5), 6.75 (0.4)

Recurrence model Truncated exponential (1.0)

Activity Rates for Zone 3			Activity Rates for Zone 4			Activity Rates for Zone 3-4			Activity Rates for Zone 5		
N(M>5)	b-value	Weight	N(M>5)	b-value	Weight	N(M>5)	b-value	Weight	N(M>5)	b-value	Weight
0.2279E-01	0.763	0.102	0.1660E-01	0.711	0.106	0.7653E-02	0.718	0.112	0.1660E-01	0.711	0.106
0.1479E-01	0.895	0.139	0.1062E-01	0.849	0.147	0.4746E-02	0.866	0.164	0.1062E-01	0.849	0.147
0.9522E-02	1.027	0.075	0.6721E-02	0.987	0.081	0.2908E-02	1.013	0.096	0.6721E-02	0.987	0.081
0.3289E-01	0.763	0.133	0.2523E-01	0.711	0.131	0.1244E-01	0.718	0.127	0.2523E-01	0.711	0.131
0.2135E-01	0.895	0.222	0.1614E-01	0.849	0.218	0.7713E-02	0.866	0.210	0.1614E-01	0.849	0.218
0.1374E-01	1.027	0.142	0.1021E-01	0.987	0.140	0.4727E-02	1.013	0.135	0.1021E-01	0.987	0.140
0.5254E-01	0.763	0.036	0.4482E-01	0.711	0.034	0.2791E-01	0.718	0.033	0.4482E-01	0.711	0.034
0.3411E-01	0.895	0.083	0.2867E-01	0.849	0.078	0.1731E-01	0.866	0.070	0.2867E-01	0.849	0.078
0.2195E-01	1.027	0.069	0.1814E-01	0.987	0.064	0.1061E-01	1.013	0.055	0.1814E-01	0.987	0.064

Activity Rates for Zone 6			Activity Rates for Zone 3-5&6			Activity Rates for Zone 7			Activity Rates for Zones 3+7		
N(M>5)	b-value	Weight	N(M>5)	b-value	Weight	N(M>5)	b-value	Weight	N(M>5)	b-value	Weight
0.5089E-02	0.713	0.117	0.2572E-02	0.707	0.124	0.7787E-02	0.671	0.114	0.3088E-01	0.732	0.101
0.3124E-02	0.864	0.174	0.1561E-02	0.861	0.190	0.5664E-02	0.823	0.174	0.2048E-01	0.859	0.134
0.1893E-02	1.014	0.104	0.9351E-03	1.016	0.116	0.4073E-02	0.975	0.107	0.1346E-01	0.986	0.071
0.8425E-02	0.713	0.124	0.4286E-02	0.707	0.120	0.1289E-01	0.671	0.126	0.4343E-01	0.732	0.132
0.5171E-02	0.864	0.204	0.2602E-02	0.861	0.196	0.9377E-02	0.823	0.204	0.2880E-01	0.859	0.222
0.3134E-02	1.014	0.131	0.1558E-02	1.016	0.126	0.6743E-02	0.975	0.130	0.1893E-01	0.986	0.141
0.2243E-01	0.713	0.031	0.1630E-01	0.707	0.029	0.3432E-01	0.671	0.035	0.6565E-01	0.732	0.037
0.1377E-01	0.864	0.065	0.9895E-02	0.861	0.057	0.2496E-01	0.823	0.065	0.4353E-01	0.859	0.088
0.8344E-02	1.014	0.050	0.5927E-02	1.016	0.043	0.1795E-01	0.975	0.046	0.2861E-01	0.986	0.074

****

Embedded within the above zones are three faults

1st source - combine F16, F17, F19, and F22 into a single line source
2nd source - F26 as a single line source
3rd source - F29 as a single line source

all three fault-specific sources have the same recurrence parameters and these are identical to F4 given above

****

Zone 8 - Colorado Plateau

Probability active = 1.0

Maximum Magnitudes 6.25 (0.2), 6.75 (0.6), 7.0 (0.2)

Recurrence model - Truncated exponential (1.0)

Activity Rates		
N(M>5)	b-value	Weight
0.3241E-02	0.671	0.105
0.2386E-02	0.817	0.156
0.1739E-02	0.964	0.093
0.5147E-02	0.671	0.132
0.3790E-02	0.817	0.213
0.2761E-02	0.964	0.137
0.1039E-01	0.671	0.038
0.7653E-02	0.817	0.073
0.5575E-02	0.964	0.053

Table 1 (cont'd)
Seismicity Parameters for Palo Verde Seismic Source Zones

****

Zone 9 - Colorado Plateau

Probability active = 1.0

Maximum Magnitudes 6.25 (0.2), 6.75 (0.6), 7.0 (0.2)

Recurrence model - Truncated exponential (1.0)

Activity Rates N(M>5)	b -value	Weight
0.1620E-01	0.671	0.105
0.1193E-01	0.817	0.156
0.8693E-02	0.964	0.093
0.2573E-01	0.671	0.132
0.1895E-01	0.817	0.213
0.1380E-01	0.964	0.137
0.5197E-01	0.671	0.038
0.3827E-01	0.817	0.073
0.2788E-01	0.964	0.053

****

Zone 10 - Colorado Plateau

Probability active = 1.0

Maximum Magnitudes 6.25 (0.2), 6.75 (0.6), 7.0 (0.2)

Recurrence model - Truncated exponential (1.0)

Activity Rates N(M>5)	b -value	Weight
0.3241E-02	0.671	0.105
0.2386E-02	0.817	0.156
0.1739E-02	0.964	0.093
0.5147E-02	0.671	0.132
0.3790E-02	0.817	0.213
0.2761E-02	0.964	0.137
0.1039E-01	0.671	0.038
0.7653E-02	0.817	0.073
0.5575E-02	0.964	0.053

****

Combined Zones 11 and 12 - Southern Basin and Range

Probability active = 1.0

maximum Magnitudes 6.0 (0.1), 6.5 (0.6), 6.75 (0.3)

Recurrence model - Truncated exponential (1.0)

Activity Rates N(M>5)	b -value	Weight
0.2979E-01	0.540	0.095
0.1453E-01	0.770	0.139
0.6811E-02	1.000	0.085
0.4300E-01	0.540	0.123
0.2097E-01	0.770	0.222
0.9832E-02	1.000	0.152
0.6868E-01	0.540	0.034
0.3350E-01	0.770	0.083
0.1571E-01	1.000	0.067

Table 1 (cont'd)
Seismicity Parameters for Palo Verde Seismic Source Zones

****

Zone 13 - Salton Trough/Gulf of California

Probability active = 1.0

maximum Magnitudes 6.0 (0.1), 6.5 (0.7), 7.0 (0.2)

Recurrence model - Truncated exponential (1.0)

Activity Rates N(M>5)	b -value	Weight
0.7741E+00	0.970	0.080
0.7741E+00	1.081	0.119
0.7741E+00	1.193	0.071
0.9211E+00	0.970	0.141
0.9211E+00	1.081	0.227
0.9211E+00	1.193	0.145
0.1114E+01	0.970	0.054
0.1114E+01	1.081	0.096
0.1114E+01	1.193	0.067

****

Zone 14 - Pinto Mountain and associated faults

Probability active = 1.0

maximum Magnitudes 6.5 (0.2), 7.0 (0.5), 7.25 (0.3)

Recurrence model - Truncated exponential (1.0)

Activity Rates N(M>5)	b -value	Weight
0.3921E-01	0.478	0.082
0.2382E-01	0.716	0.135
0.1404E-01	0.954	0.089
0.5583E-01	0.478	0.126
0.3391E-01	0.716	0.221
0.1999E-01	0.954	0.151
0.8590E-01	0.478	0.045
0.5217E-01	0.716	0.088
0.3076E-01	0.954	0.063

****

Zone 15 - San Andreas (represent by line source F35 extending outside of 300km circle to specified total lengths)

Probability active = 1.0

Case 1 Total length 130 km, Maximum Magnitude 7.55 (0.4)

Recurrence model - characteristic (1.0)

Activity Rates exponential N(m=5-7.05)	b-value	characteristic N(m=7.05-7.55)	Weight
5.55E-02	0.7	8.55E-03	0.040
6.32E-02	0.8	8.60E-03	0.120
7.25E-02	0.9	8.65E-03	0.040
6.66E-02	0.7	1.03E-02	0.120
7.58E-02	0.8	1.03E-02	0.360
8.70E-02	0.9	1.04E-02	0.120
7.77E-02	0.7	1.20E-02	0.040
8.84E-02	0.8	1.20E-02	0.120
1.01E-01	0.9	1.21E-02	0.040

Table 1 (cont'd)
Seismicity Parameters for Palo Verde Seismic Source Zones

Case 2 Total length 175 km, Maximum Magnitude 7.75 (0.5)

Recurrence model - characteristic (1.0)

Activity Rates exponential N(m=5-7.25)	b-value	characteristic N(m=7.25-7.75)	Weight
5.22E-02	0.7	5.77E-03	0.040
6.20E-02	0.8	5.81E-03	0.120
7.44E-02	0.9	5.83E-03	0.040
6.27E-02	0.7	6.92E-03	0.120
7.44E-02	0.8	6.97E-03	0.360
8.93E-02	0.9	7.00E-03	0.120
7.31E-02	0.7	8.07E-03	0.040
8.68E-02	0.8	8.13E-03	0.120
1.04E-01	0.9	8.17E-03	0.040

Case 3 Total length 400 km, Maximum Magnitude 8.15 (0.1)

Recurrence model - characteristic (1.0)

Activity Rates exponential N(m=5-7.65)	b-value	characteristic N(m=7.65-8.15)	Weight
5.79E-02	0.7	3.31E-03	0.040
7.50E-02	0.8	3.33E-03	0.120
9.84E-02	0.9	3.35E-03	0.040
6.94E-02	0.7	3.97E-03	0.120
9.00E-02	0.8	4.00E-03	0.360
1.18E-01	0.9	4.02E-03	0.120
8.10E-02	0.7	4.63E-03	0.040
1.05E-01	0.8	4.67E-03	0.120
1.38E-01	0.9	4.69E-03	0.040

****

Zone 16 - Sand Hills fault (represent by line source F36)

Probability active = 0.3

Maximum Magnitude 7.0 (0.2)

Recurrence model - characteristic (1.0)

Activity Rates exponential N(m=5-6.50)	b-value	characteristic N(m=6.50-7.00)	Weight
1.39E-03	0.7	5.49E-04	0.040
1.41E-03	0.8	5.53E-04	0.120
1.44E-03	0.9	5.56E-04	0.040
2.78E-03	0.7	1.10E-03	0.140
2.83E-03	0.8	1.11E-03	0.420
2.89E-03	0.9	1.11E-03	0.140
2.78E-02	0.7	1.10E-02	0.020
2.83E-02	0.8	1.11E-02	0.060
2.89E-02	0.9	1.11E-02	0.020

Table 1 (cont'd)
Seismicity Parameters for Palo Verde Seismic Source Zones

Maximum Magnitude 7.25 (0.6)

Recurrence model - characteristic (1.0)

Activity Rates			
exponential N(m=5-6.75)	b-value	characteristic N(m=6.75-7.25)	Weight
9.05E-04	0.7	2.32E-04	0.040
9.68E-04	0.8	2.33E-04	0.120
1.04E-03	0.9	2.34E-04	0.040
1.81E-03	0.7	4.63E-04	0.140
1.94E-03	0.8	4.66E-04	0.420
2.08E-03	0.9	4.69E-04	0.140
1.81E-02	0.7	4.63E-03	0.020
1.94E-02	0.8	4.66E-03	0.060
2.08E-02	0.9	4.69E-03	0.020

Maximum Magnitude 7.5 (0.2)

Recurrence model - characteristic (1.0)

Activity Rates			
exponential N(m=5-7.00)	b-value	characteristic N(m=7.00-7.50)	Weight
5.83E-04	0.7	9.77E-05	0.040
6.57E-04	0.8	9.83E-05	0.120
7.46E-04	0.9	9.88E-05	0.040
1.17E-03	0.7	1.95E-04	0.140
1.31E-03	0.8	1.97E-04	0.420
1.49E-03	0.9	1.98E-04	0.140
1.17E-02	0.7	1.95E-03	0.020
1.31E-02	0.8	1.97E-03	0.060
1.49E-02	0.9	1.98E-03	0.020

****

Zone 17 - Imperial/San Andreas stepover region

Probability active = 1.0

Maximum Magnitudes 6.25 (0.2), 6.5 (0.6), 6.75 (0.2)

Recurrence model - Truncated exponential (1.0)

Activity Rates		
N(M>5)	b -value	Weight
0.2769E+00	0.721	0.075
0.2301E+00	0.805	0.116
0.1908E+00	0.889	0.072
0.3158E+00	0.721	0.139
0.2625E+00	0.805	0.227
0.2176E+00	0.889	0.148
0.3633E+00	0.721	0.056
0.3020E+00	0.805	0.099
0.2506E+00	0.889	0.068

Table 1 (cont'd)
Seismicity Parameters for Palo Verde Seismic Source Zones

****

Zone 19 - Imperial Fault - represent by line source F37

Probability active = 1.0

Maximum Magnitude 7.05 (0.7)

Recurrence model - characteristic (0.5)

Activity Rates: exponential N(m=5-6.55)	b-value	characteristic N(m=6.55-7.05)	Weight
3.02E-02	0.7	7.09E-03	0.080
3.29E-02	0.8	7.21E-03	0.240
3.61E-02	0.9	7.30E-03	0.080
7.55E-02	0.7	1.77E-02	0.080
8.24E-02	0.8	1.80E-02	0.240
9.03E-02	0.9	1.83E-02	0.080
1.06E-01	0.7	2.48E-02	0.040
1.15E-01	0.8	2.52E-02	0.120
1.26E-01	0.9	2.56E-02	0.040

Recurrence model - truncated exponential (0.5)

Activity Rates: N(m=5)	b-value	Weight
1.57E-01	0.7	0.080
1.87E-01	0.8	0.240
2.20E-01	0.9	0.080
3.93E-01	0.7	0.080
4.68E-01	0.8	0.240
5.50E-01	0.9	0.080
5.50E-01	0.7	0.040
6.55E-01	0.8	0.120
7.70E-01	0.9	0.040

Maximum Magnitude 7.25 (0.3)

Recurrence model - characteristic (0.5)

Activity Rates: exponential N(m=5-6.75)	b-value	characteristic N(m=6.75-7.25)	Weight
1.84E-02	0.7	3.08E-03	0.080
2.09E-02	0.8	3.13E-03	0.240
2.38E-02	0.9	3.16E-03	0.080
4.60E-02	0.7	7.70E-03	0.080
5.22E-02	0.8	7.82E-03	0.240
5.96E-02	0.9	7.90E-03	0.080
6.44E-02	0.7	1.08E-02	0.040
7.31E-02	0.8	1.09E-02	0.120
8.35E-02	0.9	1.11E-02	0.040

Recurrence model - truncated exponential (0.5)

Activity Rates: N(m=5)	b-value	Weight
1.10E-01	0.7	0.080
1.37E-01	0.8	0.240
1.68E-01	0.9	0.080
2.76E-01	0.7	0.080
3.43E-01	0.8	0.240
4.21E-01	0.9	0.080
3.86E-01	0.7	0.040
4.80E-01	0.8	0.120
5.89E-01	0.9	0.040

GEOMATRIX

Table 1 (cont'd)
Seismicity Parameters for Palo Verde Seismic Source Zones

****

Zone 20 - San Jacinto Fault Zone - represent by line source F41 (use 75 km length)

Probability active = 1.0

Maximum Magnitude 7.00 (0.2)

Recurrence model - characteristic (0.6)

Activity Rates			
exponential N(m=5-6.55)	b-value	characteristic N(m=6.55-7.05)	Weight
2.78E-02	0.7	1.10E-02	0.080
2.83E-02	0.8	1.11E-02	0.240
2.89E-02	0.9	1.11E-02	0.080
6.95E-02	0.7	2.75E-02	0.080
7.06E-02	0.8	2.76E-02	0.240
7.22E-02	0.9	2.78E-02	0.080
9.73E-02	0.7	3.84E-02	0.040
9.89E-02	0.8	3.87E-02	0.120
1.01E-01	0.9	3.89E-02	0.040

Recurrence model - truncated exponential (0.4)

Activity Rates		
N(m=5)	b-value	Weight
2.34E-01	0.7	0.080
2.76E-01	0.8	0.240
3.21E-01	0.9	0.080
5.85E-01	0.7	0.080
6.89E-01	0.8	0.240
8.01E-01	0.9	0.080
8.19E-01	0.7	0.040
9.64E-01	0.8	0.120
1.12E+00	0.9	0.040

Maximum Magnitude 7.15 (0.6)

Recurrence model - characteristic (0.6)

Activity Rates			
exponential N(m=5-6.55)	b-value	characteristic N(m=6.55-7.05)	Weight
2.15E-02	0.7	6.54E-03	0.080
2.26E-02	0.8	6.59E-03	0.240
2.38E-02	0.9	6.62E-03	0.080
5.38E-02	0.7	1.64E-02	0.080
5.64E-02	0.8	1.65E-02	0.240
5.94E-02	0.9	1.66E-02	0.080
7.53E-02	0.7	2.29E-02	0.040
7.89E-02	0.8	2.31E-02	0.120
8.32E-02	0.9	2.32E-02	0.040

Recurrence model - truncated exponential (0.4)

Activity Rates		
N(m=5)	b-value	Weight
1.80E-01	0.7	0.080
2.18E-01	0.8	0.240
2.62E-01	0.9	0.080
4.49E-01	0.7	0.080
5.46E-01	0.8	0.240
6.56E-01	0.9	0.080
6.29E-01	0.7	0.040
7.65E-01	0.8	0.120
9.19E-01	0.9	0.040

Table 1 (cont'd)
Seismicity Parameters for Palo Verde Seismic Source Zones

Maximum Magnitude 7.25 (0.2)

Recurrence model - characteristic (0.6)

Activity Rates exponential N(m=5-6.55)	b-value	characteristic N(m=6.55-7.05)	Weight
1.81E-02	0.7	4.63E-03	0.080
1.94E-02	0.8	4.66E-03	0.240
2.08E-02	0.9	4.69E-03	0.080
4.53E-02	0.7	1.16E-02	0.080
4.84E-02	0.8	1.17E-02	0.240
5.21E-02	0.9	1.17E-02	0.080
6.34E-02	0.7	1.62E-02	0.040
6.77E-02	0.8	1.63E-02	0.120
7.29E-02	0.9	1.64E-02	0.040

Recurrence model - truncated exponential (0.4)

Activity Rates N(m=5)	b-value	Weight
1.51E-01	0.7	0.080
1.87E-01	0.8	0.240
2.29E-01	0.9	0.080
3.76E-01	0.7	0.080
4.67E-01	0.8	0.240
5.74E-01	0.9	0.080
5.27E-01	0.7	0.040
6.54E-01	0.8	0.120
8.03E-01	0.9	0.040

****

Zone 21 - Cerro Prieto - represent by line source F38

Probability active = 1.0

Maximum Magnitude 7.45 (0.4)

Recurrence model - characteristic (1.0)

Activity Rates exponential N(m=5-6.95)	b-value	characteristic N(m=6.95-7.45)	Weight
1.15E-01	0.7	2.09E-02	0.066
1.28E-01	0.8	2.10E-02	0.198
1.44E-01	0.9	2.11E-02	0.066
1.53E-01	0.7	2.79E-02	0.068
1.70E-01	0.8	2.80E-02	0.204
1.91E-01	0.9	2.82E-02	0.068
1.72E-01	0.7	3.13E-02	0.066
1.92E-01	0.8	3.16E-02	0.198
2.15E-01	0.9	3.17E-02	0.066

Maximum Magnitude 7.75 (0.5)

Recurrence model - characteristic (1.0)

Activity Rates exponential N(m=5-7.25)	b-value	characteristic N(m=7.25-7.75)	Weight
6.71E-02	0.7	7.41E-03	0.066
7.98E-02	0.8	7.46E-03	0.198
9.56E-02	0.9	7.50E-03	0.066
8.95E-02	0.7	9.88E-03	0.068
1.06E-01	0.8	9.95E-03	0.204
1.28E-01	0.9	1.00E-02	0.068
1.01E-01	0.7	1.11E-02	0.066
1.20E-01	0.8	1.12E-02	0.198
1.43E-01	0.9	1.13E-02	0.066

GEOMATRIX

Table 1 (cont'd)
Seismicity Parameters for Palo Verde Seismic Source Zones

Maximum Magnitude 8.05 (0.1)

Recurrence model - characteristic (1.0)

Activity Rates			
exponential N(m=5-7.55)	b-value	characteristic N(m=7.55-8.05)	Weight
3.90E-02	0.7	2.63E-03	0.066
4.95E-02	0.8	2.65E-03	0.198
6.35E-02	0.9	2.66E-03	0.066
5.21E-02	0.7	3.51E-03	0.068
6.60E-02	0.8	3.53E-03	0.204
8.46E-02	0.9	3.55E-03	0.068
5.86E-02	0.7	3.95E-03	0.066
7.43E-02	0.8	3.97E-03	0.198
9.52E-02	0.9	3.99E-03	0.066

****

Zone 22 - Laguna Salada

Probability active = 1.0

Maximum Magnitudes 7.25 (0.67), 7.5 (0.33)

Recurrence model - Truncated exponential (1.0)

Activity Rates		
N(M>5)	b -value	Weight
0.2357E+00	0.685	0.075
0.1929E+00	0.777	0.117
0.1573E+00	0.869	0.073
0.2729E+00	0.685	0.138
0.2232E+00	0.777	0.227
0.1820E+00	0.869	0.148
0.3194E+00	0.685	0.056
0.2613E+00	0.777	0.098
0.2131E+00	0.869	0.067

****

Zone 23 - Sierra Juarez

Probability active = 1.0

Maximum Magnitudes 7.0 (0.67), 7.25 (0.33)

Recurrence model - Truncated exponential (1.0)

Activity Rates		
N(M>5)	b -value	Weight
0.1936E+00	0.693	0.101
0.1572E+00	0.730	0.115
0.1275E+00	0.768	0.048
0.2129E+00	0.693	0.113
0.1728E+00	0.730	0.228
0.1401E+00	0.768	0.140
0.2351E+00	0.693	0.038
0.1908E+00	0.730	0.103
0.1547E+00	0.768	0.095

GEOMATRIX

Table 1 (cont'd)
Seismicity Parameters for Palo Verde Seismic Source Zones

****

Zone 24 - northern extension of Cerro Prieto

Probability active = 0.5

Maximum Magnitudes 6.5 (0.5), 7.0 (0.4), 7.2 (0.1)

Recurrence model - Truncated exponential (1.0)

Activity Rates N(M>5)	b -value	Weight
0.2663E-01	0.723	0.109
0.1551E-01	0.822	0.120
0.8967E-02	0.920	0.045
0.3126E-01	0.723	0.125
0.1820E-01	0.822	0.229
0.1052E-01	0.920	0.138
0.3718E-01	0.723	0.030
0.2166E-01	0.822	0.100
0.1252E-01	0.920	0.105

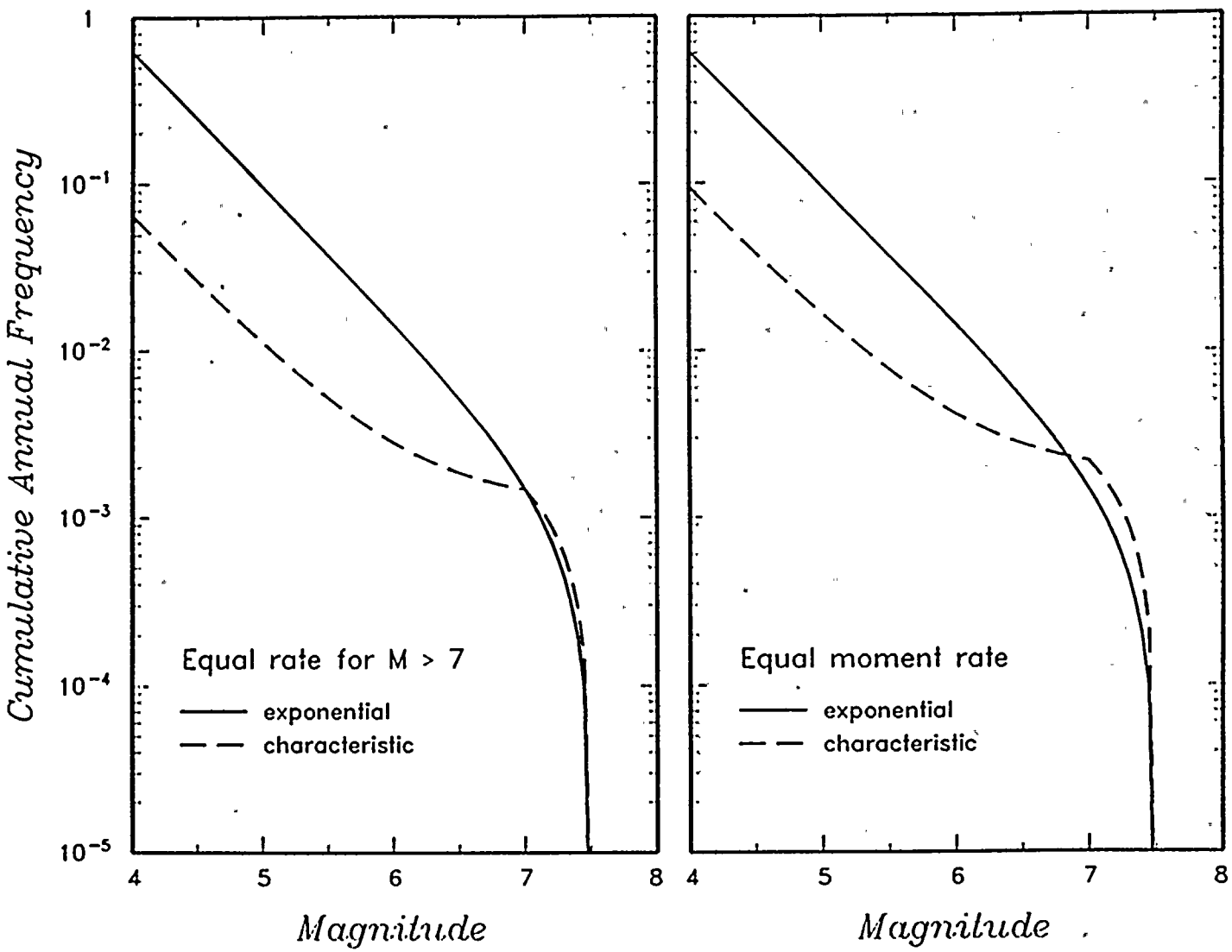

Figure 1. Recurrence models used for fault specific sources.

GEOMATRIX

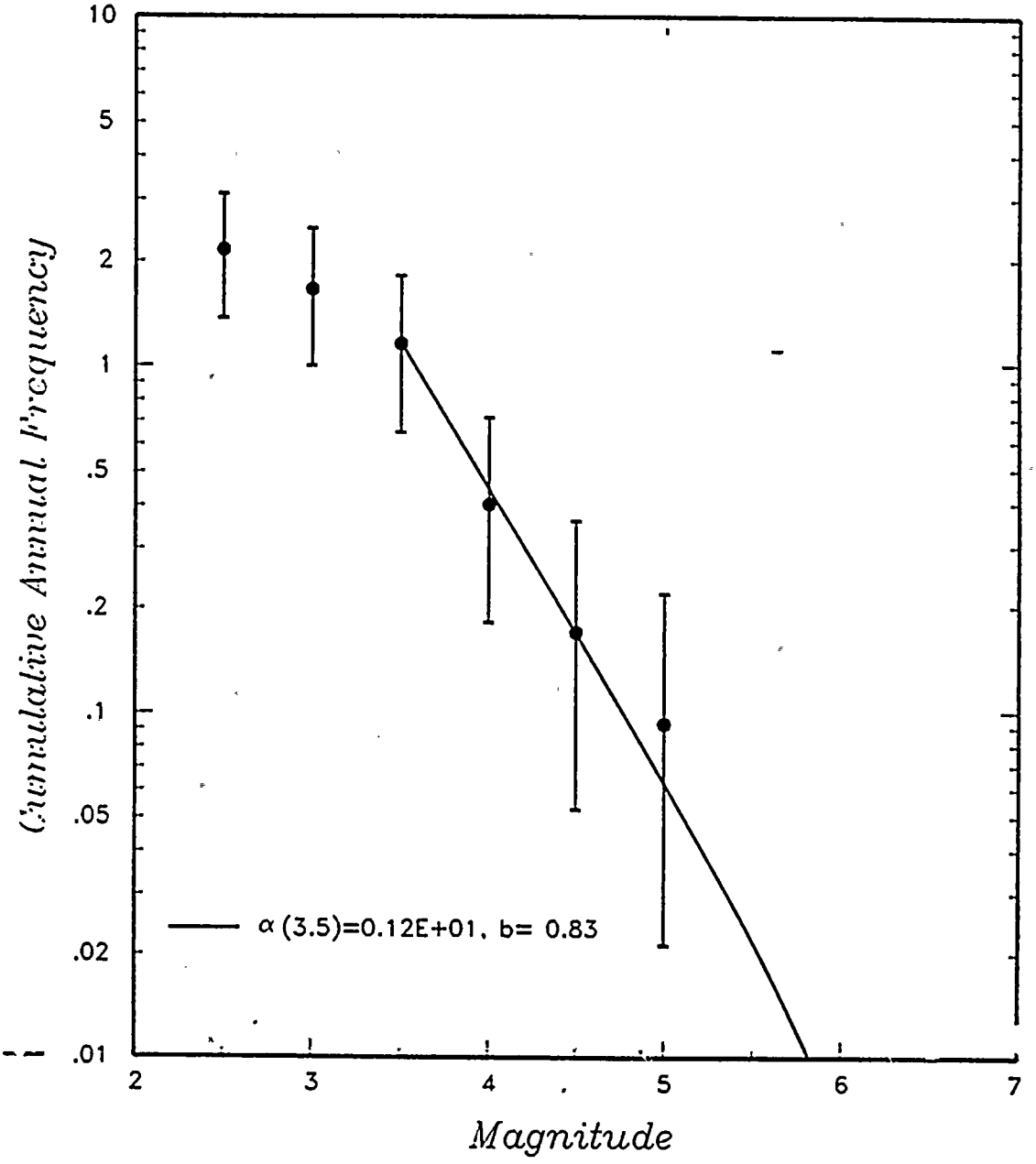

Figure 2. Regional earthquake recurrence for study region east of the Salton Trough/Gulf of California.

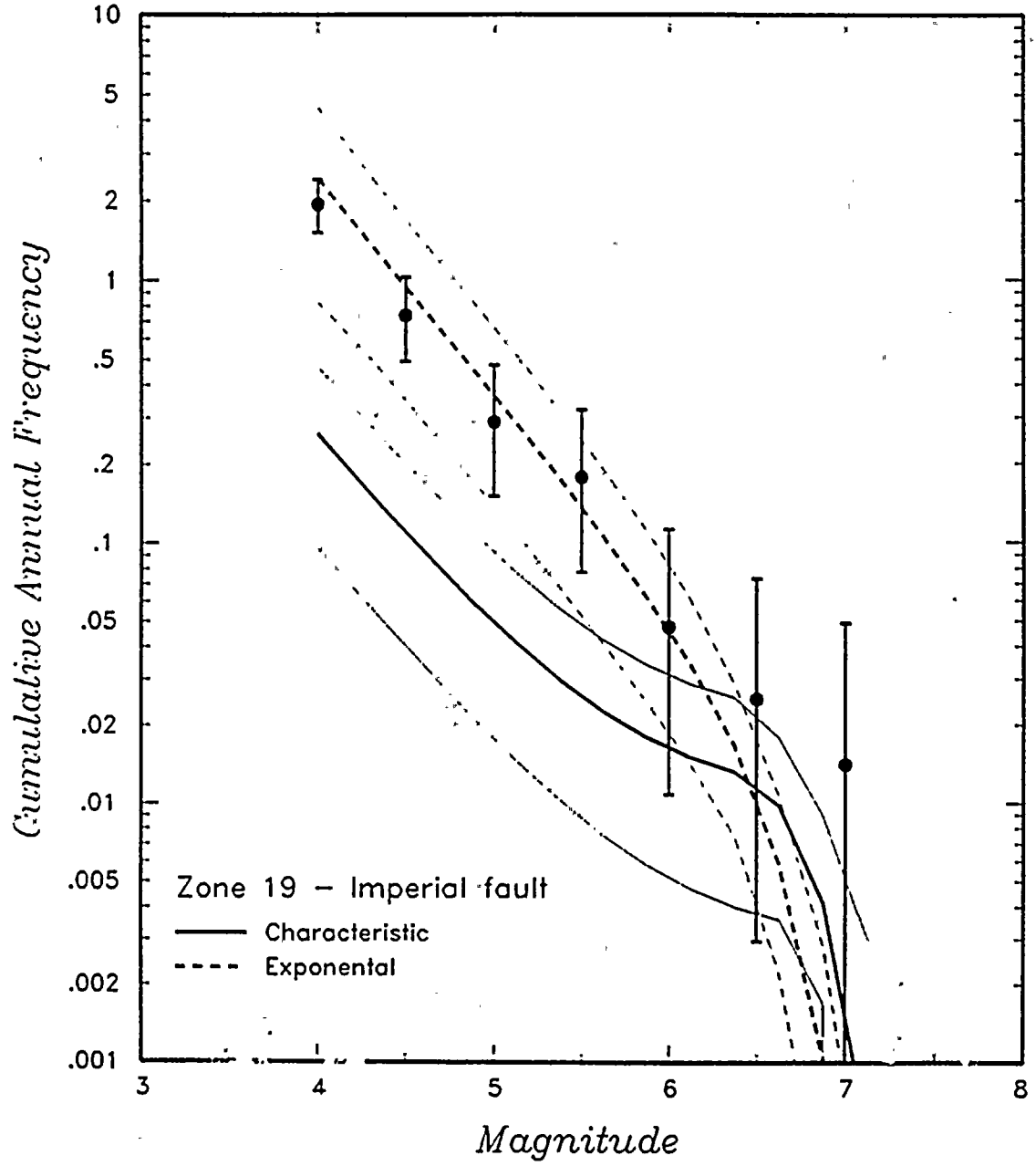

Figure 3. Comparison of observed seismicity rates (solid dots with 90% confidence intervals) with slip rate based recurrence estimates (and 90% confidence intervals) for the Imperial fault.

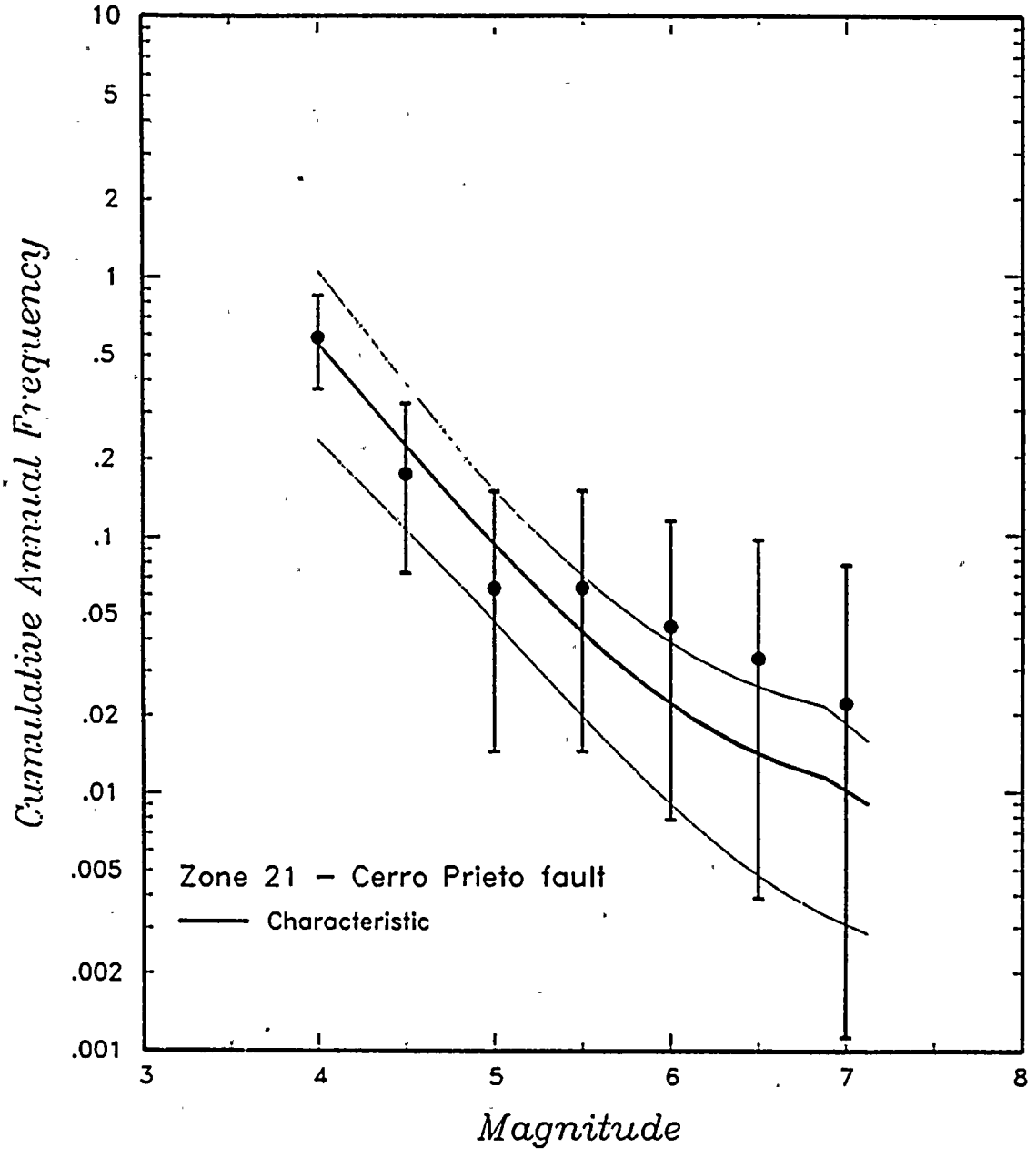

Figure 4. Comparison of observed seismicity rates (solid dots with 90% confidence intervals) with slip rate based recurrence estimates (and 90% confidence intervals) for the Cerro Prieto fault.

APPENDIX B

Seismic Source and Seismicity Parameter Interpretation, James M. Montgomery Consulting Engineers Team

TABLE OF CONTENTS

SECTION 1

INTRODUCTION

This study was carried out by James M. Montgomery, Consulting Engineers, Inc. (JMM) in association with its subconsultants, Golder Associates Inc., and Mr. Bruce Schell, consulting geologist. The work was accomplished between September 1 and November 15, 1991; and was conducted for Risk Engineering, Inc. (REI) as part of their larger study to evaluate the probabilistic seismic hazard to the Palo Verde Nuclear Generating Station, located approximately 35 miles west of Phoenix, Arizona (Figure 1).

The scope of work defined by REI for the JMM team included the following:

1) Identification and description of seismic sources within 300 km of the PVNGS that may be capable of generating earthquakes greater than magnitude 5.

2) Development of maximum magnitudes for each of the seismic sources along with a distribution of magnitudes and associated weights.

3) Development of activity rate, b-value, and estimates of probability of activity for each of the seismic sources.

4) Documentation of the methodology used to select and evaluate each of the seismic sources.

The JMM team was one of two consulting groups participating in this study that were independently evaluating the seismologic and geoscience data relevant to the project. Due to the specialized nature of the study and the limited schedule, the scope focussed on compiling and evaluating existing data and on developing information from conversations with knowledgeable professionals that are actively investigating regional neotectonics and specific Quaternary faults in Arizona. There were no new field investigations carried out by the JMM team for this contract nor was there any original research undertaken to develop new data. However, unpublished information of recent Quaternary fault investigations in Arizona was available to the JMM team through B. Schell. For the most part, the primary data sources are publicly available in published form.

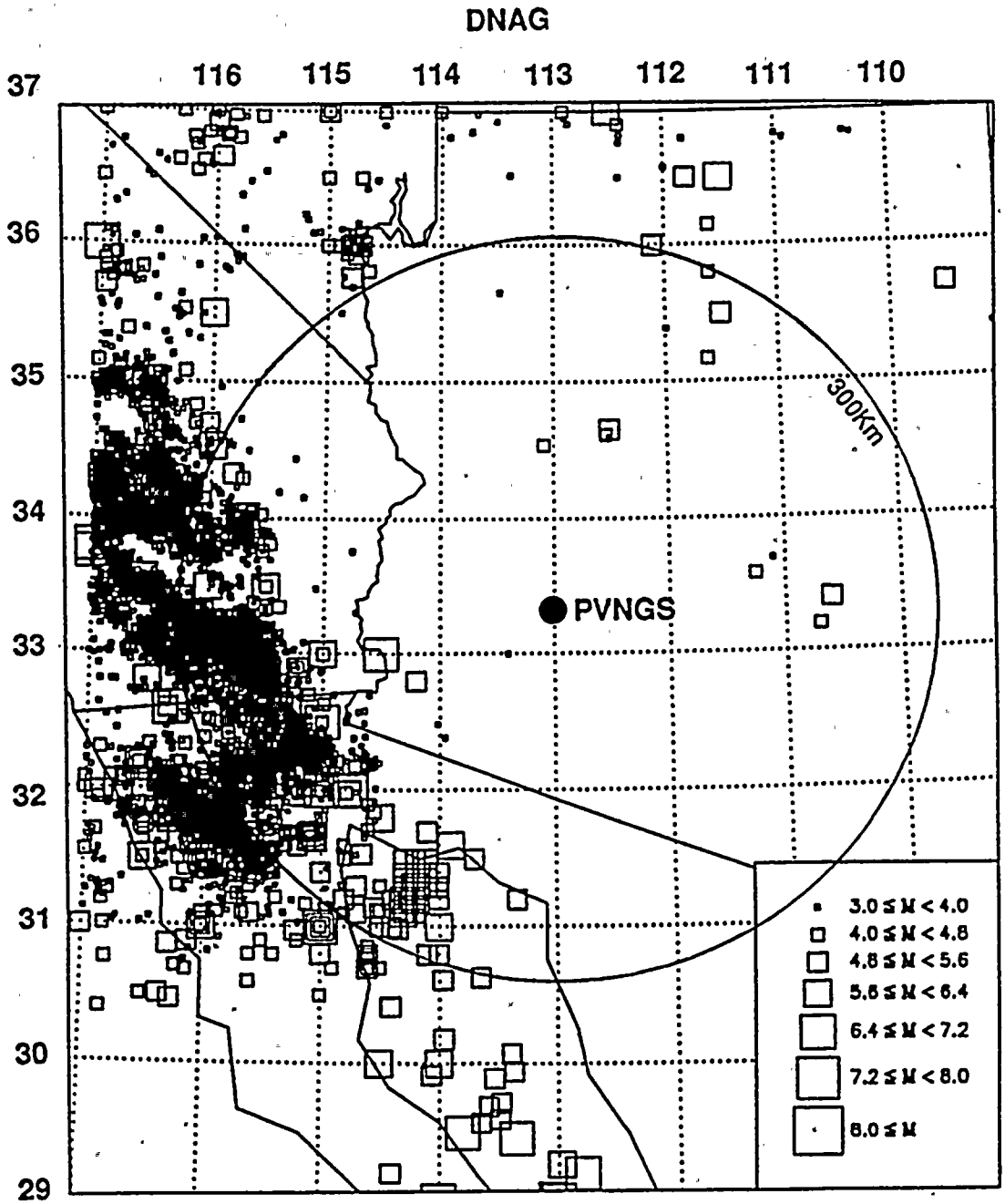

LOCATION MAP
SEISMICITY WITHIN 300 KM OF PVNGS
FIGURE B-1

The main goal was to carry out this study using methods that would ensure a high confidence that the following objectives were satisfied:

1) The data base of potential seismic sources is comprehensive and identifies all known or suspected Quaternary faults or other potential seismic sources within 300 km of PVNGS.

2) The criteria for defining seismic potential and screening the region are defendable, documentable, and accurately represent current concepts regarding causes of earthquakes in Arizona and surrounding regions.

3) The development of probability distributions for magnitude, activity rates, and alternative hypotheses is based on accepted methods, and the distributions represent a reasonably conservative range of interpretations that are supported by the data.

SECTION 2

METHODOLOGY

Figure 2 provides an overview of the methodology used in this seismic evaluation. The process has been divided into seven basic steps:

1) Research and compilation of the data base,

2) Identification of preliminary neotectonic zones and seismic sources,

3) Development and application of criteria for evaluating the seismic potential,

4) Screening and refinement of the neotectonic zones and seismic sources,

5) Evaluation and assignment of appropriate seismic parameters and weights,

6) Definition of the probabilistic relationships between the seismic sources and the neotectonic zones, and

7) Documentation.

The following subsections highlight the important aspects of the methodology. Later sections describe the details of the process and summarize the results.

2.1 RESEARCH AND DATA COMPILATION

The primary sources of information for this study are listed in the reference section following the report text. For the most part, the data were obtained from the following general published sources:

1) Open-file maps and reports from the Arizona Bureau of Geology and Mineral Technology (ABGMT), the Arizona Geological Survey (AGS), and the U.S. Geological Survey (USGS), and other federal agencies,

2) Published seismologic data bases from federal agencies (Geological Society of America DNAG) and special studies from the USGS (Stover, et. al. 1983),

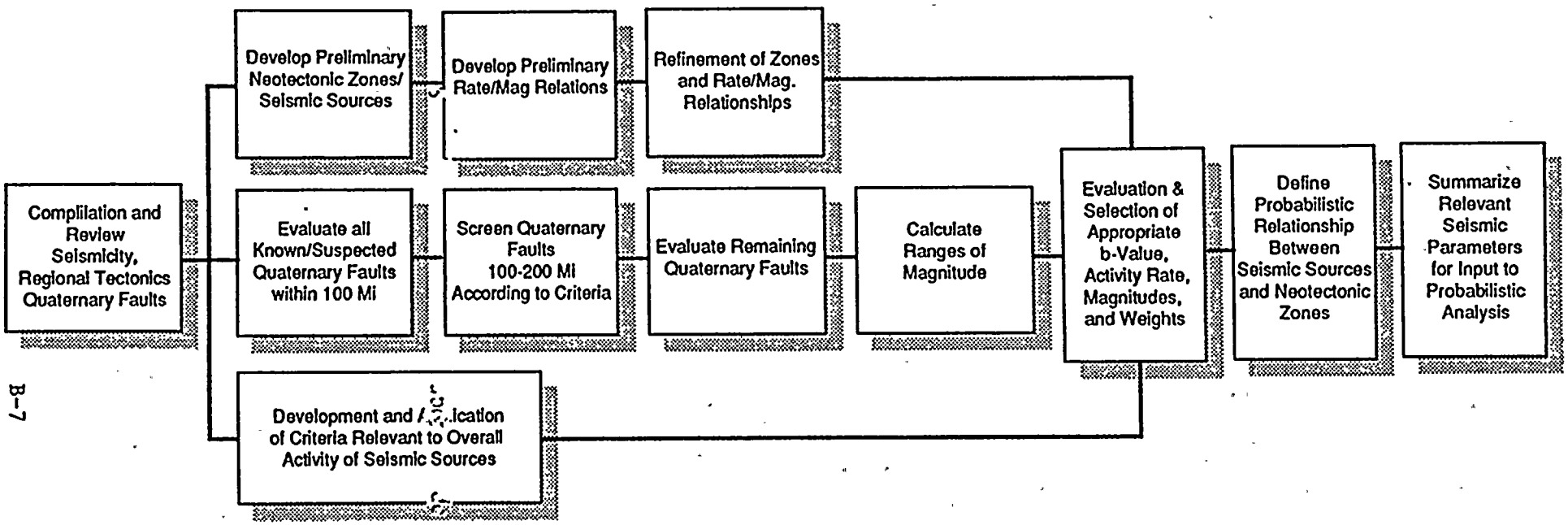

METHODOLOGY FLOW DIAGRAM
FIGURE B-2

3) Published articles from a variety of state and federal agencies,

4) Safety Analysis Reports (PSAR, FSAR) for the PVNGS.

During the compilation of data on Quaternary faults, contact was made with researchers regarding current opinions on the age and activity of selected features. As explained in a later section, in some instances certain faults were removed or modified from published maps based on that personal communication, even though the field work is not yet documented in the literature.

The data that characterize Quaternary faults in terms of their ability to generate earthquakes were summarized and tabulated (Table B-1).

2.2 PRELIMINARY IDENTIFICATION OF NEOTECTONIC ZONES AND POTENTIAL SEISMIC SOURCES

The preliminary identification of neotectonic zones and potential seismic sources involved the following:

1) Preparation of base maps and overlays (1:1,000,000 scale) of the 300 km radius showing the distribution of historic seismicity, known or suspected Quaternary faults, Quaternary volcanic rocks, and previous interpretations of neotectonic zones or provinces from published sources.

2) Comparison of the regional tectonic characteristics in Arizona and surrounding areas with the data presented on the maps and overlays noted in item 1).

3) Creation of boundaries around regions of similar tectonic and seismic characteristics within a 300 km radius.

4) Creation of envelops around specific Quaternary faults (potential seismic sources) that might be associated with historic seismicity and might provide analogs for other, similar faults in a particular neotectonic zone. The width of the envelops around selected faults was based on the assumption that the faults could dip at a angle up to 45 degrees for the full thickness of the crust.

REI digitized the neotectonic regions and seismic source envelops and provided an analysis of the seismicity (if any) within each area. The REI results were presented to JMM as semi-log plots of annual rate of seismic activity vs. magnitude along with a best fit line to mathematically define the slope of historic seismicity.

2.3 DEVELOPMENT OF CRITERIA FOR EVALUATING SEISMIC POTENTIAL OF SPECIFIC FEATURES

The workscope defined by REI required that each specific seismic source should have an evaluation of its capability to generate earthquakes greater than magnitude 5. To accomplish this and document the results, a matrix was created to evaluate each seismic source in terms of the following criteria:

1) Spatial association between the Quaternary fault or volcanic source and the distribution of historic seismicity,

2) Evidence for recency of movement or activity on the feature during the Quaternary or Holocene,

3) Orientation of the feature relevant to the regional stress system,

4) Quality of the data and confidence in the conclusions drawn about the particular feature.

Each criterion was divided into three possible ranges of scores (i.e., evidence for high, intermediate, or low activity) which sum to a probability of 1.0. The final evaluation of activity (probability) is the sum of the high and intermediate scores for all criteria. The scores were assigned by a group of four lead professionals from the JMM team. Examples of the matrix and the scoring system are included in Table B-3.

2.4 SCREENING AND REFINING OF NEOTECTONIC ZONES AND POTENTIAL SEISMIC SOURCES

The Quaternary faults identified during the data search were screened for further analysis based on the following criteria:

1) All known or suspected Quaternary faults identified within 100 miles of the PVNGS were compiled on the maps and included for additional analysis,

2) All known or suspected Quaternary faults identified between 100 and 200 miles of the PVNGS were screened based on specific criteria derived from an NRC methodology outlined in CFR Title 10, Part 100, Table B-1 . The subcriteria define a fault length vs site distance relationship to determine whether additional analyses should be carried out. Faults that did not meet the following relationship were screened out:

Fault Length (miles)	Distance from Site (miles)
1	0 to 20
5	>20 to 50
10	>50 to 100
20	>100 to 150
40	>150 to 200

The purpose of the screening was to focus the analysis on the faults that would have the most contribution to the seismic risk to PVNGS.

3) Of the faults that were screened out based on the subcriteria in item 2), several of the longer ones (i.e., Bright Angel, Mesa Butte, and Santa Rita) were selected for analysis in order to test their contribution to the seismic risk.

2.5 EVALUATION AND ASSIGNMENT OF APPROPRIATE SEISMIC PARAMETERS

The seismic parameters required by the REI scope included the following:

1) The range of maximum magnitudes for each seismic source or neotectonic zone along with weights for each magnitude,

2) The annualized activity rate for earthquakes greater than magnitude 5 for each seismic source,

3) The slope (b-value) of earthquake recurrence for each seismic source along with weights, and

4) The overall probability of activity of the seismic source.

2.5.1 Maximum Magnitudes

A range of maximum magnitudes was determined for each seismic source. In some cases, multiple rupture alternatives were developed for a single fault, and a range of maximum magnitudes was developed for each alternative. The maximum magnitudes were calculated using a number of equations applicable to the type of fault and expected sense of movement. The equations included variables and relations such as the following:

1) Maximum fault length to earthquake magnitude,

2) Fault rupture length to earthquake magnitude,

3) Fault rupture area to earthquake magnitude,

4) Fault slip rate to earthquake magnitude,

5) Seismic moment and moment magnitude.

For normal faults, which represent the largest number of faults in the region, six magnitude calculations were made for each seismic source. For strike slip faults, nine magnitude calculations were made for each seismic source. The procedure to develop the magnitude range included selecting the low, high, and mean values of each calculation set. Probabilities were assigned for each of the three magnitudes within

each alternative based on the collective judgment of the four project team members. The judgments were based on meetings or conference calls where each fault was discussed individually and compared with other faults in the analysis.

Examples of the magnitude calculations including rupture alternatives, assumptions, equations, magnitude values, and equation references are included for each fault in Table B-2.

2.5.2 Annualized Activity Rate and b-Value

To determine the appropriate annualized activity rate (for earthquakes greater than magnitude 5) and b-value for each seismic source or neotectonic zone, the following procedure was used:

1) Annual rate vs magnitude plots generated by REI were reviewed for each neotectonic zone and seismic source (where available) in terms of adequacy of the data quantity, quality, and accuracy of the seismicity catalogue;

2) b-values derived from historical seismicity in a zone or seismic source were compared to those developed from broader data sets from the southwest U.S.,

3) b-value slopes derived from the historic seismicity were evaluated against the geologic/tectonic data for the appropriate zone or seismic source. The purpose was to evaluate the best fit between the slope of historical seismicity and the estimated maximum magnitude considered to be characteristic of a particular fault or zone. In several cases, recurrence data and maximum magnitude estimations for particular faults could be compared with the b-value slopes developed from historical seismicity to judge the appropriateness of the slope and to constrain the placement of the line.

4) Appropriate b-values and activity rates were selected based on directly applicable data or the use of analogous information derived from the region.

For this analysis, the probability distributions assigned to activity rates and b-values were identical to those assigned to the range of maximum magnitudes. Examples are included in the Zone and Seismic Source Summary Sheets included in Table B-4 and Table B-5.

2.5.3 Overall Probability of Activity

The overall probability of activity for a particular fault was evaluated and assigned based on the matrix and criteria described in the section on criteria development on page 3. Examples of the system used to evaluate and document the probability of activity are included in Table B-3.

2.6 DEFINITION OF THE PROBABILISTIC RELATIONSHIPS

The probabilistic framework was defined between the neotectonic zones and the Quaternary faults according to the following criteria:

1) Each Quaternary fault is considered an independent seismic source that can act alone or in combination with other seismic sources within the same neotectonic zone,

2) Each neotectonic zone containing the independent seismic sources has a background level of seismic activity (with a maximum random event) that is mutually exclusive with earthquakes produced by the independent seismic sources (i.e., faults) within the same neotectonic zone,

3) For neotectonic zones not containing any Quaternary faults or specific seismic sources, a range of maximum earthquakes, b-value slopes, and activity levels can be defined which can occur randomly anywhere within the neotectonic zone,

4) The only exception to the above criteria is the Salton Trough neotectonic zone and the San Andreas fault zone, which are considered for this study to represent an identical seismic exposure to the PVNGS in terms of maximum magnitude and source-site distance. Although conservative, this interpretation is considered justified because of the poorly-defined location of the fault elements within the Salton Trough, the high levels of historical seismicity, and the large distance to the site.

SECTION 3

NEOTECTONIC ZONES

Plate 1 (pocket drawing) shows the boundaries of the eleven neotectonic zones that have been interpreted within the 300 km radius from the site. The majority of these zones have been previously identified and described by previous researchers in the southwestern U.S. The interpretation shown on Plate 1 is primarily a compilation based on work by Menges and Pearthree (1983), Menges (1984), Schell and Wilson (1981), and Schell et. al. (1985). The zones include the following:

1) Salton Trough

2) Eastern Transverse Ranges

3) Mojave Basin and Range

4) Lake Mead Basin and Range

5) Sonoran Desert Basin and Range

6) Mexican Basin and Range

7) Pinacate Volcanic Field

8) Arizona Mountains

9) Hurricane-Wasatch

10) San Francisco Volcanic Field

11) Colorado Plateau

The term neotectonic refers to tectonic processes that are active and reflective of the current stress regime of the region. The most definitive data for identifying and describing neotectonic regimes are the distribution and characteristics of young faults, seismicity, geomorphology, and young volcanism. To some extent, the time span over which the neotectonic processes have been in action varies among the neotectonic zones. For the most part, previous researchers have considered features which occurred within the Quaternary (about 1.8 to 2.0 million years) as evidence of neotectonic activity, although the Quaternary Period is primarily based on climatic rather than tectonic criteria.

The boundary of the Salton Trough neotectonic zone includes the San Andreas fault zone east of the Salton Sea and the Sand Hills-Algondones fault zone southeast of Yuma. The southern part of the zone parallels the Gulf of California. This boundary also envelops most of the intense seismicity associated with the Salton Trough-Gulf of California.

3.2 EASTERN TRANSVERSE RANGES

The Eastern Transverse Ranges neotectonic zone includes the east-west trending mountain ranges located east of the San Andreas fault zone. This zone and its associated faulting has been uplifted through compression related the kinematic constraints of the bend in the San Andreas fault system. The northern edge of the zone has been uplifted along a major reverse fault system which separates it from the Mojave block. Major left-lateral faults in the province are the Pinto Mountain and Blue Cut faults which have been included in the analysis of seismic sources for this study. Seismicity is abundant in this zone although there have been no major historic surface ruptures associated with the earthquakes.

3.3 MOJAVE BASIN AND RANGE

The Mojave Basin and Range neotectonic zone is distinguished by abundant northwest trending, right-lateral, strike slip faults, many of which show evidence of Quaternary displacement. Although these faults are long, their cumulative displacements are generally less than 5 to 10 km suggesting that the initiation of strike slip faulting in the Mojave could be as recent as Pliocene. The northwest trending faults are often terminated at both the northern and southern margin of the zone by east-west trending faults. Seismicity is most evident in the eastern part of the zone in proximity to the major northwest trending faults. Earthquakes in 1947, 1975, and 1979 were accompanied by surface rupture on the Manix, Galway Lake, and Johnson Valley-Homestead Valley faults, respectively.

3.4 LAKE MEAD BASIN AND RANGE

The Lake Mead Basin and Range is distinguished from the surrounding zones by a) an abundance of northeast striking faults, b) more intense seismicity, and c) focal mechanisms with tensional axes oriented northwest-southeast. The seismicity is more intense within this zone compared to the Sonoran Desert Basin and Range to the south. Part of the increased seismicity has been induced by the reservoir at Lake Mead and by activities at the Nevada Test Site. Late Quaternary faults in the Lake Mead Basin and Range neotectonic zone are similar in orientation to the faults of central Nevada (north trending) except that they commonly change strike (i.e., northeast) at their southern end.

3.5 SONORAN DESERT BASIN AND RANGE

The part of the Sonoran Desert Basin and Range neotectonic zone within a 300 km radius of PVNGS lies between the mountains to the northeast (Arizona Mountains

The province boundaries shown on Plate 1 have been depicted as solid lines divided into a series of straight segments. Even though the zone boundaries are often irregular, this segmentation has been used to simplify the digitizing process of the maps. In addition, a number of boundaries are transitional and can not always be clearly defined by a single line. Where transitions among zones was fairly broad, the line was placed in the most reasonably conservative location.

The majority of the area within the 300-km radius encompasses a single large tectonic province and its transition areas, namely, the Basin and Range province. As summarized by Schell et. al. (1985), the following generalizations about the Basin and Range province and the later identification of neotectonic zones still apply to the tectonic analysis of the site region:

> "The major part of the area comprising these provinces was part of one continuous large tectonic province, the Basin and Range province, until sometime between late Miocene and early Pliocene when the present tectonic (neotectonic) regime came into effect. Neotectonic characteristics such as young faults, volcanism, seismicity, and geomorphology indicate a modern tectonic regime of somewhat coherent crustal blocks extending westward relative to the North American continental interior. These coherent blocks are separated by zones of more active extension where most of the stress is released by tensional faults. The Sonoran neotectonic province is one of the coherent blocks and is characterized by a near lack of Quaternary faults, seismicity, and volcanism, and it has a relatively mature physiography, all of which are evidence of tectonic stability. The province is nearly surrounded by zones of active extension such as the Mexican Basin and Range, Arizona Mountain, Southern Nevada, and Salton Trough-Gulf of California neotectonic provinces. Young faults, relatively young volcanism, frequent earthquakes, and immature physiography characterize these provinces. Complexities in the overall crustal extension, typical of the southeastern U.S. occur in the Salton Trough, Eastern Transverse Ranges, and Mojave provinces but these complexities are compatible with the regional extensional tectonic regime."

The following subsections briefly summarize the salient characteristics of the neotectonic zones shown on Plate 1. Many of the following descriptions have been abstracted from the PVNGS FSAR (ANPP, 1983) and Schell et. al. (preprint,1985).

3.1 SALTON TROUGH

The Salton Trough neotectonic zone is the most seismically active area within 300 km of the PVNGS. In this region,the Salton Trough zone defines the broad boundary between the North American and the Pacific lithospheric plates. This zone incorporates a) major right lateral, strike slip fault zones (i.e., San Andreas, San Jacinto, Whittier-Elsinore, Imperial, and Cerro Prieto), b) a crustal rift zone which includes numerous short spreading centers and transform faults within the Gulf of California, and c) peripheral zones of primarily normal and normal oblique faulting (i.e., Sand Hills-Algodones and Sierra Juarez-San Pedro Martir fault zones).

neotectonic zone) and the Salton Trough-Gulf of California depression to the southwest. This neotectonic zone is characterized by relatively small, randomly oriented mountain ranges that comprise about 20 percent of the surface area within the zone. The mountain ranges are surrounded by broad pediments indicating long periods of erosion without vertical changes. The geomorphology of river terraces along the Colorado and Gila Rivers provide additional evidence of long term stability of the region. Late Quaternary faults within the province are few and are very minor features that are generally less than 5 miles long. Examples of Quaternary faulting include the Sand Tank fault and Gila Mountain fault both of which have been included in this study.

Seismicity within the Sonoran Desert Basin and Range is infrequent, scattered and of small magnitude. The only appreciable seismicity is along the southwestern border near the Pinacate volcanic field. These events are believed to be poorly located earthquakes associated with the Pinacate volcanic field and the Salton Trough.

The youngest volcanic rocks in the zone are in the Sentinel-Arlington volcanic field which represent a primarily Pliocene episode of volcanism.

3.6 ARIZONA MOUNTAINS

The Arizona Mountain neotectonic zone represents the mountainous terrain between the relatively flat Colorado Plateau and the desert plains and low relief ranges of the Sonoran Desert Basin and Range. The relief in the Arizona Mountains is due to epeirogenic upwarping with accompanying crustal extension and subsidence of the valley blocks. The valley fault blocks of the Arizona Mountains are similar to but not as well developed as the tectonic style of the Great Basin. The bounding faults are also much younger (Quaternary movement) than the range bounding faults of the Sonoran Desert Basin and Range. The major differences between the Arizona Mountains and the surrounding neotectonic zones are geomorphology, age and rate of faulting, age of volcanic activity, and seismicity. The major faults of this zone are the northwest striking basin bounding faults of the grabens such as the Chino area Verde Valleys. There are also other numerous Quaternary faults shown on Plate 1. The southwest boundary of the Arizona Mountains primarily follows the physiographic and topographic change from rugged mountains to the plains and scattered ranges of the Sonoran Desert Basin and Range neotectonic zone.

Seismicity in the Arizona Mountains neotectonic zone consists of small to moderate sized earthquakes in a loosely defined belt extending from the Hurricane-Wasatch zone and the Rio Grande Rift.

3.7 MEXICAN BASIN AND RANGE

The Mexican Basin and Range neotectonic zone is an area demonstrating extensional tectonics similar to the Great Basin. Evidence for the present-day activity comes from the youthful geomorphology and the greater number and density of late Quaternary faults compared to the Sonoran Desert. In the northern part of the zone, the valley floors generally lie between 4000 and 4500 feet above sea level and ranges reach a

maximum heights of about 9,500 to 10,000 feet above sea level. North of the Arizona-Mexico border, the north-south structural trend turns north-northwest and the basins have a more open appearance. For this study, the northern boundary of the zone includes all of the mountain ranges with elevations above about 9,000 feet.

The earthquake record for this zone is sparse however this may be due to a lack of adequate coverage by seismographic stations, especially for smaller events in the remote areas of the province. At least two large events have been associated with this zone (1887 and 1923), however they occurred on faults well outside the 300 km radius.

3.8 PINACATE VOLCANIC FIELD

The Pinacate Volcanic Field neotectonic zone is south-southwest of the PVNGS and extends from approximately the Arizona border south to the Salton Trough. The zone encompasses a large Quaternary volcanic flow (about 1000 sq. mi.) and possibly some short Quaternary faults that may be associated with the volcanism. Although no Quaternary faults that could produce moderate to large earthquakes have been mapped in this zone, the Pinacate Volcanic Field was designated as a possible source of volcanic earthquakes.

3.9 HURRICANE-WASATCH

The Hurricane-Wasatch neotectonic zone marks the western transition from the Colorado Plateau to the Great Basin. The main characteristics of this zone are the great length of fault zones and the relatively high rate of seismicity. This zone coincides with a major portion of the southern Intermountain Seismic Belt as it enters Arizona from Utah. Several major north-trending fault systems are within the boundaries of this zone: i.e., the Hurricane, Wasatch, Sevier, Toroweap, and Mainstreet faults, all which have demonstrated late Quaternary displacement but no historic surface faulting. Earthquake focal mechanisms indicate predominantly east-west extension along west dipping normal faults, which is consistent the geometry of the larger faults in this neotectonic zone.

3.10 SAN FRANCISCO VOLCANIC FIELD

The San Francisco Volcanic Field is a subdivision of the Colorado Plateau. It is characterized by young volcanism, northeast trending faults, and moderately active seismicity. Volcanism in the San Francisco Peaks has been active in the Holocene and may still be capable of eruptions. Northwest striking faults are not as prominent in this zone and northeast trending faults such as the Bright Angel and Mesa Butte faults are the most prominent.

3.11 COLORADO PLATEAU

The Colorado Plateau neotectonic zone lies at the northeast corner of the 300 km radius from the site. This neotectonic zone is represented by a relatively flat-lying

undeformed sequence of Paleozoic through Tertiary strata overlying deformed Precambrian basement. There are no known Quaternary faults within the zone and the seismicity is rare and widely scattered. The boundaries have been drawn north of the Mogollon Rim and east of the San Francisco Volcanic Fields.

3.12 QUATERNARY FAULTS

Plate 1 shows the location of 23 Quaternary faults or fault systems that were evaluated as potential seismic sources for the PVNGS study. Each fault has been assigned a number (as shown on Plate 1) which remains consistent throughout the text and appendices. The primary sources of tectonic data for the faults in Arizona were Scarborough et. al. (1986), Menges and Pearthree (1983), Schell and Wilson (1983), numerous reports and theses, and Schell (personal communication, 1991). Quaternary faults data for California were from California Division of Mines and Geology (1975, 1987) and Wesnousky (1986).

As described in the Methodology section, all known or suspected Quaternary faults within the 300 km radius were identified and screened according to the criteria outlined in CFR Title 10, Part 100, Table B-1 . In general, the identified Quaternary faults were included or excluded based on their length and distance from the site (see page 4 for the screening parameters). The application of the CFR Title 10 criteria excluded so many of the Quaternary faults that the criteria were first modified to include all Quaternary faults within 100 miles of the site. This modification returned the following faults for further evaluation: Sand Tank (#1), Sugarloaf Peak (#3), Carefree (#4), Tonto Basin (#5), Horseshoe Dam (#6), Turret Peak (#7), Prescott Valley (#9), Williamson Valley (#10), and Gila Mountain (#23). Quaternary faults beyond the 100 mile radius were evaluated according to the CFR Title 10 criteria with the following exceptions which were included for further evaluation: Santa Rita (#2), Mesa Butte (#15), and Bright Angel (#16).

The Quaternary faults which required evaluations based upon CFR Title 10 criteria were the Verde (#8), Big Chino (#14), Aubrey (#17), Toroweap (#18), Hurricane (#19), Pinto Mountain (#20), Blue Cut (#21), and the San Andreas (#22). The following three faults or fault systems were included in the study although they have not been proven to be Quaternary in age: Chavez Mountain (#11), Lake Mary-Mormon Lake (#12), and Munds Park (#13).

In some cases, suspected Quaternary faults were removed from consideration based on more recent inspections or investigations that have not been documented yet (Schell, Pearthree, personal communication 1991). Examples of faults that were removed by this process include the Rio Sonoyta fault, Catalina fault, and the Cook's Mesa fault.

Table B-1 contains tables that summarize the fault characteristics most important to evaluating the seismic potential. The particular fault characteristics important to this study include the neotectonic zone containing the fault, distance to the site, and fault geometry, such as, sense of slip strike, total and segment length, and down dip width. Fault characteristics relevant to Quaternary deformation include total displacement and slip rate, as well as recent displacement history, such as, number of events in the late Quaternary, most recent displacement, displacement per event, and recurrence interval.

This study focussed on the particular Quaternary faults which had been evaluated or investigated in detail by previous workers. These faults were then used as analogs for the faults which had relatively little available information. A fault was considered to have detailed information if data concerning rates of Quaternary deformation were available, such as slip rate, most recent displacement, displacement per event, and recurrence interval. The faults which were particularly useful as analogs were the following: Sand Tank (#1), Verde (#8), Big Chino (#14), Toroweap (#18), Hurricane (#19), Pinto Mountain (#20), and the San Andreas (#22).

3.13 ACTIVITY RATE AND b-VALUE

The activity rates and b-values selected for specific faults and neotectonic zones are summarized in Tables B-4 & B-5. Two earthquake data catalogues were used to evaluate the distribution of seismicity for this study: DNAG (1852 to 1985) for the entire 300 km radius and beyond, and Stover et. al.1983, (1830 to 1982), for the area within the Arizona state boundaries. The Stover catalogue was used as a cross reference on the DNAG data because Stover did considerable research in analyzing and relocating some of the larger earthquakes reported in Arizona. An example of an important relocation includes the 1852 Ft. Yuma event (magnitude 7) which, in the Stover catalogue, has been moved south from the Sonoran Desert Basin and Range to the Salton Trough (Stover et al, 1983; ANPP, 1983).

As described in the Methodology section (page 4), the seismicity was evaluated for each neotectonic zone and for selected Quaternary faults with associated seismicity. The annual rate vs. magnitude relationships developed from the historical seismicity were compared to the available Quaternary tectonic data (recurrence estimates) and maximum magnitude calculations from applicable faults. Where the annual rate vs magnitude relation (i.e., the slope or b-value) was consistent with the rates and magnitudes based on geologic/tectonic data, then the curve was selected for use on the tables in Tables B-4 & B-5. The annual rate vs magnitude relations for the following faults showed good correlation with the tectonic data and magnitude estimates:

1) San Andreas fault (DNAG)

2) Blue Cut fault (DNAG)

3) Hurricane-Toroweap fault (Stover)

4) Mesa Butte fault

In several cases, the activity rate and b-value from the neotectonic zone were assigned to specific faults within the zone. This was useful where not enough seismic record existed to create a b-value for a specific fault or where the b-value for specific faults did not fit the geologic/tectonic data. Examples include 1) the Arizona Mountains b-value (Stover) was applied to all faults within the Arizona Mountains neotectonic zone (faults #3 through #10 in Tables B-4 & B-5) and to the Mexican Basin and

Range (fault #2), and 2) the Sonoran Desert Basin and Range curve (DNAG) was applied to the faults #1 and #23 in the Sonoran Desert Basin and Range neotectonic zone. In addition, since there was little or no seismicity reported from the Pinacate Volcanic Field, the Sonoran Desert Basin and Range curve (DNAG) was applied to this neotectonic zone.

Due to the low level of historical seismicity in the Sonoran Desert Basin and Range neotectonic zone (the host zone for PVNGS), the DNAG and Stover earthquake catalogues were used to develop a range of b-values and activity rates. Three b-values (0.8, 0.9, and 1.0) were interpreted from the Stover data, and one steeper b-value (1.36) was interpreted from the DNAG data. The JMM team selected this range to be representative of b-values from the southwest U.S. and North America. Weights were assigned to each b-value along with a range of magnitudes that reflect the maximum random earthquake within this neotectonic zone (Table B-4).

In several cases, the b-values developed for specific faults with adequate data served as analogs for other faults with less data in the same neotectonic zone. Examples include 1) the curve for the Mesa Butte fault (DNAG) which was used for all faults analyzed in the San Francisco Volcanic Field neotectonic zone (faults #11 through #13, and #15 through #16), and 2) the curve for the Hurricane-Toroweap faults (Stover) was used for faults #14, #18 and #19.

For neotectonic zones not requiring any specific analyses of Quaternary faults (such as the Colorado Plateau, Mojave Basin and Range, and Lake Mead Basin and Range), the b-values were selected based on the historical seismicity.

Copies of the selected annual rate vs magnitude curves are included in Figures B-3 through B-14.

3.14 MAXIMUM MAGNITUDES

The approach to developing the maximum magnitudes for the selected Quaternary faults is described in the Methodology section (page 4). Table B-2 contains the calculation sheets for the maximum magnitudes for the 23 faults evaluated. The assumptions regarding the rupture lengths, fault dimensions and geometry, weights for various rupture alternatives, and magnitude formulae are included on the calculation sheets.

The determination of maximum magnitude for neotectonic zones (i.e., for zones where no specific Quaternary faults were evaluated as part of this study) was based on the collective judgment of the four members of the project team. The deliberations considered such factors as the number of Quaternary faults that were screened out by the criteria, the historic seismicity, evidence for Quaternary deformation or volcanism, and maximum earthquakes from analogous areas in the western US and the world.

The determination of the background seismicity for neotectonic zones that did contain specific Quaternary faults was based on the collective judgement of the project team. The factors considered were the same as summarized above for the determination of maximum magnitude.

REFERENCES

Anderson, L.W. & Piety, L.A.; 1987; Quaternary History of the Tonto Basin and Vicinity, Salt River, Arizona; Geol. Soc. Am.; Abstracts with programs; Vol. 19; p. 572.

Anderson, R.E. & Mehnert; H.H., 1979; Reinterpretations of the History of the Hurricane Fault; in Utah, in Newman, G.W., and Goode, H.D., eds., 1979 Basin and Range Symposium; Rocky Mountain Assoc. Geol. and Utah Geol. Assoc.; p. 145-165.

Arizona Nuclear Power Project; 1991; Updated Final Safety Analysis Report, Section 2.5 and Related Geology and Seismology Graphics; p. 202.

Baldersman, M.A., Johnson, C.A., Miller, D.G., and Schmidt, D.L.; 1978; The 1852 Fort Yuma Earthquake; Bull. Seismol. Soc. Am.; Vol. 68; p. 699-709.

Brumbaugh; 1990; Depth of Fredonia, Az earthquakes of 15 Feb 62. BSSA; Vol. 80; p. 1762-1764.

Brumbaugh, D.S.; 1980; Analysis of the Williams, Arizona Earthquake of November 4, 1971; Seismological Society of America; Bulletin; Vol. 70; No. 3; p. 885-891.

Bull, W.B. & Pearthree, P.A.; 1988; Frequency and Size of Quaternary Surface Ruptures of Pitaycachi fault, northeastern Sonora Mexico; Bull. Seis. Soc. Am.; Vol. 78; February.

Demsey, Karen A. & Pearthree, Philip A.; 1988; Late Quaternary Surface-Rupture History of the Sand Tank Fault, and Associated Seismic Hazard for the proposed Superconducting Super Collider Site, Maricopa County, Arizona; Arizona Geological Survey; Open-File Report 90-1; p. 27.

Dohrenwend, J.C., Menges, C.M., Schell, B.A., & Moring, B.C.; 1991 (in press); Reconnaissance Photogeologic Map of Young Faults in the Las Vegas 1 x 2 Quadrangle, Nevada, Utah, and Arizona; U.S. Geological Survey; Miscellaneous Field Investigations Map, 1:250,000.

Dubois, Susan M. Smith, Ann W., Nye, Nan K., & Nowak, Thaddeus A. Jr.; 1982; Arizona Earthquakes, 1776-1980; State of Arizona, Bureau of Geology and Mineral Technology, Geological Survey Branch; Bulletin 193; p. 456.

DuBois, Susan M., Sbar, Marc L., & Nowak, Thaddeus A.; 1981; Historical Seismicity in Arizona; Arizona Bureau of Geology and Mineral Technology, University of Arizona; Open File Report 82-21; p. 199.

Eberhart-Phillips, Donna, Richardson, Randall M., Sbar, Marc L., & Herrmann, Robert B.; 1981; Analysis of the 4 February 1976 Chino Valley, Arizona, Earthquake; Bulletin of the Seismological Society of America; Vol. 71; No. 3; p. 787-801.

Hamblin, W.K., & Best, M.G.; 1979; Patterns and Rates of Recurrent Movement along the Wasatch-Hurricane-Sevier Fault Zone During Late Cenozoic Time; U.S. Geol. Survey; Summaries of Technical Reports; Vol. VIII; p. 126-127.

Hanks, T.C., and Kanamori, H., 1979, A moment magnitude scale: Journal of Geophysical Research, v. 84, no. 20, p. 2981-2987.

Huntoon, P.W.; 1977; Holocene Faulting in the Western Grand Canyon, Arizona, Geol. Soc. Am Bull; Vol. 88; p. 1619-1622.

Huntoon, P.W.; 1979; Holocene Faulting in the Western Grand Canyon, Arizona, discussion and reply, Geological Society of America Bulletin Part 1; Vol. 90; p. 221-224.

Huntoon, P.W., & Sears, J.W.; 1975; Bright Angel and Eminence Faults, Eastern Grand Canyon, Arizona; Geol. Soc. Am. Bull.; Vol. 86; p. 465-472.

Jackson, Garret W.; 1990; Tectonic Geomorphology of the Toroweap Fault, Western Grand Canyon, Arizona; Implications for Transgression of Faulting on the Colorado Plateau; Arizona Geological Survey; Open-File Report 90-4; p. 66.

Johnson, R.A., Loy, K., Wallace, T., & Pearthree, P.A.; 1990; The Santa Rita Fault; Reactivation of a low angle Detachment Fault; Geol. Soc. Am.; Abstracts with Programs; Vol. 22, p. 32.

Menges, Christopher M. & Pearthree; 1983; Map of Neotectonic (Latest Pliocene-Quaternary) Deformation in Arizona; Bureau of Geology and Mineral Technology; Open File Report 83-22.

Menges, Christopher M.; 1983 (revised 1984); The Neotectonic Framework of Arizona: Implications for the Regional Character of Basin-Range Tectonism; State of Arizona, Arizona Bureau of Geology and Mineral Technology; (Part of final report, Contract #14-08-0001-19861); Open-File Report 83-19; p. 109.

Morrison, R.B., Menges, C.M., & Lepley, L.K.; 1981; Neotectonic Maps of Arizona; Arizona Geol. Soc. Dig; Vol. 13; p. 179-183.

Pearthree, Philip A.; 1986; Late Quaternary Faulting and Seismic Hazard in Southeastern Arizona and Adjacent Portions of New Mexico and Sonora, Mexico; Arizona Bureau of Geology and Mineral Technology, University of Arizona; Open-File Report 86-8; p. 17.

Pearthree, Philip A., Scarborough, Robert B.; 1984; Reconnaissance Analysis of Possible Quaternary Faulting in Central Arizona; Arizona Bureau of Geology and Mineral Technology; Open-File Report 85-4; p. 27.

Pearthree, Philip A., Menges, Christopher M., & Mayer, Larry; 1983; Distribution, Recurrence, and Possible Tectonic Implications of Late Quaternary Faulting in Arizona; State of Arizona, Bureau of Geology and Mineral Technology; Open-File Report 83-20; p. 36.

Piety, L.A. & Anderson, L.W.; 1990; Recurrent Late Quaternary Faulting on Horsehoe Fault, Verde River Valley, Central AZ.; Geol. Soc. Am; Abstracts with Programs; Vol. 22; p. 76.

Sanchez, P.E., & Brumbaugh, D.S.; 1990; Seismicity and Seismotectonics of Verde Valley and Transition Zone of Central AZ; Geol. Soc. Am.; Abstracts with Programs; Vol. 22; p. 80.

Scarborough, Robert B., Menges, C.M., & Pearthree, Philip A.; 1983(ca); Late Pliocene-Quaternary (Post 4 M.Y.) Faults, Folds, and Volcanic Rocks in Arizona; Arizona Bureau of Geology and Mineral Technology; Map 22.

Schell, B.A. & Wilson, K.L. (Ertec Western, Inc.); 1981; Regional Neotectonic Analysis of the Sonoran Desert; Ertec Western, Inc.; Report 79-288; U.S.G.S. Contract No. 14-08-001-18284; U.S. Geological Survey; Open-File Report 82-57; p. 70.

Schell, B.A., Erickkson, L.G., Murphy, B.E., Baylon, D., Kling, M., & Gregory, J.L.; 1985; Application of Seismotectonic Zoning to Regional Screening, Characterization, and Selection, Association of Engineering Geologists Annual Meeting, Abstract with Program, p. 74.

Shafiqullah, M., Damon, P.E., Lynch, D.J., Reynolds, S.J., Rehrig, W.A., & Raymond R.H.; 1980; K-Ar Geochronology and Geologic History of Southwestern Arizona and Adjacent Areas; AZ. Geol. Soc. Digest; Vol. XII; p. 201-260.

Shoemaker E.M., Squires, R.L., & Abrams, M.J.; 1978; Bright Angel and Mesa Butte Fault Systems of Northern Arizona; Geol. Soc. Am.; Memoir 152; p. 341-367.

Slammons, D.B., 1982, Determination of design earthquake magnitudes for microsonation: Proceedings of Third International Earthquake Microsonation Conference, v.1, p. 119-130.

Soule, Charles Henry; 1978; Tectonic Geomorphology of Big Chino; M.S., Thesis; The University of Arizona; p. 1-102.

Weide, David L.; 1985; Soils and Quaternary Geology of the Southwestern United States; Department of Geoscience, University of Nevada; Special Paper 203; p. 150.

Woodward-Clyde Consultants, 1979, Report of the evaluation of maximum earthquake and site ground motion parameters associated with the offshore zone of deformation, San Onofre Nuclear Generating Station; unpublished report for Southern California Edison Company, p. 241.

Wyss, M., 1979, Estimating maximum expectable magnitude of earthquakes from fault dimensions: Geology, v. 7, no. 7, p. 336-340.

TABLE B-1

913-7064 Palo Verde Nuclear Generating Station (PVNGS): Seismic Study

FAULT	PROVINCE/ DOMAIN	SITE DIST. (km)	FAULT GEOMETRY					TOTAL DISPL. (m or km)	SLIP RATE (mm/yr)	# EVENTS L. QUAT.	MOST RECENT DISPL.(yrs)	DISPL./ EVENT (m)	RECURR. INTERVAL (yrs)	COMMENTS
			SENSE OF SLIP	STRIKE	TOTAL LENGTH (km)	SEGMENT LENGTH (km)	DOWN DIP WIDTH (km)							
1. Sand Tank	Sonoran Desert Basin and Range	55	N	N15-50E	3.5	3.5	---	2 m	0.01-0.04	---	8-20 ka	---	50-200 ka	AGS OFR 90-1
2. Santa Rita	Mexican Basin and Range	255	N	N50E-NS	60	2, 4(2), 5, 6(2), 8, 9	---	1-7 m	---	2 events in last 200 ka	60-100 ka	---	---	ABGMT Map 22 Johnson et al, 1990
3. Sugarloaf Peak	Arizona Mountains	130	N	N15W	7	---	---	<1 m	---	---	L. Pleist.-Holo.	---	---	ABGMT Map 22 ABGMT OFR 85-4
4. Carefree	Arizona Mountains	105	---	50W-N	10	2.5, 6	---	1-3 m	---	---	<30 ka	---	---	ABGMT Map 22 ABGMT OFR 85-4
5. Tonto Basin	Arizona Mountains	150	N	N15E-N30W	19	4, 13	---	---	---	---	Plio.-Quat.	---	---	ABGMT Map 22
6. Horseshoe Dam	Arizona Mountains	65	N	N5E-N25W	21	10, 11	---	7.5 m	---	2 in last 300 ka	>12 ka, L.Pleist.-E. Holo.	1	---	Piety and Anderson, 1990
7. Turret Peak	Arizona Mountains	135	N	N45E	10	10	---	---	---	---	Plio.-Quat.	---	---	ABGMT Map 22
8. Verde	Arizona Mountains	140	N	N30W	90	3(2), 10, 17, 17.5, 35	---	0.5-6 m	---	---	5-15 ka, <150 ka-4 m.y.	---	---	ABGMT Map 22 Pearthree and others, 1983
9. Prescott Valley	Arizona Mountains	145	N	N15W	4	---	---	---	---	---	30 ka-4 m.y.	---	---	ABGMT Map 22

TABLE B-1 (Cont'd)

913-7064 Palo Verde Nuclear Generating Station (PVNGS): Seismic Study

FAULT	PROVINCE/ DOMAIN	SITE DIST. (km)	FAULT GEOMETRY					TOTAL DISPL. (m or km)	SLIP RATE (mm/yr)	# EVENTS L..QUAT.	MOST RECENT DISPL.(yrs)	DISPL./ EVENT (m)	RECURR. INTERVAL (yrs)	COMMENTS
			SENSE OF SLIP	STRIKE	TOTAL LENGTH (km)	SEGMENT LENGTH (km)	DOWN DIP WIDTH (km)							
10. Williamson Valley	Arizona Mountains	150	N	N12W	2.5-3	---	---	---	---	---	30 ka-4 m.y.	---	---	ABGMT Map 22
11. Chavez Mtn.	San Francisco Volcanic Field	220	N	N40W	40	7, 7.5(2), 15	---	---	---	---	---	---	---	ABGMT Map 22 ABGMT OFR 83-22
12. Lake Mary-Mormon Lake	San Francisco Volcanic Field	220	N	N80W-N5E	35	5, 7, 7.5, 12, 15	---	<130 m	---	---	Most >2-3 m.y., and L. to M Holo.	---	---	ABGMT Map 22 ABGMT OFR 83-22
13. Munds Park	San Francisco Volcanic Field	210	N	N50-60W	35	5, 7, 10, 12	---	<45-90 m	---	---	>2-3 m.y.	---	---	ABGMT Map 22 ABGMT OFR 83-22
14. Big Chino	Hurricane-Wasatch	180	N	N45W	50	---	10-15	---	0.6-1.2	At least 5	E. Holo. (?)	2-3.5	20-50 ka (assume 2m)	ABGMT Map 22 Soule, 1978 Eberhart-Phillips et al, 1981
15. Mesa Butte	San Francisco Volcanic Field	270	N	N40E	>150	35, 38	---	100-150 m	---	---	<620 ka and 510 ka	---	---	ABGMT Map 22 Shoemaker et al, 1977
16. Bright Angel	San Francisco Volcanic Field	295	N	N35E	>100	65	---	<100	---	---	Plio-Quat.	---	---	ABGMT Map 22 Shoemaker et al, 1977
17. Aubrey	Hurricane-Wasatch	200	N	N35W-N20E	70	22.5, 45(2)	---	4-7 m	---	---	<30 ka and <4 m.y.	---	---	ABGMT Map 22
18. Toroweap	Hurricane-Wasatch	270	N	N25E-N20W	480	45(2)	---	150-265, 137	0.056-0.11, 0.074	3	3 and 5 ka	2.2	20-40 ka	Jackson, 1990 Anderson and Christensen, 1989 ABGMT Map 22

TABLE B-1 (Cont'd)

913-7064 Palo Verde Nuclear Generating Station (PVNGS): Seismic Study

FAULT	PROVINCE/ DOMAIN	SITE DIST. (km)	FAULT GEOMETRY					TOTAL DISPL. (m or km)	SLIP RATE (mm/yr)	# EVENTS L. QUAT.	MOST RECENT DISPL.(yrs)	DISPL./ EVENT (m)	RECURR. INTERVAL (yrs)	COMMENTS
			SENSE OF SLIP	STRIKE	TOTAL LENGTH (km)	SEGMENT LENGTH (km)	DOWN DIP WIDTH (km)							
19. Hurricane	Hurricane-Wasatch	250	N	N20E-NS	>170	25(2), 65	---	7-12 m	0.17 +/- 0.03	---	<30 ka, <30-150 ka <4 m.y.	---	12 ka (assume 2m	ABGMT Map 22 Hamblin and Best,
20. Pinto Mountain	Transverse Ranges	290	SS, LL	N50E-N20W	73	73	---	16 km	0.3-5.3	---	---	---	2885	Dibblee, 1967, 1975 Weanousky, 1986 CDMG, 1975
21. Blue Cut	Transverse Ranges	245	SS, LL	N2-4E	80	80	---	---	>0.01	---	---	---	---	Weanousky, 1986 CDMG, 1975
22. San Andreas	Salton Trough	230	SS, RL	N35-40W	1100	210	20	>330 km	10-35	---	23	1-4	150-350	Weanousky, 1986 Crowell, 1981 CDMG, 1975
23. Gila Mountain	Sonoran Desert	155	N	N60W	3	---	---	---	---	---	Plio.-Qual.	---	---	ABGMT Map 22
Pitaycachi	Sonoran Desert	440	N	N5-10E	75	<1 (several), 2-5 (several), 12, 18	---	9-13 m	1	2 events since L. mid Pleist.	1887 A.D.	0.25-4	100-200 ka	Bull and Pearthree, 1988

TABLE B-2

FAULT NAME/NO.:	SAND TANK FAULT/#1	P-1	P-2	P-3	REFS
	Fault Type N	0.85	0.15		AGS 0FR 90-1
	Orientation:				Crust=15km
	Total fault length (L, km) =	3.5	30		Dip=55
	Rupture length (L, m)	3500	15000		Downdip=18km
	Rupture area (A, sq. km)	64	270		
	Maximum surface displacement (D, m)	2	1.1		
	Average surface displacement (D, cm)	110	110		
	Slip rate (S, mm/yr)				

FAULT NAME/NO.: SAND TANK FAULT/#1								
Parameter (Reference)	Fault Type	Limits	Equation	Computed Ms P-1	P-2	P-3	s
Total fault length (Slemmons,1982)	SS	Ms>6.0	Ms=6.618+0.0012(L)	6.6	6.7	6.6	0.221
Rupture length (Slemmons, (1982)	N	-	Ms=0.809+1.341LogL	5.6	6.4	ERR	0.318
	R	-	Ms=2.021+1.142LogL	6.1	6.8	ERR	0.197
	SS	-	Ms=1.404+1.169LogL	5.5	6.3	ERR	0.205
(Bonilla and others, 1984)	R	Ms>6.0	Ms=5.71+0.916LogL	6.2	6.8	ERR	0.274
	SS	Ms>6.0	Ms=6.24+0.619LogL	6.6	7.0	ERR	0.293
Rupture area (Wyss, 1979)	All	Ms>5.6	Ms=4.15+LogA	6.0	6.6	ERR	0.3
(WCC, 1982)	All	4<Ms<6, A>5	Ms=4.257+0.656LogA	5.4	5.9	ERR	-
Maximum surface displacement (Slemmons, 1982)	N	-	Ms=6.668+0.750LogD	6.9	6.7	ERR	0.340
	R	-	Ms=6.793+1.306LogD	7.2	6.8	ERR	0.374
	SS	-	Ms=6.974+0.804LogD	7.2	7.0	ERR	0.315
(Bonilla and others, 1984)	N	Ms>6.0	Ms=6.81+0.741LogD	7.0	6.8	ERR	0.188
	SS	Ms>6.0	Ms=7.00+0.782LogD	7.2	7.0	ERR	0.331
Slip rate (WWC, 1979)	SS	-	Ms=7.223+1.263LogS	ERR	ERR	ERR	-
Seismic moment (Schwartz et al.,1984)	All	3<Ml<7 5<Ms<7.5 Mm>7.5	Mm=2/3logMo-10.7 Mo=ADu	6.2	6.6	ERR	0.24
MEAN				6.2	6.5	ERR	
MAXIMUM				7.0	6.8	ERR	
MINIMUM				5.4	5.9	ERR	

TABLE B-2 (Con't)

FAULT NAME/NO.:	SANTA RITA/#2	P-1	P-2	P-3	REFS
	Fault Type N	0.3	0.7		ABGMT Map 22
	Orientatio				Johnson, 1990
	Total fault length (L, km) =	60	9		Crust=15km
	Rupture length (L, m)	30000	9000		Dip=75
	Rupture area (A, sq. km)	496	148		Downdip=16.5km
	Maximum surface displacement (D, m)	3.5	0.5		
	Average surface displacement (D, cm)	150	50		Assumed
	Slip rate (S, mm/yr)				

FAULT NAME/NO.: SANTA RITA/#2								
Parameter (Reference)	Fault Type	Limits	Equation	Computed Ms P-1	P-2	P-3	s
Total fault length (Slemmons,1982)	SS	Ms>6.0	Ms=6.618+0.0012(L)	6.7	6.6	6.6	0.221
Rupture length (Slemmons, (1982)	N	-	Ms=0.809+1.341LogL	6.8	6.1	ERR	0.318
	R	-	Ms=2.021+1.142LogL	7.1	6.5	ERR	0.197
	SS	-	Ms=1.404+1.169LogL	6.6	6.0	ERR	0.205
(Bonilla and others, 1984)	R	Ms>6.0	Ms=5.71+0.916LogL	7.1	6.6	ERR	0.274
	SS	Ms>6.0	Ms=6.24+0.619LogL	7.2	6.8	ERR	0.293
Rupture area (Wyss, 1979)	All	Ms>5.6	Ms=4.15+LogA	6.8	6.3	ERR	0.3
(WCC, 1982)	All	4<Ms<6, A>5	Ms=4.257+0.656LogA	6.0	5.7	ERR	-
Maximum surface displacement (Slemmons, 1982)	N	-	Ms=6.668+0.750LogD	7.1	6.4	ERR	0.340
	R	-	Ms=6.793+1.306LogD	7.5	6.4	ERR	0.374
	SS	-	Ms=6.974+0.804LogD	7.4	6.7	ERR	0.315
(Bonilla and others, 1984)	N	Ms>6.0	Ms=6.81+0.741LogD	7.2	6.6	ERR	0.188
	SS	Ms>6.0	Ms=7.00+0.782LogD	7.4	6.8	ERR	0.331
Slip rate (WWC, 1979)	SS	-	Ms=7.223+1.263LogS	ERR	ERR	ERR	-
Seismic moment (Schwartz et al.,1984)	All	3<Ml<7 5<Ms<7.5 Mm>7.5	Mm=2/3logMo-10.7 Mo=ADu	6.9	6.2	ERR	0.24
MEAN				6.8	6.2	ERR	
MAXIMUM				7.2	6.6	ERR	
MINIMUM				6.0	5.7	ERR	

TABLE B-2 (Con't)

FAULT NAME/NO.:	SUGARLOAF PEAK/#3	P-1	P-2	P-3	REFS
	Fault Type N	1			ABGMT Map 22
	Orientatio				ABGMT OFR 85-4
	Total fault length (L, km) =	7			Crust=20km
	Rupture length (L, m)	7000			Dip=55 assumed
	Rupture area (A, sq. km)	171			Downdip=24.5km
	Maximum surface displacement (D, m)	0.75			Assumed
	Average surface displacement (D, cm)	75			
	Slip rate (S, mm/yr)				

FAULT NAME/NO.: SUGARLOAF PEAK/#3

Parameter (Reference)	Fault Type	Limits	Equation	Computed Ms P-1	P-2	P-3	s
Total fault length (Slemmons,1982)	SS	Ms>6.0	Ms=6.618+0.0012(L)	6.6	6.6	6.6	0.221
Rupture length (Slemmons, (1982)	N	-	Ms=0.809+1.341LogL	6.0	ERR	ERR	0.318
	R	-	Ms=2.021+1.142LogL	6.4	ERR	ERR	0.197
	SS	-	Ms=1.404+1.169LogL	5.9	ERR	ERR	0.205
(Bonilla and others, 1984)	R	Ms>6.0	Ms=5.71+0.916LogL	6.5	ERR	ERR	0.274
	SS	Ms>6.0	Ms=6.24+0.619LogL	6.8	ERR	ERR	0.293
Rupture area (Wyss, 1979)	All	Ms>5.6	Ms=4.15+LogA	6.4	ERR	ERR	0.3
(WCC, 1982)	All	4<Ms<6, A>5	Ms=4.257+0.656LogA	5.7	ERR	ERR	-
Maximum surface displacement (Slemmons, 1982)	N	-	Ms=6.668+0.750LogD	6.6	ERR	ERR	0.340
	R	-	Ms=6.793+1.306LogD	6.6	ERR	ERR	0.374
	SS	-	Ms=6.974+0.804LogD	6.9	ERR	ERR	0.315
(Bonilla and others, 1984)	N	Ms>6.0	Ms=6.81+0.741LogD	6.7	ERR	ERR	0.188
	SS	Ms>6.0	Ms=7.00+0.782LogD	6.9	ERR	ERR	0.331
Slip rate (WWC, 1979)	SS	-	Ms=7.223+1.263LogS	ERR	ERR	ERR	-
Seismic moment (Schwartz et al.,1984)	All	3<Ml<7 5<Ms<7.5 Mm>7.5	Mm=2/3logMo-10.7 Mo=ADu	6.4	ERR	ERR	0.24
MEAN				6.3	ERR	ERR	
MAXIMUM				6.7	ERR	ERR	
MINIMUM				5.7	ERR	ERR	

TABLE B-2 (Con't)

FAULT NAME/NO.:	CAREFREE/#4	P-1	P-2	P-3	REFS
	Fault Type N	0.7	0.3		ABGMT Map 22
	Orientatio				ABGMT OFR 85-4
	Total fault length (L, km) =	10	6		Crust=20km
	Rupture length (L, m)	10000	6000		Dip=55 assumed
	Rupture area (A, sq. km)	90	108		Downdip=24.5km
	Maximum surface displacement (D, m)	1	1		
	Average surface displacement (D, cm)	100	50		
	Slip rate (S, mm/yr)				

FAULT NAME/NO.: CAREFREE/#4 Parameter (Reference)	Fault Type	Limits	Equation	Computed Ms P-1	P-2	P-3	s
Total fault length (Slemmons,1982)	SS	Ms>6.0	Ms=6.618+0.0012(L)	6.6	6.6	6.6	0.221
Rupture length (Slemmons,	N	-	Ms=0.809+1.341LogL	6.2	5.9	ERR	0.318
(1982)	R	-	Ms=2.021+1.142LogL	6.6	6.3	ERR	0.197
	SS	-	Ms=1.404+1.169LogL	6.1	5.8	ERR	0.205
(Bonilla and others, 1984)	R	Ms>6.0	Ms=5.71+0.916LogL	6.6	6.4	ERR	0.274
	SS	Ms>6.0	Ms=6.24+0.619LogL	6.9	6.7	ERR	0.293
Rupture area (Wyss, 1979)	All	Ms>5.6	Ms=4.15+LogA	6.1	6.2	ERR	0.3
(WCC, 1982)	All	4<Ms<6, A>5	Ms=4.257+0.656LogA	5.5	5.6	ERR	-
Maximum surface	N	-	Ms=6.668+0.750LogD	6.7	6.7	ERR	0.340
displacement (Slemmons,	R	-	Ms=6.793+1.306LogD	6.8	6.8	ERR	0.374
1982)	SS	-	Ms=6.974+0.804LogD	7.0	7.0	ERR	0.315
(Bonilla and others, 1984)	N	Ms>6.0	Ms=6.81+0.741LogD	6.8	6.8	ERR	0.188
	SS	Ms>6.0	Ms=7.00+0.782LogD	7.0	7.0	ERR	0.331
Slip rate (WWC, 1979)	SS	-	Ms=7.223+1.263LogS	ERR	ERR	ERR	-
Seismic moment (Schwartz et al.,1984)	All	3<Ml<7 5<Ms<7.5 Mm>7.5	Mm=2/3logMo-10.7 Mo=ADu	6.3	6.1	ERR	0.24
MEAN				6.3	6.2	ERR	
MAXIMUM				6.8	6.8	ERR	
MINIMUM				5.5	5.6	ERR	

TABLE B-2 (Cont'd)

FAULT NAME/NO.:	TONTO BASIN/#5	P-1	P-2	P-3	REFS
	Fault Type N	0.5	0.5		ABGMT Map 22
	Orientatio				Crust=20km
	Total fault length (L, km) =	19	13		Dip=55 assumed
	Rupture length (L, m)	19000	13000		Downdip=24.5km
	Rupture area (A, sq. km)	465	319		
	Maximum surface displacement (D, m)	1	0.5		Assumed
	Average surface displacement (D, cm)	100	50		
	Slip rate (S, mm/yr)				

FAULT NAME/NO.:	TONTO BASIN/#5						
Parameter (Reference)	Fault Type	Limits	Equation	Computed Ms P-1	P-2	P-3	s
Total fault length (Slemmons,1982)	SS	Ms>6.0	Ms=6.618+0.0012(L)	6.6	6.6	6.6	0.221
Rupture length (Slemmons, (1982)	N	-	Ms=0.809+1.341LogL	6.5	6.3	ERR	0.318
	R	-	Ms=2.021+1.142LogL	6.9	6.7	ERR	0.197
	SS	-	Ms=1.404+1.169LogL	6.4	6.2	ERR	0.205
(Bonilla and others, 1984)	R	Ms>6.0	Ms=5.71+0.916LogL	6.9	6.7	ERR	0.274
	SS	Ms>6.0	Ms=6.24+0.619LogL	7.0	6.9	ERR	0.293
Rupture area (Wyss, 1979)	All	Ms>5.6	Ms=4.15+LogA	6.8	6.7	ERR	0.3
(WCC, 1982)	All	4<Ms<6, A>5	Ms=4.257+0.656LogA	6.0	5.9	ERR	-
Maximum surface displacement (Slemmons, 1982)	N	-	Ms=6.668+0.750LogD	6.7	6.4	ERR	0.340
	R	-	Ms=6.793+1.306LogD	6.8	6.4	ERR	0.374
	SS	-	Ms=6.974+0.[illegible]4LogD	7.0	6.7	ERR	0.315
(Bonilla and others, 1984)	N	Ms>6.0	Ms=6.81+0.741LogD	6.8	6.6	ERR	0.188
	SS	Ms>6.0	Ms=7.00+0.782LogD	7.0	6.8	ERR	0.331
Slip rate (WWC, 1979)	SS	-	Ms=7.223+1.263LogS	ERR	ERR	ERR	-
Seismic moment (Schwartz et al.,1984)	All	3<Ml<7 5<Ms<7.5 Mm>7.5	Mm=2/3logMo-10.7 Mo=ADu	6.7	6.4	ERR	0.24
MEAN				6.6	6.4	ERR	
MAXIMUM				6.8	6.7	ERR	
MINIMUM				6.0	5.9	ERR	

TABLE B-2 (Cont'd)

FAULT NAME/NO.:	HORSESHOE DAM/#6	P-1	P-2	P-3	REFS
	Fault Type N	1			Piety et al, 1990
	Orientatio				Crust=20km
	Total fault length (L, km) =	21			Dip=55 assumed
	Rupture length (L, m)	10500			Downdip=24.5km
	Rupture area (A, sq. km)	260			
	Maximum surface displacement (D, m)	1			
	Average surface displacement (D, cm)	100			
	Slip rate (S, mm/yr)				

FAULT NAME/NO.: HORSESHOE DAM/#6

Parameter (Reference)	Fault Type	Limits	Equation	Computed Ms P-1	P-2	P-3	s
Total fault length (Slemmons,1982)	SS	Ms>6.0	Ms=6.618+0.0012(L)	6.6	6.6	6.6	0.221
Rupture length (Slemmons,	N	-	Ms=0.809+1.341LogL	6.2	ERR	ERR	0.318
(1982)	R	-	Ms=2.021+1.142LogL	6.6	ERR	ERR	0.197
	SS	-	Ms=1.404+1.169LogL	6.1	ERR	ERR	0.205
(Bonilla and others, 1984)	R	Ms>6.0	Ms=5.71+0.916LogL	6.6	ERR	ERR	0.274
	SS	Ms>6.0	Ms=6.24+0.619LogL	6.9	ERR	ERR	0.293
Rupture area (Wyss, 1979)	All	Ms>5.6	Ms=4.15+LogA	6.6	ERR	ERR	0.3
(WCC, 1982)	All	4<Ms<6, A>5	Ms=4.257+0.656LogA	5.8	ERR	ERR	-
Maximum surface	N	-	Ms=6.668+0.750LogD	6.7	ERR	ERR	0.340
displacement (Slemmons,	R	-	Ms=6.793+1.306LogD	6.8	ERR	ERR	0.374
1982)	SS	-	Ms=6.974+0.804LogD	7.0	ERR	ERR	0.315
(Bonilla and others, 1984)	N	Ms>6.0	Ms=6.81+0.741LogD	6.8	ERR	ERR	0.188
	SS	Ms>6.0	Ms=7.00+0.782LogD	7.0	ERR	ERR	0.331
Slip rate (WWC, 1979)	SS	-	Ms=7.223+1.263LogS	ERR	ERR	ERR	-
Seismic moment (Schwartz et al.,1984)	All	3<Ml<7 5<Ms<7.5 Mm>7.5	Mm=2/3logMo-10.7 Mo=ADu	6.6	ERR	ERR	0.24
MEAN				6.4	ERR	ERR	
MAXIMUM				6.8	ERR	ERR	
MINIMUM				5.8	ERR	ERR	

TABLE B-2 (Cont'd)

FAULT NAME/NO.:	TURRET PEAK/#7	P-1	P-2	P-3	REFS
	Fault Type N	1	0		ABGMT Map 22
	Orientatio				Crust=20km
	Total fault length (L, km) =	10	0		Dip=55 assumed
	Rupture length (L, m)	10000	0		Downdip=24.5km
	Rupture area (A, sq. km)	245	0		
	Maximum surface displacement (D, m)	1	0		Assumed
	Average surface displacement (D, cm)	50	0		
	Slip rate (S, mm/yr)				

FAULT NAME/NO.: TURRET PEAK/#7

Parameter (Reference)	Fault Type	Limits	Equation	Computed Ms P-1	P-2	P-3	s
Total fault length (Slemmons,1982)	SS	Ms>6.0	Ms=6.618+0.0012(L)	6.6	6.6	6.6	0.221
Rupture length (Slemmons, (1982)	N	-	Ms=0.809+1.341LogL	6.2	ERR	ERR	0.318
	R	-	Ms=2.021+1.142LogL	6.6	ERR	ERR	0.197
	SS	-	Ms=1.404+1.169LogL	6.1	ERR	ERR	0.205
(Bonilla and others, 1984)	R	Ms>6.0	Ms=5.71+0.916LogL	6.6	ERR	ERR	0.274
	SS	Ms>6.0	Ms=6.24+0.619LogL	6.9	ERR	ERR	0.293
Rupture area (Wyss, 1979)	All	Ms>5.6	Ms=4.15+LogA	6.5	ERR	ERR	0.3
(WCC, 1982)	All	4<Ms<6, A>5	Ms=4.257+0.656LogA	5.8	ERR	ERR	-
Maximum surface displacement (Slemmons, 1982)	N	-	Ms=6.668+0.750LogD	6.7	ERR	ERR	0.340
	R	-	Ms=6.793+1.306LogD	6.8	ERR	ERR	0.374
	SS	-	Ms=6.974+0.804LogD	7.0	ERR	ERR	0.315
(Bonilla and others, 1984)	N	Ms>6.0	Ms=6.81+0.741LogD	6.8	ERR	ERR	0.188
	SS	Ms>6.0	Ms=7.00+0.782LogD	7.0	ERR	ERR	0.331
Slip rate (WWC, 1979)	SS	-	Ms=7.223+1.263LogS	ERR	ERR	ERR	-
Seismic moment (Schwartz et al.,1984)	All	3<Ml<7 5<Ms<7.5 Mm>7.5	Mm=2/3logMo-10.7 Mo=ADu	6.3	ERR	ERR	0.24
MEAN				6.4	ERR	ERR	
MAXIMUM				6.8	ERR	ERR	
MINIMUM				5.8	ERR	ERR	

TABLE B-2 (Cont'd)

FAULT NAME/NO.:	VERDE/#8	P-1	P-2	P-3	REFS
	Fault Type N	0.3	0.7		ABGMT Map 22
	Orientatio				Pearthree e.a.1983
	Total fault length (L, km) =	90	35		Crust=20km
	Rupture length (L, m)	45000	35000		Dip=55 assumed
	Rupture area (A, sq. km)	1103	858		Downdip=24.5km
	Maximum surface displacement (D, m)	2	1		Derived
	Average surface displacement (D, cm)	100	50		Assumed
	Slip rate (S, mm/yr)				

FAULT NAME/NO.: VERDE/#8 Parameter (Reference)	Fault Type	Limits	Equation	Computed Ms P-1	P-2	P-3	s
Total fault length (Slemmons,1982)	SS	Ms>6.0	Ms=6.618+0.0012(L)	6.7	6.7	6.6	0.221
Rupture length (Slemmons,	N	-	Ms=0.809+1.341LogL	7.0	6.9	ERR	0.318
(1982)	R	-	Ms=2.021+1.142LogL	7.3	7.2	ERR	0.197
	SS	-	Ms=1.404+1.169LogL	6.8	6.7	ERR	0.205
(Bonilla and others, 1984)	R	Ms>6.0	Ms=5.71+0.916LogL	7.2	7.1	ERR	0.274
	SS	Ms>6.0	Ms=6.24+0.619LogL	7.3	7.2	ERR	0.293
Rupture area (Wyss, 1979)	All	Ms>5.6	Ms=4.15+LogA	7.2	7.1	ERR	0.3
(WCC, 1982)	All	4<Ms<6, A>5	Ms=4.257+0.656LogA	6.3	6.2	ERR	-
Maximum surface displacement (Slemmons,	N	-	Ms=6.668+0.750LogD	6.9	6.7	ERR	0.340
	R	-	Ms=6.793+1.306LogD	7.2	6.8	ERR	0.374
1982)	SS	-	Ms=6.974+0.804LogD	7.2	7.0	ERR	0.315
(Bonilla and others, 1984)	N	Ms>6.0	Ms=6.81+0.741LogD	7.0	6.8	ERR	0.188
	SS	Ms>6.0	Ms=7.00+0.782LogD	7.2	7.0	ERR	0.331
Slip rate (WWC, 1979)	SS	-	Ms=7.223+1.263LogS	ERR	ERR	ERR	-
Seismic moment (Schwartz et al.,1984)	All	3<Ml<7 5<Ms<7.5 Mm>7.5	Mm=2/3logMo-10.7 Mo=ADu	7.0	6.7	ERR	0.24
MEAN				6.9	6.7	ERR	
MAXIMUM				7.2	7.1	ERR	
MINIMUM				6.3	6.2	ERR	

TABLE B-2 (Cont'd)

FAULT NAME/NO.:	PRESCOTT VALLEY/#9	P-1	P-2	P-3	REFS
	Fault Type N	1	0		ABGMT Map 22
	Orientatio				Crust=20km
	Total fault length (L, km) =	4	0		Dip=55 assumed
	Rupture length (L, m)	4000	0		Downdip=24.5km
	Rupture area (A, sq. km)	98	0		
	Maximum surface displacement (D, m)	1	0		Assumed
	Average surface displacement (D, cm)	50	0		Assumed
	Slip rate (S, mm/yr)				

FAULT NAME/NO.: PRESCOTT VALLEY/#9

Parameter (Reference)	Fault Type	Limits	Equation	Computed Ms P-1	P-2	P-3	s
Total fault length (Slemmons,1982)	SS	Ms>6.0	Ms=6.618+0.0012(L)	6.6	6.6	6.6	0.221
Rupture length (Slemmons, (1982)	N	-	Ms=0.809+1.341LogL	5.6	ERR	ERR	0.318
	R	-	Ms=2.021+1.142LogL	6.1	ERR	ERR	0.197
	SS	-	Ms=1.404+1.169LogL	5.6	ERR	ERR	0.205
(Bonilla and others, 1984)	R	Ms>6.0	Ms=5.71+0.916LogL	6.3	ERR	ERR	0.274
	SS	Ms>6.0	Ms=6.24+0.619LogL	6.6	ERR	ERR	0.293
Rupture area (Wyss, 1979)	All	Ms>5.6	Ms=4.15+LogA	6.1	ERR	ERR	0.3
(WCC, 1982)	All	4<Ms<6, A>5	Ms=4.257+0.656LogA	5.6	ERR	ERR	-
Maximum surface displacement (Slemmons, 1982)	N	-	Ms=6.668+0.750LogD	6.7	ERR	ERR	0.340
	R	-	Ms=6.793+1.306LogD	6.8	ERR	ERR	0.374
	SS	-	Ms=6.974+0.804LogD	7.0	ERR	ERR	0.315
(Bonilla and others, 1984)	N	Ms>6.0	Ms=6.81+0.741LogD	6.8	ERR	ERR	0.185
	SS	Ms>6.0	Ms=7.00+0.782LogD	7.0	ERR	ERR	0.331
Slip rate (WWC, 1979)	SS	-	Ms=7.223+1.263LogS	ERR	ERR	ERR	-
Seismic moment (Schwartz et al.,1984)	All	3<Ml<7 5<Ms<7.5 Mm>7.5	Mm=2/3logMo-10.7 Mo=ADu	6.1	ERR	ERR	0.24
MEAN				6.2	ERR	ERR	
MAXIMUM				6.8	ERR	ERR	
MINIMUM				5.6	ERR	ERR	

TABLE B-2 (Cont'd)

FAULT NAME/NO.:	WILLIAMSON VALLEY/#10	P-1	P-2	P-3	REFS
	Fault Type N	1			ABGMT Map 22
	Orientatio				Crust=20km
	Total fault length (L, km) =	3			Dip=55 assumed
	Rupture length (L, m)	3000			Downdip=24.5km
	Rupture area (A, sq. km)	73			
	Maximum surface displacement (D, m)	1			Assumed
	Average surface displacement (D, cm)	50			Assumed
	Slip rate (S, mm/yr)				

FAULT NAME/NO.:	WILLIAMSON VALLEY/#10						
Parameter (Reference)	Fault Type	Limits	Equation	Computed Ms P-1	P-2	P-3	s
Total fault length (Slemmons,1982)	SS	Ms>6.0	Ms=6.618+0.0012(L)	6.6	6.6	6.6	0.221
Rupture length (Slemmons, (1982)	N	-	Ms=0.809+1.341LogL	5.5	ERR	ERR	0.318
	R	-	Ms=2.021+1.142LogL	6.0	ERR	ERR	0.197
	SS	-	Ms=1.404+1.169LogL	5.5	ERR	ERR	0.205
(Bonilla and others, 1984)	R	Ms>6.0	Ms=5.71+0.916LogL	6.1	ERR	ERR	0.274
	SS	Ms>6.0	Ms=6.24+0.619LogL	6.5	ERR	ERR	0.293
Rupture area (Wyss, 1979)	All	Ms>5.6	Ms=4.15+LogA	6.0	ERR	ERR	0.3
(WCC, 1982)	All	4<Ms<6, A>5	Ms=4.257+0.656LogA	5.5	ERR	ERR	-
Maximum surface displacement (Slemmons, 1982)	N	-	Ms=6.668+0.750LogD	6.7	ERR	ERR	0.340
	R	-	Ms=6.793+1.306LogD	6.8	ERR	ERR	0.374
	SS	-	Ms=6.974+0.804LogD	7.0	ERR	ERR	0.315
(Bonilla and others, 1984)	N	Ms>6.0	Ms=6.81+0.741LogD	6.8	ERR	ERR	0.188
	SS	Ms>6.0	Ms=7.00+0.782LogD	7.0	ERR	ERR	0.331
Slip rate (WWC, 1979)	SS	-	Ms=7.223+1.263LogS	ERR	ERR	ERR	-
Seismic moment (Schwartz et al.,1984)	All	3<Ml<7 5<Ms<7.5 Mm>7.5	Mm=2/3logMo-10.7 Mo=ADu	6.0	ERR	ERR	0.24
MEAN				6.1	ERR	ERR	
MAXIMUM				6.8	ERR	ERR	
MINIMUM				5.5	ERR	ERR	

TABLE B-2 (Cont'd)

FAULT NAME/NO.:	CHAVEZ MTN/#11	P-1	P-2	P-3	REFS
	Fault Type N	0.5	0.5		ABGMT Map 22
	Orientatio				Crust=35km
	Total fault length (L, km) =	40	15		Dip=55 assumed
	Rupture length (L, m)	20000	15000		Downdip=43km
	Rupture area (A, sq. km)	854	641		
	Maximum surface displacement (D, m)	2	1		Assumed
	Average surface displacement (D, cm)	100	50		Assumed
	Slip rate (S, mm/yr)				

FAULT NAME/NO.: Parameter (Reference)	CHAVEZ MTN/#11 Fault Type	Limits	Equation	Computed Ms P-1	P-2	P-3	s
Total fault length (Slemmons,1982)	SS	Ms>6.0	Ms=6.618+0.0012(L)	6.7	6.6	6.6	0.221
Rupture length (Slemmons, (1982)	N	-	Ms=0.809+1.341LogL	6.6	6.4	ERR	0.318
	R	-	Ms=2.021+1.142LogL	6.9	6.8	ERR	0.197
	SS	-	Ms=1.404+1.169LogL	6.4	6.3	ERR	0.205
(Bonilla and others, 1984)	R	Ms>6.0	Ms=5.71+0.916LogL	6.9	6.8	ERR	0.274
	SS	Ms>6.0	Ms=6.24+0.619LogL	7.0	7.0	ERR	0.293
Rupture area (Wyss, 1979)	All	Ms>5.6	Ms=4.15+LogA	7.1	7.0	ERR	0.3
(WCC, 1982)	All	4<Ms<6, A>5	Ms=4.257+0.656LogA	6.2	6.1	ERR	-
Maximum surface displacement (Slemmons, 1982)	N	-	Ms=6.668+0.750LogD	6.9	6.7	ERR	0.340
	R	-	Ms=6.793+1.306LogD	7.2	6.8	ERR	0.374
	SS	-	Ms=6.974+0.804LogD	7.2	7.0	ERR	0.315
(Bonilla and others, 1984)	N	Ms>6.0	Ms=3.81+0.74LogD	7.0	6.8	ERR	0.188
	SS	Ms>6.0	Ms=7.00+0.782LogD	7.2	7.0	ERR	0.331
Slip rate (WWC, 1979)	SS	-	Ms=7.223+1.263LogS	ERR	ERR	ERR	-
Seismic moment (Schwartz et al.,1984)	All	3<Ml<7 5<Ms<7.5 Mm>7.5	Mm=2/3logMo-10.7 Mo=ADu	6.9	6.6	ERR	0.24
MEAN				6.8	6.6	ERR	
MAXIMUM				7.1	7.0	ERR	
MINIMUM				6.2	6.1	ERR	

TABLE B-2 (Cont'd)

FAULT NAME/NO.:	LAKE MARY/MORMON LAKE/#1	P-1	P-2	P-3	REFS
	Fault Type N	0.5	0.5		ABGMT Map 22
	Orientatio				Crust=35km
	Total fault length (L, km) =	35	15		Dip=55 assumed
	Rupture length (L, m)	17500	15000		Downdip=43km
	Rupture area (A, sq. km)	747	641		
	Maximum surface displacement (D, m)	1	1		Assumed
	Average surface displacement (D, cm)	50	50		Assumed
	Slip rate (S, mm/yr)				

FAULT NAME/NO.: LAKE MARY/MORMON LAKE/#12

Parameter (Reference)	Fault Type	Limits	Equation	Computed Ms P-1	P-2	P-3	s
Total fault length (Slemmons,1982)	SS	Ms>6.0	Ms=6.618+0.0012(L)	6.7	6.6	6.6	0.221
Rupture length (Slemmons, (1982)	N	-	Ms=0.809+1.341LogL	6.5	6.4	ERR	0.318
	R	-	Ms=2.021+1.142LogL	6.9	6.8	ERR	0.197
	SS	-	Ms=1.404+1.169LogL	6.4	6.3	ERR	0.205
(Bonilla and others, 1984)	R	Ms>6.0	Ms=5.71+0.916LogL	6.8	6.8	ERR	0.274
	SS	Ms>6.0	Ms=6.24+0.619LogL	7.0	7.0	ERR	0.293
Rupture area (Wyss, 1979)	All	Ms>5.6	Ms=4.15+LogA	7.0	7.0	ERR	0.3
(WCC, 1982)	All	4<Ms<6, A>5	Ms=4.257+0.656LogA	6.1	6.1	ERR	-
Maximum surface displacement (Slemmons, 1982)	N	-	Ms=6.668+0.750LogD	6.7	6.7	ERR	0.340
	R	-	Ms=6.793+1.306LogD	6.8	6.8	ERR	0.374
	SS	-	Ms=6.974+0.804LogD	7.0	7.0	ERR	0.315
(Bonilla and others, 1984)	N	Ms>6.0	Ms=6.81+0.741LogD	6.8	6.8	ERR	0.188
	SS	Ms>6.0	Ms=7.00+0.782LogD	7.0	7.0	ERR	0.331
Slip rate (WWC, 1979)	SS	-	Ms=7.223+1.263LogS	ERR	ERR	ERR	-
Seismic moment (Schwartz et al.,1984)	All	3<Ml<7 5<Ms<7.5 Mm>7.5	Mm=2/3logMo-10.7 Mo=ADu	6.7	6.6	ERR	0.24
MEAN				6.6	6.6	ERR	
MAXIMUM				7.0	7.0	ERR	
MINIMUM				6.1	6.1	ERR	

TABLE B-2 (Cont'd)

FAULT NAME/NO.:	MUNDS PARK/#13	P-1	P-2	P-3	REFS
	Fault Type N	0.5	0.5		ABGMT Map 22
	Orientatio				Crust=35km
	Total fault length (L, km) =	35	12		Dip=55 assumed
	Rupture length (L, m)	17500	12000		Downdip=43km
	Rupture area (A, sq. km)	747	513		
	Maximum surface displacement (D, m)	1	1		Assumed
	Average surface displacement (D, cm)	50	50		Assumed
	Slip rate (S, mm/yr)				

FAULT NAME/NO.: Parameter (Reference)	MUNDS PARK/#13 Fault Type	Limits	Equation	Computed Ms P-1	P-2	P-3	s
Total fault length (Slemmons,1982)	SS	Ms>6.0	Ms=6.618+0.0012(L)	6.7	6.6	6.6	0.221
Rupture length (Slemmons, (1982)	N	-	Ms=0.809+1.341LogL	6.5	6.3	ERR	0.318
	R	-	Ms=2.021+1.142LogL	6.9	6.7	ERR	0.197
	SS	-	Ms=1.404+1.169LogL	6.4	6.2	ERR	0.205
(Bonilla and others, 1984)	R	Ms>6.0	Ms=5.71+0.916LogL	6.8	6.7	ERR	0.274
	SS	Ms>6.0	Ms=6.24+0.619LogL	7.0	6.9	ERR	0.293
Rupture area (Wyss, 1979)	All	Ms>5.6	Ms=4.15+LogA	7.0	6.9	ERR	0.3
(WCC, 1982)	All	4<Ms<6, A>5	Ms=4.257+0.656LogA	6.1	6.0	ERR	-
Maximum surface displacement (Slemmons, 1982)	N	-	Ms=6.668+0.750LogD	6.7	6.7	ERR	0.340
	R	-	Ms=6.793+1.306LogD	6.8	6.8	ERR	0.374
	SS	-	Ms=6.974+0.804LogD	7.0	7.0	ERR	0.315
(Bonilla and others, 1984)	N	Ms>6.0	Ms=6.81+0.741LogD	6.8	6.8	ERR	0.188
	SS	Ms>6.0	Ms=7.00+0.782LogD	7.0	7.0	ERR	0.331
Slip rate (WWC, 1979)	SS	-	Ms=7.223+1.263LogS	ERR	ERR	ERR	-
Seismic moment (Schwartz et al.,1984)	All	3<Ml<7 5<Ms<7.5 Mm>7.5	Mm=2/3logMo-10.7 Mo=ADu	6.7	6.6	ERR	0.24
MEAN				6.6	6.5	ERR	
MAXIMUM				7.0	6.9	ERR	
MINIMUM				6.1	6.0	ERR	

TABLE B-2 (Cont'd)

FAULT NAME/NO.:	BIG CHINO/#14	P-1	P-2	P-3	REFS
	Fault Type N	0.5	0.5		ABGMT Map 22
	Orientatio				Crust=35km
	Total fault length (L, km) =	50	35		Dip=55 assumed
	Rupture length (L, m)	25000	35000		Downdip=43km
	Rupture area (A, sq. km)	1068	1505		
	Maximum surface displacement (D, m)	3.5	2		
	Average surface displacement (D, cm)	250	150		Assumed
	Slip rate (S, mm/yr)				

FAULT NAME/NO.:- BIG CHINO/#14

Parameter (Reference)	Fault Type	Limits	Equation	Computed Ms P-1	P-2	P-3	s
Total fault length (Slemmons,1982)	SS	Ms>6.0	Ms=6.618+0.0012(L)	6.7	6.7	6.6	0.221
Rupture length (Slemmons, (1982)	N	-	Ms=0.809+1.341LogL	6.7	6.9	ERR	0.318
	R	-	Ms=2.021+1.142LogL	7.0	7.2	ERR	0.197
	SS	-	Ms=1.404+1.169LogL	6.5	6.7	ERR	0.205
(Bonilla and others, 1984)	R	Ms>6.0	Ms=5.71+0.916LogL	7.0	7.1	ERR	0.274
	SS	Ms>6.0	Ms=6.24+0.619LogL	7.1	7.2	ERR	0.293
Rupture area (Wyss, 1979)	All	Ms>5.6	Ms=4.15+LogA	7.2	7.3	ERR	0.3
(WCC, 1982)	All	4<Ms<6, A>5	Ms=4.257+0.656LogA	6.2	6.3	ERR	-
Maximum surface displacement (Slemmons, 1982)	N	-	Ms=6.668+0.750LogD	7.1	6.9	ERR	0.340
	R	-	Ms=6.793+1.306LogD	7.5	7.2	ERR	0.374
	SS	-	Ms=6.974+0.804LogD	7.4	7.2	ERR	0.315
(Bonilla and others, 1984)	N	Ms>6.0	Ms=6.81+0.741LogD	7.2	7.0	ERR	0.188
	SS	Ms>6.0	Ms=7.00+0.782LogD	7.4	7.2	ERR	0.331
Slip rate (WWC, 1979)	SS	-	Ms=7.223+1.263LogS	ERR	ERR	ERR	-
Seismic moment (Schwartz et al.,1984)	All	3<Ml<7 5<Ms<7.5 Mm>7.5	Mm=2/3logMo-10.7 Mo=ADu	7.2	7.2	ERR	0.24
MEAN				6.9	6.9	ERR	
MAXIMUM				7.2	7.3	ERR	
MINIMUM				6.2	6.3	ERR	

TABLE B-2 (Cont'd)

FAULT NAME/NO.:	MESA BUTTE/#15	P-1	P-2	P-3	REFS
	Fault Type N	0.3	0.7		ABGMT Map 22
	Orientatio				Shoemaker e.a.,1977
	Total fault length (L, km) =	150	38		Crust=35km
	Rupture length (L, m)	75000	38000		Dip=55 assumed
	Rupture area (A, sq. km)	3204	1623		Downdip=43km
	Maximum surface displacement (D, m)	2.5	2		Assumed
	Average surface displacement (D, cm)	100	100		Assumed
	Slip rate (S, mm/yr)				

FAULT NAME/NO.:	MESA BUTTE/#15						
Parameter (Reference)	Fault Type	Limits	Equation	Computed Ms P-1	P-2	P-3	s
Total fault length (Slemmons,1982)	SS	Ms>6.0	Ms=6.618+0.0012(L)	6.8	6.7	6.6	0.221
Rupture length (Slemmons, (1982)	N	-	Ms=0.809+1.341LogL	7.3	7.0	ERR	0.318
	R	-	Ms=2.021+1.142LogL	7.6	7.3	ERR	0.197
	SS	-	Ms=1.404+1.169LogL	7.1	6.8	ERR	0.205
(Bonilla and others, 1984)	R	Ms>6.0	Ms=5.71+0.916LogL	7.4	7.2	ERR	0.274
	SS	Ms>6.0	Ms=6.24+0.619LogL	7.4	7.2	ERR	0.293
Rupture area (Wyss, 1979)	All	Ms>5.6	Ms=4.15+LogA	7.7	7.4	ERR	0.3
(WCC, 1982)	All	4<Ms<6, A>5	Ms=4.257+0.656LogA	6.6	6.4	ERR	-
Maximum surface displacement (Slemmons, 1982)	N	-	Ms=6.668+0.750LogD	7.0	6.9	ERR	0.340
	R	-	Ms=6.793+1.306LogD	7.3	7.2	ERR	0.374
	SS	-	Ms=6.974+0.804LogD	7.3	7.2	ERR	0.315
(Bonilla and others, 1984)	N	Ms>6.0	Ms=6.81+0.741LogD	7.1	7.0	ERR	0.188
	SS	Ms>6.0	Ms=7.00+0.782LogD	7.3	7.2	ERR	0.331
Slip rate (WWC, 1979)	SS	-	Ms=7.223+1.263LogS	ERR	ERR	ERR	-
Seismic moment (Schwartz et al.,1984)	All	3<Ml<7 5<Ms<7.5 Mm>7.5	Mm=2/3logMo-10.7 Mo=ADu	7.3	7.1	ERR	0.24
MEAN				7.2	6.9	ERR	
MAXIMUM				7.7	7.4	ERR	
MINIMUM				6.6	6.4	ERR	

TABLE B-2 (Cont'd)

FAULT NAME/NO.:	BRIGHT ANGEL/#16	P-1	P-2	P-3	REFS
	Fault Type N	0.5	0.5		ABGMT Map 22
	Orientatio				Crust=35km
	Total fault length (L, km) =	100	65		Dip=55 assumed
	Rupture length (L, m)	50000	65000		Downdip=43km
	Rupture area (A, sq. km)	2136	2777		
	Maximum surface displacement (D, m)	2	2.5		Assumed
	Average surface displacement (D, cm)	100	100		Assumed
	Slip rate (S, mm/yr)				

FAULT NAME/NO.: BRIGHT ANGEL/#16

Parameter (Reference)	Fault Type	Limits	Equation	Computed Ms P-1	P-2	P-3	s
Total fault length (Slemmons,1982)	SS	Ms>6.0	Ms=6.618+0.0012(L)	6.7	6.7	6.6	0.221
Rupture length (Slemmons, (1982)	N	-	Ms=0.809+1.341LogL	7.1	7.3	ERR	0.318
	R	-	Ms=2.021+1.142LogL	7.4	7.5	ERR	0.197
	SS	-	Ms=1.404+1.169LogL	6.9	7.0	ERR	0.205
(Bonilla and others, 1984)	R	Ms>6.0	Ms=5.71+0.916LogL	7.3	7.4	ERR	0.274
	SS	Ms>6.0	Ms=6.24+0.619LogL	7.3	7.4	ERR	0.293
Rupture area (Wyss, 1979)	All	Ms>5.6	Ms=4.15+LogA	7.5	7.6	ERR	0.3
(WCC, 1982)	All	4<Ms<6, A>5	Ms=4.257+0.656LogA	6.4	6.5	ERR	-
Maximum surface displacement (Slemmons, 1982)	N	-	Ms=6.668+0.750LogD	6.9	7.0	ERR	0.340
	R	-	Ms=6.793+1.306LogD	7.2	7.3	ERR	0.374
	SS	-	Ms=6.974+0.804LogD	7.2	7.3	ERR	0.315
(Bonilla and others, 1984)	N	Ms>6.0	Ms=6.81+0.741LogD	7.0	7.1	ERR	0.188
	SS	Ms>6.0	Ms=7.00+0.782LogD	7.2	7.3	ERR	0.331
Slip rate (WWC, 1979)	SS	-	Ms=7.223+1.263LogS	ERR	ERR	ERR	-
Seismic moment (Schwartz et al.,1984)	All	3<Ml<7 5<Ms<7.5 Mm>7.5	Mm=2/3logMo-10.7 Mo=ADu	7.2	7.2	ERR	0.24
MEAN				7.0	7.1	ERR	
MAXIMUM				7.5	7.6	ERR	
MINIMUM				6.4	6.5	ERR	

TABLE B-2 (Cont'd)

FAULT NAME/NO.:	AUBREY/#17	P-1	P-2	P-3	REFS
	Fault Type N	0.5	0.5		ABGMT Map 22
	Orientatio				Crust=35km
	Total fault length (L, km) =	70	45		Dip=55 assumed
	Rupture length (L, m)	35000	45000		Downdip=43km
	Rupture area (A, sq. km)	1495	1922		
	Maximum surface displacement (D, m)	2	2		Assumed
	Average surface displacement (D, cm)	100	100		Assumed
	Slip rate (S, mm/yr)				

FAULT NAME/NO.: AUBREY/#17

Parameter (Reference)	Fault Type	Limits	Equation	Computed Ms P-1=	P-2	P-3	s
Total fault length (Slemmons,1982)	SS	Ms>6.0	Ms=6.618+0.0012(L)	6.7	6.7	6.6	0.221
Rupture length (Slemmons, (1982)	N	-	Ms=0.809+1.341LogL	6.9	7.0	ERR	0.318
	R	-	Ms=2.021+1.142LogL	7.2	7.3	ERR	0.197
	SS	-	Ms=1.404+1.169LogL	6.7	6.8	ERR	0.205
(Bonilla and others, 1984)	R	Ms>6.0	Ms=5.71+0.916LogL	7.1	7.2	ERR	0.274
	SS	Ms>6.0	Ms=6.24+0.619LogL	7.2	7.3	ERR	0.293
Rupture area (Wyss, 1979)	All	Ms>5.6	Ms=4.15+LogA	7.3	7.4	ERR	0.3
(WCC, 1982)	All	4<Ms<6, A>5	Ms=4.257+0.656LogA	6.3	6.4	ERR	-
Maximum surface displacement (Slemmons, 1982)	N	-	Ms=6.668+0.750LogD	6.9	6.9	ERR	0.340
	R	-	Ms=6.793+1.306LogD	7.2	7.2	ERR	0.374
	SS	-	Ms=6.974+0.804LogD	7.2	7.2	ERR	0.315
(Bonilla and others, 1984)	N	Ms>6.0	Ms=6.81+0.741LogD	7.0	7.0	ERR	0.188
	SS	Ms>6.0	Ms=7.00+0.782LogD	7.2	7.2	ERR	0.331
Slip rate (WWC, 1979)	SS	-	Ms=7.223+1.263LogS	ERR	ERR	ERR	-
Seismic moment (Schwartz et al.,1984)	All	3<Ml<7 5<Ms<7.5 Mm>7.5	Mm=2/3logMo-10.7 Mo=ADu	7.1	7.1	ERR	0.24
MEAN				6.9	7.0	ERR	
MAXIMUM				7.3	7.4	ERR	
MINIMUM				6.3	6.4	ERR	

TABLE B-2 (Cont'd)

FAULT NAME/NO.:	TOROWEAP/#18	P-1	P-2	P-3	REFS
	Fault Type N	0.3	0.7		Jackson 1990
	Orientatio				Anderson e.a.,1989
	Total fault length (L, km) =	480	45		Crust=35km
	Rupture length (L, m)	240000	45000		Dip=55 assumed
	Rupture area (A, sq. km)	10254	1922		Downdip=43km
	Maximum surface displacement (D, m)	2.2	2.2		
	Average surface displacement (D, cm)	100	100		Assumed
	Slip rate (S, mm/yr)				

FAULT NAME/NO.:	TOROWEAP/#18						
Parameter (Reference)	Fault Type	Limits	Equation	Computed Ms P-1	P-2	P-3	s
Total fault length (Slemmons,1982)	SS	Ms>6.0	Ms=6.618+0.0012(L)	7.2	6.7	6.6	0.221
Rupture length (Slemmons,	N	-	Ms=0.809+1.341LogL	8.0	7.0	ERR	0.318
(1982)	R	-	Ms=2.021+1.142LogL	8.2	7.3	ERR	0.197
	SS	-	Ms=1.404+1.169LogL	7.7	6.8	ERR	0.205
(Bonilla and others, 1984)	R	Ms>6.0	Ms=5.71+0.916LogL	7.9	7.2	ERR	0.274
	SS	Ms>6.0	Ms=6.24+0.619LogL	7.7	7.3	ERR	0.293
Rupture area (Wyss, 1979)	All	Ms>5.6	Ms=4.15+LogA	8.2	7.4	ERR	0.3
(WCC, 1982)	All	4<Ms<6, A>5	Ms=4.257+0.656LogA	6.9	6.4	ERR	-
Maximum surface	N	-	Ms=6.668+0.750LogD	6.9	6.9	ERR	0.340
displacement (Slemmons,	R	-	Ms=6.793+1.306LogD	7.2	7.2	ERR	0.374
1982)	SS	-	Ms=6.974+0.804LogD	7.2	7.2	ERR	0.315
(Bonilla and others, 1984)	N	Ms>6.0	Ms=6.81+0.741LogD	7.1	7.1	ERR	0.188
	SS	Ms>6.0	Ms=7.00+0.782LogD	7.3	7.3	ERR	0.331
Slip rate (WWC, 1979)	SS	-	Ms=7.223+1.263LogS	ERR	ERR	ERR	-
Seismic moment (Schwartz et al.,1984)	All	3<Ml<7 5<Ms<7.5 Mm>7.5	Mm=2/3logMo-10.7 Mo=ADu	7.6	7.1	ERR	0.24
MEAN				7.4	7.0	ERR	
MAXIMUM				8.2	7.4	ERR	
MINIMUM				6.9	6.4	ERR	

TABLE B-2 (Cont'd)

FAULT NAME/NO.:	HURRICANE/#19	P-1	P-2	P-3	REFS
	Fault Type N	0.3	0.7		ABGMT Map 22
	Orientatio				Hamblin e.a.
	Total fault length (L, km) =	170	65		Crust=35km
	Rupture length (L, m)	85000	65000		Dip=55 assumed
	Rupture area (A, sq. km)	3631	2777		Downdip=43km
	Maximum surface displacement (D, m)	2.5	2.5		Assumed
	Average surface displacement (D, cm)	100	100		Assumed
	Slip rate (S, mm/yr)				

FAULT NAME/NO.: Parameter (Reference)	HURRICANE/#19 Fault Type	Limits	Equation	Computed Ms P-1	P-2	P-3	s
Total fault length (Slemmons,1982)	SS	Ms>6.0	Ms=6.618+0.0012(L)	6.8	6.7	6.6	0.221
Rupture length (Slemmons, (1982)	N	-	Ms=0.809+1.341LogL	7.4	7.3	ERR	0.318
	R	-	Ms=2.021+1.142LogL	7.7	7.5	ERR	0.197
	SS	-	Ms=1.404+1.169LogL	7.2	7.0	ERR	0.205
(Bonilla and others, 1984)	R	Ms>6.0	Ms=5.71+0.916LogL	7.5	7.4	ERR	0.274
	SS	Ms>6.0	Ms=6.24+0.619LogL	7.4	7.4	ERR	0.293
Rupture area (Wyss, 1979)	All	Ms>5.6	Ms=4.15+LogA	7.7	7.6	ERR	0.3
(WCC, 1982)	All	4<Ms<6, A>5	Ms=4.257+0.656LogA	6.6	6.5	ERR	-
Maximum surface displacement (Slemmons, 1982)	N	-	Ms=6.668+0.750LogD	7.0	7.0	ERR	0.340
	R	-	Ms=6.793+1.306LogD	7.3	7.3	ERR	0.374
	SS	-	Ms=6.971+0.804LogD			ERR	0.315
(Bonilla and others, 1984)	N	Ms>6.0	Ms=6.81+0.741LogD	7.1	7.1	ERR	0.188
	SS	Ms>6.0	Ms=7.00+0.782LogD	7.3	7.3	ERR	0.331
Slip rate (WWC, 1979)	SS	-	Ms=7.223+1.263LogS	ERR	ERR	ERR	-
Seismic moment (Schwartz et al.,1984)	All	3<Ml<7 5<Ms<7.5 Mm>7.5	Mm=2/3logMo-10.7 Mo=ADu	7.3	7.2	ERR	0.24
MEAN				7.2	7.1	ERR	
MAXIMUM				7.7	7.6	ERR	
MINIMUM				6.6	6.5	ERR	

TABLE B-2 (Cont'd)

FAULT NAME/NO.:	PINTO MTN/#20	P-1	P-2	P-3	REFS
	Fault Type SS	0.2	0.1	0.7	Diblee, 1975
	Orientatio				Wesnousky, 1986
	Total fault length (L, km) =	73	73	73	Crust=20km
	Rupture length (L, m)	36500	36500	36500	Dip=75 assumed
	Rupture area (A, sq. km)	766	766	766	Downdip=21km
	Maximum surface displacement (D, m)	2	2	2	Assumed
	Average surface displacement (D, cm)	200	200	200	Assumed
	Slip rate (S, mm/yr)	0.3	5.3	1	

FAULT NAME/NO.: PINTO MTN/#20

Parameter (Reference)	Fault Type	Limits	Equation	Computed Ms P-1	P-2	P-3	s
Total fault length (Slemmons,1982)	SS	Ms>6.0	Ms=6.618+0.0012(L)	6.7	6.7	6.7	0.221
Rupture length (Slemmons, (1982)	N	-	Ms=0.809+1.341LogL	6.9	6.9	6.9	0.318
	R	-	Ms=2.021+1.142LogL	7.2	7.2	7.2	0.197
	SS	-	Ms=1.404+1.169LogL	6.7	6.7	6.7	0.205
(Bonilla and others, 1984)	R	Ms>6.0	Ms=5.71+0.916LogL	7.1	7.1	7.1	0.274
	SS	Ms>6.0	Ms=6.24+0.619LogL	7.2	7.2	7.2	0.293
Rupture area (Wyss, 1979)	All	Ms>5.6	Ms=4.15+LogA	7.0	7.0	7.0	0.3
(WCC, 1982)	All	4<Ms<6, A>5	Ms=4.257+0.656LogA	6.1	6.1	6.1	-
Maximum surface displacement (Slemmons, 1982)	N	-	Ms=6.668+0.750LogD	6.9	6.9	6.9	0.340
	R	-	Ms=6.793+1.306LogD	7.2	7.2	7.2	0.374
	SS	-	Ms=6.974+0.804LogD	7.2	7.2	7.2	0.315
(Bonilla and others, 1984)	N	Ms>6.0	Ms=6.81+0.741LogD	7.0	7.0	7.0	0.188
	SS	Ms>6.0	Ms=7.00+0.782LogD	7.2	7.2	7.2	0.331
Slip rate (WWC, 1979)	SS	-	Ms=7.223+1.263LogS	6.6	8.1	7.2	-
Seismic moment (Schwartz et al.,1984)	All	3<Ml<7 5<Ms<7.5 Mm>7.5	Mm=2/3logMo-10.7 Mo=ADu	7.1	7.1	7.1	0.24
MEAN				6.9	7.1	7.0	
MAXIMUM				7.2	8.1	7.2	
MINIMUM				6.1	6.1	6.1	

TABLE B-2 (Cont'd)

FAULT NAME/NO.:	BLUE CUT/#21	P-1	P-2	P-3	REFS
	Fault Type SS	1			Wesnousky, 1986
	Orientatio				Crust=20km
	Total fault length (L, km) =	80			Dip=75 assumed
	Rupture length (L, m)	40000			Downdip=21km
	Rupture area (A, sq. km)	840			
	Maximum surface displacement (D, m)	2			Assumed
	Average surface displacement (D, cm)	200			Assumed
	Slip rate (S, mm/yr)	0.05			

FAULT NAME/NO.: BLUE CUT/#21

Parameter (Reference)	Fault Type	Limits	Equation	Computed Ms P-1	P-2	P-3	s
Total fault length (Slemmons,1982)	SS	Ms>6.0	Ms=6.618+0.0012(L)	6.7	6.6	6.6	0.221
Rupture length (Slemmons, (1982)	N	-	Ms=0.809+1.341LogL	7.0	ERR	ERR	0.318
	R	-	Ms=2.021+1.142LogL	7.3	ERR	ERR	0.197
	SS	-	Ms=1.404+1.169LogL	6.8	ERR	ERR	0.205
(Bonilla and others, 1984)	R	Ms>6.0	Ms=5.71+0.916LogL	7.2	ERR	ERR	0.274
	SS	Ms>6.0	Ms=6.24+0.619LogL	7.2	ERR	ERR	0.293
Rupture area (Wyss, 1979)	All	Ms>5.6	Ms=4.15+LogA	7.1	ERR	ERR	0.3
(WCC, 1982)	All	4<Ms<6, A>5	Ms=4.257+0.656LogA	6.2	ERR	ERR	-
Maximum surface displacement (Slemmons, 1982)	N	-	Ms=6.668+0.750LogD	6.9	ERR	ERR	0.340
	R	-	Ms=6.793+1.306LogD	7.2	ERR	ERR	0.374
	SS	-	Ms=6.974+0.804LogD	7.2	ERR	ERR	0.315
(Bonilla and others, 1984)	N	Ms>6.0	Ms=6.81+0.741LogD	7.0	ERR	ERR	0.188
	SS	Ms>6.0	Ms=7.00+0.782LogD	7.2	ERR	ERR	0.331
Slip rate (WWC, 1979)	SS	-	Ms=7.223+1.263LogS	5.6	ERR	ERR	-
Seismic moment (Schwartz et al.,1984)	All	3<Ml<7 5<Ms<7.5 Mm>7.5	Mm=2/3logMo-10.7 Mo=ADu	7.1	ERR	ERR	0.24
MEAN				6.8	ERR	ERR	
MAXIMUM				7.2	ERR	ERR	
MINIMUM				5.6	ERR	ERR	

TABLE B-2 (Cont'd)

FAULT NAME/NO.:	SAN ANDREAS/#22	P-1	P-2	P-3	REFS
	Fault Type SS	0.2	0.2	0.6	Crowell, 1981
	Orientatio				Wesnousky, 1986
	Total fault length (L, km) =	1100	1100	210	Crust=20km
	Rupture length (L, m)	550000	550000	210000	Dip=90 assumed
	Rupture area (A, sq. km)	11000	11000	4200	Downdip=20km
	Maximum surface displacement (D, m)	1	4	2	Assumed
	Average surface displacement (D, cm)	100	200	100	Assumed
	Slip rate (S, mm/yr)	10	35	10	

FAULT NAME/NO.: SAN ANDREAS/#22							
Parameter (Reference)	Fault Type	Limits	Equation	Computed Ms P-1	P-2	P-3	s
Total fault length (Slemmons,1982)	SS	Ms>6.0	Ms=6.618+0.0012(L)	7.9	7.9	6.9	0.221
Rupture length (Slemmons, (1982)	N	-	Ms=0.809+1.341LogL	8.5	8.5	7.9	0.318
	R	-	Ms=2.021+1.142LogL	8.6	8.6	8.1	0.197
	SS	-	Ms=1.404+1.169LogL	8.1	8.1	7.6	0.205
(Bonilla and others, 1984)	R	Ms>6.0	Ms=5.71+0.916LogL	8.2	8.2	7.8	0.274
	SS	Ms>6.0	Ms=6.24+0.619LogL	7.9	7.9	7.7	0.293
Rupture area (Wyss, 1979)	All	Ms>5.6	Ms=4.15+LogA	8.2	8.2	7.8	0.3
(WCC, 1982)	All	4<Ms<6, A>5	Ms=4.257+0.656LogA	6.9	6.9	6.6	-
Maximum surface displacement (Slemmons, 1982)	N	-	Ms=6.668+0.750LogD	6.7	7.1	6.9	0.340
	R	-	Ms=6.793+1.306LogD	6.8	7.6	7.2	0.374
	SS	-	Ms=6.974+0.804LogD	7.0	7.5	7.2	0.315
(Bonilla and others, 1984)	N	Ms>6.0	Ms=6.81+0.741LogD	6.8	7.3	7.0	0.188
	SS	Ms>6.0	Ms=7.00+0.782LogD	7.0	7.5	7.2	0.331
Slip rate (WWC, 1979)	SS	-	Ms=7.223+1.263LogS	8.5	9.2	8.5	-
Seismic moment (Schwartz et al.,1984)	All	3<Ml<7 5<Ms<7.5 Mm>7.5	Mm=2/3logMo-10.7 Mo=ADu	7.6	7.8	7.4	0.24
MEAN				7.7	7.9	7.4	
MAXIMUM				8.5	9.2	8.5	
MINIMUM				6.9	6.9	6.6	

TABLE B-2 (Cont'd)

FAULT NAME/NO.:	GILA MTN/#23	P-1	P-2	P-3	REFS
	Fault Type N	1			AGS OFR 90-1
	Orientation:				Crust=15km
	Total fault length (L, km) =	3			Dip=55
	Rupture length (L, m)	3000			Downdip=18km
	Rupture area (A, sq. km)	54			
	Maximum surface displacement (D, m)	1			Assumed
	Average surface displacement (D, cm)	50			Assumed
	Slip rate (S, mm/yr)				

FAULT NAME/NO.: GILA MTN/#23 Parameter (Reference)	Fault Type	Limits	Equation	Computed Ms – P-1	P-2	P-3	s
Total fault length (Slemmons,1982)	SS	Ms>6.0	Ms=6.618+0.0012(L)	6.6	6.6	6.6	0.221
Rupture length (Slemmons, (1982)	N	-	Ms=0.809+1.341LogL	5.5	ERR	ERR	0.318
	R	-	Ms=2.021+1.142LogL	6.0	ERR	ERR	0.197
	SS	-	Ms=1.404+1.169LogL	5.5	ERR	ERR	0.205
(Bonilla and others, 1984)	R	Ms>6.0	Ms=5.71+0.916LogL	6.1	ERR	ERR	0.274
	SS	Ms>6.0	Ms=6.24+0.619LogL	6.5	ERR	ERR	0.293
Rupture area (Wyss, 1979)	All	Ms>5.6	Ms=4.15+LogA	5.9	ERR	ERR	0.3
(WCC, 1982)	All	4<Ms<6, A>5	Ms=4.257+0.656LogA	5.4	ERR	ERR	-
Maximum surface displacement (Slemmons, 1982)	N	-	Ms=6.668+0.750LogD	6.7	ERR	ERR	0.340
	R	-	Ms=6.793+1.306LogD	6.8	ERR	ERR	0.374
	SS	-	Ms=6.974+0.804LogD	7.0	ERR	ERR	0.315
(Bonilla and others, 1984)	N	Ms>6.0	Ms=6.81+0.741LogD	6.8	ERR	ERR	0.188
	SS	Ms>6.0	Ms=7.00+0.782LogD	7.0	ERR	ERR	0.331
Slip rate (WWC, 1979)	SS	-	Ms=7.223+1.263LogS	ERR	ERR	ERR	-
Seismic moment (Schwartz et al.,1984)	All	3<Ml<7 5<Ms<7.5 Mm>7.5	Mm=2/3logMo-10.7 Mo=ADu	5.9	ERR	ERR	0.24
MEAN				6.0	ERR	ERR	
MAXIMUM				6.8	ERR	ERR	
MINIMUM				5.4	ERR	ERR	

TABLE B-3

	Probability that the Given				
	Feature Exhibits a Given				
	Level of Each Characteristic				
Physical Characteristic	*Feature #1*	*Feature #2*	*Feature #3*	*Feature #4*	*Feature #5*
	Sand Tank	*Santa Rita*	*Sugar Loaf*	*Carefree*	*Tonto Basin*
1. Spatial association between fault and/or					
volcanic sources and seismicity.					
a. Moderate to large earthquakes	0.00	0.00	0.00	0.15	0.15
b. Small earthquakes only	0.10	0.10	0.30	0.70	0.70
c. No seismicity	0.90	0.90	0.70	0.15	0.15
Subtotal (Sum to 1.0)	1.00	1.00	1.00	1.00	1.00
2. Geologic evidence of surface rupture					
a. Holocene movements (one or more)	0.50	0.00	0.50	0.10	0.10
b. Late Quat. movements (multiple)	0.50	1.00	0.50	0.90	0.90
c. No Quaternary movement	0.00	0.00	0.00	0.00	0.00
Subtotal (Sum to 1.0)	1.00	1.00	1.00	1.00	1.00
3. Geometry of feature relative to stress					
orientation and/or sense of slip					
a. Favorable geometry/sense of slip	0.50	0.30	1.00	0.90	0.90
b. Ambiguous geometry/sense of slip	0.50	0.70	0.00	0.10	0.10
c. Unfavorable geometry/sense of slip	0.00	0.00	0.00	0.00	0.00
Subtotal (Sum to 1.0)	1.00	1.00	1.00	1.00	1.00
4. Confidence in Quality of Information					
a. Specific Investigations on Source	1.00	1.00	0.20	0.10	0.20
b. Good regional information only	0.00	0.00	0.70	0.30	0.70
c. General information only	0.00	0.00	0.10	0.60	0.10
Subtotal (Sum to 1.0)	1.00	1.00	1.00	1.00	1.00
Overall Probability of Activity					
a. Category - High	0.50	0.33	0.43	0.31	0.34
b. Category - Moderate	0.28	0.45	0.38	0.50	0.60
c. Category - Low	0.23	0.23	0.20	0.19	0.06
Probability of Activity (High + Moderate Scores	0.78	0.78	0.80	0.81	0.94

TABLE B-3 (Cont'd)

	Probability that the Given				
	Feature Exhibits a Given				
	Level of Each Characteristic				
Physical Characteristic	*Feature #6*	*Feature #7*	*Feature #8*	*Feature #9*	*Feature #10*
	Horseshoe D	*Turret Peak*	*Verde*	*Prescott V.*	*Williamson*
1. Spatial association between fault and/or					
volcanic sources and seismicity.					
a. Moderate to large earthquakes	0.00	0.00	0.30	0.15	0.15
b. Small earthquakes only	0.50	0.50	0.50	0.70	0.70
c. No seismicity	0.50	0.50	0.20	0.15	0.15
Subtotal (Sum to 1.0)	1.00	1.00	1.00	1.00	1.00
2. Geologic evidence of surface rupture					
a. Holocene movements (one or more)	0.10	0.00	0.50	0.00	0.00
b. Late Quat. movements (multiple)	0.90	0.50	0.50	0.50	0.50
c. No Quaternary movement	0.00	0.50	0.00	0.50	0.50
Subtotal (Sum to 1.0)	1.00	1.00	1.00	1.00	1.00
3. Geometry of feature relative to stress					
orientation and/or sense of slip					
a. Favorable geometry/sense of slip	1.00	1.00	1.00	1.00	1.00
b. Ambiguous geometry/sense of slip	0.00	0.00	0.00	0.00	0.00
c. Unfavorable geometry/sense of slip	0.00		0.00	0.00	0.00
Subtotal (Sum to 1.0)	1.00	1.00	1.00	1.00	1.00
4. Confidence in Quality of Information					
a. Specific Investigations on Source	1.00	0.10	0.20	0.10	0.10
b. Good regional information only	0.00	0.40	0.70	0.40	0.40
c. General information only	0.00	0.50	0.10	0.50	0.50
Subtotal (Sum to 1.0)	1.00	1.00	1.00	1.00	1.00
Overall Probability of Activity					
a. Category - High	0.53	0.28	0.50	0.31	0.31
b. Category - Moderate	0.35	0.35	0.43	0.40	0.40
c. Category - Low	0.13	0.38	0.08	0.29	0.29
Probability of Activity (High + Moderate Scores	0.88	0.63	0.93	0.71	0.71

TABLE B-3 (Cont'd)

	Probability that the Given				
	Feature Exhibits a Given				
	Level of Each Characteristic				
Physical Characteristic	*Feature #11*	*Feature #12*	*Feature #13*	*Feature #14*	*Feature #15*
	Chavez Mtn.	*Lake Mary*	*Munds Park*	*Big Chino*	*Mesa Butte*
1. Spatial association between fault and/or					
volcanic sources and seismicity.					
a. Moderate to large earthquakes	0.10	0.10	0.10	0.10	0.75
b. Small earthquakes only	0.60	0.60	0.60	0.80	0.25
c. No seismicity	0.30	0.30	0.30	0.10	0.00
Subtotal (Sum to 1.0)	1.00	1.00	1.00	1.00	1.00
2. Geologic evidence of surface rupture					
a. Holocene movements (one or more)	0.00	0.00	0.00	1.00	0.10
b. Late Quat. movements (multiple)	0.70	0.70	0.70	0.00	0.90
c. No Quaternary movement	0.30	0.30	0.30	0.00	0.00
Subtotal (Sum to 1.0)	1.00	1.00	1.00	1.00	1.00
3. Geometry of feature relative to stress					
orientation and/or sense of slip					
a. Favorable geometry/sense of slip	1.00	1.00	1.00	1.00	0.00
b. Ambiguous geometry/sense of slip	0.00	0.00	0.00	0.00	0.50
c. Unfavorable geometry/sense of slip	0.00	0.00	0.00	0.00	0.50
Subtotal (Sum to 1.0)	1.00	1.00	1.00	1.00	1.00
4. Confidence in Quality of Information					
a. Specific Investigations on Source	0.10	0.10	0.10	1.00	0.30
b. Good regional information only	0.40	0.40	0.40	0.00	0.60
c. General information only	0.50	0.50	0.50	0.00	0.10
Subtotal (Sum to 1.0)	1.00	1.00	1.00	1.00	1.00
Overall Probability of Activity					
a. Category - High	0.30	0.30	0.30	0.78	0.29
b. Category - Moderate	0.43	0.43	0.43	0.20	0.56
c. Category - Low	0.28	0.28	0.28	0.03	0.15
Probability of Activity (High + Moderate Scores	0.73	0.73	0.73	0.98	0.85

TABLE B-3 (Cont'd)

	Probability that the Given				
	Feature Exhibits a Given				
	Level of Each Characteristic				
Physical Characteristic	*Feature #16*	*Feature #17*	*Feature #18*	*Feature #19*	*Feature #20*
	Bright Angel	*Aubrey*	*Toroweap*	*Hurricane*	*Pinto Mtn.*
1. Spatial association between fault and/or					
volcanic sources and seismicity.					
a. Moderate to large earthquakes	0.75	0.00	0.10	0.10	1.00
b. Small earthquakes only	0.25	0.80	0.90	0.90	0.00
c. No seismicity	0.00	0.20	0.00	0.00	0.00
Subtotal (Sum to 1.0)	1.00	1.00	1.00	1.00	1.00
2. Geologic evidence of surface rupture					
a. Holocene movements (one or more)	0.00	0.00	1.00	0.20	1.00
b. Late Quat. movements (multiple)	0.50	0.80	0.00	0.80	0.00
c. No Quaternary movement	0.50	0.20	0.00	0.00	0.00
Subtotal (Sum to 1.0)	1.00	1.00	1.00	1.00	1.00
3. Geometry of feature relative to stress					
orientation and/or sense of slip					
a. Favorable geometry/sense of slip	0.00	1.00	1.00	1.00	1.00
b. Ambiguous geometry/sense of slip	0.50	0.00	0.00	0.00	0.00
c. Unfavorable geometry/sense of slip	0.50	0.00	0.00	0.00	0.00
Subtotal (Sum to 1.0)	1.00	1.00	1.00	1.00	1.00
4. Confidence in Quality of Information					
a. Specific Investigations on Source	0.30	0.30	1.00	0.80	0.40
b. Good regional information only	0.50	0.60	0.00	0.20	0.60
c. General information only	0.20	0.10	0.00	0.00	0.00
Subtotal (Sum to 1.0)	1.00	1.00	1.00	1.00	1.00
Overall Probability of Activity					
a. Category - High	0.26	0.33	0.78	0.53	0.85
b. Category - Moderate	0.44	0.55	0.23	0.48	0.15
c. Category - Low	0.30	0.13	0.00	0.00	0.00
Probability of Activity (High + Moderate Scores	0.70	0.88	1.00	1.00	1.00

TABLE B-3 (Cont'd)

	Probability that the Given				
	Feature Exhibits a Given				
	Level of Each Characteristic				
Physical Characteristic	*Feature #21*	*Feature #22*	*Feature #23*		
	Blue Cut	*San Andreas*	*Gila Mtn.*	*Pinacate V.F.*	
1. Spatial association between fault and/or					
volcanic sources and seismicity.					
a. Moderate to large earthquakes	1.00	1.00	0.00	0.20	0.00
b. Small earthquakes only	0.00	0.00	0.50	0.60	0.00
c. No seismicity	0.00	0.00	0.50	0.20	0.00
Subtotal (Sum to 1.0)	1.00	1.00	1.00	1.00	0.00
2. Geologic evidence of surface rupture or erupt.					
a. Holocene movements/erupts (one or more)	0.10	1.00	0.00	1.00	0.00
b. Late Quat. movements/erupts (multiple)	0.90	0.00	0.50	0.00	0.00
c. No Quaternary movement/eruptions	0.00	0.00	0.50	0.00	0.00
Subtotal (Sum to 1.0)	1.00	1.00	1.00	1.00	0.00
3. Geometry of feature relative to stress					
orientation and/or sense of slip					
a. Favorable geometry/sense of slip	1.00	1.00	1.00	0.30	0.00
b. Ambiguous geometry/sense of slip	0.00	0.00	0.00	0.40	0.00
c. Unfavorable geometry/sense of slip	0.00	0.00	0.00	0.30	0.00
Subtotal (Sum to 1.0)	1.00	1.00	1.00	1.00	0.00
4. Confidence in Quality of Information					
a. Specific Investigations on Source	0.40	1.00	0.10	0.20	0.00
b. Good regional information only	0.60	0.00	0.30	0.00	0.00
c. General information only	0.00	0.00	0.60	0.80	0.00
Subtotal (Sum to 1.0)	1.00	1.00	1.00	1.00	0.00
Overall Probability of Activity					
a. Category - High	0.63	1.00	0.28	0.43	#NUM!
b. Category - Moderate	0.38	0.00	0.33	0.25	#NUM!
c. Category - Low	0.00	0.00	0.40	0.33	#NUM!
Probability of Activity (High + Moderate Scores	1.00	1.00	0.60	0.68	#NUM!

ANNUAL RATE/MAGNITUDE CURVE

SONORAN DESERT B/R (STOVER)

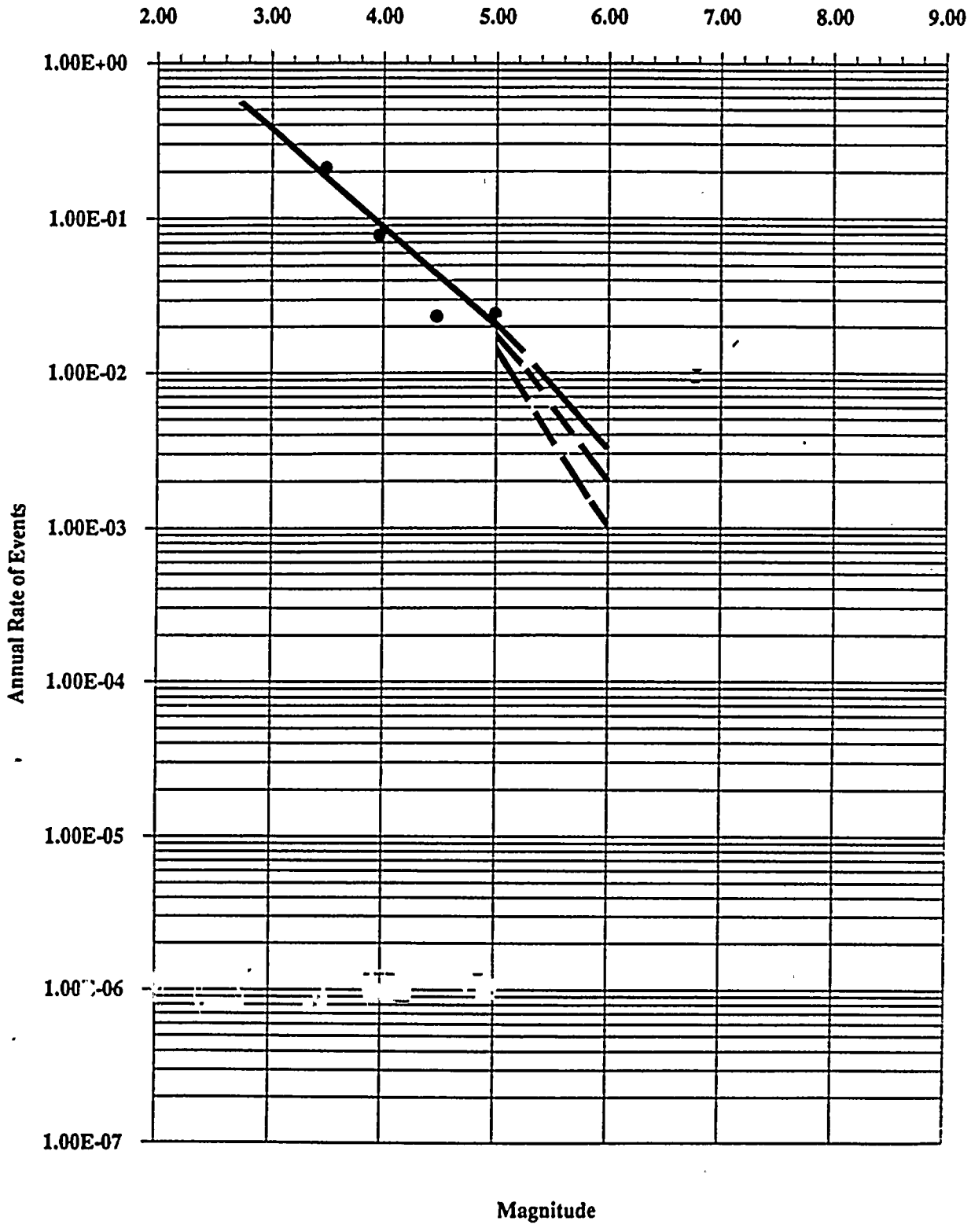

FIGURE B-3

ANNUAL RATE/MAGNITUDE CURVE

SONORAN DESERT B/R (DNAG)

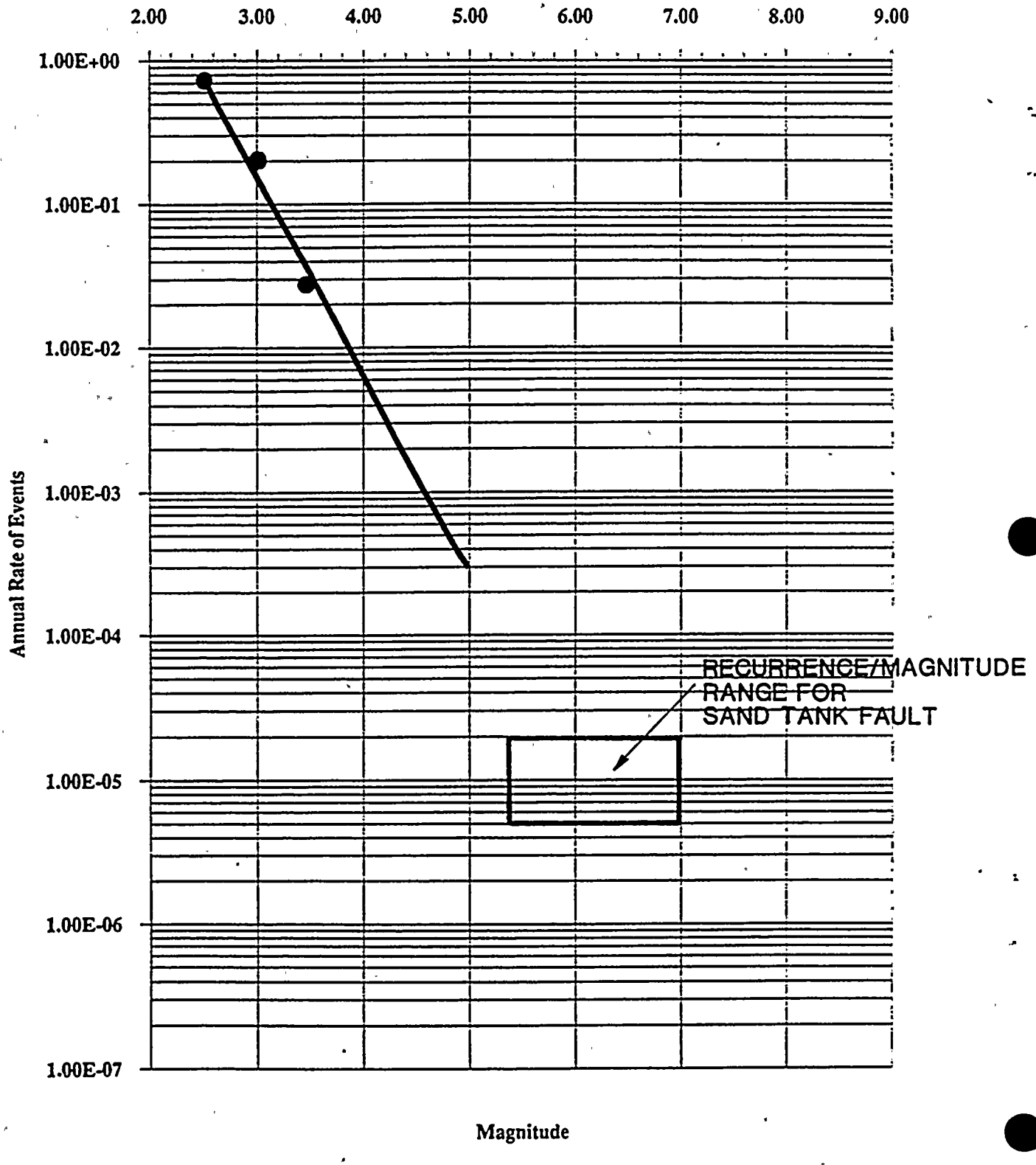

FIGURE B-4

ANNUAL RATE/MAGNITUDE CURVE

SALTON TROUGH (DNAG)

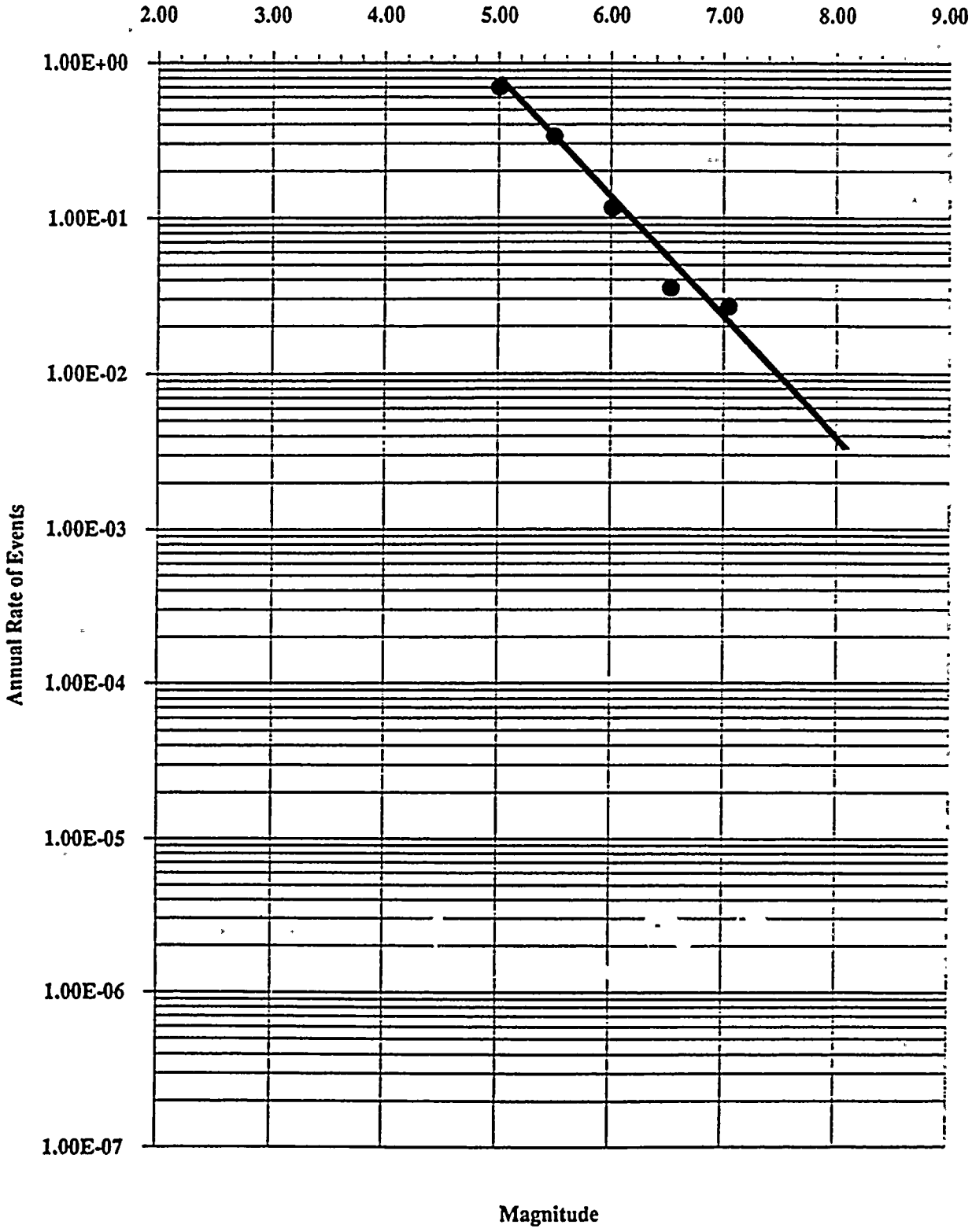

FIGURE B-5

ANNUAL RATE/MAGNITUDE CURVE

EAST TRANSVERSE RANGES (DNAG)

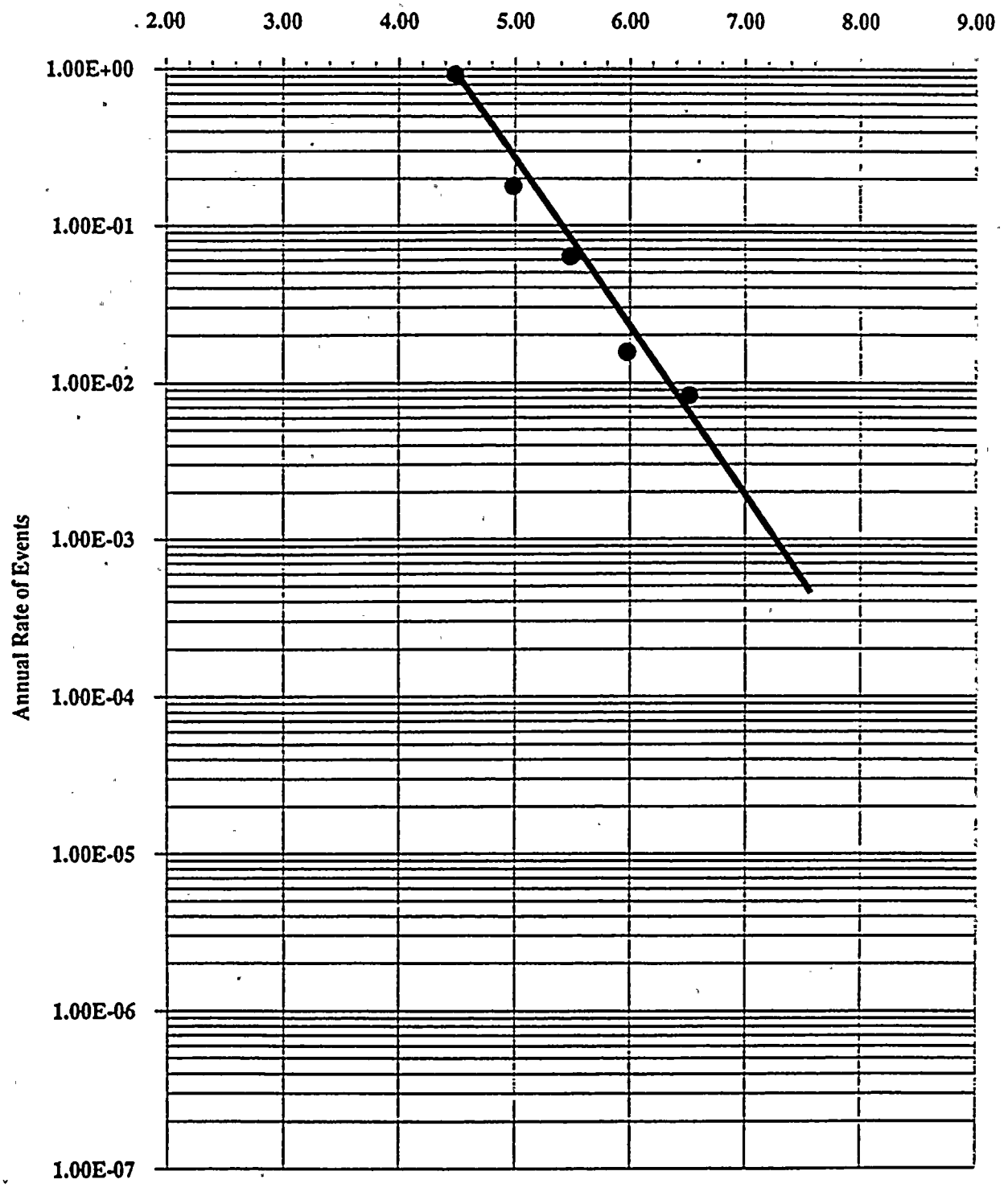

FIGURE B-6

ANNUAL RATE/MAGNITUDE CURVE

BLUE CUT F.Z. (DNAG)

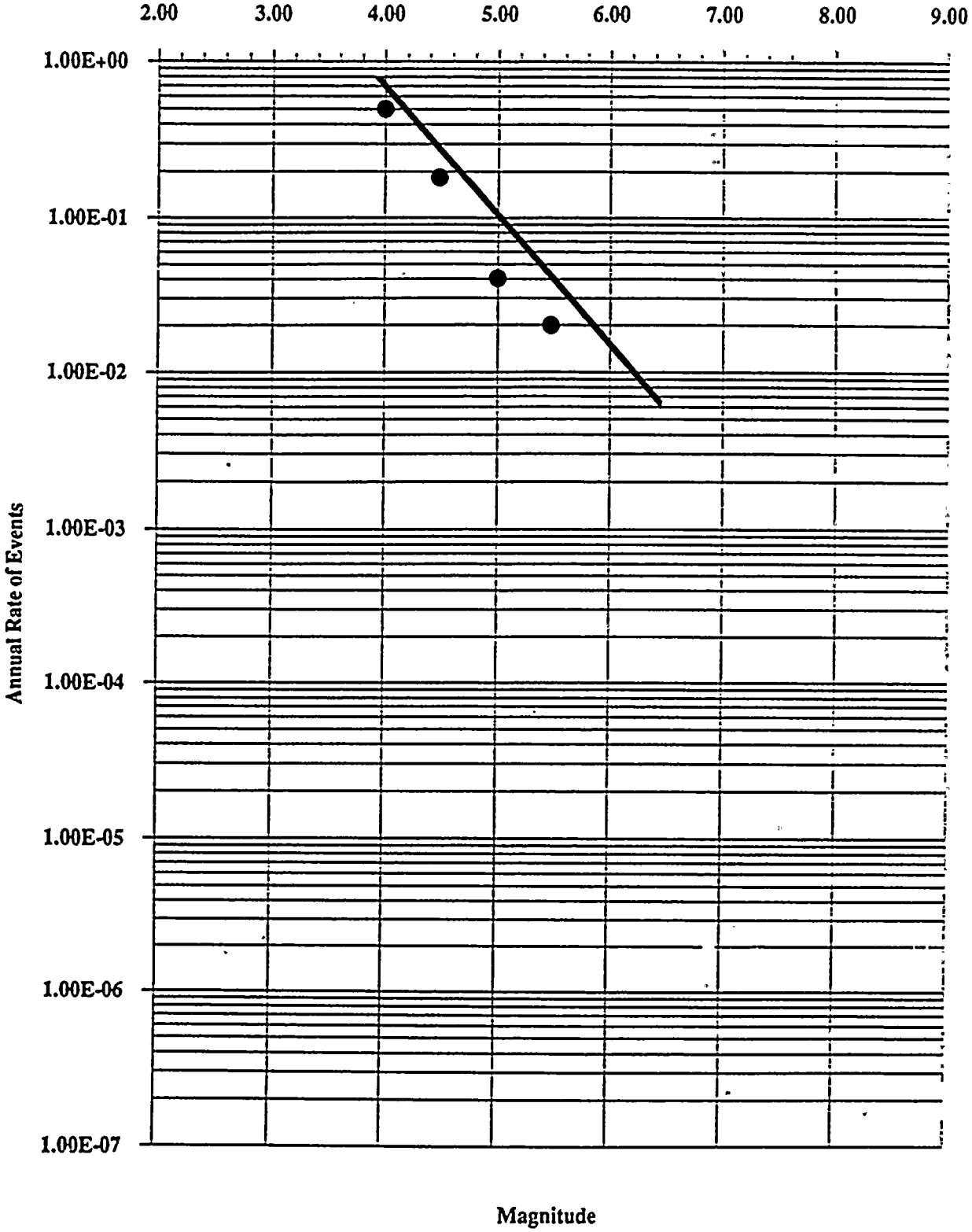

FIGURE B-7

ANNUAL RATE/MAGNITUDE CURVE

MOJAVE BASIN AND RANGE (DNAG)

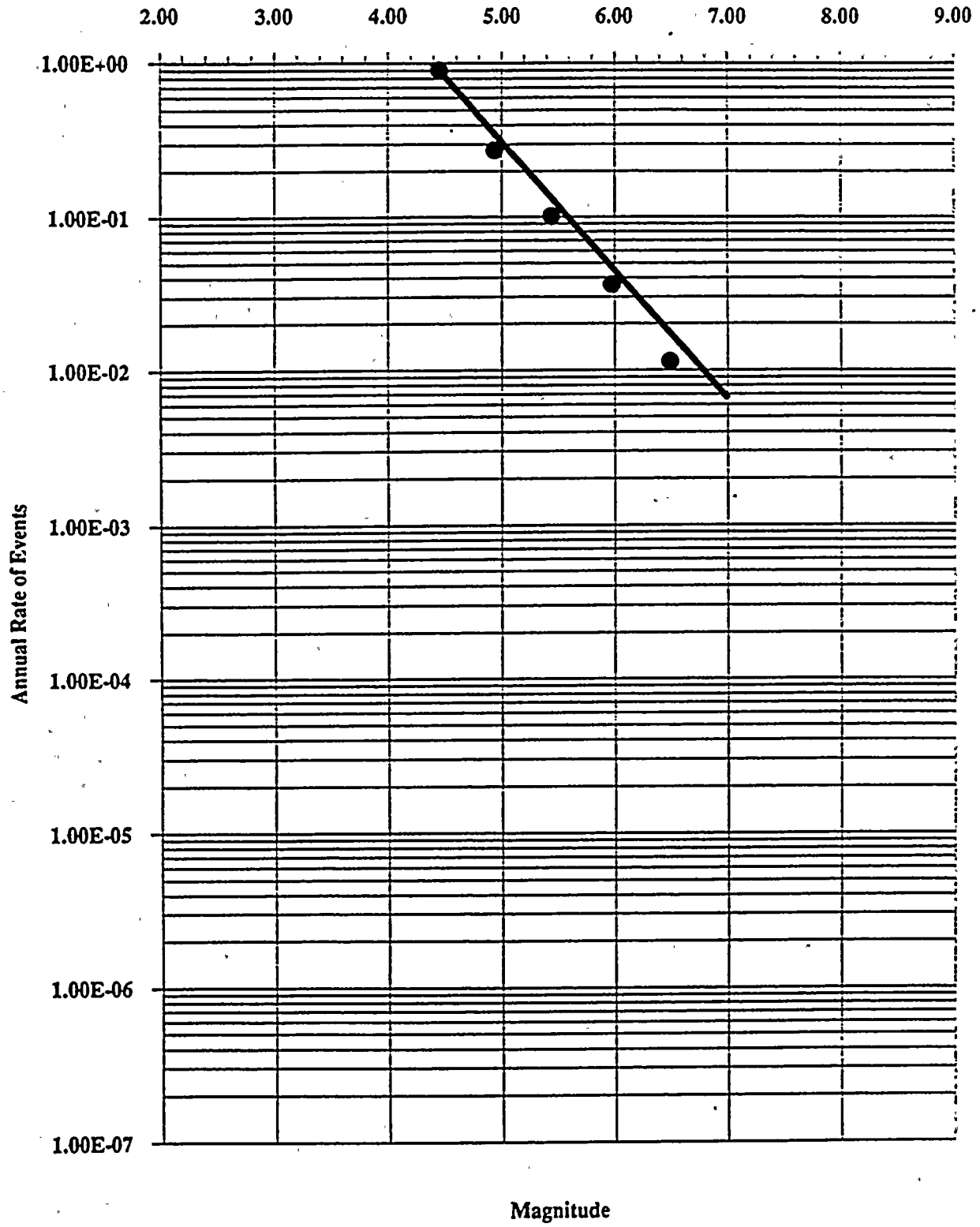

FIGURE B-8

ANNUAL RATE/MAGNITUDE CURVE

LAKE MEAD BASIN AND RANGE (DNAG)

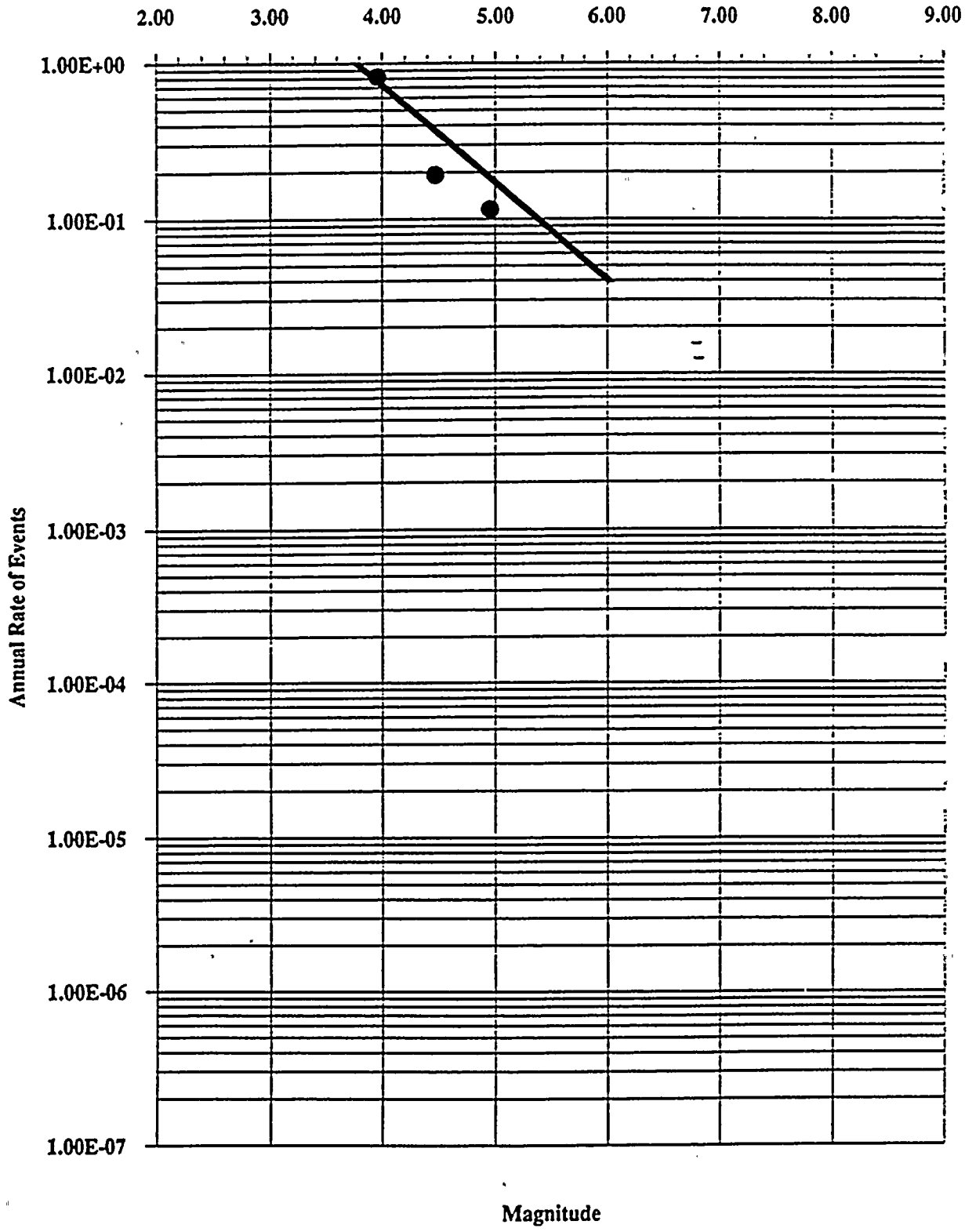

FIGURE B-9

ANNUAL RATE/MAGNITUDE CURVE

ARIZONA MOUNTAINS (STOVER)

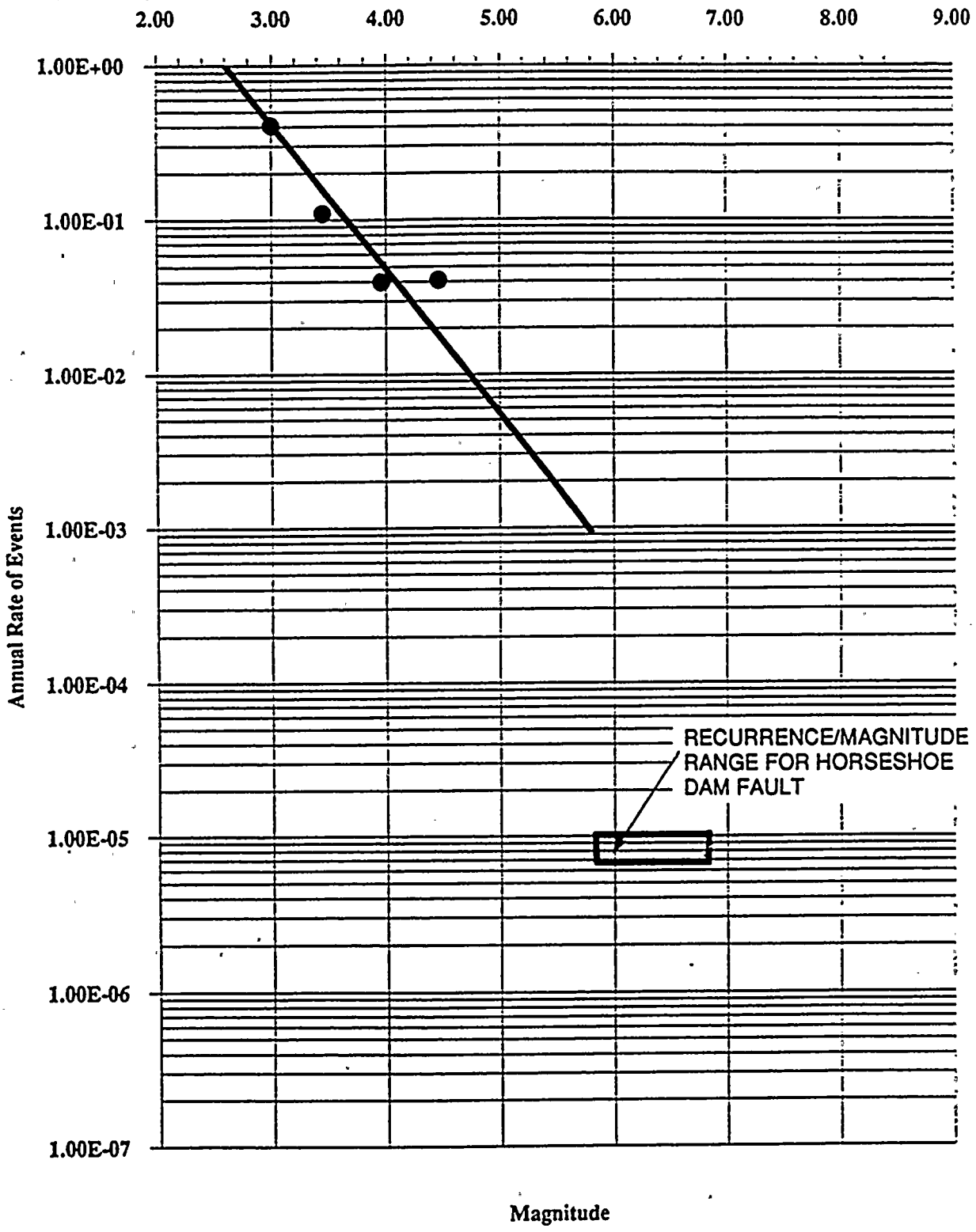

FIGURE B-10

ANNUAL RATE/MAGNITUDE CURVE

HURRICANE-TOROWEAP F.Z. (STOVER)

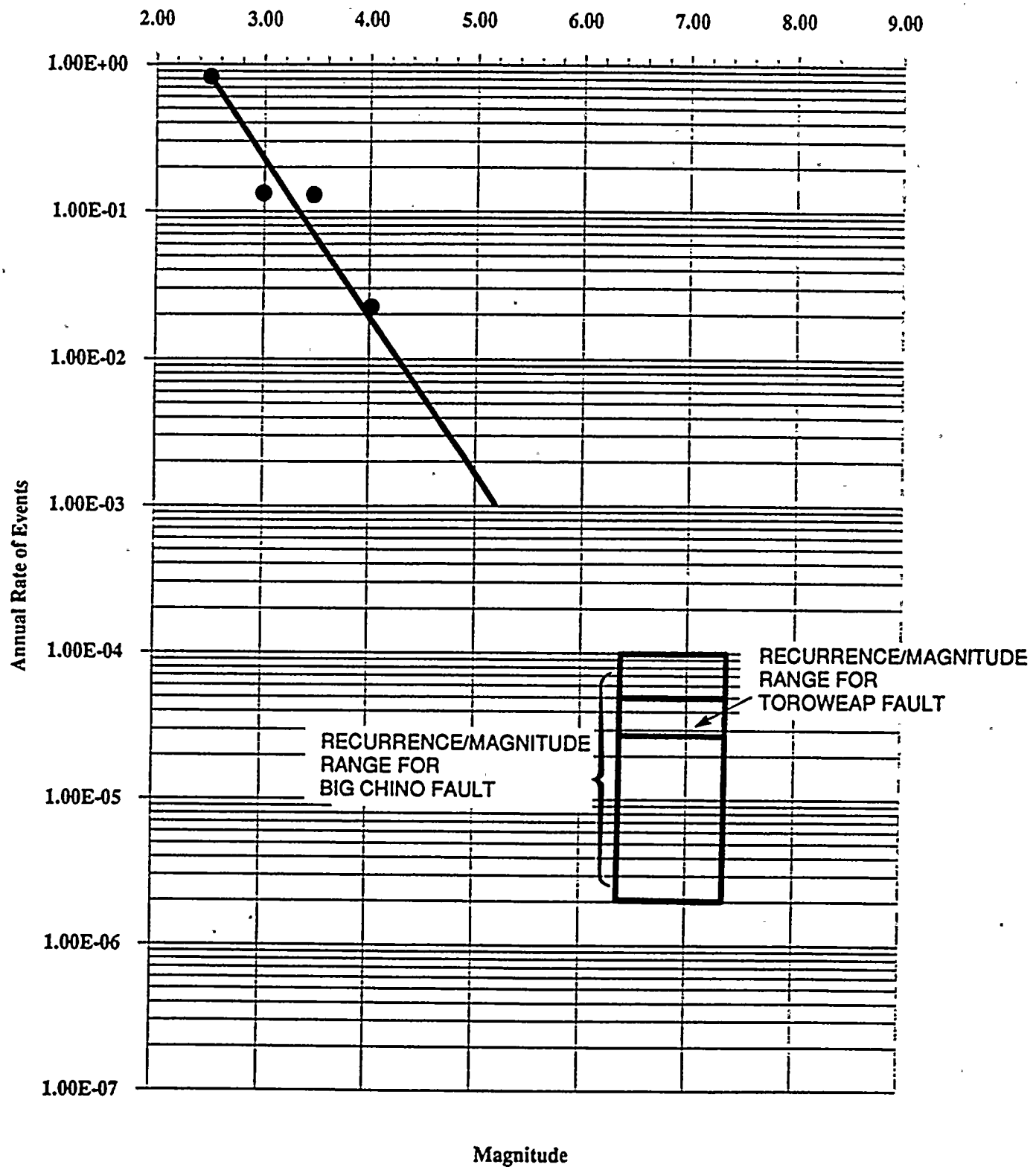

FIGURE B-11

ANNUAL RATE/MAGNITUDE CURVE

MESA BUTTE F.Z. (DNAG)

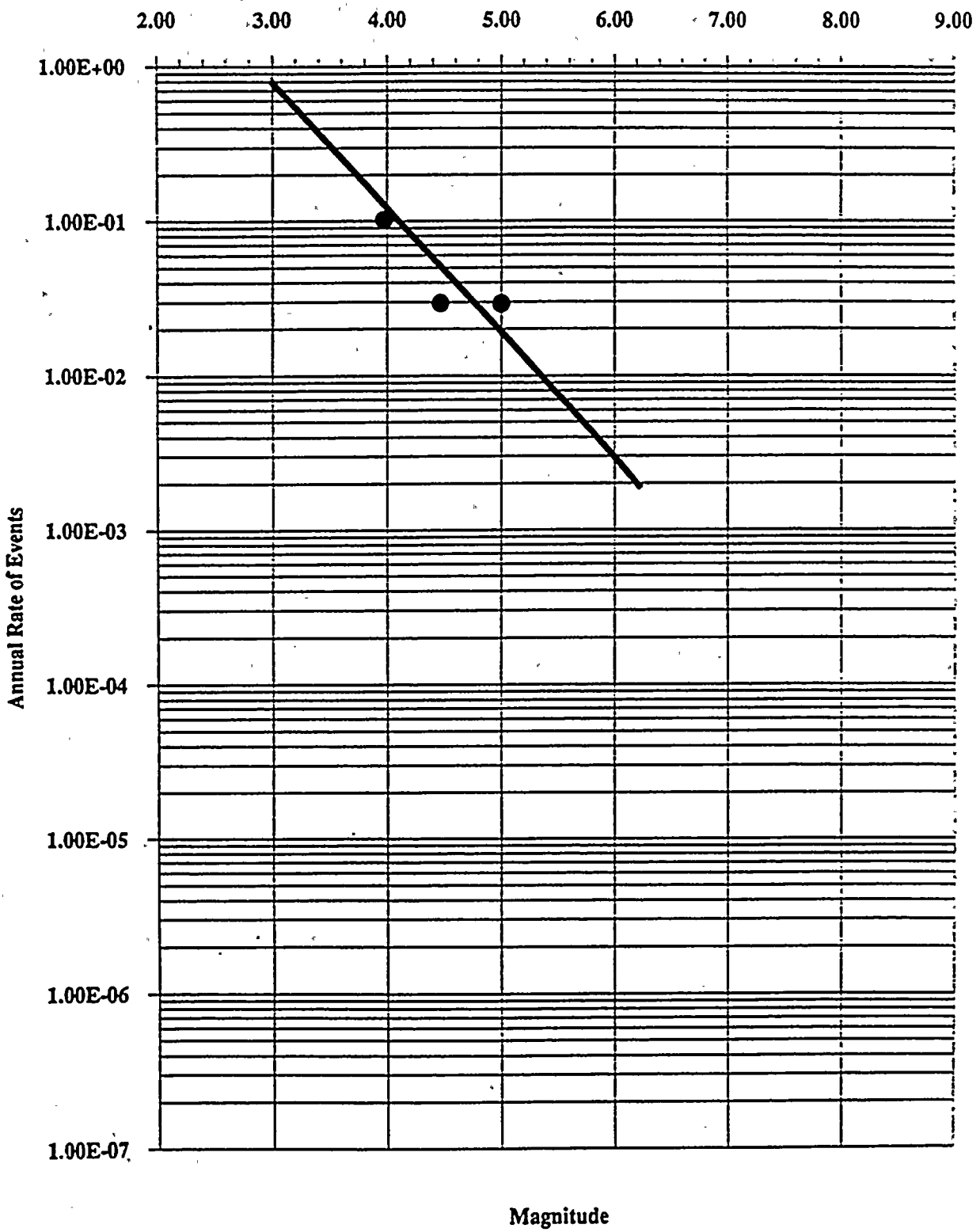

FIGURE B-12

ANNUAL RATE/MAGNITUDE CURVE

SAN FRANCISCO VOLCANIC FIELD (STOVER)

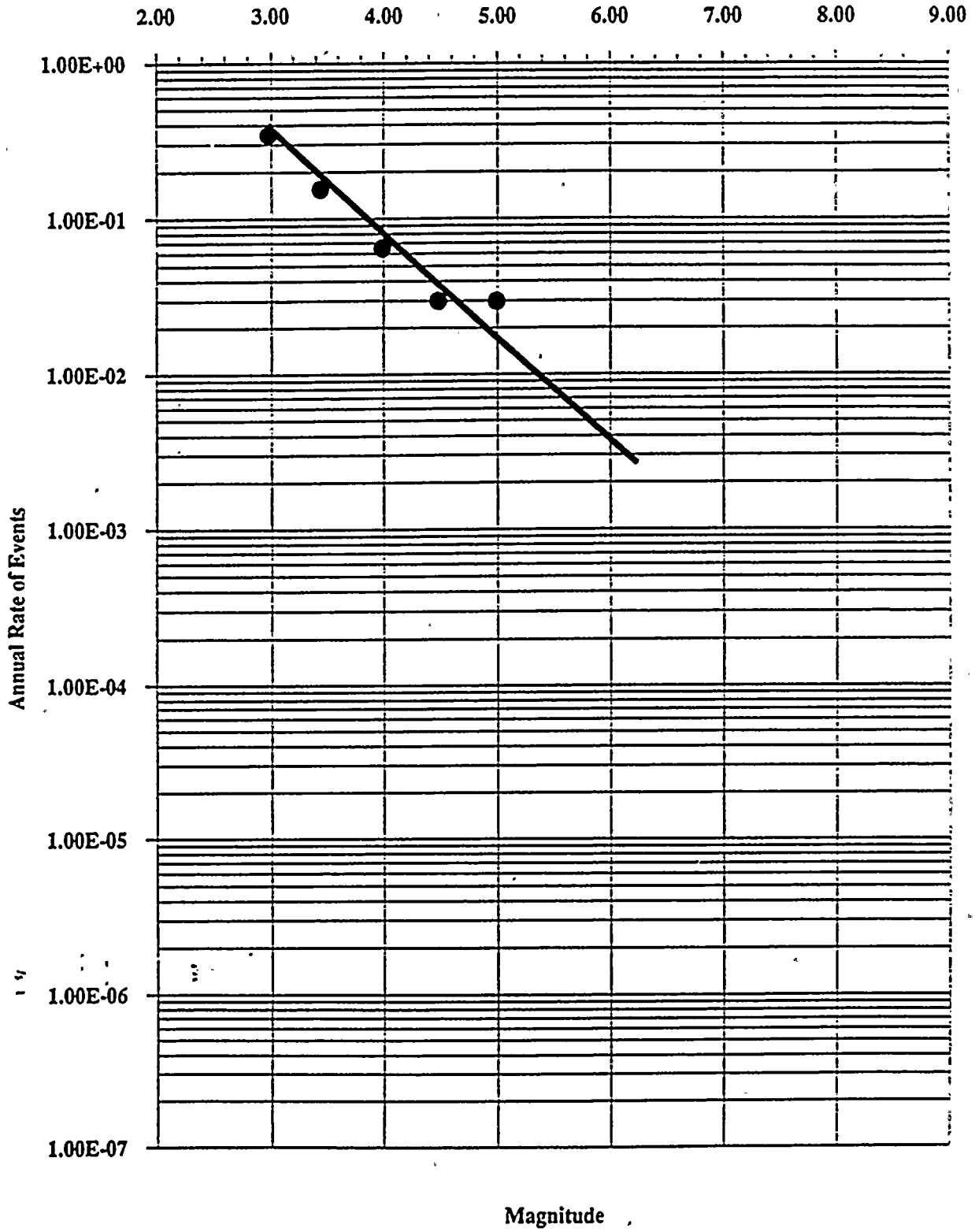

FIGURE B-13

ANNUAL RATE/MAGNITUDE CURVE

COLORADO PLATEAU (STOVER)

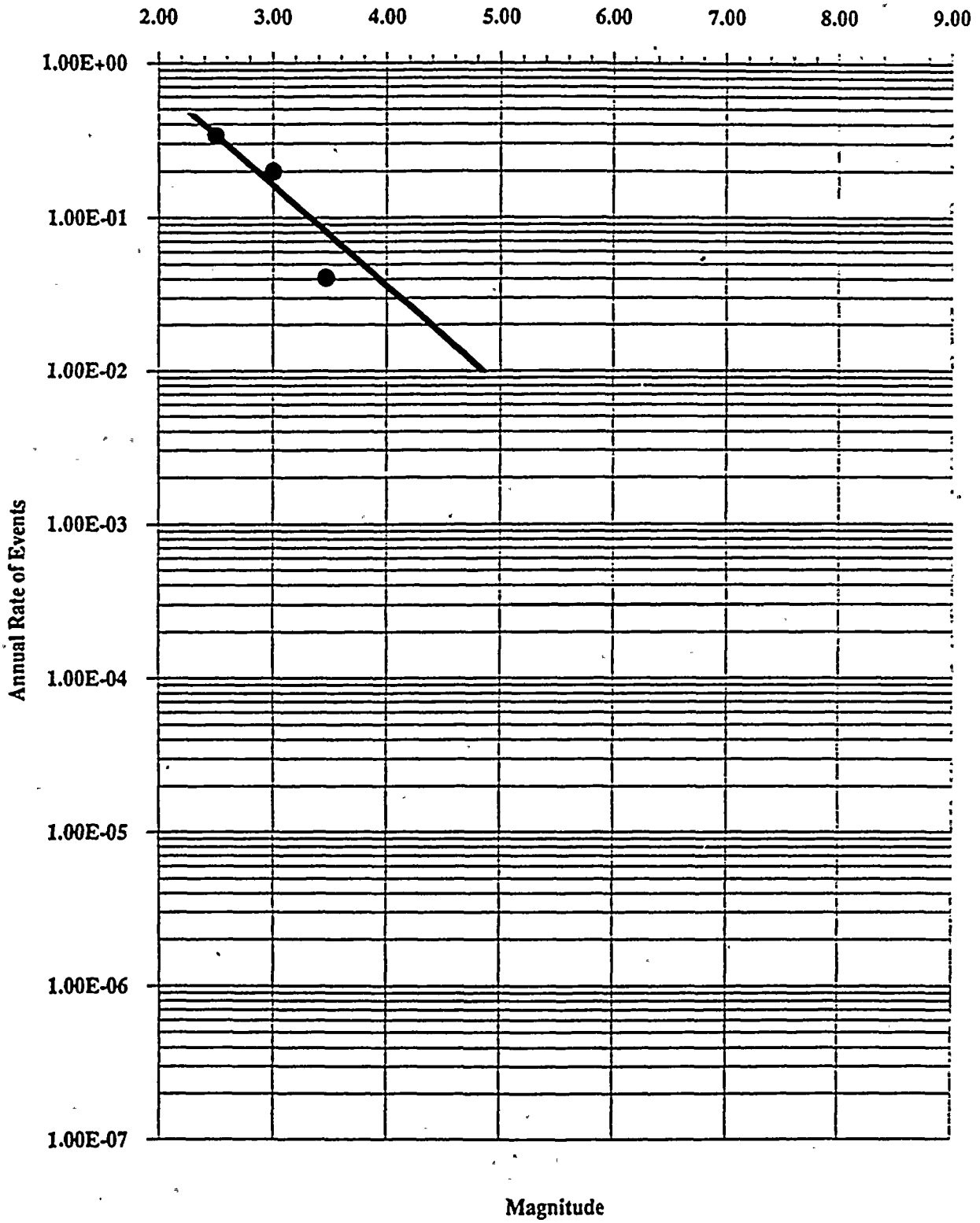

FIGURE B-14

PVNGS SUMMARY SHEET #1

TABLE B-4

FAULT OR SEISMIC SOURCE	SEISMIC	DISTANCE	PROB OF ACTIVITY		MAXIMUM	MAG	ACT	b-VALUE	WEIGHT	COMMENTS
Name and Number	ZONE	TO	FAULT	SCENARIO	MAGNITUDE	WEIGHT	RATE			
		SITE (km)			(Ms)		(yr)			
Sand Tank Fault #1	Sonoran Desert B/R	55	0.78	P-1 (0.85)	5.4	0.30	0.0003	1.3623	0.30	P-1 and P-2 are mutually exclusive.
					6.2	0.60	0.0003	1.3623	0.60	Fault#1 is an independent event.
					7.0	0.10	0.0003	1.3623	0.10	Mutually exclusive to background
				P-2 (0.15)	5.9	0.60	0.0003	1.3623	0.60	seismicity for Sonoran Desert B/R
					6.5	0.30	0.0003	1.3623	0.30	
					6.8	0.10	0.0003	1.3623	0.10	
Santa Rita Fault #2	Mexican B/R	255	0.78	P-1 (0.3)	6.0	0.25	0.0045	0.9886	0.25	P-1 and P-2 aare mutually exclusive
					6.8	0.50	0.0045	0.9886	0.50	Fault #2 is an independent event.
					7.2	0.25	0.0045	0.9886	0.25	Mutually exclusive to the
				P-2 (0.7)	5.7	0.25	0.0045	0.9886	0.25	background seismicity for the
					6.2	0.50	0.0045	0.9886	0.50	Mexican B/R zone.
					6.6	0.25	0.0045	0.9886	0.25	
Sugarloaf Peak Fault #3	Arizona Mountains	130	0.80	P-1 (1.0)	5.7	0.50	0.0045	0.9886	0.50	Fault #3 is an independent event.
					6.3	0.30	0.0045	0.9886	0.30	Mutually exclusive to background
					6.7	0.20	0.0045	0.9886	0.20	seismicity of Arizona Mountains.
Carefree Fault #4	Arizona Mountains	105	0.81	P-1 (0.7)	5.5	0.25	0.0045	0.9886	0.25	P-1 and P-2 are mutually exclusive
					6.3	0.55	0.0045	0.9886	0.55	Fault #4 is an independent event.
					6.8	0.20	0.0045	0.9886	0.20	Mutually exclusive to background
				P-2 (0.3)	5.6	0.25	0.0045	0.9886	0.25	seismicity of Arizona Mountains.
					6.2	0.65	0.0045	0.9886	0.65	
					6.8	0.10	0.0045	0.9886	0.10	
Tonto Basiin Fault #5	Arizona Mountains	150	0.94	P-1 (0.5)	6.0	0.15	0.0045	0.9886	0.15	P-1 and P-2 are mutually exclusive
					6.6	0.55	0.0045	0.9886	0.55	Fault #5 is an independent event.
					6.8	0.30	0.0045	0.9886	0.30	Mutually exclusive to background
				P-2 (0.5)	5.9	0.15	0.0045	0.9886	0.15	seismicity of Arizona Mountains.
					6.4	0.55	0.0045	0.9886	0.55	
					6.7	0.30	0.0045	0.9886	0.30	

PVNGS SUMMARY SHEET #2

TABLE B-4 (Cont'd)

FAULT OR SEISMIC SOURCE Name and Number	SEISMIC ZONE	DISTANCE TO SITE (km)	PROB OF ACTIVITY FAULT	PROB OF ACTIVITY SCENARIO	MAXIMUM MAGNITUDE (Ms)	MAG WEIGHT	ACT RATE (yr)	b-VALUE	WEIGHT	COMMENTS
Horseshoe Dam Fault #6	Arizona Mountains	65	0.88	P-1 (1.0)	5.8	0.15	0.0045	0.9886	0.15	Fault #6 is an independent event.
					6.4	0.60	0.0045	0.9886	0.60	Mutually exclusive to background
					6.8	0.25	0.0045	0.9886	0.25	seismicity of Arizona Mountains.
Turret Peak Fault #7	Arizona Mountains	135	0.68	P-1 (1.0)	5.8	0.25	0.0045	0.9886	0.25	Fault #7 is an independent event.
					6.4	0.60	0.0045	0.9886	0.60	Mutually exclusive to background
					6.8	0.15	0.0045	0.9886	0.15	seismicity of Arizona Mountains.
Verde Fault #8	Arizona Mountains	140	0.93	P-1 (0.3)	6.3	0.10	0.0045	0.9886	0.10	5464646
					6.9	0.50	0.0045	0.9886	0.50	Fault #8 is an independent event.
					7.2	0.40	0.0045	0.9886	0.40	Mutually exclusive to background
				P-2 (0.7)	6.2	0.10	0.0045	0.9886	0.10	seismicity of Arizona Mountains.
					6.7	0.40	0.0045	0.9886	0.40	
					7.1	0.50	0.0045	0.9886	0.50	
Prescott Valley Fault #9	Arizona Mountains	145	0.71	P-1 (1.0)	5.6	0.35	0.0045	0.9886	0.35	Fault #9 is an independent event.
					6.2	0.50	0.0045	0.9886	0.50	Mutually exclusive to background
					6.8	0.15	0.0045	0.9886	0.15	seismicity of Arizona Mountains.
Williamson Valley Fault #10	Arizona Mountains	150	0.71	P-1 (1.0)	5.5	0.35	0.0045	0.9886	0.35	Fault #10 is an independent event.
					6.1	0.50	0.0045	0.9886	0.50	Mutually exclusive to background
					6.8	0.15	0.0045	0.9886	0.15	seismicity of Arizona Mountains.
Chavez Mountain Fault #11	San Francisco V.F.	220	0.73	P-1 (0.5)	6.2	0.40	0.0173	0.7924	0.40	P-1 and P-2 are mutually exclusive.
					6.8	0.50	0.0173	0.7924	0.50	Fault #11 is an independent event.
					7.1	0.10	0.0173	0.7924	0.10	Mutually exclusive to background
				P-2 (0.5)	6.1	0.35	0.0173	0.7924	0.35	seismicity of San Francisco VF.
					6.6	0.55	0.0173	0.7924	0.55	
					7.0	0.10	0.0173	0.7924	0.10	

PVNGS SUMMARY SHEET #3

TABLE B-4 (Cont'd)

FAULT OR SEISMIC SOURCE	SEISMIC	DISTANCE	PROB OF ACTIVITY		MAXIMUM	MAG	ACT	b-VALUE	WEIGHT	COMMENTS
Name and Number	ZONE	TO	FAULT	SCENARIO	MAGNITUDE	WEIGHT	RATE			
		SITE (km)			(Ms)		(yr)			
Lake Mary/Mormon Lake Fault #12	San Francisco V.F.	220	0.73	P-1 (0.5)	6.1	0.35	0.0173	0.7924	0.35	P-1 and P-2 are mutually exclusive.
					6.6	0.55	0.0173	0.7924	0.55	Fault #12 is an independent event.
					7.0	0.10	0.0173	0.7924	0.10	Mutually exclusive to background
				P-2 (0.5)	6.1	0.35	0.0173	0.7924	0.35	seismicity of San Francisco VF.
					6.6	0.55	0.0173	0.7924	0.55	
					7.0	0.10	0.0173	0.7924	0.10	
Munds Park Fault #13	San Francisco V.F.	210	0.73	P-1 (0.5)	6.1	0.35	0.0173	0.7924	0.35	P-1 and P-2 are mutually exclusive.
					6.6	0.55	0.0173	0.7924	0.55	Fault #14 is an independent event.
					7.0	0.10	0.0173	0.7924	0.10	Mutually exclusive to background
				P-2 (0.5)	6.0	0.35	0.0173	0.7924	0.35	seismicity of San Francisco VF.
					6.5	0.55	0.0173	0.7924	0.55	
					6.9	0.10	0.0173	0.7924	0.10	
Big Chino Fault #14	Hurricane-Wasatch	180	0.98	P-1 (0.5)	6.2	0.10	0.0017	1.0758	0.10	P-1 and P-2 are mutually exclusive.
					6.9	0.40	0.0017	1.0758	0.40	Fault #13 is an independent event.
					7.2	0.50	0.0017	1.0758	0.50	Mutually exclusive to background
				P-2 (0.5)	6.3	0.10	0.0017	1.0758	0.10	seismicity of the Hurricane-Wasatch
					6.9	0.40	0.0017	1.0758	0.40	
					7.3	0.50	0.0017	1.0758	0.50	
Mesa Butte Fault #15	San Francisco V.F.	270	0.85	P-1 (0.3)	6.6	0.50	0.0173	0.7924	0.50	P-1 and P-2 are mutually exclusive.
					7.2	0.40	0.0173	0.7924	0.40	Fault #12 is an independent event.
					7.7	0.10	0.0173	0.7924	0.10	Mutually exclusive to background
				P-2 (0.7)	6.4	0.40	0.0173	0.7924	0.40	seismicity of San Francisco VF.
					6.9	0.50	0.0173	0.7924	0.50	
					7.4	0.10	0.0173	0.7924	0.10	
Bright Angel Fault #16	San Francisco V.F.	295	0.70	P-1 (0.5)	6.4	0.45	0.0173	0.7924	0.45	P-1 and P-2 are mutually exclusive.
					7.0	0.45	0.0173	0.7924	0.45	Fault #12 is an independent event.
					7.5	0.10	0.0173	0.7924	0.10	Mutually exclusive to background
				P-2 (0.5)	6.5	0.45	0.0173	0.7924	0.45	seismicity of San Francisco VF.
					7.1	0.45	0.0173	0.7924	0.45	
					7.6	0.10	0.0173	0.7924	0.10	

PVNGS SUMMARY SHEET #4

TABLE B-4 (Cont'd)

FAULT OR SEISMIC SOURCE	SEISMIC	DISTANCE	PROB OF ACTIVITY		MAXIMUM	MAG	ACT	b-VALUE	WEIGHT	COMMENTS
Name and Number	ZONE	TO	FAULT	SCENARIO	MAGNITUDE	WEIGHT	RATE			
		SITE (km)			(Ms)		(yr)			
Aubrey Fault #17	Hurricane-Wasatch	200	0.88	P-1 (0.5)	6.3	0.10	0.0017	1.0758	0.10	P-1 and P-2 are mutually exclusive.
					6.9	0.50	0.0017	1.0758	0.50	Fault #17 is an independent event.
					7.3	0.40	0.0017	1.0758	0.40	Mutually exclusive to background
				P-2 (0.5)	6.4	0.10	0.0017	1.0758	0.10	seismicity for the Hurricane-Wasatch
					7.0	0.50	0.0017	1.0758	0.50	
					7.4	0.40	0.0017	1.0758	0.40	
Toroweap Fault #18	Hurricane-Wasatch	270	1.00	P-1 (0.3)	6.9	0.25	0.0017	1.0758	0.25	P-1 and P-2 are mutually exclusive.
					7.4	0.70	0.0017	1.0758	0.70	Fault #18 is an independent event.
					8.2	0.05	0.0017	1.0758	0.05	Mutually exclusive to background
				P-2 (0.7)	6.4	0.10	0.0017	1.0758	0.10	seismicity for the Hurricane-Wasatch
					7.0	0.30	0.0017	1.0758	0.30	
					7.4	0.60	0.0017	1.0758	0.60	
Hurricane Fault #19	Hurricane-Wasatch	250	1.00	P-1 (0.3)	6.6	0.10	0.0017	1.0758	0.10	P-1 and P-2 are mutually exclusive.
					7.2	0.50	0.0017	1.0758	0.50	Fault #19 is an independent event.
					7.7	0.40	0.0017	1.0758	0.40	Mutually exclusive to background
				P-2 (0.7)	6.5	0.10	0.0017	1.0758	0.10	seismicity for the Hurricane-Wasatch
					7.1	0.50	0.0017	1.0758	0.50	
					7.6	0.40	0.0017	1.0758	0.40	
Pinto Mountain Fault #20	Transverse Ranges	290	1.00	P-1 (0.2)	6.1	0.10	0.0977	0.8266	0.10	P-1,P-2,P-3 are mutually exclusive.
					6.9	0.55	0.0977	0.8266	0.55	Fault #20 is an independent event.
					7.2	0.35	0.0977	0.8266	0.35	Mutually exclusive to background
				P-2 (0.1)	6.1	0.10	0.0977	0.8266	0.10	seismicity for the Transverse Ranges
					7.1	0.80	0.0977	0.8266	0.80	
					8.1	0.10	0.0977	0.8266	0.10	
				P-3 (0.7)	6.1	0.10	0.0977	0.8266	0.10	
					7.0	0.45	0.0977	0.8266	0.45	
					7.2	0.45	0.0977	0.8266	0.45	

PVNGS SUMMARY SHEET #5

TABLE B-4 (Cont'd)

FAULT OR SEISMIC SOURCE	SEISMIC	DISTANCE	PROB OF ACTIVITY		MAXIMUM	MAG	ACT	b-VALUE	WEIGHT	COMMENTS
Name and Number	ZONE	TO	FAULT	SCENARIO	MAGNITUDE	WEIGHT	RATE			
		SITE (km)			(Ms)		(yr)			
Blue Cut Fault #21	Transverse Ranges	245	1.00	P-1 (1.0)	5.6	0.10	0.0970	0.8266	0.10	Fault #21 is an independent event.
					6.8	0.60	0.0970	0.8266	0.60	Mutually exclusive to background
					7.2	0.30	0.0970	0.8266	0.30	seismicity for the Transverse Ranges
San Andreas Fault #22	Salton Trough	250	1.00	P-1 (0.2)	6.9	0.10	0.7669	0.7748	0.10	P-1,P-2,P-3 are mutually exclusive.
					7.7	0.60	0.7669	0.7748	0.60	For this study, the San Andreas FZ
					8.5	0.30	0.7669	0.7748	0.30	and the Salton Trough Zone aare
				P-1 (0.2)	6.9	0.10	0.7669	0.7748	0.10	considered identical.
					7.9	0.85	0.7669	0.7748	0.85	
					9.2	0.05	0.7669	0.7748	0.05	
				P-1 (0.6)	6.6	0.10	0.7669	0.7748	0.10	
					7.4	0.70	0.7669	0.7748	0.70	
					8.5	0.20	0.7669	0.7748	0.20	
Gila Mountain Fault #23	Sonoran Desert B/R	155	0.60	P-1 (1.0)	5.4	0.40	0.0003	1.3623	0.40	Fault #23 is an independent event.
					6.0	0.55	0.0003	1.3623	0.55	Mutually exclusive to background
					6.8	0.05	0.0003	1.3623	0.05	seismicity for the Sonoran
										Desert B/R.

TABLE B-5

SEISMIC ZONE	DISTANCE TO SITE (km)	RELATION TO SEISMIC SOURCES	MAXIMUM MAGNITUDE (Ms)	MAG WEIGHT	ACT RATE (yr)	b-VALUE	WEIGHT	COMMENTS
Salton Trough	156	Identical	6.9	0.10	0.7669	0.7748	0.10	Salton Trough and San Andreas FZ.
			7.7	0.60	0.7669	0.7748	0.60	are considered the same for this study
			8.5	0.30	0.7669	0.7748	0.30	
Transverse Ranges	191	Default to Background						Mutually exclusive with Faults #20
			6.0	0.40	0.2314	1.0335	0.40	and #21.
			6.5	0.60	0.2314	1.0335	0.60	
Mojave Desert B/R	226	Maximum Event	P-1 (1.0)					Single Regional Source Zone
			6.8	0.30	0.2986	0.8142	0.30	
			7.3	0.70	0.2986	0.8142	0.70	
Lake Mead B/R	280	Maximum Event	P-1 (1.0)					Single Regional Source Zone
			6.8	0.30	0.1677	0.6283	0.30	
			7.3	0.70	0.1677	0.6283	0.70	
Mexican B/R	188	Default to Background						Mutually exclusive with Fault #2
			5.0	0.30	0.0045	0.9886	0.30	
			5.5	0.70	0.0045	0.9886	0.70	
Pinacate V. F.	137	Maximum Event	P-1 (1.0)					Single Regional Source Zone
			5.0	0.30	0.0003	1.3623	0.30	
			5.5	0.70	0.0003	1.3623	0.70	
Arizona Mountains	70	Default to Background						Mutually exclusive with Faults #3,
			5.0	0.30	0.0045	0.9886	0.30	#4, #5, #6, #7, #8, #9, and #10.
			5.5	0.70	0.0045	0.9886	0.70	
Hurricane/Wasatch	178	Default to Background						Mutually exclusive with Faults #14,
			6.0	0.40	0.0152	0.6102	0.40	#17, #18, and #19.
			7.3	0.60	0.0152	0.6102	0.60	
San Francisco V. F.	180	Default to Background						Mutually exclusive with Faults #11,
			5.5	0.30	0.0172	0.658	0.30	#12, #13, #15, and #16.
			6.0	0.70	0.0172	0.658	0.70	
Colorado Plateau	280	Maximum Event	P-1 (1.0)					Single Regional Source Zone
			5.8	0.50	0.0072	0.672	0.50	
			6.0	0.50	0.0072	0.672	0.50	

Appendix C
SEISMICITY CATALOGS

This appendix contains listings of the DNAG and Stover earthquake catalogs (1,2). Table C–1 contains a listing of the main events in the DNAG catalog. For the sake of brevity, this listing contains only earthquakes with $M > 3$ within 300 km of the PVNGS site, and earthquakes with $M > 5$ within 500 km of the site. The seismicity calculations documented in Section 4 used a wider range of magnitudes and distances; namely, all $M > 2$ events falling within the seismic sources specified by the Teams.

Table C–2 contains a listing of the Stover catalog for Arizona. The earlier events in this catalog do not have assigned magnitudes. For these events, we derived a moment magnitude estimate from epicentral intensity, using the expression $M = 1 + \frac{2}{3}I_0$.

C.1 REFERENCES

1. E. R. Engdahl and W. A. Rinehart. "Seismicity Map of North America". In *Observatory Seismology*, ed. by J. J. Litehiser, Univ. of Calif. Press, Berkeley, Calif., 1989.

2. C. W. Stover, B. G. Reagor, and S. T. Algermissen. *Seismicity Map of the State of Arizona.* Miscellaneous Field Studies Map MF-1852, US Geological Survey, 1986.

TABLE B-5 (Cont'd)

SEISMIC ZONE	DISTANCE TO SITE (km)	RELATION TO SEISMIC SOURCES	MAXIMUM MAGNITUDE (Ms)	MAG WEIGHT	ACT RATE (yr)	b-VALUE	WEIGHT	COMMENTS
Sonoran Desert B/R	8	Default to Background	5.0	0.55	0.0250	0.80	0.10	Mutually exclusive with Faults #1
			5.5	0.40	0.0250	0.80	0.10	and #21.
			6.0	0.05	0.0250	0.80	0.10	
		Default to Background	5.0	0.55	0.0240	0.90	0.35	
			5.5	0.40	0.0240	0.90	0.35	
			6.0	0.05	0.0240	0.90	0.35	
		Default to Background	5.0	0.55	0.0170	1.00	0.45	
			5.5	0.40	0.0170	1.00	0.45	
			6.0	0.05	0.0170	1.00	0.45	
		Default to Background	5.0	0.55	0.0003	1.36	0.10	
			5.5	0.40	0.0003	1.36	0.10	
			6.0	0.05	0.0003	1.36	0.10	

Table C-1

DNAG Earthquake Catalog

Year	Date MM	DD	HH	Lat. Deg(N)	Long. Deg(W)	M
1852	11	29	20	32.500	115.000	6.6
1868	5			33.500	115.500	6.3
1872	5	03	01	33.000	115.000	5.9
1887	5	03	21	31.000	109.000	7.0
1890	2	09	12	33.500	116.500	6.0
1892	2	24	07	32.599	116.300	6.9
1892	5	28	11	33.500	116.000	6.0
1894	10	23	23	32.800	116.500	6.1
1899	12	25	12	33.800	117.000	6.7
1902	12	12	23	29.000	114.000	7.1
1906	4	19	00	32.500	115.500	6.0
1908	11	04	08	36.000	117.000	6.5
1912	8	18	21	36.500	111.500	5.7
1915	6	23	03	32.800	115.500	6.3
1915	6	23	04	32.800	115.500	6.3
1915	11	21	00	32.000	115.000	7.1
1916	11	10	09	35.500	116.000	6.1
1918	4	21	22	33.750	117.000	6.8
1923	11	07	23	31.000	116.000	6.3
1927	1	01	08	32.500	115.500	5.8
1931	10	01	11	30.000	114.500	6.0
1932	7	07	16	29.000	113.000	6.8
1932	12	29	05	32.700	114.600	3.7
1934	5	14	13	31.000	114.500	5.5
1934	11	25	08	32.083	116.666	5.0
1934	12	30	13	32.250	115.500	6.5
1934	12	30	13	31.000	115.000	6.5
1934	12	30	13	32.250	115.500	6.5
1934	12	31	18	32.000	114.750	7.1
1935	1	02	07	32.800	114.200	5.0
1935	1	10	08	36.000	112.100	5.0
1935	2	24	01	31.983	115.200	6.0
1935	2	24	01	31.983	115.200	6.0
1935	4	29	20	31.750	116.500	5.0
1935	9	08	17	32.900	115.216	5.0
1935	10	11	14	32.900	115.216	5.0
1935	10	24	14	34.100	116.800	5.3
1935	12	20	07	33.166	115.500	5.0
1936	4	29	08	31.666	115.083	5.0
1937	2	27	01	31.866	116.566	5.0

DNAG Earthquake Catalog (continued)

1937	3	25	16	33.400	116.250	6.0
1938	6	06	02	32.900	115.216	5.0
1939	2	26	23	33.000	109.000	5.5
1939	5	02	13	29.500	113.800	6.8
1939	5	02	13	29.500	113.800	6.5
1939	5	04	20	35.768	114.785	5.0
1939	9	21	21	30.000	114.000	6.0
1940	5	18	05	34.083	116.300	5.5
1940	5	18	05	34.066	116.333	5.5
1940	5	18	07	34.066	116.333	5.0
1940	5	19	04	32.733	115.500	7.1
1940	5	19	04	32.765	115.483	5.5
1940	5	19	05	32.765	115.483	5.5
1940	5	19	06	32.765	115.483	5.0
1940	5	19	06	32.765	115.483	5.5
1940	5	19	06	32.765	115.483	5.5
1940	6	04	10	33.000	116.433	5.1
1940	7	07	18	31.666	115.083	5.0
1940	12	07	22	31.666	115.083	6.0
1941	1	09	10	31.700	115.100	5.5
1941	2	05	13	31.700	115.100	5.0
1941	4	09	17	31.000	114.000	6.0
1942	3	03	01	34.000	115.750	5.0
1942	5	23	15	32.983	115.983	5.0
1942	9	09	05	36.000	114.700	5.0
1942	10	21	16	32.966	116.000	6.5
1942	10	21	16	32.966	116.000	5.0
1942	10	21	16	32.966	116.000	5.0
1942	10	22	01	33.233	115.716	5.8
1942	10	22	18	32.966	116.000	5.0
1943	8	29	03	34.266	116.966	5.5
1943	12	22	15	34.333	115.800	5.5
1944	6	12	10	33.966	116.716	5.1
1944	6	12	11	33.983	116.700	5.3
1945	1	07	22	36.500	111.800	5.1
1945	3	20	21	34.250	116.166	5.0
1945	5	12	07	31.600	115.600	5.2
1945	8	15	17	33.216	116.133	5.7
1946	1	08	18	33.000	115.833	5.4
1946	7	18	14	34.533	115.983	5.8
1946	9	28	07	33.950	116.850	5.0
1947	4	10	15	34.983	116.550	6.4
1947	4	10	16	34.966	116.550	5.1

DNAG Earthquake Catalog (continued)

1947	4	10	17	34.950	116.533	5.0
1947	4	11	07	34.966	116.550	5.0
1947	7	24	22	34.016	116.500	5.5
1947	7	25	00	34.016	116.500	5.0
1947	7	25	06	34.016	116.500	5.2
1947	7	26	02	34.016	116.500	5.1
1948	12	04	23	33.933	116.383	6.5
1949	5	02	11	34.016	115.683	5.9
1949	9	16	20	31.000	115.000	5.1
1949	11	04	20	32.200	116.550	5.7
1949	11	05	04	32.200	116.550	5.1
1950	1	17	00	35.700	109.500	5.0
1950	7	28	17	33.116	115.566	5.6
1950	7	29	14	33.116	115.566	5.5
1951	1	24	07	32.983	115.733	6.4
1951	9	02	16	31.000	117.000	5.2
1952	2	20	13	36.000	114.700	5.0
1952	5	24	04	35.939	114.732	5.0
1952	10	20	07	36.000	114.800	5.0
1953	5	04	14	32.700	114.600	3.0
1953	6	14	04	32.950	115.716	5.5
1953	10	10	18	31.800	116.100	5.0
1953	10	13	08	30.000	114.000	6.1
1954	2	01	04	32.300	115.300	5.2
1954	2	01	04	32.300	115.300	5.6
1954	2	01	13	32.300	115.300	5.1
1954	3	19	09	33.283	116.183	6.2
1954	3	19	09	33.283	116.183	5.0
1954	3	19	10	33.283	116.183	5.5
1954	3	23	04	33.283	116.183	5.1
1954	4	29	11	29.200	112.800	7.0
1954	5	31	08	31.600	115.200	5.2
1954	10	17	22	31.500	116.500	5.7
1954	10	24	09	31.500	116.000	6.0
1954	10	24	11	31.500	116.000	5.4
1954	11	12	12	31.500	116.000	6.3
1954	11	12	13	31.500	116.000	5.0
1954	11	14	05	31.500	116.000	5.4
1955	4	25	10	32.333	115.000	5.2
1955	11	26	17	31.600	116.100	5.4
1955	12	17	06	33.000	115.500	5.4
1956	2	09	14	31.750	115.916	6.8
1956	2	09	14	31.700	115.900	5.6

DNAG Earthquake Catalog (continued)

1956	2	09	15	31.600	115.700	5.3
1956	2	09	15	31.750	115.916	6.1
1956	2	09	16	31.600	115.700	5.8
1956	2	09	16	31.750	115.916	5.7
1956	2	09	18	31.750	115.916	5.7
1956	2	10	04	31.583	115.666	5.0
1956	2	10	15	31.750	115.916	5.0
1956	2	10	18	31.750	115.916	5.5
1956	2	11	02	31.750	115.916	5.1
1956	2	11	05	31.700	115.900	5.0
1956	2	11	06	31.750	115.916	5.0
1956	2	11	06	31.583	115.666	5.4
1956	2	14	14	31.500	115.500	5.0
1956	2	14	18	31.500	115.500	6.3
1956	2	15	01	31.500	115.500	6.4
1956	2	15	02	31.500	115.500	5.3
1956	2	15	07	31.500	115.500	5.2
1956	2	15	08	31.500	115.500	5.0
1956	2	16	08	31.500	115.500	5.0
1956	2	25	08	31.500	115.500	5.1
1956	3	03	18	31.583	115.666	5.1
1956	3	09	00	31.750	115.916	5.0
1956	3	10	14	31.500	115.500	5.0
1956	5	10	11	31.833	116.000	5.0
1956	8	25	15	31.500	115.500	5.0
1956	12	13	13	31.000	115.000	6.0
1957	4	25	21	33.200	115.800	5.2
1957	4	25	22	33.183	115.850	5.1
1957	5	26	15	33.216	116.000	5.0
1958	4	19	09	36.000	114.800	5.0
1958	12	01	03	32.250	115.750	5.8
1958	12	01	03	32.250	115.750	5.0
1958	12	01	06	32.250	115.750	5.5
1959	7	21	17	37.000	112.500	5.7
1959	10	13	08	35.500	111.500	5.0
1962	1	27	23	30.800	114.600	5.3
1962	5	27	01	31.700	115.600	5.1
1963	3	25	09	36.018	114.771	5.0
1963	6	11	15	31.783	116.266	5.8
1963	8	06	23	33.783	116.916	5.0
1963	9	23	14	33.700	116.916	5.3
1963	10	20	13	31.100	115.600	5.0
1964	2	03	08	31.500	114.200	5.0

DNAG Earthquake Catalog (continued)

1964	5	15	19	31.500	113.700	5.0
1964	7	22	10	31.700	114.100	5.0
1964	8	30	21	29.200	114.400	5.2
1965	2	11	21	31.600	113.900	5.6
1965	9	25	17	34.700	116.500	5.2
1965	9	26	07	34.700	116.016	5.0
1965	12	30	16	33.566	116.550	5.9
1966	8	07	17	31.800	114.500	6.3
1966	10	09	08	31.200	113.333	5.4
1967	4	26	07	31.140	114.547	5.0
1967	5	04	22	30.416	114.403	5.2
1967	5	07	18	37.000	115.000	5.1
1967	9	21	00	31.416	115.950	5.2
1967	12	05	11	30.800	114.100	5.4
1967	12	05	18	30.800	114.000	5.0
1968	4	09	02	33.183	116.116	7.1
1968	4	09	03	33.100	116.033	5.2
1968	4	23	13	31.966	116.683	5.0
1969	3	20	08	31.400	114.000	5.2
1969	3	20	08	31.300	114.200	5.9
1969	3	20	08	31.400	114.100	5.2
1969	3	21	03	31.300	114.700	5.2
1969	3	21	03	31.200	114.300	5.6
1969	3	21	04	31.200	114.200	5.2
1969	3	21	04	31.300	114.300	5.1
1969	3	21	04	31.200	114.400	5.0
1969	3	21	04	31.000	114.500	5.2
1969	3	21	04	31.200	114.200	5.1
1969	3	21	04	31.200	114.200	5.8
1969	3	21	05	31.400	114.300	5.0
1969	3	21	05	31.300	114.300	5.0
1969	3	21	05	31.400	114.200	5.3
1969	3	21	06	31.300	114.000	5.1
1969	3	21	06	31.100	114.300	5.7
1969	3	21	07	31.300	114.200	5.6
1969	3	21	07	31.300	114.100	5.0
1969	3	21	07	31.000	114.400	5.0
1969	3	21	08	31.100	114.200	5.1
1969	3	21	08	31.200	114.200	5.5
1969	3	21	09	31.200	114.000	5.0
1969	3	21	10	31.300	114.000	5.0
1969	3	21	10	31.200	114.300	5.5
1969	3	21	12	31.200	114.200	5.2

DNAG Earthquake Catalog (continued)

1969	3	21	12	31.200	114.266	5.3
1969	3	21	15	31.200	114.300	5.1
1969	3	21	16	31.300	114.300	5.1
1969	3	21	17	31.290	114.010	5.2
1969	3	21	18	31.100	114.300	5.3
1969	3	22	07	31.400	114.100	5.5
1969	3	23	11	31.400	115.000	5.2
1969	3	23	15	31.500	114.100	5.2
1969	3	24	09	31.300	114.200	5.3
1969	3	28	15	31.500	114.300	5.3
1969	4	28	23	33.333	116.333	6.1
1969	6	10	03	31.616	116.200	5.0
1969	12	25	12	33.400	110.600	5.1
1970	10	04	17	30.629	113.645	5.1
1970	10	12	20	30.072	113.384	5.1
1971	1	23	22	32.550	115.783	5.1
1971	9	30	22	33.033	115.816	5.1
1972	2	20	06	29.895	113.532	5.4
1973	10	11	00	29.719	113.473	5.0
1973	10	13	01	29.575	113.644	5.1
1975	2	16	00	32.700	114.600	3.7
1975	6	01	01	34.515	116.495	5.4
1975	7	08	09	29.459	113.346	6.5
1975	7	17	18	31.927	115.777	5.0
1975	9	13	02	30.891	116.115	5.4
1975	9	13	02	30.868	116.277	5.1
1976	1	10	12	32.083	115.471	5.0
1976	2	04	00	34.655	112.500	5.2
1976	2	04	05	34.600	112.500	3.7
1976	2	04	09	34.600	112.500	3.7
1976	2	04	13	34.600	112.500	3.7
1976	2	09	03	34.614	112.530	4.6
1976	2	23	14	34.539	113.083	4.2
1976	8	18	04	32.700	114.600	3.7
1976	11	04	10	33.120	115.594	5.3
1976	12	07	12	31.977	114.778	5.7
1976	12	15	17	29.947	113.364	5.0
1977	11	10	14	33.000	113.400	3.7
1977	11	14	02	32.820	115.470	5.0
1977	11	21	02	29.269	112.970	5.6
1978	3	11	23	32.290	115.080	5.0
1978	5	05	21	32.210	115.303	5.5
1978	11	29	14	30.177	113.956	5.4

DNAG Earthquake Catalog (continued)

1979	3	15	20	34.309	116.440	5.3
1979	3	15	21	34.327	116.444	5.7
1979	3	15	23	34.329	116.442	5.0
1979	7	01	09	32.398	114.630	3.1
1979	7	03	03	32.492	114.638	3.0
1979	10	15	23	32.630	115.330	7.0
1979	10	15	23	32.765	115.440	5.2
1979	10	16	01	32.908	115.528	5.1
1979	10	16	05	32.927	115.539	5.6
1979	10	16	06	32.928	115.539	5.5
1979	10	16	06	33.013	115.555	6.1
1979	10	16	11	32.907	115.566	5.2
1979	10	16	23	32.650	115.340	5.5
1979	10	17	22	33.045	115.490	5.0
1979	12	11	20	33.700	111.100	3.7
1980	2	25	10	33.501	116.513	5.6
1980	6	09	03	32.185	115.075	6.5
1980	8	30	04	29.603	113.483	5.4
1980	9	15	22	33.590	111.250	4.3
1980	9	21	02	29.694	113.576	5.3
1981	3	16	06	32.574	114.686	3.1
1981	4	26	12	33.098	115.631	6.3
1982	2	07	19	29.035	113.053	5.7
1984	6	27	20	29.918	114.060	5.2
1984	9	06	20	30.614	113.966	5.2
1985	3	30	18	32.487	114.012	3.3
1985	5	08	23	31.890	115.821	5.1
1985	7	06	10	30.986	114.347	5.0
1985	7	16	17	34.543	116.842	5.2
1985	8	17	18	32.387	113.952	3.3

Table C-2

Stover Earthquake Catalog

Year	Date MM	DD	HH	Lat. Deg(N)	Long. Deg(W)	M	Io
1870	03	11	17	34.550	112.470		5
1870	08	12		34.550	112.470		4
1871	02	07	22	34.100	112.440		5
1875	01	22	22	33.650	114.500		5
1876	04	20	14	32.700	114.600		5
1877	09	21	02	32.700	114.600		5
1878	12	17	23	32.700	114.600		6
1884	09	02		32.700	114.600		4
1884	09	27	06	32.700	114.600		3
1888	08	19	10	32.700	114.600		4
1888	08	19	11	32.700	114.600		6
1888	08	19	14	32.700	114.600		5
1888	11	13	08	32.700	114.600		6
1888	11	25	11	32.200	111.000		4
1890	06	11	01	32.700	114.600		6
1890	06	11	03	32.700	114.600		3
1890	09	23	07	32.700	114.600		5
1891	04	27	04	35.200	114.500		3
1892	02	02	08	35.200	111.600		6
1893	06	05	13	31.700	110.100		5
1893	09	20	08	32.700	114.600		3
1897	02	12	13	32.700	114.600		3
1899	09	20		35.200	114.100		4
1899	10	07	06	31.700	110.100		5
1899	10	07	09	31.700	110.100		3
1905	11	14	23	32.700	114.600		4
1906	01	25	21	35.200	111.700		7
1906	01	28	17	35.200	111.700		3
1907	02	04	06	32.700	114.600		4
1910	09	24	04	35.800	111.500		7
1912	08	18	21	36.000	111.500		7
1912	08	19	10	36.000	111.500		3
1913	12	06	00	35.200	112.200		5
1915	06	27	08	33.400	111.800		3
1916	03	30	05	31.400	110.900		6
1916	12	12	12	34.000	110.000		5
1918	04	28	12	35.200	111.600		4
1919	05	23	11	35.200	111.600		3
1921	03	26	00	32.700	114.600		4
1921	03	26	23	32.700	114.600		3

Stover Earthquake Catalog (continued)

1921	03	28		32.700	114.600		3
1921	04	06	21	34.900	110.200		5
1922	06	17	23	34.000	111.200		5
1923	09	28		35.200	111.700		4
1923	09	30	18	34.000	111.200		4
1923	12	02	17	32.700	114.600		4
1924	03	21	19	32.700	114.600		4
1927	09	05	22	32.700	114.600		4
1931	04	17	12	34.500	110.000		5
1931	07	28	08	35.000	112.000		5
1932	12	29	05	32.700	114.600		4
1933	11	27		34.400	112.900		3
1934	01	11	07	31.900	109.800		4
1934	03	12		35.000	110.700		3
1934	12	25	10	37.000	112.500		4
1934	12	25	12	36.900	112.500		4
1935	01	01	08	36.000	112.100		4
1935	01	02	07	32.800	114.200		6
1935	01	03	14	36.900	112.500		4
1935	01	05	04	36.000	112.100		4
1935	01	10	08	36.000	112.100		6
1935	10	28	02	33.500	112.100		3
1935	12	05	21	36.900	112.500		4
1936	01	12		36.000	112.100		3
1936	01	22	03	36.300	113.500	4.3	.
1936	02	25	06	35.200	114.100		4
1937	04	08	12	35.700	109.500		5
1937	07	20	22	35.300	112.900		5
1937	07	21	03	35.300	112.900		3
1937	07	21	23	33.500	112.100		4
1937	07	22	03	33.500	112.100		3
1937	12	17	23	35.200	111.700		4
1939	02	19	11	36.100	112 100		3
1939	02	20	23	36.100	112.100		3
1939	03	09	13	36.100	112.100		5
1939	03	09	18	36.100	112.100		3
1940	05	19	18	32.700	114.200		5
1940	06	06	05	32.700	114.300		4
1940	10	16	13	35.200	111.700		4
1941	03	21		35.900	114.600		4
1941	03	22	12	36.000	114.600	3.5	4
1941	03	28	05	35.900	114.600		3
1941	05	21	16	35.900	114.600		4

Stover Earthquake Catalog (continued)

1941	09	03	21	36.000	114.700	3.5	3
1941	09	05	13	36.000	114.700		3
1942	09	09	05	36.000	114.700		5
1942	10	01	18	36.000	114.700	3.5	.
1943	07	20	06	36.000	114.000		4
1944	01	31	04	36.900	112.400		4
1945	07		11	36.100	112.100		4
1946	11	26	22	36.100	114.000		4
1947	10	27	04	35.500	112.000		4
1948	01	24	02	36.000	111.600		3
1948	01	25		36.000	111.600		3
1948	08	08	23	36.100	112.100		5
1948	12	03	18	35.000	110.700		4
1949	11	02	02	37.000	113.500	4.7	6
1950	01	17	00	35.700	109.500		6
1951	03	05	23	36.900	112.500		4
1951	04	12	06	32.000	113.000	4.5	.
1952	02	08	08	36.000	114.700	3.4	5
1952	02	20	13	36.000	114.700	3.6	6
1953	05	04	14	32.700	114.600		3
1953	05	18	07	36.000	114.500	3.8	3
1953	10	08	20	34.750	111.000		5
1958	09	18	06	31.400	109.900		4
1959	02	11	14	35.200	111.700		5
1959	07	21	17	36.800	112.370	5.6	6
1959	10	05	08	36.800	112.400		3
1959	10	13	08	35.500	111.500	5.0	5
1959	11	10	06	36.800	112.400		4
1961	06	18	08	32.400	112.500	4.7	.
1961	12	03	19	32.380	109.960	2.6	.
1962	01	17	16	36.800	112.400		4
1962	01	20	15	36.450	110.400	2.6	.
1962	02	15	07	36.900	112.400	4.5	5
1962	02	15	09	37.000	112.900	4.4	.
1962	03	02	08	36.960	113.480	2.6	.
1962	03	04	16	32.910	109.540	2.7	.
1962	03	07	19	32.290	109.770	2.9	.
1962	03	09	18	33.050	109.340	2.9	.
1962	03	11	20	33.140	109.310	2.8	.
1962	03	16	23	36.880	109.720	2.8	.
1962	03	17	22	34.880	112.090	2.9	.
1962	03	22	19	33.080	109.420	2.6	.
1962	03	23	19	33.050	109.430	2.6	.

Stover Earthquake Catalog (continued)

1963	05	10	23	35.040	113.820	2.7	.
1963	05	19	22	35.460	114.210	2.9	.
1963	05	27	22	36.050	114.650	2.5	.
1963	06	15	19	34.570	112.070	2.6	.
1963	06	29	03	34.810	114.540	2.7	.
1963	09	11	11	33.200	110.700		5
1963	10	03	18	33.100	109.350	3.1	.
1963	10	07	16	33.380	109.160	2.8	.
1963	10	09	19	33.080	109.430	2.7	.
1963	10	19	17	32.900	109.600	2.9	.
1963	10	20	18	33.060	109.450	2.8	.
1963	10	21	11	33.200	110.700	3.5	.
1963	12	05	20	32.840	109.550	2.7	.
1965	03	13	08	32.200	111.400	4.4	.
1965	05	03	03	36.000	114.700	4.2	3
1965	06	07	14	36.000	112.200	3.5	.
1966	01	22	12	36.570	111.990	2.7	.
1966	04	28	00	35.600	113.000	2.9	.
1966	05	05	06	36.820	112.390	2.6	.
1967	07	20	13	36.300	112.100	3.8	.
1967	08	07	16	36.500	112.400	3.8	.
1967	08	07	16	36.400	112.600	3.9	.
1967	09	04	23	36.150	111.600	4.2	.
1969	12	25	12	33.400	110.600		6
1970	04	25	08	36.019	114.734	3.0	.
1970	04	26	02	36.004	114.688	2.7	.
1970	09	16	12	35.200	111.700		3
1970	11	24	16	36.357	112.273	3.0	.
1970	12	03	03	35.874	111.906	2.8	.
1970	12	16	13	36.844	113.715	2.6	.
1971	03	27	04	36.762	112.393	2.6	.
1971	05	01	03	36.518	113.375	2.9	.
1971	05	23	21	35.017	113.888	3.0	.
1971	11	04	02	35.220	112.168	3.7	5
1971	12	15	12	36.791	111.824	3.0	.
1972	04	20	13	35.311	111.640		4
1973	02	09	17	36.430	110.425	3.2	.
1973	12	26	06	36.081	114.639	3.1	3
1974	03	04	08	32.550	114.779	2.7	.
1974	10	04	18	34.540	113.019	3.2	.
1974	12	20	03	33.860	111.880	2.5	2
1974	12	24	05	33.864	111.879	3.0	5
1975	02	16	00	32.700	114.600		4

Stover Earthquake Catalog (continued)

1962	03	30	17	32.650	109.170	2.7	.
1962	03	31	17	33.070	109.390	2.7	.
1962	04	25	21	33.040	109.350	2.7	.
1962	04	29	15	33.040	109.420	2.6	.
1962	05	01	17	32.930	109.490	2.7	.
1962	05	09	16	32.060	110.320	2.9	.
1962	10	01	13	36.140	111.740	2.5	.
1962	10	09	10	33.020	109.440	2.7	.
1962	10	15	21	33.620	109.230	2.7	.
1962	10	21	16	33.120	109.320	2.9	.
1962	10	22	16	33.060	109.420	2.7	.
1962	10	25	16	33.340	109.190	2.6	.
1962	10	30	15	33.260	109.340	2.5	.
1962	11	03	19	33.090	109.350	2.8	.
1962	11	05	20	33.040	109.430	2.5	.
1962	11	16	17	33.070	109.370	2.8	.
1962	11	17	16	33.180	109.330	2.6	.
1962	11	20	20	33.070	109.450	2.6	.
1962	11	23	16	33.460	109.090	2.5	.
1962	11	30	19	33.050	109.430	2.7	.
1962	12	01	19	33.010	109.470	2.7	.
1962	12	03	20	33.030	109.450	2.6	.
1962	12	05	19	33.400	109.120	2.6	.
1962	12	15	16	33.180	109.330	2.5	.
1962	12	28	16	33.360	109.140	2.8	.
1963	01	12	16	33.110	109.360	2.5	.
1963	01	12	21	33.190	109.220	2.7	.
1963	02	05	19	32.900	109.420	2.7	.
1963	02	07	20	32.790	109.620	2.8	.
1963	03	03	20	33.490	109.070	2.5	.
1963	03	06	20	33.230	109.270	2.6	.
1963	03	08	16	33.030	109.300	2.7	.
1963	03	10	19	33.070	109.400	2.6	.
1963	03	19	21	33.010	109.450	2.7	.
1963	04	08	19	32.940	109.540	2.5	.
1963	04	17	20	32.790	109.560	2.6	.
1963	04	19	16	33.000	109.450	2.7	.
1963	04	21	22	33.100	109.140	2.8	.
1963	04	22	22	32.540	112.080	2.7	.
1963	04	25	20	33.050	109.420	2.6	.
1963	05	01	16	32.890	109.540	2.7	.
1963	05	02	19	33.020	109.390	2.8	.
1963	05	05	16	33.130	109.250	2.7	.

Stover Earthquake Catalog (continued)

1975	09	08	22	32.550	114.329	2.9	.
1975	10	06	22	34.160	114.209	2.7	.
1976	02	04	00	34.655	112.500	4.6	6
1976	02	04	05	34.600	112.500		4
1976	02	04	09	34.600	112.500		4
1976	02	04	13	34.600	112.500		4
1976	02	05	21	34.703	112.574	2.9	.
1976	02	07	05	34.710	112.490	2.6	.
1976	02	07	08	34.594	112.621	2.9	.
1976	02	07	13	34.710	112.500	2.8	.
1976	02	08	09	32.500	114.800		3
1976	02	09	03	34.614	112.530	3.3	2
1976	02	21	03	34.524	112.705	2.8	.
1976	02	23	14	34.679	112.432	3.5	6
1976	02	28	20	35.910	111.788	3.0	.
1976	04	19	23	35.390	109.100	3.5	5
1976	05	04	10	34.702	112.535	3.0	2
1976	05	20	19	35.470	109.040	2.5	4
1976	08	18	04	32.700	114.600		4
1977	08	12	04	36.790	110.920	2.6	.
1977	10	21	02	34.630	112.480	2.5	5
1977	11	10	14	33.000	113.400		4
1977	11	29	21	36.820	110.990	3.0	.
1979	08	05	19	36.796	113.984	3.7	.
1979	12	11	20	33.700	111.100		4
1980	06	01	08	35.391	111.986	3.6	2
1980	09	15	22	33.590	111.250		5
1981	01	12	08	35.658	113.469	3.5	.
1981	01	18	23	34.150	110.790	3.0	.
1981	03	16	06	32.570	114.690	3.1	.
1981	05	29	03	36.830	110.370	3.0	.
1981	07	14	19	36.820	110.310	3.0	.
1981	12	06	09	35.170	111.620		5
1982	01	07	16	36.950	112.880	2.9	.
1982	02	11	02	36.980	113.980	2.9	.
1982	11	01	23	36.030	114.380	3.3	4
1982	11	19	20	36.030	112.010	3.0	.
1983	02	16	08	36.040	114.722	3.0	4
1983	02	23	11	35.973	114.711	3.9	4
1983	08	31	08	36.135	112.037	3.3	.
1984	04	14	09	36.503	113.383	2.6	.
1984	07	07	18	32.460	114.010	3.0	.
1984	07	18	14	36.216	111.844	3.0	.

Stover Earthquake Catalog (continued)

1985	01	30	13	34.750	112.137	3.0	4
1985	03	30	18	32.487	114.012	3.3	.
1985	04	14	21	35.174	109.071	3.3	3
1985	07	23	20	36.010	114.638	3.6	.
1985	08	12	21	35.976	114.644	3.3	.
1985	11	16	12	36.088	114.653	3.1	.

ENCLOSURE 3